RISK-CONSCIOUS DESIGN OF OFF-GRID SOLAR ENERGY HOUSES

A Thesis
Presented to
The Academic Faculty

by

Huafen Hu

In Partial Fulfillment
of the Requirements for the Degree
Doctor of Philosophy in the
College of Architecture

Georgia Institute of Technology
December 2009

RISK-CONSCIOUS DESIGN OF OFF-GRID SOLAR ENERGY HOUSES

Approved by:

Prof. Godfried Augenbroe, Advisor
College of Architecture
Georgia Institute of Technology

Dr. Ruchi Choudhary
College of Engineering
University of Cambridge, UK

Dr. Ellis Johnson
School of Industrial and Systems Engineering
Georgia Institute of Technology

Dr. Russell Gentry
College of Architecture
Georgia Institute of Technology

Dr. Pieter de Wilde
School of Architecture
University of Plymouth, UK

Date Approved: Oct 30th, 2009

To my parents and grandparents

ACKNOWLEDGEMENTS

This dissertation would not have been completed without support and contribution from many people.

I could never find the adequate word to express my gratitude to my advisor Prof. Augenbroe. Thank you for all the advice and friendly atmosphere that stimulate my self-growth during the past five years! I enjoy all the lectures on building physics 101 but have harvested even more during those conversations reaching for wisdom and happiness in life. Because of you I have had a lot more than the doctoral degree from Georgia Tech. I am truly grateful for having you as the advisor from all aspects!

I would like to thank Dr. Johnson, my advisor in the minor area of my doctoral study, for serving in the thesis committee. Thank you for all your advice and inspiring suggestions to my research and projects! I wish I had more time to catch up on mathematics with you!

I would like to thank Dr. Choudhary and Dr. Gentry for their support in my dissertation work. Thank you for offering me the wonderful opportunity to work for the Solar Decathlon project. The project not only provides a great chance to enrich my field experience in building simulation but also motivates the initialization of this dissertation. Thank you to the Georgia Tech Solar Decathlon team for having made the event true!

I owe special thanks to Dr. de Wilde for having flied such a long way to join us in the thesis defense in Atlanta. I feel greatly flattered. Thank you for your support and all the fine remarks on the thesis!

To all my colleagues and friends in building technology program, Yeonsook, Jason, Paola, Fei, Zhengwei, Atefe, Jihyun, Sanghoon,Yuming, Seanhay, thank you for all the

help and friendship in the past five years. Also to all my officemates in room 217, Jin Kook, Jaemin, Yeon-Suk, Hugo, because of you I have had a life at Georgia Tech. Special thanks to Paola: you saved me from a terrible thesis presentation!! Thank you for having pulled me through that desperate time! I will also have to thank Matt for offering the super computation power. Without it I would have not been able to finish the dissertation in time.

I would also like to take the opportunity to thank all the friends whom I have come cross in my personal life, Haiying, Bo, Ruoting, Rulan, Jing, Ning, Hui, Glendon, Kin, Kong, Rannie, Bin… I always enjoy the great time with you! Thank you for joining me in the way! It is and will always be my pleasure to have you around!

TABLE OF CONTENTS

LIST OF TABLES

LIST OF FIGURES

SUMMARY

Zero energy houses and (near) zero energy buildings are among the most ambitious targets of society moving towards an energy efficient built environment. The "zero" energy consumption is most often judged on a yearly basis and should thus be interpreted as yearly net zero energy. The fully self sustainable, i.e. off-grid, home poses a major challenge due to the dynamic nature of building load profiles, ambient weather condition and occupant needs. In current practice, the off-grid status is accomplishable only by relying on backup generators or utilizing a large energy storage system.

The research develops a risk based holistic system design method to guarantee a match between onsite sustainable energy generation and energy demand of systems and occupants. Energy self-sufficiency is the essential constraint that drives the design process. It starts with information collection of occupants' need in terms of life style, risk perception, and budget planning. These inputs are stated as probabilistic risk constraints that are applied during design evolution. Risk expressions are developed based on the relationships between power unavailability criteria and "damages" as perceived by occupants. A power reliability assessment algorithm is developed to aggregate the system underperformance causes and estimate all possible power availability outcomes of an off-grid house design. Based on these foundations, the design problem of an off-grid house is formulated as a stochastic programming problem with probabilistic constraints. The results show that inherent risks in weather patterns dominate the risk level of off-grid houses if current power unavailability criteria are used. It is concluded that a realistic and economic design of an off-grid house can only be

achieved after an appropriate design weather file is developed for risk conscious design methods.

The second stage of the research deals with the potential risk mitigation when an intelligent energy management system is installed. A stochastic model based predictive controller is implemented to manage energy allocation to sub individual functions in the off-grid house during operation. The controller determines in real time the priority of energy consuming activities and functions. The re-evaluation of the risk indices show that the proposed controller helps occupants to reduce damages related to power unavailability, and increase thermal comfort performance of the house.

The research provides a risk oriented view on the energy self-sufficiency of off-grid solar houses. Uncertainty analysis is used to verify the match between onsite sustainable energy supply and demand under dynamic ambient conditions in a manner that reveals the risks induced by the fact that new technologies may not perform as well as expected. Furthermore, taking occupants' needs based on their risk perception as constraints in design evolution provides better guarantees for right sized system design.

CHAPTER 1 INTRODUCTION

1.1 Sustainable energy

Sustainable energy resources have been attracting more and more attention because of our current energy and environmental concerns. In the past three decades the U.S. yearly energy consumption has increased from 76 quadrillion Btu in 1976 to near 100 quadrillion Btu in 2006 and meanwhile the yearly carbon dioxide emission has increased from 4735 million metric tons in 1980 to 5945 million metric tons in 2005 [1]. Using renewable energy is believed to be the ultimate solution to energy conservation and green house gas reduction [2].

Currently renewable energy is being employed as either main or complementary energy sources for both residential and commercial buildings with the primary aim to reduce the buildings' demand for traditional electricity from the public grid, or to take the building totally off the grid. This relieves national power plants from overload situations and may save billions of investment dollars that would be required to increase plants' capacities to meet the increasing countrywide electricity demand. If new urban development could be totally off-grid, it additionally saves otherwise needed infrastructure investments. Based on the annual energy outlook 2008 (AEO 2008) the total electricity consumption will grow from 3814 billion kWh in 2006 to 4972 billion kWh in 2030 in the U.S. [3]. It also predicts that using renewable technologies for electricity generation will be stimulated by improved technology, increases in fossil fuel prices, and tax credits provided by the government. Total renewable generation is predicted to grow from 385 billion kWh in 2006 to 658 billion kWh in 2030. On the supply market side, the U.S. PV industry has set

their goal of meeting 10% of U.S. peak generation capacity by 2030 which represents an energy equivalent of some 180 million barrels of oil in that year [4].

1.2 Motivation

Despite all the ambition and enthusiasm that people have about clean energy the actual market penetration of installing a renewable power system is still low. It is mainly caused by two reasons. The first obstacle is the high capital cost due to expensive raw materials and relatively low efficiencies especially compared to solar water systems. The second reason is its unpredictability in terms of power generation which is determined by the partially unpredictability of the dynamic nature of natural resources like solar radiation and wind.

According to AEO 2008 the percentage of the electricity generated by renewable energy over the total electricity generation across the country will only increase from 10% in 2006 to 13% in 2030. Unaffordable cost is considered as one of main factors that prevents the wide spread adoption of renewable energy. Take solar energy as an example: the 2004 solar electricity cost is estimated to be 18.2 cents/kWh based on present federal policies for a grid-connected commercial system, investment tax credit, and accelerated depreciation [5] while the average retail price of electricity in 2004 is 6.95 cents/kWh [6]. This high cost is why building renewable power systems is still limited to governmental, institutional, and public projects where other than return on investment (ROI) considerations drive adoption. During the past decade numerous efforts have been contributed to lower renewable power price down, including investment tax credit provided by the government and rapidly advanced technology offered by the renewable power industry. One of the most promising news on renewable power price is that PV

module costs are expected to decrease 40% by 2010 [7]. A considerable reduction in renewable power price can thus be expected to happen in the next few years.

Another factor that stops renewable power from being widely used is its momentary unpredictability. One common point among most of the renewable energy sources, such as solar and wind, is that its productivity highly depends on the natural resources and can therefore not be guaranteed at critical times of necessity without a storage component that can be charged in times of abundance and discharged at times when the need is greater than what can be covered by the natural resources at that time. This is another main reason, other than large initial capital investments, that stops people from choosing to live in an off-grid house. The necessity for storage to bridge periods of scarce supplies may be such that large size storage components lead to expensive "over engineered" solutions. The alternative, an off-grid house with back-up generators can be equally unattractive if the capacity and operation time of the generators exceed acceptable limits. It has to be well understood that the house and its systems operate in highly variable conditions and use scenarios. The design parameters should therefore be chosen to give sufficient guarantee that minimal requirements with respect to reliability are met. This objective relates primarily to the system sizing, as far as the scope of this thesis is concerned. The sizing is driven by performance evaluation metrics and assessment against minimum levels of compliance to system performance requirements. Their derivation can become complex, especially for an off-grid system which intends to achieve complete energy self-sufficiency, at least within certain yet to be determined margins of continuous power availability. Power reliability is the primary issue that has to be resolved for people to feel comfortable living in an off-grid without a back-up generator.

1.3 People's attitude towards adoption of new technologies to live off-grid

Living off-grid with power supplied from renewable energy resources reflects not only people's enthusiasms of contributing to the global sustainability but also their attitude towards adopting renewable energy technologies regardless the inconvenience brought by its nature of uncertainty. In general technology acceptance has three dimensions: 1) characteristics of individuals; 2) characteristics of technologies; and 3) characteristics of the implemented context. And often the characteristic of the technology contains two determinants: performance expectancy and effort expectancy.

A research conducted by Beamish et al. reveals that user satisfaction and perceived benefits and problems are the two main influencing factors that affect the adoption and usage of a new technology. Beamish et al. examine how user's perception of passive solar, active solar, and earth-sheltered housing options may influence their actions towards adopting them. Their analysis of results indicates that the design/appearance is a major factor in consumer acceptability and a lack of understanding of those housing options in terms of potential benefits and problems with innovative energy-efficient measures implemented might have been a negative impact on consumers' attitude towards adoption [8].

Then the question is how to help consumers better understand the potential benefits and problems and what key information a designer should provide before their design gets adopted? Rogers develops a model of an innovation related decision process [9]. In his model a decision process regarding adopting an innovative technology includes five steps as shown in Figure 1.1.

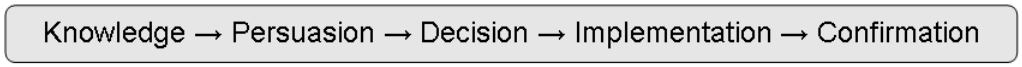

Figure 1.1 A model of the innovation related decision process [9]

The persuasion stage in Rogers' process model studies the characteristics of the technology perceived by the consumers. The perceived characteristics include the following six attributes:

1) Relative advantage: the degree to which the innovation is superior to prior innovations;
2) Risk: the degree to which economic, physical, psychological, functional, and social ills are perceived in a innovation.
3) Compatibility: the degree to which an innovation is consistent with the values and experiences of potential adopters.
4) Complexity: the degree to which an innovation is difficult to understand and use.
5) Divisibility: the degree to which an innovation can be tried on a limited basis.
6) Communicability: the degree to which results of an innovation are easily and effectively disseminated.

Meanwhile Weber et al. have conducted a research of people's propensity to adopt innovative housing (passive and active solar, earth sheltered and retrofitted). Weber et al. mainly examine the relationship between people's attitude towards innovative housing options and their level of knowledge about the innovative technology. As the first step Weber et al. develop a series of knowledge indices which include individual ones representing occupants' knowledge of the four different innovative housing options and a total knowledge index summing people's knowledge of all four housing options. Their

analysis of results shows that the knowledge indices can produce valid results in terms of predicting consumers' acceptance of innovative housing types. It also indicates that the better their knowledge of innovative housing type is, the better/easier decision consumers could make to adopt/reject the new housing options.

1.4 User involvement in sustainable design

It is well understood that user involvement is critical in our pursuit of environmental sustainability. Yet its full potential can only be achieved by: 1) redefining the fundamental concept of user need, and 2) engaging users to share a part of the responsibilities regarding the liability.

1.4.1 The concept of "Normality"

One of the basic intentions of system invention is to define and maintain a normal way of life. In the context of design, "normality" is represented by a set of performance criteria that describe the need a design intends to fulfill. Whether the predefined performance criteria are justified for innovative design remains unexamined. Take thermal comfort evaluation as an example. The fundamental thermal comfort criterion is derived by Fanger based on systematic analysis of human response to different thermal environments [10]. Subsequent studies have shown that this criterion can be relaxed if natural ventilation is used instead of mechanical ventilation [11-13]. It raises the question: is the conventional definition of need suitable in our path toward a sustainable environment? User involvement in design will not significantly accelerate the step toward sustainability unless it challenges the purpose, norms, conventions around which contemporary concepts of need are built [14].

1.4.2 Occupants' responsibility

After establishing the definition of "normal" life (i.e. performance criteria) it is up to designers to ensure that the system will provide a comfortable and healthy living environment under the very dynamic and unpredictable ambient environment. Because of liability issues, designers generally have to oversize a system to guarantee a certain level of system performance under all scenarios. It often results in unnecessary energy waste during normal operation which occurs for the most part of a system's service time.

Take passive building design practice as an example. Regardless of all the incredible enthusiasms the world has about sustainability, one possible reason why passive building design did not become standard practice by the end of the 20th century is the perceived demands designers made on occupants' time and efforts which were not incorporated as part of their responsibility [15]. Using natural ventilation to keep the indoor environment healthy and/or thermally comfortable has become one of the most attractive but also challenging way to implement energy saving strategies in building design. Meguro [16] has interviewed people from different disciplines but all now working in natural ventilation practice field and she concluded three common reasons that compromise building performance when passive ventilation scheme is implemented. Occupants' unawareness of building operation requirements is one of them. Natural ventilation takes place through sophisticated positioning and operation of building envelope openings according to the specific local weather, which often needs occupants' interventions. If occupants do not understand how those envelope openings shall be operated under different weather conditions they might counter-react to the passive ventilation scheme and turn the building configuration into a different one away from design conditions

under which a passive ventilation scheme is developed and evaluated. Only when occupants become active players the energy saving intended by implementing natural ventilation can be maximally attained. Similar arguments about natural ventilation can be found in a design practice presented in [17] and a dissertation research on occupants' input to building energy simulation [18].

As a matter of fact customers' willingness to share part of responsibility in meeting performance requirements is not specific to attaining building energy savings or sustainability in general. It is encountered in other industry fields as well. One of the latest researches in power reliability, conducted by Oak Ridge National Laboratory (ORNL) addresses the need for customers to take some responsibility, together with the utility providers, to meet reliability demands for today's 21st century power service system [19]. The study points out that it might not be appropriate for distributed energy resources (DER) themselves to be dedicated to meet the power quality and reliability needs of individual customers through market-based solutions because only the customer truly knows the value of increased power reliability/quality for their particular circumstances. Therefore researchers have defined multiple levels of power quality/reliability for different load needs and some customers could even trade their rights of power interrupt back to the power systems if they are willing to accept power service with a lower reliability than the basic regulated service. In fact current power plant capacities are expected to expand in order to meet the fast growing power demand and "responsive load" has been proposed to be one of the solutions which requires customers to cut off their electricity consumption during peak load periods [20]. Utility companies have been investing and implementing pilot program(s) to encourage

customers to contribute more proactively to help power systems provide more reliable and higher quality service without the need of capital investments in power plant capacity expansion. Georgia Power has offered a program called "power credit program" to get their customers' permission so that they can manage their air conditioning (AC) running time to reduce HVAC power consumption in times when power demand peaks in the summer [21]. In return customers will receive $20 credit plus $2 for every interrupt to their AC systems. Similar programs are also available from other power companies who provide service to the areas where AC equipments are the main contributors to peak electricity demand, like Nevada Power [22] and Idaho Power [23]. More aggressive measures are on the way to demonstrate the potential benefits that might be brought by implementing multiple levels of reliability in power service proposed in [19]. The introduction of these customer-active measures are bringing extensive benefits for both utility companies and customers: 1) it provides economic benefits for environmental impact aware customers by offering reward credits, electricity service at reduced rates, and/or tax credits; 2) it relieves pressure on utility companies by helping them reduce capital investments that would otherwise be spent to expand power plant capacity in order to meet the increasing electricity demand especially during peak period. The ultimately goal is to establish a more compact power infrastructure and cut off some redundancy which would otherwise exist to ensure regulated power reliability during peak load periods.

The fact that industry is calling on their customers for inputs and offering a flexible choice for reliability reflects the strong desire to break away from exiting rigid design criteria and embrace a more flexible and customer centric design space. A shared

responsibility with respect to system reliability provides designers more flexibility to implement bolder energy efficient measures and meanwhile improve the awareness of sustainability opportunities hidden in the daily lives of consumers. Appropriate economic measures can be expected to be implemented to motivate and practice this holistic cooperation.

In this thesis we will explore how the same thinking can and should be applied to the right-sizing and right engineering of off grid solar houses.

1.5 Hypothesis

This work is driven by one major hypothesis and two associated hypotheses.

- Hypothesis 1: Current reliability based sizing methods are inadequate for (near) zero energy solar houses as they do not relate system failure rates to occupant risk acceptance attitudes
- Hypothesis 2: A new integrated design procedure can be developed that enables the combined building and system design of near zero solar energy houses to meet occupant/owner oriented reliability and ROI expectations in the light of quantifiable uncertainties in system behavior
- Hypothesis 3: The role of intelligent, embedded simulation based control can increase the reliability of solar energy houses significantly.

1.6 Goals of this research

The goals of this research are:

(1) To investigate the potential causes of system underperformance;

(2) To establish a systematic approach of developing expressions of risk and reliability in off-grid house design;

(3) To use expressions of risk as design targets and thus ensure system performance at a level that the various stakeholders will gain confidence in experimental technologies.

1.7 Research approach, methodology, and assumptions

This research is carried out in the form of case study. An existing off-grid solar energy house, designed by the Georgia Tech team as their entry to the Solar Decathlon, is used as the demonstration case throughout the whole dissertation.

Figure 1.2 shows the framework of the research methodology of this dissertation. It includes three main parts:

- The development of an occupant oriented power reliability assessment method: this covers the first stage and will be used as an instrument to evaluate power reliability of an off-grid solar house design.
- The development of a mode-based control: A stochastic model based predictive controller is developed in the second stage. The predictive controller is proposed to help daily operation in an off-grid solar house and improve user satisfaction with respect to power reliability.
- The development of approaches for reliability based design optimizations: Design optimizations will be conducted in the third stage to find the suitable trade-off between power reliability and an increase in design capital cost.

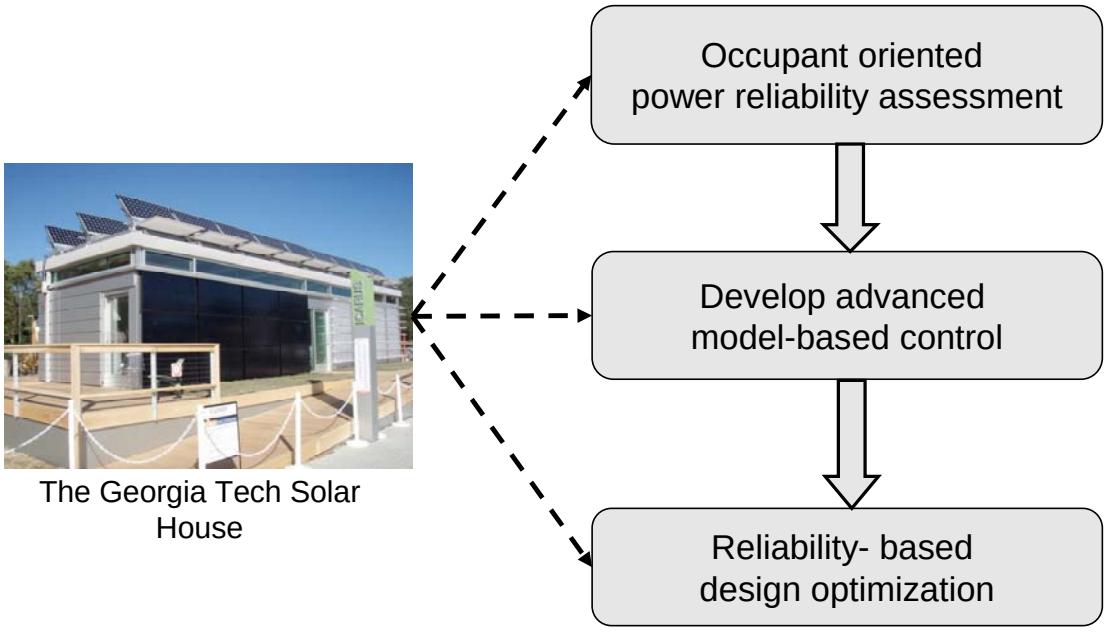

Figure 1.2 A framework of the thesis research methodology

An off-grid solar house design involves work from multiple disciplines. A large number of challenges have to be solved before reaching the final goal – an off-grid residence satisfying its occupants at all different performance aspects. This research mainly focuses on the aspect of power self-sufficiency which is a necessary requirement for the success of an off-grid house design.

1.8 Thesis outline

This thesis is organized as follows:

Chapter 1 presents the motivation of this research and describes the research hypotheses, research goals, methodology, and the main focus of this dissertation.

Chapter 2 provides an overview of the power reliability concept in power industry. A literature review of power reliability assessment study, especially when renewable power generation presents, is also included in this chapter.

Chapter 3 introduces the role of occupants' preference in power reliability analysis and develops a framework of occupant oriented reliability assessment for off-grid solar house design.

Chapter 4 investigates the potential causes of power unavailability in off-grid solar houses focusing on the role that uncertainties play in power reliability analyses.

Chapter 5 presents a case study in which the occupant oriented power reliability assessment approach is demonstrated.

Chapter 6 develops a stochastic model based predictive controller and demonstrates how it can be used to manage energy distribution and increase the general power reliability in the case presented in Chapter 5.

Chapter 7 introduces a value based approach to help size the energy system of off-grid solar house. A design optimization using the value-based approach is conducted on the case presented in Chapter 5. The difference of outcomes is investigated with and without a stochastic model-based controller installed, in order to verify the relevance of adding intelligent control to the house.

Chapter 8 develops a risk based design optimization (sizing) approach for off-grid solar house design, in which the occupants' demands on power reliability are applied as probabilistic constraints with the aim to guarantee certain levels of power reliability (formulated as probabilities).

Chapter 9 completes the dissertation with conclusions and insights that point to future and continuing work.

CHAPTER 2 POWER RELIABILITY

2.1 Power reliability

2.1.1 Definition

Power reliability analysis addresses specific performance aspects that impact reliability of power systems. The North American Electric Reliability Council (NERC) has introduced a definition of the reliability of an electric system which includes two basic functional aspects [24, 25]:

- Adequacy: The ability of the electric system to supply the aggregate electrical power demand and energy consumption requirements of customers at all times, taking into account scheduled and reasonably expected unscheduled outages of system elements.
- Security: The ability of the electric system to withstand sudden disturbances such as electric short circuits or unanticipated loss of system elements.

Most of current researches on power reliability modeling are focusing on the adequacy aspect due to the complexities associated with modeling power system in security aspect. This research will only deal with power adequacy aspect. Meanwhile we will continue using the term “power reliability” but only in the narrower definition: the ability to provide power service to its customers in the desired amount at when they want.

An electric power system is generally composed of three main functional zones: generation, transmission, and distribution systems, all of which work together to generate, transport and deliver the required amount of electric power to customers when

they want. These zones are modeled as system hierarchical levels in reliability assessment as shown in Figure 2.1 [25]. The hierarchical level 1 (HL1) is only concerned with the generation system. Hierarchical level 2 (HL2) concerns both generation system and transportation system. Hierarchical level 3 (HL3) covers all three functional systems in an electric power system which deals with reliability assessment at customer load point. Due to inherent complexities, reliability evaluation of an electric power system at HL3 is usually not conducted directly in practice.

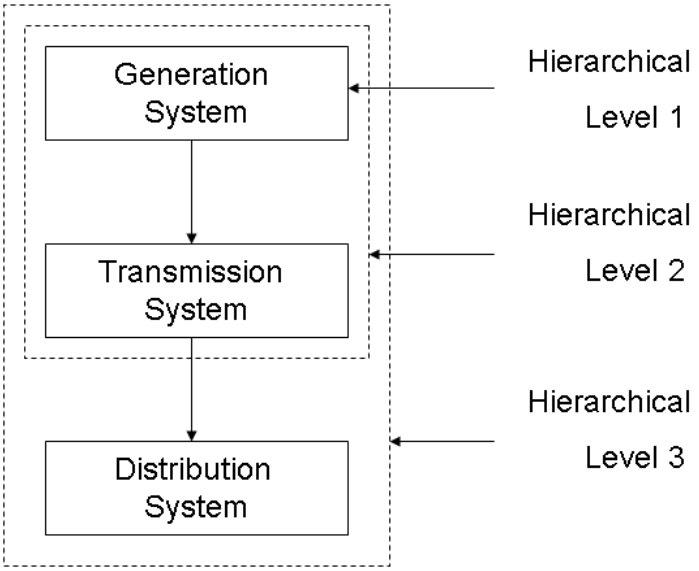

Figure 2.1 Hierarchical levels in an electric power system

2.1.2 Evaluation techniques

There are two different categories of approaches: the analytical approach and the Monte Carlo (MC) approach. Detailed reviews on power system reliability assessment methods can be found in recent dissertation research in the electric engineering field [26-29]. Below is a short summary of the difference between the analytical approach and the MC approach.

As indicated by its name, the analytical approach represents the concerned system using analytical model(s) and evaluates reliability indices directly through the models using mathematical solutions. The MC approach estimates the system reliability indices by simulating the actual process and random behavior of the system. In general the analytical techniques are more efficient and seen as preferable if: 1) there are no complex operating conditions involved, and 2) fairly reasonable analytical models are available to represent the to-be-evaluated system. When a system is operated under complex conditions and/or the failure probability of a system is relatively large, MC approaches are often preferable since MC simulations can not only evaluate the system reliability indices but also provide distributions of reliability indices which help provide a better understanding of the investigated reliability issues. And obviously when there is no reasonable analytical model exiting for the investigated system MC approach will become the only candidate. Billinton and Li [25] lists a few main advantages of using MC in power reliability evaluations:

- In theory MC approaches can include some system effects or system processes which are usually simplified in analytical approaches;
- The required number of samples for a given accuracy level is independent of the size of the system and therefore it is suitable for large scale power system evaluation;
- MC approaches can provide probability distribution of reliability indices which analytical methods generally cannot;

- MC approaches can simulate the probability distributions of certain system components associated with system failures which analytical methods cannot perform;
- MC approaches can also simulate the uncertain effects from operating conditions, such as dynamic weather conditions.

However, as concluded by Billion and Li, regardless all the advantages described above we have to realize that the analytical methods also have their own advantages and the quality of the reliability analysis is only as good as the approximation of system models, the appropriateness of evaluation techniques, and the quality of the inputs.

2.1.3 Modeling techniques and common reliability indices

There are mainly two types of modeling methods in power system reliability assessment: deterministic modeling methods and probabilistic modeling methods. The deterministic methods have been used to check satisfactory reliability levels in the power industry during the past decades. In recent days, probabilistic modeling methods have gradually taken the lead due to the increasing complexities in modern power system and the growing sophistication and fidelity of computational approaches. Two main reasons that result in this shift from deterministic methods to probabilistic methods are: 1) deterministic methods can not catch the stochastic nature of power system behaviors, customer loads, and other external influences.; 2) the evaluation techniques of probability theory [28, 30] have become very powerful. Detailed reviews on today's power reliability modeling methods can be found in [26] and [28].

Accordingly two types of reliability indices are currently used in the power industry depending on the modeling methods selected: deterministic reliability indices and

probabilistic reliability indices. Karki [28] reviewed the deterministic and probabilistic adequacy indices used in Canadian utilities. More power reliability indices, at different hierarchy levels and derived from different modeling methods, can be found in [28], [25], and [30]. Table 2.1 lists a few of the most commonly used adequacy indices.

Table 2.1 Some common adequacy indices

Methods	Criteria	Further explanations
Deterministic	Percent margin	The capacity reserve requirement is a fixed percentage of the total installed capacity.
	Loss of largest unit	The capacity reserve requirement is at least equal to the capacity of the largest unit.
Probabilistic	Loss of load expectation	The expected number of days or hours in a year that the system generation capacity is not adequate.
	Expected unserved energy	The expected energy in kWh that cannot be supplied by the system in a year.

2.1.4 Power reliability assessment in the 21st century

One big transition in the power industry today is that the electric power industry has begun to look at reliability and power quality as two tightly interrelated aspects of utility performance [19]. Utility performance is no longer considered to be independent from customers' need and responsibilities. ORNL lists two important characteristics of the reliability prospective of 21st-century power systems [19]:

- It may not be appropriate to require the utility alone to meet reliability; the customer shall have to accept some responsibility;
- The "reliability" of electric service is a function of the loads served, as well as of the characteristics of the electricity provided.

This new concept makes it possible for customers to receive and to pay the power service based on their own needs and desires. Some customers could pay less if they are willing to trade their rights of being guaranteed power service at the regulated level of reliability and quality. Conversely, some customers could choose to pay extra to receive power service at higher reliability requirements or at a higher quality level.

2.2 Reliability assessment in renewable power systems

2.2.1 Main characteristics

One common point among most of the renewable energy sources, such as solar and wind, is that its productivity highly depends on the natural resources and can therefore not be guaranteed at all times. This varying and uncertain nature makes both sizing and performance evaluation of a renewable power system difficult, especially for an off-grid system which intends to achieve complete energy self-sufficiency (or more accurately phrased "acceptable reliability level in terms of energy availability"). Given the fundamental similarity among different renewable energy systems the following treatment will primarily take solar energy as an example, i.e. focus on solar electricity generation system design and associated challengers in terms of its ability to support off-grid buildings.

2.2.2 Adequacy indices, modeling methods, and evaluation techniques

Due to the complexity in modeling a renewable power system, especially in taking dynamic weather effects into account, current adequacy assessments of renewable power systems are conducted using MC simulations in stead of analytical methods. Both deterministic and probabilistic criteria have been used in reliability evaluations. Similar to the trend in general power system reliability evaluation, probabilistic indices have become popular for renewable systems assessment. A treatment of deterministic indices for reliability evaluation of renewable power systems can be found in [28]. The following section will focus on probabilistic modeling.

A well-known probabilistic performance parameter used to evaluate the reliability of off-grid solar power systems is the loss of load probability (LOLP), defined as the ratio between energy deficit and energy demand over the total operation time of the installation [31]. It represents how often the supply system (PV + storage) will not be able to meet energy load. El-Maghraby et al. [31] and Tsalides and Thanailakis [32] conducted two of the earliest investigations that applied the concept of LOLP to evaluate a design of stand-alone PV system in the mid 1980s. LOLP links PV system design parameters to overall reliability and has since been used to estimate reliability of off-grid solar power system in many instances.

Karki [28] conducted a thorough review of the indices used for reliability evaluation of power system investigating the difference between a traditional power system and a renewable power system. He concluded that reliability assessment of solar and/or wind electric power systems would require a probabilistic reliability evaluation approach because of its varying capacity which is due to the unpredictability of local weather and

its dynamic nature. Karki developed a reliability evaluation model for an isolated renewable power system using sequential MC simulations which are used to generate synthetic data for hourly atmospheric condition based on the historical monthly mean values. Several follow-up researches from the same research community have extended this stochastic reliability assessment to general power systems where renewable energy is involved [27, 29]. Figure 2.2 shows the main framework of reliability evaluation of off-grid solar and wind power systems developed by this research community. The first step generates hourly atmospheric condition based on monthly average atmospheric data using the sequential MC simulations. Step 2 models the renewable energy conversion devices to estimate the actual hourly outputs from the renewable power system. The synthetic weather data generated from the first step will be used as input parameters for the second step. The third step compares the hourly energy generated in the second step with the chronological hourly loads that are either from the Reliability Test System (RTS) used by the Institute of Electrical and Electronics Engineers (IEEE) or other typical residential load models to obtain the desired adequacy indices which are then translated to reliability indices using certain reliability evaluation models. The random nature of renewable power resources has been well captured using a sequential MC simulation technique in those researches [27-29].

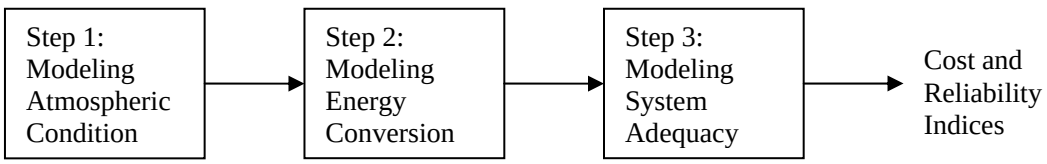

Figure 2.2. Renewable energy evaluation steps[28]

2.3 Risk in design compliance

Every design is meant to perform a required function, under given environmental and operational conditions for a stated period of time. Risk analysis (or reliability analysis as its complementary goal) is often conducted in the end to evaluate how well a design is compliant with a design performance requirement.

Risk has different definitions depending on the specific discipline and application contexts. In general, risk is defined as the probability that an unfavorable outcome occurs [33]. It presents the chance of loss or injury. In situations where casualties and/or severe damage may be caused, such as a nuclear accident or other public health hazard, risk is measured as a combination of the probability of an occurrence of an unfavorable event and the severity of damage (casualties or illness) it causes, as shown in Equation 2-1.

$$Risk = \Pr(\textit{an unwanted event}) \times (\textit{impact of the event occurring}) \qquad (2\text{-}1)$$

In engineering the unfavorable outcome can occur when the design performance does not meet the design requirement. It is difficult to measure impacts caused by such an event in dollar values and hence difficult to design for a certain acceptable risk. Instead, engineering disciplines typically aim at a system design that meets the design requirement under all conditions or define a maximum allowance of violation of the design compliance, in case a design does not comply with its performance requirement under all circumstances.

Equation 2-2 shows the mathematical definition of risk when a design is required to meet a minimum performance requirement. The expression assumes that a set of model parameters can only be estimated within an uncertainty range.

$$Risk(PI) = \Pr(PI(\overline{X}, \omega) \le PI_{req}) \quad (2\text{-}2)$$

Where

$\overline{X}$	the vector of design variables;
ω	the vector of relevant uncertain parameters;
PI	the concerned performance indicator;
PI_{req}	the design requirement of concerned design PI;
$Risk(PI)$	the calculated risk index with respect to the concerned design PI.

Figure 2.3 illustrates the risk definition. The curve shows the probability density function of the performance indicator of a design and the red dot represents the design requirement (i.e. the minimum required performance). The red area represents the probability that this design performs worse than the minimum requirement and will be calculated as the corresponding risk index defined in Equation 2-2.

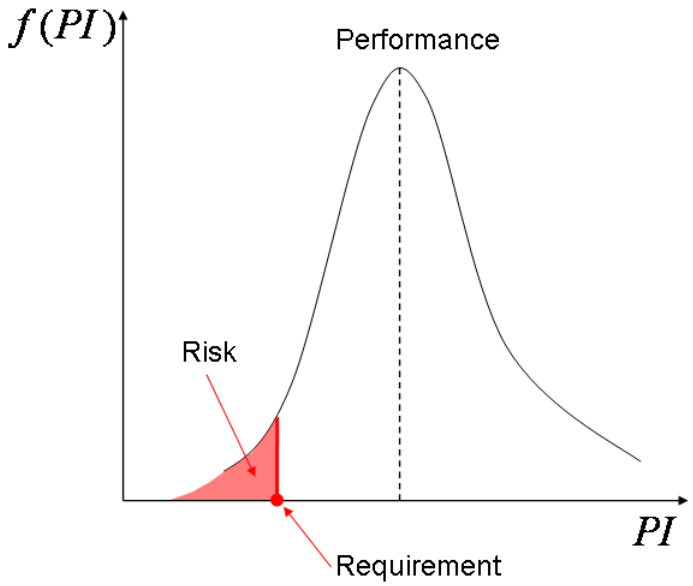

Figure 2.3 Distribution functions of design performance parameter and its requirement

2.4 Reliability during service life

Risk definitions in Equation 2-1 and Equation 2-2 are given at any time t and in reality we are usually concerned with risk issues during the whole service life (SL) period. Marteinsson (2005) and Stojanovic (2007) have reviewed different definitions of service life and opted for the one defined in the standard ISO 15686-1 [34] as:

Service life (SL): "Period of time after installation during which a building or its parts meets or exceeds the performance requirements".

System performance deteriorates gradually as time goes by due to degradation whereas the performance level may intermittently get improved through maintenance interventions.

Let η represent the system parameters that degrade over time and a mathematical definition of service life risk index could be written as follows, based on Equation 2-2:

$$Risk(PI,t) = \Pr(PI(\overline{X},\eta(t),\omega) \le PI_{req}) \tag{2-3}$$

If $\varepsilon_{PI,req}$ represents the maximum allowable risk level, Equation 2-4 shows the complete design compliance, including both design requirement and its minimum allowable violation. The time length between installation time and the time when calculated reliability equals the minimal acceptable reliability is the service life. Figure 2.4 shows the time dependent system risk and its relationship with system performance and the performance requirement. The maintenance process has been ignored in the schematic figure for simplicity.

$$\begin{gathered} Risk(PI,t) = \Pr(PI(\overline{X},\eta(t),\omega) \le PI_{req}) \\ Risk(PI,t) \le \varepsilon_{PI,req} \end{gathered} \tag{2-4}$$

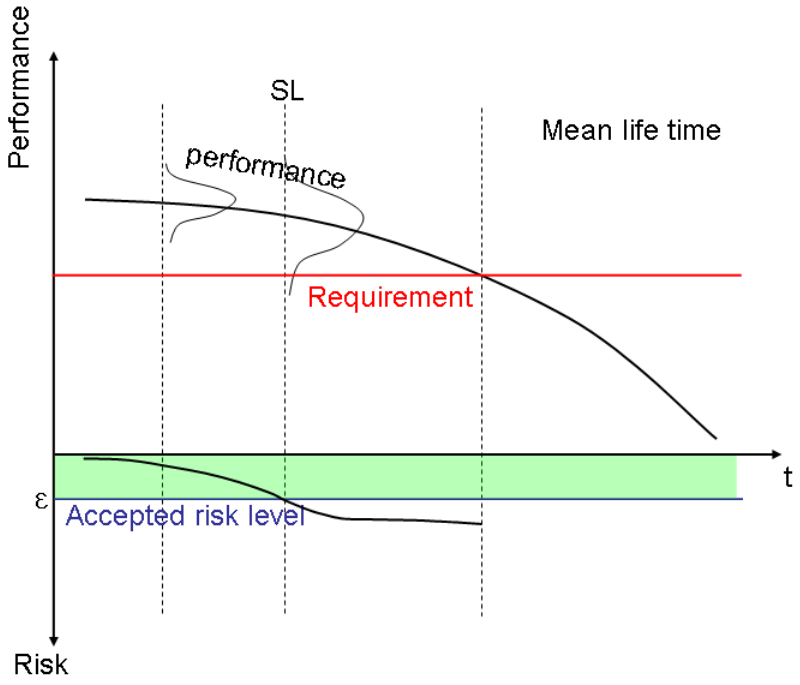

Figure 2.4 System reliability and performance over time (constant performance requirements)

2.5 Risk and uncertainty

As stated before risk is the probability that an unfavorable event occurs. In order to measure risk we have to analyze uncertainty. Uncertainty is defined as the indefiniteness about the outcome of a situation [33]. The reason that a system/component outcome varies might be: 1) certain part of the system/component may not perform as designed or at least not as its design idealization predicts; 2) the operating condition might not be the same as the during design assumed condition; 3) the intended function requirement might not be the same as what the system/component is designed for in the first place (functional mismatch). All of those possible reasons are represented as uncertainties in the mathematical concept of risk analysis. In the analysis they will be modeled as uncertain variables with corresponding probability density functions.

In addition to uncertainties related to properties of the studied system there is another type of uncertainty that is due to reliability modeling itself. In practice risk analysts will have to derive/choose deterministic/stochastic models of the system or individual components before performing a risk analysis. In reality there is no perfect modeling approach that can capture all aspects of a system and predict its full spectrum of behavior during operation. Certain model simplifications have to be made. Figure 2.5 illustrates the schematic modeling steps. Two conflicting interests always exist during the model development process [24]:

- The model shall be sufficiently simple to be handled by available mathematical and statistical methods;
- The model shall be sufficiently "realistic" such that the deduced results are of practical relevance.

Choosing the appropriate model with the proper level of accuracy depends on the analysts' knowledge of the system and their experience in the field. The errors due to the estimators' lack of knowledge are unpredictable and hard to be taken into account in risk assessments [35]. This thesis will not research the potential risk raised by human errors. All other sources of uncertainty relevant to the power reliability of off-grid solar houses will be discussed in detail in Chapter 3.

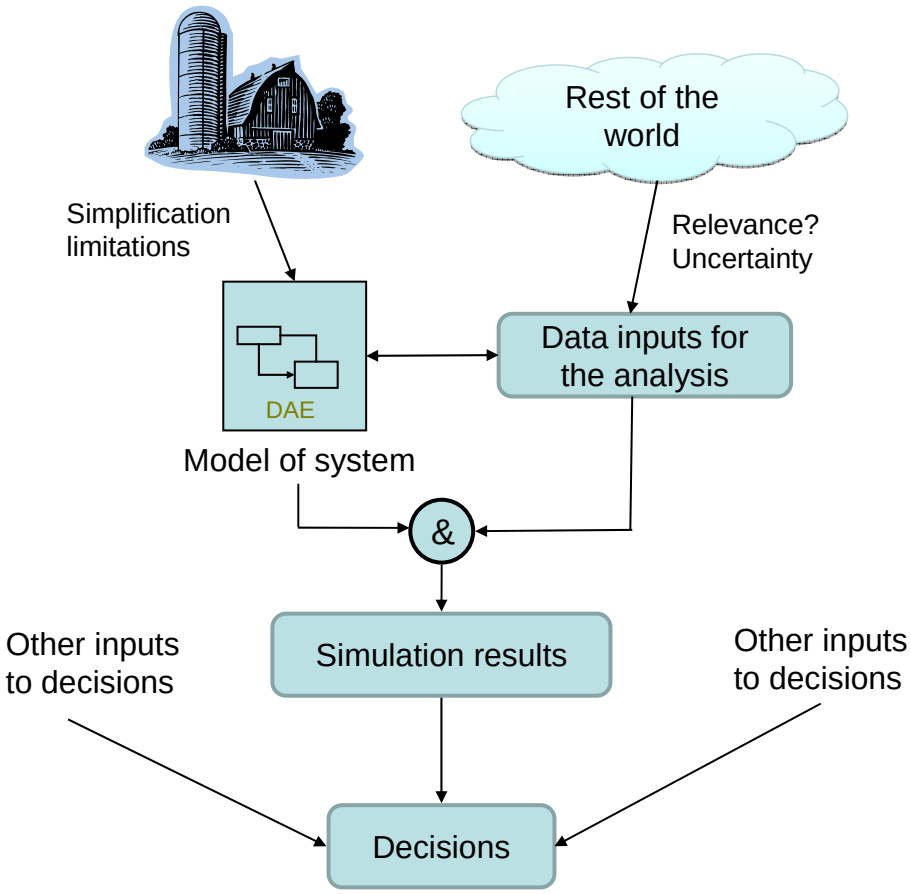

Figure 2.5 Modeling and uncertainties [24]

2.6 Probabilistic values and expected values

As discussed earlier in this chapter there are two types of power reliability indices: deterministic indices and probabilistic indices. Although probabilistic power reliability assessment typically produces probability distributions of predicted (simulated) reliability indices, in most instances we will choose expected values as performance indicators and use those to evaluate a design candidate. The expected value is a single performance parameter but an expected value is not a deterministic parameter. It is the long-run average of the phenomenon under study. Expectation indices provide valid power reliability indicators which reflect various factors such as system component availability

and capacity, load characteristics and uncertainty, system configurations and operational conditions [25].

However an expected value is not a probability neither [19]. Take LOLP as an example. LOLP is a projected value of how much time, in the long run, and as an average over many different realizations the load on a power system is expected to be greater than the capacity of the generating resources. The expected value is used to characterize the adequacy of generation to serve the load but this is not a true measure of the reliability of electric services. For instance, the expected value of the loss of load (LOL) may be 0.05 (percentage of time that power is not available (i.e. LOLP), computed as the mean over all realizations). Another and probably better measure of power reliability could be the probability that the LOL is greater that 0.05. Obviously the second probabilistic power reliability measure better reflects the true definition of risk in terms of design compliance which is the probability of undesired outcome (i.e. LOL > 0.05) while the expected value (LOLP) represents the average system performance (i.e. mean LOL).

Explained mathematically the expected value of a discrete random variable is the sum of the probability of each possible outcome of the experiment multiplied by the outcome value in probability theory. If x is a discrete random variable with probability mass function $p(x)$ then the expected value becomes

$$E(X) = \sum_i x_i \, p(x_i) \tag{2-5}$$

If the probability distribution of x admits a probability density function then the expected value can be calculated as

$$E(X) = \int_{-\infty}^{\infty} xf(x)dx \tag{2-6}$$

As used in the earlier section $f(x)$ denotes the probability density function of random variable x. Expected value gives a rational average expectation of future occurrence. The expected value of a certain outcome (value of a PI) is not enough to know the probability of an occurrence during which the value of this particular PI is lower than its corresponding requirement criterion. Figure 2.6 shows different system risk possibilities even if their expected values of PI are the same. $F(x)$ represents the cumulative distribution which is defined in equation 2-7. Only when the probability density function of a PI ($f(PI(\overline{X}))$) is symmetrical, as is the case in a normal distribution, one can use expected value based design criteria, as expressed in equation 2-8 for the case of 50% risk criterion. . When dealing with complicated system configurations, especially when multiple nonlinear relationships are involved (and outcomes cannot be expected to have a normal distribution), any expected value based risk analysis will show an incomplete picture.

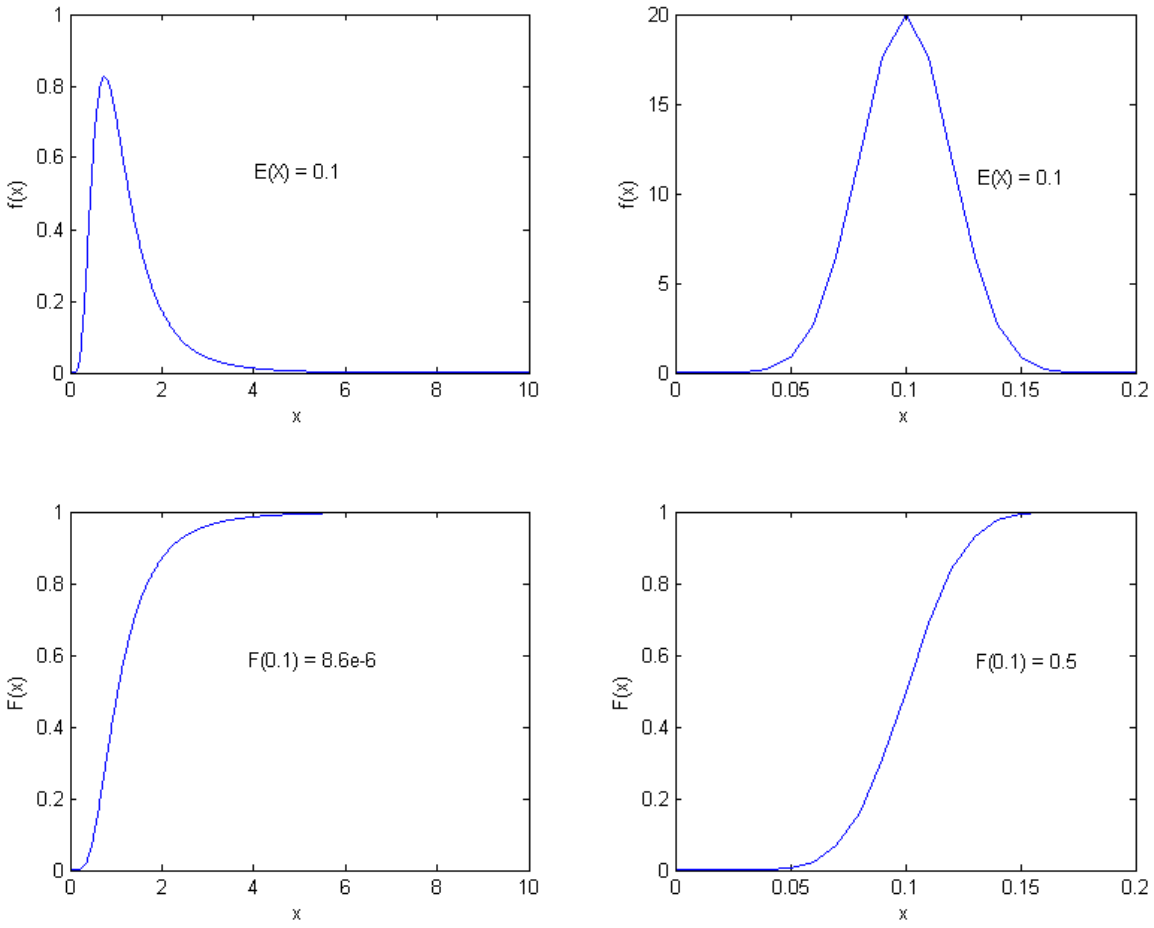

Figure 2.6 Different cumulative probabilities vs. the same expected values

$$F(x_c) = \Pr(x \le x_t) \tag{2-7}$$

$$50\% = \Pr(PI(\overline{X}) \ge E(PI(\overline{X}))) \tag{2-8}$$

Figure 2.7 illustrates the difference between making design decisions based on an expected value based criterion and a probability based criterion. Given a design performance measure PI and its corresponding probabilistic design compliance threshold a design process (as indicated in black solid line in Figure 2.7) shall end up with the design option $\overline{X}_{design}$. While using an expected value based criteria E_{req} (as indicated in the dotted line in Figure 2.7) the design option $\overline{X}''_{design}$ will be selected. The design option

$\overline{X}_{design}$ and $\overline{X}''_{design}$ may not be the same, and in many practical instances they will indeed differ. Instead of working with the probability distribution, designers tend to favor expected value based criteria. And the adjustment of the expected value criterion, is commonly realized by applying an additional "safety factor". The value of the safety factor must then be chosen such that the "real" probabilistic design compliance criterion is met if the adjusted expected value based criterion is met. But the use of the adjusted expected value based criteria in the system design often causes extra waste of resources and fails to answer the question how likely it is that a minimum required design compliance criterion is met by the proposed design. The answer may for instance reveal the necessity for the occupant of a zero energy house to include a backup system. This dissertation will follow the design process shown in the solid line black boxes in Figure 2.7. More details will be discussed in Chapter 3.

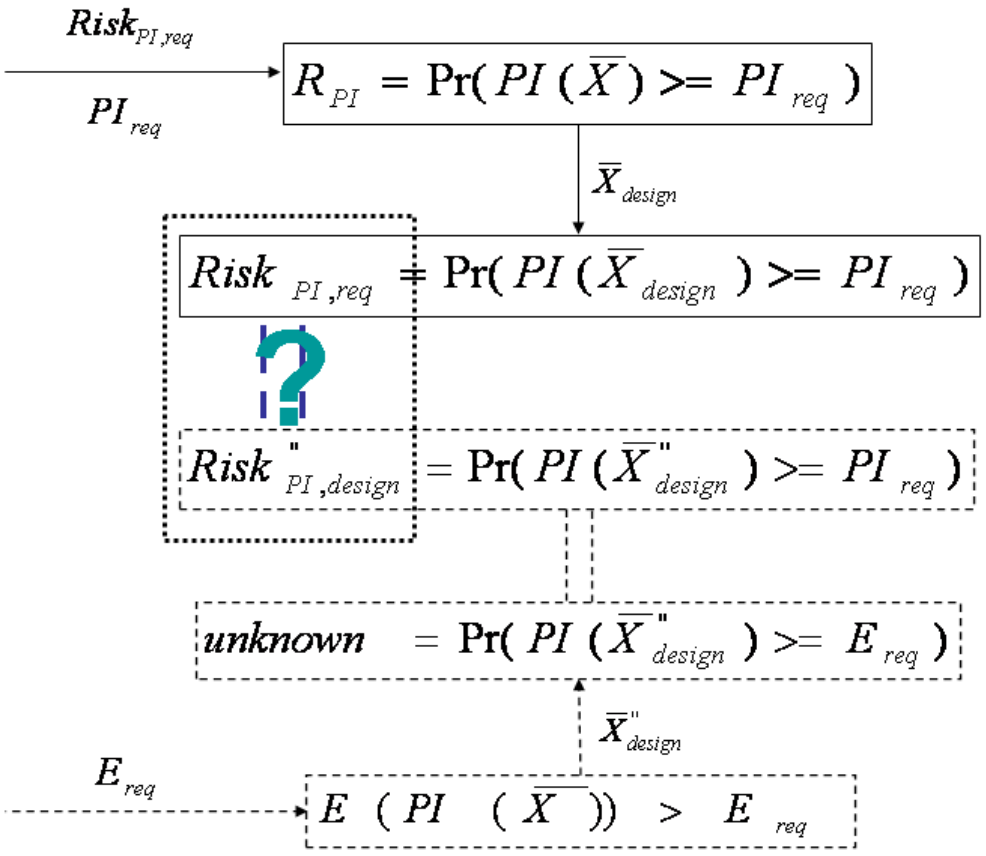

Figure 2.7 Different design results between an expected value based criterion and a probability based criterion

CHAPTER 3 OCCUPANT ORIENTED RELIABILITY ASSESSMENT

3.1 Motivations

Chapter 1 and Chapter 2 have addressed why a constant value performance criterion fails to support our design evolution toward sustainable environment: 1) it demands a full performance compliance under all circumstances which results in oversized systems, given the conventional deterministic performance simulation; 2) it does not reflect people's attitude toward undesired outcomes even if a stochastic performance evaluation is conducted, during which, an expected value of the performance indicator is used to check the compliance against the constant value design criterion. Moreover in the case that a stochastic performance evaluation is conducted the use of a constant value design criterion leads to a total neglect of the full future of possible system performance that has already been provided by simulations. Meanwhile the use of a constant value performance criterion also prevents the possibility for users to share responsibility with designers in sustainable practices as most of the experimental novel designs have difficulty to maintain system performance at a constant level. By demanding a constant performance it rules out the use of certain sustainable design features, such as natural ventilation.

In the context of off-grid solar houses occupants/owners will be particularly interested in the reliability of PV system to provide electricity in the amount they want and when they need it. They are willing accept a certain percentage of non compliance, but they will put strict limits on the risk that are willing to accept. One can expect that occupants' attitude

toward power reliability is flexible in an off-grid solar house especially when there is a trade-off with initial investments. Developers, investors, owners, occupants should all be actively involved in the reliability analysis. Each stakeholder will have different perspectives on gaining confidence in the expectations about the viability of an off-grid house by gaining a clear picture of how often, how long and why energy unavailability will happen. Moreover their consciousness of the underlying physical systems and associated risk will enhance their willingness to accept experimental features and grant experimentation with new technologies in sustainable design practices.

Another special characteristic of off-grid solar houses is that the installed PV system has to provide electricity for occupants to conduct multiple tasks, albeit with fairly flexible schedules. For instance, a household may have time to do laundry either Monday morning or Friday afternoon depending on the occupants' preference and/or private agenda. Such specific flexibility in the schedules that electricity is needed for doing the laundry can be used to increase system reliability as there will be times that laundry is shifted to the next available time. The otherwise consumed electricity can be used to meet other more critical needs and the power reliability in general is improved. This is not different from the power quality consumer contract that the power provider industry is trending towards, as mentioned in the previous chapter. Often it is hard and expensive for power utility companies to meet all power needs at the same level of reliability because that means that they have to expand the capacity of power plants accordingly. In the current market, the power industry typically uses real time rates that vary based on time of day, peak demand, duration of peak demand etc to urge customers to avoid consumption during peak period. Through the leverage of electricity price, utility

companies gain some strength in controlling the expansion of their generation capacity and power customers receive the opportunities to save utility costs by re-arranging their consumption profile accordingly. A common classification of loads and their corresponding power adequacy criteria are shown below [36, 37]:

- The critical ones; where it is acceptable that the supply system may fail to meet these loads for up to 88 hours per annum or 1% of the year;
- The non-critical ones; where it is acceptable that the supply system may fail to meet these loads for up to 438 hours per annum or 5% of the year.

The judgment on a load's criticality is based on the damage that a power interruption to the load could cause to customers. Therefore the classification of loads in terms of their criticality is subjective and may change under different contexts.

For power reliability assessment in off-grid solar houses a refined load classification needs to be established due to the very subjective response from occupants in terms of the severity of energy shortage affecting different residential functions and household necessities. A regular residential house will serve as an example. The residential living may include some (or all) of the following energy consumers: TV, computer, microwave, oven, refrigerator, freezer, air conditioner, air heater, hot water heater, phone and other device chargers. Depending on the personal attitude of the occupants their tolerance in terms of the duration of energy shortage leading to postponing certain energy functions may differ. Traditional power reliability engineers usually don't focus on one single house but look more broadly at all the houses within a certain region, which does not allow them the opportunity to apply a finer load classification system in power reliability assessment. It will be hard, if not impossible to establish a reference tolerance level that

applies to every occupant. Therefore power reliability engineers tend to over-ensure the reliability of a system by raising the evaluation criteria so that the majority of the customers will be satisfied with the power service they receive from their utility company. In cases of reliability assessment of an off-grid house, a unique reliability evaluation criterion could be tailored for every particular occupant (or developer) to meet his or her minimal reliability tolerance level which will help stop design from being over-ensured and meanwhile will help improve designs approaching the best utility for all stakeholders.

Adopting the concept of reliability and considering an off-grid house as one single system we can now identify the main aspects of a design analysis related to power adequacy of an off-grid house design as below:

- Its required function: to provide a comfortable and healthy environment for occupants. A full blown quantitative measure of the performance of the living environment will be too complicated as it includes many sub-aspects such as lighting, acoustic, thermal comfort, power service, water service and etc.
- The environmental conditions: the system operates in unknown weather conditions, provided by mother nature. The best guess is to use known weather data in the same location to generate a statistically representative time series that substitutes for the unknown weather conditions. This is very customary in the field of building simulation, where it is customary to work with a full year of hourly data. The 365x24 data points for temperature, humidity, solar irradiation and wind conditions have been carefully constructed from known weather data. One of the commonly used yearly weather data sets is TMY weather data set [38,

39]. There is proof that this time series performs well for the customary analysis of building performance, e.g. used for energy performance, system sizing, control design etc. [40]. Recent research has embedded the potential affects of global warming, especially relevant in longer term predictions [41]. However, for reliability analysis there is a lack of research to determine the adequate construction method and length of time series. As this important topic is not in the scope of this thesis, we will use the time series that is currently used in regular building performance analysis. Meanwhile experiments will be conducted to test whether the used weather data introduces a bias in the results for the considered case.

- Daily operation schedule: its daily operation is highly unpredictable as household composition, user behavior etc may be highly personal and unpredictable.
- Service life time: the expected period of service depends on the type of stakeholders. For an owner it could be the period of time during his/her ownership and for an occupant it could be during his/her expectation of occupying the home. For the type of risk assessment in the scope of this study we will take system's service life time as the period of study.

3.2 Definitions

As indicated by its name an occupant oriented reliability assessment grants occupants authority to define their own acceptable levels of power reliability for both performance requirements PI_{req} and the corresponding risk based compliance criteria $\varepsilon_{PI,req}$, as expressed in Equation 3-1 and 3-2. Meanwhile because of multiple simultaneous tasks

occupants shall also indicate the task sequence or prioritization of distributing electricity when the available electricity is not sufficient for all the tasks.

$$Risk(PI) = \Pr(PI > PI_{req}) \text{ if } PI_{req} \text{ represents the minimum requirement} \quad (3\text{-}1)$$

$$Risk(PI) = \Pr(PI < PI_{req}) \text{ if } PI_{req} \text{ represents the maximum allowance} \quad (3\text{-}2)$$

Therefore two sets of inputs will be required/collected from potential occupants before an occupied oriented reliability assessment is conducted:

- The task priority sequence in which electricity is distributed when electricity is not sufficient to meet all the needs;
- The performance requirements PI_{req} and the corresponding reliability criteria $\varepsilon_{PI,req}$.

3.3 Basic assumptions

There are two basic assumptions made in this research:

- Although the term "power reliability" is adopted in this thesis, the causes of reliability investigated are different from those currently assessed by the power industry. The industrial power reliability engineers are primarily concerned with the effects from equipment failures. In the scope of this thesis, the focus is on uncertainties in predicted system behavior, such as resulting from the lack of perfect knowledge of physical properties, component parameter uncertainties, deterioration effects etc. System unreliability due to equipment failures is considered to be less influential compared to these sources of uncertainty and underperformance of the systems and is therefore ignored. The other main difference is that system failure is a temporary

nuisance, whereas our focus is on the prediction of reliability of the system if all systems work as designed and specified, but are affected by sources of uncertainties that cannot be controlled. The main sources and causes of uncertainty are reviewed later in this chapter.

- Occupants' opinions are used in this research in two ways: 1) to determine design criteria for power reliability and its compliance level; and 2) to determine the sequence of energy delivery among domestic appliances. Both settings may vary if residents change. This research assumes that change of residents will not influence the total energy demand significantly and the off-grid design can be re-adjusted for new residents by 1) to re-adjust the solar power generation system; and 2) to reprogram the sequence of energy delivery.

3.4 The methodology

3.4.1 Evaluation flowchart

After adopting a set of evaluation criteria and setting the priority sequence of electricity distribution, a traditional reliability analysis in terms of energy sufficiency can be performed. Figure 3.1 shows the flowchart of an occupant oriented reliability evaluation process.

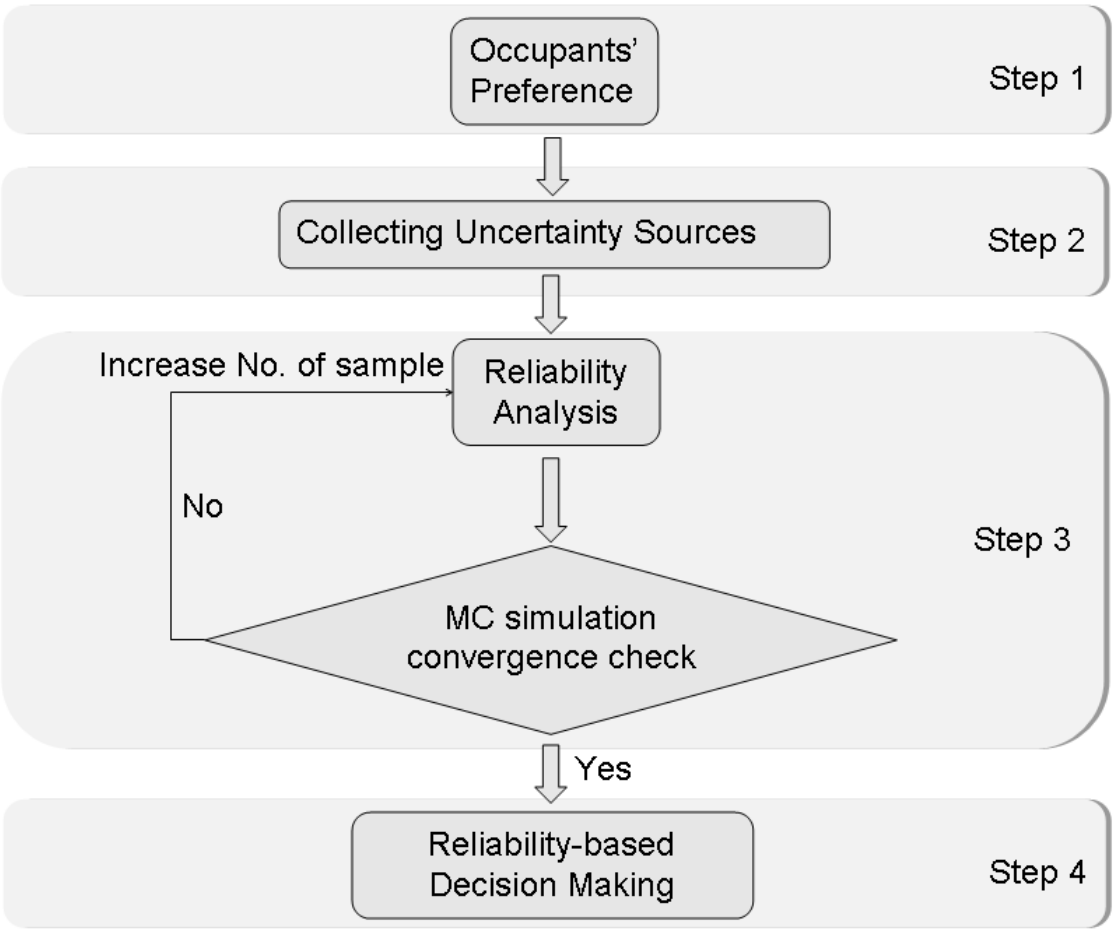

Figure 3.1 The evaluation flowchart of an occupant oriented reliability analysis

Step 1: Collect inputs from occupants, including their priority settings for the sequence of electricity distribution, their performance requirements, and their reliability criteria;

Step 2: Collect and analyze uncertainties with respect to the system performance;

Step 3: Start reliability analysis with a pre-set number of samples and increase the sampling number if the accuracy level of the MC simulations is not met. If multiple PIs are involved the accuracy level of MC simulations for every single PI has to be met before the evaluation is considered to converge;

Step 4: Perform necessary post analyses to help solve reliability-based decision making problems. In this stage the power reliability will be considered as an important performance aspect in off-grid solar house design and involved in design optimization. Different reliability centered design optimization approaches will be introduced and demonstrated later in this research.

3.4.2 Reliability performance indices

Regardless of the different causes of system failure investigated between general power reliability engineering and this thesis, the main performance aspect of reliability analysis remains the same: energy deficit. Thus basic reliability indices of general power reliability assessment at hierarchy level HL3 can be adopted into this research. There are three basic load-point adequacy indices: load-point failure rate λ (failures/yr), load-point outage duration r (hr/failure), and the load-point annual unavailability U (hr/yr). The overall system performance indices can be calculated from these three basic indices. A more complete list of overall system reliability indices can be found [25]. In addition to three basic reliability indices there will two energy based indices used in this study. They are energy needed (EN) and energy wasted (EW). The detailed definitions of both energy related reliability indices are shown below.

- EN: energy needed (kWh/yr)

$$EN = \sum P_{a,i} r_i \tag{3-3}$$

Where P_a is the power shortage (in kW) during a power interruption and r_i is the elapsed time (in hr) that a power outage lasts.

- EW: energy wasted (kWh/yr)

$$EW = \sum P_w D_w \tag{3-4}$$

Where P_w is the wasted power (in kW) due to storage limitation and D_w is the elapsed time (in hr) that a power waste lasts.

Table 3.1 lists the main reliability performance indicators to be used in this research. Occupants provide input for both performance requirements and reliability criteria for all three basic adequacy indices per their desires, for each house electricity consumer (or each occupant selected house electricity consumer).

Table 3.1 A list of commonly used adequacy indices in HL3

Adequacy indices	Descriptions	Units
λ	Load-point failure rate	failures/yr
r	Load-point outage duration	hr/failure
U	load-point annual unavailability	hr/yr
EN	energy needed	kWh/yr
EW	energy wasted	kWh/yr

3.4.3 The Monte Carlo simulation

The Monte Carlo (MC) simulation is a method to analyze uncertainty propagation, where the goal is to find how random variation and lack of knowledge affect the system performance. The MC simulation uses random number generators to model stochastic event occurrences. Thus the MC simulation is generally categorized as a sampling method. In order to well represent the stochastic event occurrences the number of the MC simulation samples has to be large enough, which leads to intensive computation. One

way to solve the computation intensity problem is to replace the crude MC sampling with a stratified sampling technique – Latin Hypercube Sampling (LHS).

Assume that a sample size *nsample* is needed for a k-dimensional uncertain variable X. The LHS selects *nsample* different values from each of k variables in the following manner. The uncertainty range of each variable is divided into *nsample* equally probable intervals. One value from each interval is selected randomly with respect to the probability density in the interval. The *nsample* values obtained for X_1 are paired in a random manner with the *nsample* values of X_2. These *nsample* pairs are combined in a random manner with the *nsample* values of X_3 to form *nsample* triplets, and so on, until *nsample* k-dimensional vectors are formed. The *nsample* k-dimensional vectors are the LHS sample. Detailed LHS sample procedure can be found in [42].

Then the system is simulated repeatedly using the LHS sample as inputs and *nsample* system outcomes are calculated. The distribution of system outcomes can be further analyzed for risk indices estimate.

3.4.4 Stop criteria for Monte Carlo simulations

The MC approach can only represent the random nature of an event when the sampling number is big enough. In general the larger the sampling number is the more complete the random nature of the output will be described. A classic way to evaluate the accuracy level of MC simulations in power reliability assessment was proposed by Billiton [25], as shown in equation 3-5.

$$\alpha = \frac{\sigma}{E(PI)} \tag{3-5}$$

Where,

α the accuracy level of a MC simulation expressed by the coefficient of variation (CoV);

$E(PI)$ the estimated expectation of the index;

σ the standard deviation of the estimated expectation $E(PI)$.

Equation 3-5 indicates that two measures can be utilized to reduce variation in a MC simulation: increasing the number of samples and decreasing the sample variance. Variance reduction techniques can be used to improve the effectiveness of MC simulation, such as using strategic sampling techniques. However the variance cannot be reduced to be zero and therefore it is always necessary to utilize a reasonable and sufficiently large number of samples.

When multiple indices are involved a sensitivity study shall be conducted to determine which index converges the slowest and then the CoV of the slowest converged index will be compared against the convergence criterion to determine if the MC simulation should stop. A CoV tolerance of 0.05 is usually used in power reliability assessments [25].

3.4.5 Role of uncertainties

Reliability is an indicator of how well a device or a system will perform its intended function in the light of all the existing uncertainties. As discussed in Chapter 2 the quality of a reliability assessment is partially determined by how well the associated uncertainties can be quantified and represented in models. In this study five different categories of uncertainties will be distinguished:

- Uncertainty in renewable power system component properties

A renewable power system includes a variety of components: energy generating devices, battery bank, inverters, and other system components. Their properties have been rated

by the manufacturers in standard set-ups. As the actual operation conditions are not the same as in the test set-ups, deviations will occur. Take the efficiency of PV modules as the example. The rated efficiency (i.e. nameplate efficiency ratings) is estimated through lab experiments under controlled ambient environments. The test conditions established by the Photovoltaics for Utility Systems Applications (PVUSA) are 1000 W/m^2 of array irradiance, 20°C ambient temperature, and 1 m/s wind speed [43]. Module efficiency varies when ambient conditions change. Meanwhile wiring, accidental mismatch between real power loads and invert power outputs, transformers, cabling, and occasional shading from surrounding objects all impact the power system's efficiency. A few studies have been conducted to quantify power losses caused by variations in the properties of different system components and the effect on resulting efficiency loss [44-46]. The maximum overall efficiency loss could be up to 25%.

- Uncertainty in building component properties and installed system properties

All equipments and building components have standard material properties in manufacturer's information that are "idealized" or standardized. Their onsite values are not guaranteed because of different operation environments and construction and installation circumstances, including the effects of bad or inconsistent workmanship. Recent uncertainty studies have shown the great importance of involving uncertainties in performance evaluation of building designs and especially when innovative technologies get involved. De Wit and Augenbroe [47] presented an approach to uncertainty analysis of thermal comfort performance with emphasis on quantifying modeling uncertainties. Their research showed that quantitative uncertainty assessment is essential in a design decision analysis.

- Uncertainties in dynamic weather

The actual available solar radiation at specific site principally determines the electricity production from a PV power system. Meanwhile dynamic weather also influences the electricity consumption needed by space heating and cooling. Therefore a deep investigation of weather dynamics is obviously crucial in the reliability assessment of a renewable power system. Current stand-alone PV power system design methods incorporate the characteristics of local weather patterns [48-50]. Kaplanis [37] has investigated the effects of statistical fluctuations of solar radiation on PV system sizing and proposed an approach which could lead to a considerable reduction in the estimated PV peak power as well as the capacity of the battery bank for a stand-alone PV system. Labed and Lorenzo [51] conducted another in-depth research to analyze the impact of solar radiation variability and data discrepancies from different existing weather information resources on the PV system design. Because of the natural variability of solar radiation two different radiation information resources could show discrepancies of up to 15%. They concluded that solar radiation data would contribute a significant uncertainty in PV system sizing due to three main reasons: the selection of a particular solar radiation data source, selection of any hypothetical load profile, and the random character of local solar radiation.

- Uncertainties caused by degradation

Most system degrades gradually during its lifetime, affecting material properties and system efficiencies. Adelstein and Sekulic [52] studied the performance and reliability of a 1 kW PV roofing system which was monitored for 6 years. They found out that the degradation rate of their amorphous silicon PV system was 0.985% per year in direct

current (DC) and 1.09% per year in alternating current (AC). King et al. [53] summarized that the commercial amorphous silicon PV modules initially, during the first 6 months, showed rapid degradation in terms of power and reached a "stabilized" level of about 20% below the initial (1st day) power after 1 year. Similar degradation related efficiency losses can be also observed in house equipments such as heat pumps, boilers and etc.

- Modeling uncertainties

Besides all the uncertainties in physical parameters that will be considered in the reliability studies there are uncertainties associated with the system model selection and modeling assumptions themselves. There are always several methods to model a specific component and every model has its own inherent limitations. Certain assumptions have to be made to build a reasonable computer model for a specific component to reflect its intended function under given operating conditions. Past research suggests that one proper way to study this is to introduce a surrogate parameter representing the model uncertainty and make a reasonable guess of its magnitude but this method usually leads to an iterative uncertainty refinement process if this surrogate parameter is shown to be one of the dominant parameters [54, 55]. Modeling uncertainty will not be considered in the uncertainty analysis separately in this study. It will be combined with uncertainty in model parameters when a specific model is chosen.

- Uncertainties in occupant behaviors

In addition there is another uncertainty, related to the usage scenario and occupant behavior in simulations. Occupant behavior is usually represented by occupancy schedules and is then linked with other associated control state variables such as temperature setpoints. Previous research has demonstrated that an in-depth modeling of

occupant behavior is necessary for simulations when occupant-based phenomena are involved, such as cases associated to lighting behavioral patterns and personal control of operable windows in natural ventilation scenarios [18]. However this research will adopt the classic approach and take the view that this should not be considered as an "uncertainty" but as a "usage scenario". The common usage scenarios will be chosen and fed into reliability simulation as fixed scenarios of use. Figure 3.2 shows the separate treatments of the uncertainties in the off-grid solar house model (including models of solar power system) and the usage scenarios. This separation simplifies the uncertainty analysis raised by usage scenarios but meanwhile accounts for effects that different usage scenarios may have on the power supply risks of a solar house design.

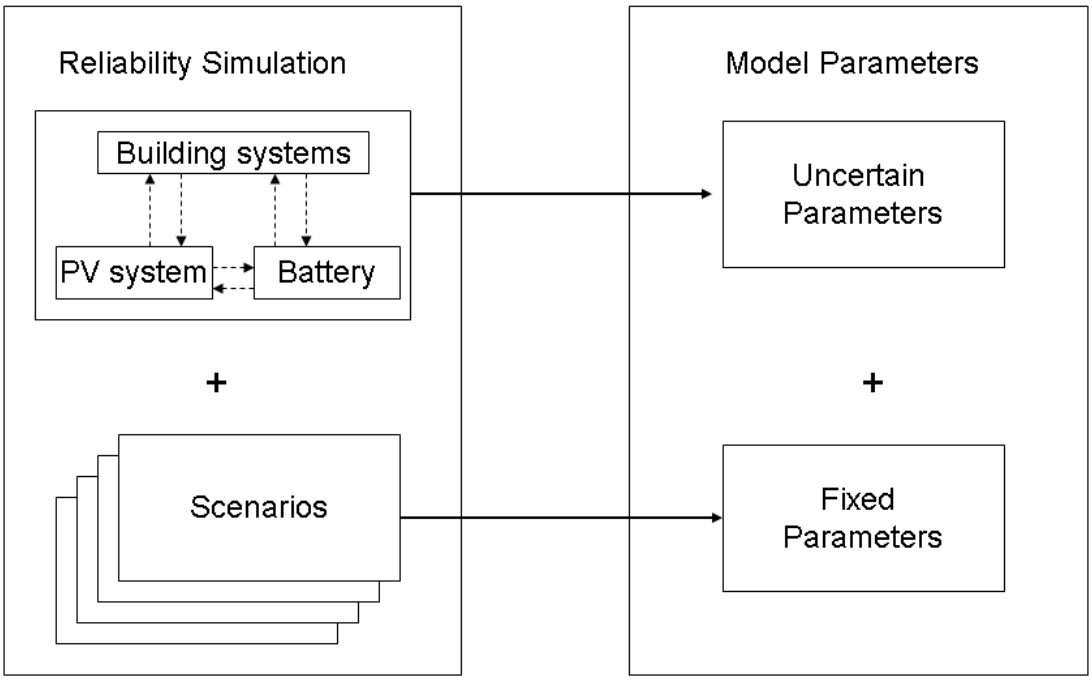

Figure 3.2. Off-grid solar house model and scenarios in reliability simulation

However, as a summary, regardless of all the inspections of associated uncertainties we should be aware that any future performance prediction is based on past observations of

variable phenomena (solar radiation, wind speed, ambient temperature, etc.) and observed statistical spreads in system and component property values. This intrinsic limitation in quantifying uncertainties is unavoidable [56].

3.5 Conclusions

An occupant oriented reliability assessment takes account of and responds to people's attitude towards energy inadequacy. It adopts customers' opinions as design criteria and literally tailors a design for its very specific owners. Meanwhile it should link reliability PIs with initial costs or operating costs or even both for every off-grid house design and create a design opportunity that could possibly benefit everyone:

- It ensures that the value of an off grid design can be predicted with greater confidence from the perspective of each stakeholder. In particular it will become apparent which sources of uncertainty have a detrimental effect on resulting performance and reliability.
- It will make the effect of different system types and components on reliability explicit, thus paving the way for performance contracting, shifting part of the responsibility for underperformance from designers to subcontractors and manufacturers.
- It puts the responsibility of ensuring reliability squarely in the hands of the designers but offers them a richer set of tools to match stakeholders' requirements by showing the potential trade-offs between lower levels of reliability and cost savings.
- It provides developers and owners with a new perspective on cost savings. Over-sizing systems to ensure default reliability criteria can be avoided if indeed they

are not deemed critical for the value perception of the system and can be relaxed. Thus the initial cost that otherwise will be spent to enlarge system capacity can be saved.

- It helps shape the next generation of off-grid house designs into a more right-sized compact system design. As a consequence it will reduce raw material consumption and operating energy consumption which results in less environmental impacts and less energy waste.

CHAPTER 4 UNCERTAINTY IN POWER RELIABILITY ANALYSES OF AN OFF-GRID SOLAR HOUSE

4.1 Introduction

As discussed in Chapter 2 there are three possible reasons that may cause the failure of a system/component: 1) certain parts of the system/component may not perform as designed; 2) the operating condition might not be the same as the design conditions; 3) the intended function requirement might not be the same as what the system/component is designed for in the first place (functional mismatch). Reliability analysis is indeed about the estimate of how often the above three circumstances happen and how significant the damage could be if any of the three circumstances takes place. A quantitative goal, in modelling and simulation studies, becomes feasible only in those situations where deep knowledge is available [57]. In other words the available knowledge of the system and its future operating environment determines the quality of a quantitative reliability assessment. This chapter will investigate the following questions:

- What are the possible reasons that may cause occupant inconveniences in an off-grid solar house due to energy shortage;
- What are the factors that have a greater chance to cause occupant inconveniences;
- What is the best estimate of the probability of those factors causing possible failure taking into account of our current (lack of) knowledge.

The three questions are the necessary pillars for a risk analysis: (1) understanding the damages caused by less than optimal behaviour of the system, (2) identifying and quantifying the risk factors, (3) quantifying the (predicted) risk in the outcomes of the

system. It is important to note that in all stages of the analysis, the focus of this thesis is on the risk stemming from incomplete knowledge of the system behaviour, and hence our inability to predict exactly how the system will perform in reality. A remedy for this lack of knowledge is to make it explicit, i.e. estimate our lack of knowledge and predict system behaviour showing the explicit dependency on this lack of knowledge. This is in the realm of classical uncertainty analysis, which indeed will form the backbone of the risk assessment. As stipulated before, this choice of risk factors limits the assessment to deal only with our incomplete knowledge of the physical behaviour of the system and its occupants under normal operating conditions. There are many other risk factors that will not be considered in this thesis, such as failure rates of imperfect system components, malfunctions caused by bad workmanship, catastrophic occurrences, such as flooding, and hurricanes. The risk associated with long term climate change is also not considered, although this will be touched upon in the discussion of the role that the choice of weather time series plays in the reliability and risk assessment.

4.2 Sources of uncertainty in power reliability analysis of off-grid solar houses

Uncertainty analysis has recently moved to the centre of attention in building simulation. This has happened for two reasons: 1) the advancement in building simulation software and increased computation power enables building analysts to provide more detailed performance evaluations, including reliability analysis; 2) our increased level of knowledge about buildings and building systems indicates that traditional deterministic building simulation does not capture building performance as it represents only one possible experiment out of many, due to the incompleteness of data at different design

stages as well as the discrepancy between system design condition and real operating condition [55].

Considering the possible causes of a system/component failure (under the limitations stated above) one can classify the sources of uncertainty in a power reliability analysis of an off-grid solar house into four categories, as shown in Figure 4.1.

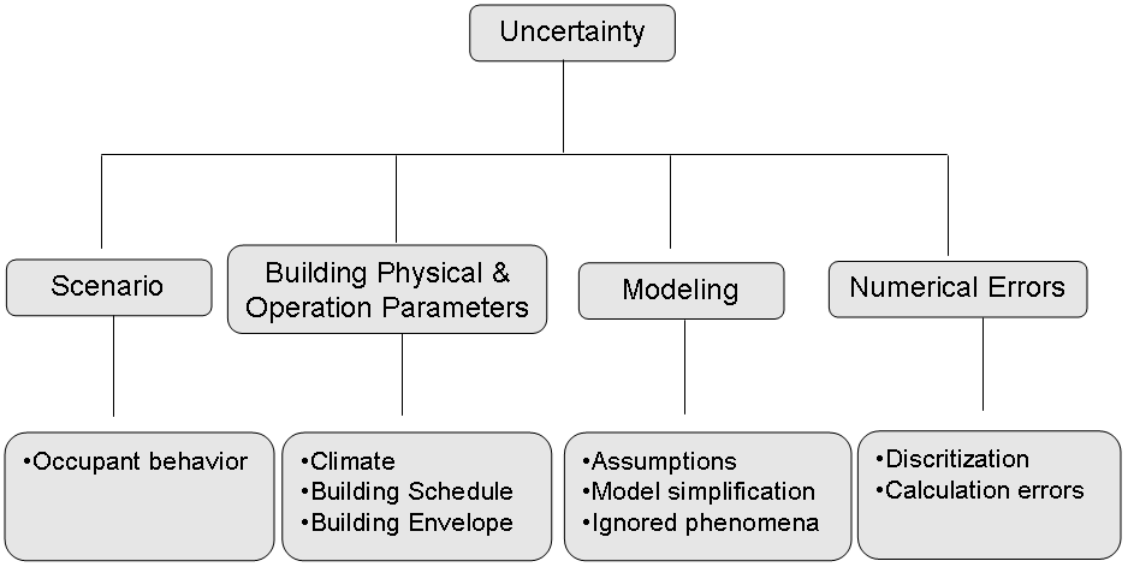

Figure 4.1 Sources of uncertainty in a power reliability analysis for off-grid solar houses

The main source of uncertainty arises from the discrepancy between design idealization (based on the design specification) and reality, especially the difference between design conditions and real building operating conditions. This research refers to this type of uncertainty as uncertainty in "building physical and operation parameters". A typical example of this type of uncertainty is the variation of material properties. Building materials come with specification sheets which list their physical properties tested under standard conditions, but they often behave differently in reality due to the discrepancy between testing conditions and real operating condition. Second order effects are usually not considered or not measured. A typical example is the dependency of the heat

conductivity of a material as a function of temperature. Meanwhile, all the materials degrade over time domain which means that their physical properties change within the service life horizon. The following section of this chapter will focus on quantification of uncertainty in this category.

In addition to the uncertainty in building physical and operation parameters there are also modeling related uncertainties which have been briefly touched in Chapter 2. Assumptions are made during the translation of physical phenomena to computational models that are used as an idealization of reality in a simulation environment. This simplification is necessary to make it feasible for us to study real problems using computational models but meanwhile it creates a discrepancy between the real phenomena and their presentation in computational models. Modeling simplification often takes place in two typical forms: 1) to replace the existing complicated phenomena by relatively simple empirical models; 2) to ignore the related secondary phenomena as they are deemed less relevant in the study of the major system behavioral issue. Either way of modeling simplifications will cause a certain level of compromise in modeling accuracy. Generally the quality control regarding modeling simplification is up to building modelers. In other words, the modeler's experience and expertise plays a major role in determining the uncertainties introduced in the modeling uncertainty category. This study will generally assume that the classical building simulation models are built at such an accuracy level that the effect of modeling uncertainties for the purpose of this thesis can be ignored. This does not hold true for the modeling of specific components such as PV panels, or batteries. In such cases the model uncertainty will be typically captured in an uncertainty range of model parameters, which thus harbor the dual effect

from incomplete knowledge of physics as well as the approximate models with which we describe the physical behavior. Examples of this will be encountered in the next section.

There is another type of uncertainty which is also unavoidable in building performance analysis. It is the uncertainty caused by numerical approximation methods employed in the computational simulations. The leading building simulation tools in the market have been verified against certain criteria (such as BESTEST [58]), to assure the accurateness of the embedded numerical algorithm. This study will therefore not consider uncertainties raised by numerical errors.

The fourth category of uncertainty is referred as uncertainty in "scenarios" in this study. The uncertainty in the scenario category is mainly related to user behavior in relation to building operation. Typical examples include window operation and thermostat settings. In residential buildings natural ventilation is a promising and attractive approach for passive cooling, especially in a location with mild weather. However whether residents will operate windows "as designed" and how often they will, is difficult or almost impossible to predict and introduce in the simulation. Depending on user responsiveness and attitude, it can be expected that an occupant may operate the windows in a regime that results in the efficiency somewhere between zero and maximum efficiency. As there is no way of knowing and also no data available to estimate user responses, the approach is taken to assume different types of occupant behavior, each type representing a certain scenario. This study will consider the "ideal" operation case as one scenario and the "worst" operation case as the other "scenario". Results from both scenarios together are expected to give us sufficient insights about what happens in reality when an occupant will operate the house somewhere in between these two extremes.

The thermostat set point is another typical uncertainty source in the scenario category. Lowering thermostats is suggested broadly these days as an option for occupants to reduce their utility bills (Figure 4.2) [59]. However it is hard to model this effect due to the subjectivity of occupants' attitude in terms of setting a higher cooling temperature or a lower heating temperature. This study will consider thermostat setting as an integer variable. Building performance will be predicted at selected thermostat settings with the intents of providing insights in building performance at any thermostat setting. In a later chapter variable thermostat settings will be investigated as part of the interventions of an intelligent controller. To summarize, this study investigates building performance in unknowable usage scenarios by conducting performance evaluations at a series of predefined usage scenarios. Figure 4.3 shows the separate treatments of the uncertainties in the off-grid solar house model and uncertainties in the category of scenarios. This separation simplifies the uncertainty analysis raised by unpredictable user behaviour but meanwhile accounts for effects that different user intervention (in response to house operations) may have on the power reliability of an off-grid solar house design.

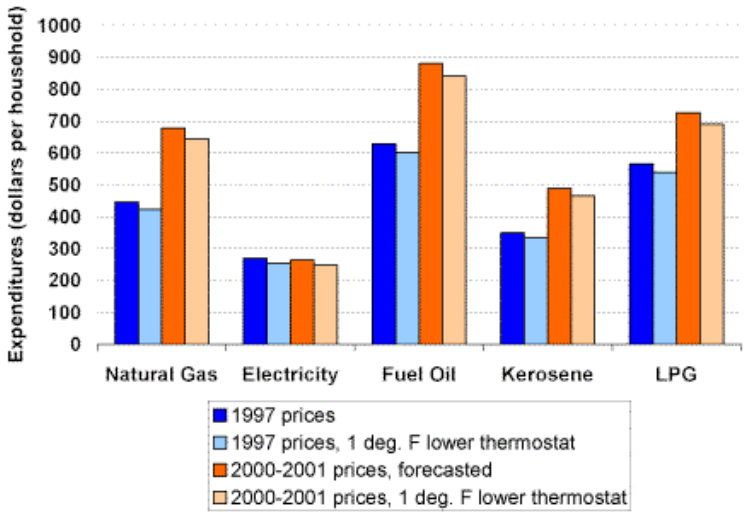

Figure 4.2 Annual Heating Energy Expenditures per Household in 1997, Based on Actual and 1° F Lower Thermostat Settings, and 1997 and Projected 2000-2001 Fuel Prices [59]

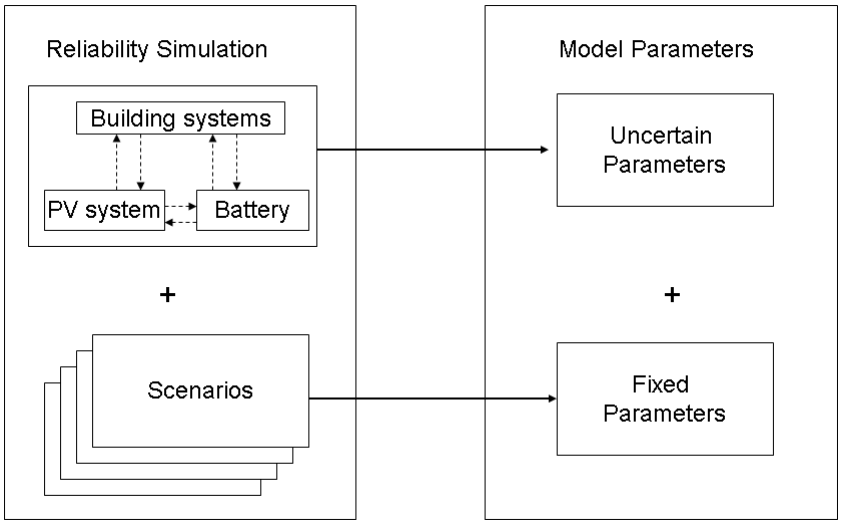

Figure 4.3 Off-grid solar house models and scenarios in reliability simulation

4.3 Uncertainty parameters in life-time reliability analysis

Uncertainty in a reliability assessment is captured in the probability distributions of model parameters. The distributions express the deviations between "as-designed" values and actual "in-use" values [55] as well as the likelihood of their occurrence. Simulations

propagate the uncertainties in model inputs through the simulations and turn them into probabilities of observed outcomes or simply, distributions of performance indicators of interest. Figure 4.4 shows the process of uncertainty propagation in a simulation.

The first step of an uncertainty analysis is to identify and quantify uncertain parameters in the concerned model. Recall the definition of reliability in Chapter 2: a power reliability analysis is all about finding out the instant relationship between load and supply. Therefore this study will classify uncertainty sources into two subgroups: uncertainties affecting power loads and uncertainties affecting power supplies. The classification will help advance the identification of uncertainty parameters in a systematic way, especially in the category of "building physical and operational parameters". Figure 4.5 shows the framework of identifying uncertain parameters by exploring uncertain sources through a strategic classification of all associated system components.

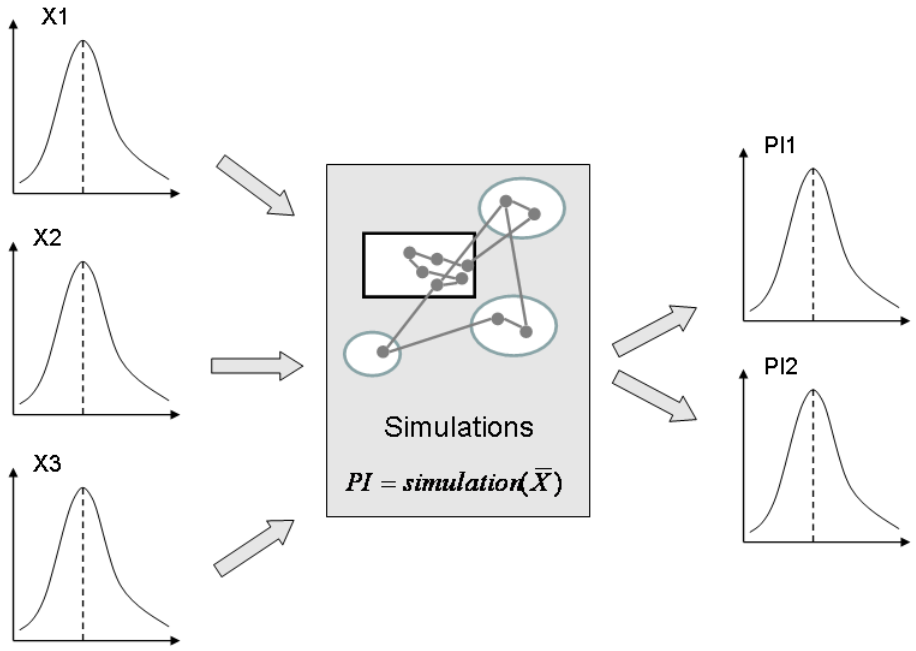

Figure 4.4 Propagations of uncertainties in a simulation

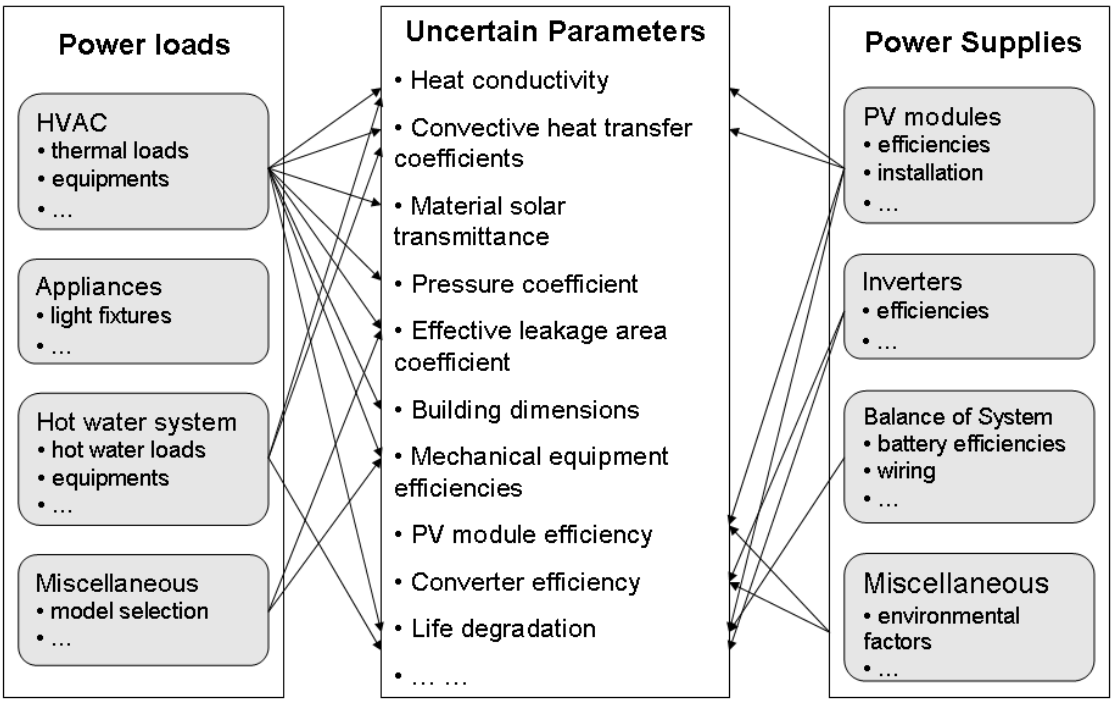

Figure 4.5 Identification of uncertain sources by exploring both load and supply sides

4.4 Quantification of uncertainty

Each estimate of energy consumption/production in a subsystem/system component may require introduction of uncertainty in one or several physical parameters. Which parameter shall be considered depends on the specific physical properties we are modelling and the specific modelling technique we choose. For instance the electricity production by a PV module is strongly linked to PV efficiency. There are two main factors contributing to the range of PV module efficiency: the PV module cell temperature and the environmental factor (wiring quality, environmental shading, and module cleanliness). The PV cell temperatures can be estimated using two methods. The first method is to model PV cells and their surrounding thermal environments using the first law of thermodynamics. Figure 4.6 shows the mechanism of heat transfer in a PV module. In this approach the main uncertainty will reside in the convective heat transfer

coefficient and material properties of the PV cell material. The second method is to model the PV cell temperatures using empirical models established by other researchers through experiments. Skoplaki and Palyvos [60] have reviewed current empirical models for PV cell temperature estimates, including both implicit methods and explicit methods. Depending on which one of the nearly 30 models a modeller chooses, different uncertain parameters must be chosen accordingly to represent the uncertainty in the prediction model. In doing so it must be ascertained that the chosen parameters can bridge the gap between the experimental condition and the operating condition.

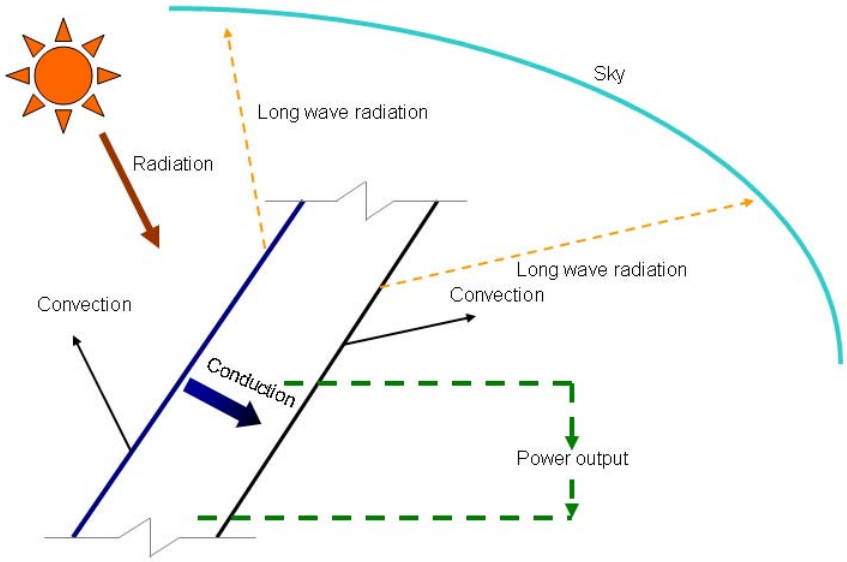

Figure 4.6 A schematic of the heat transfer mechanism of a PV module

Each energy production/consumption of a system component will have uncertainty contributed from all four source categories: uncertainty from physical properties, modeling uncertainty, uncertainty linked to varying users' behavior (called scenario uncertainty in this study), and numerical uncertainty (not considered in this study). However despite the fact that multiple uncertainty sources exist it is difficult and in most cases unnecessary to quantify the uncertainty arising from each uncertainty source

separately when modeling a system/component. This study will rely on the building modeler's expertise to select the appropriate component models based on the available information about building design. The uncertainty in the component behavior will be the result of uncertainties that arise both from the lack of knowledge about the physical properties as well as lack of knowledge about the accuracy of the component model. Rather than quantifying each uncertainty separately, an overall uncertainty range is attached to specific parameters that reflect the combination of contributions from all the sources. There is no established methodology to do this; available monitoring data, heuristics and literature search are used to make the best possible guess at the model structure and quantification of the parameter ranges.

Quantitatively each uncertainty will be represented using a reference value and a probability density function (PDF). The reference value represents the value that building modelers will typically use in a deterministic simulation. The PDF of an uncertain parameter represents the variance of the uncertain parameter in the simulation. The following section will discuss some major uncertain parameters and their ranges of values taken in general building thermal simulations based on literature review. Certain uncertainty ranges of parameters might be refined when dealing with a specific building case, as will be illustrated in the case study presented in the next chapter.

4.4.1 Material properties

Material property parameters, such as density, conductivity, thermal capacity, and etc., are important in describing the physical characteristics of each building element. Material properties inputs can be looked up in product specifications. However there is an unavoidable discrepancy between material testing conditions and operating conditions.

This part of uncertainty is often documented in product specifications as confidence limits provided by manufacturers. The normal distribution function is one of the most commonly used probability density distribution functions to represent uncertainty associated with material properties according to the central limit theory in probability and statistics [61]. Macdonald has quantified uncertainties for three major material properties according to the material type [62]. Table 4.1 shows the uncertainties of impermeable materials. A list of uncertainty ranges for specific building construction materials can be found in the document appendices. Table 4.2 shows the uncertainties related with surface properties of unpainted materials.

Table 4.1 Uncertainty quantification for impermeable materials [62]

Material property	Uncertainty
Conductivity	5%
Density	1%
Specific heat	12.25%

Table 4.2 Uncertainty in surface properties of unpainted materials [62]

	Absorptivity	Std dev	Emissivity	Std dev
Metals polished	0.32	0.07	0.05	0.01
Metals	0.56	0.12	0.24	0.06
Brick (light)	0.49	0.04	0.90	0.02
Brick (dark)	0.76	0.04	0.90	0.02
Stone (natural)	0.63	0.10	0.91	0.02
Plaster	0.40	0.03	0.90	0.02
Concrete	0.68	0.04	0.90	0.02

4.4.2 Convective heat transfer coefficients

Convection is one of three heat transfer processes (conduction, convection, and radiation) in buildings. The convective heat transmission primarily takes place at the boundaries between spaces and solid enclosures. There are two types of convection: natural convection and forced convection. There has been a large number of research projects aiming at estimating convective heat transfer coefficient since 1930's. Some disparity among them exists due to the complexity in the nature of the phenomenon. A review by Beausoleil-Morrison reveals that estimate of building energy demands can be strongly influenced by the choice of convective heat transfer modeling algorithms and a difference of 20~40% in energy demand prediction caused by the choice of different models has been observed by some researchers [63].

In building interior spaces heat convection between interior surfaces and indoor air is dominated by natural convection due to the low air flow rate along interior surfaces mandated by thermal comfort requirements. Therefore the range for internal convective heat transfer is relatively narrow. De Wit summaries that the internal convective heat transfer coefficient ranges from 1.57 W/m^2-K and 3.21 W/m^2-K when temperature difference between interior surface and indoor air equals to 2°C [54]. Awbi's chamber test shows that the internal convective heat transfer coefficient for floors varies the most as a function of temperature difference between surface temperature and air temperature [64]. Figure 4.7 shows the measured internal convective heat transfer coefficients for different chamber surfaces at different surface-air temperature difference according to his research.

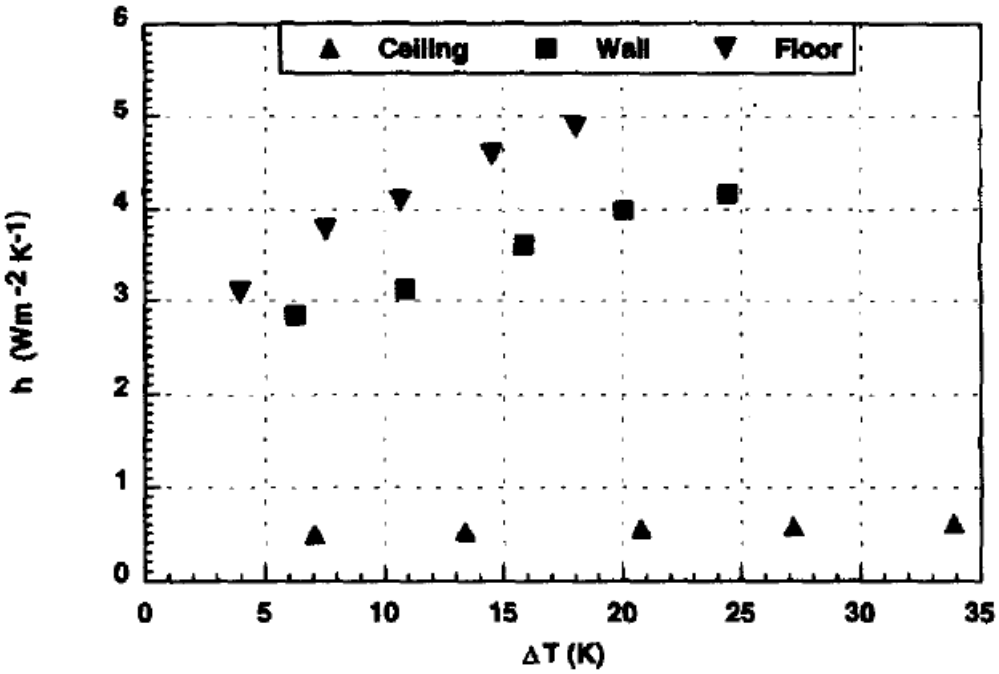

Figure 4.7 Measured convective heat transfer coefficients for chamber surfaces [64]

Unlike the interior convective heat transfer the external convective heat transfer is mostly dominated by forced convection caused by wind. The external convective heat transfer coefficient varies more rapidly depending on the wind condition, surface roughness, and etc. De Wit summarizes the uncertain range of the external convective heat transfer coefficient to be between 9 W/m^2-K and 27 W/m^2-K when wind flows parallel to the surface at a speed of 2 m/s [54]. Modeling the external convective heat transfer coefficient has been a research topic since 1920's. But there is still no satisfying method available. Below are two models of external convective heat transfer coefficient adopted by EnergyPlus [65], one of the leading energy simulation tools in the U.S. and one linear model summarized based on an extensive literature review.

- MoWiTT model

The MoWiTT model is developed by Yazdanian and Klems based on measurements taken at the Mobile Window Thermal Test facility [66]. Therefore the model only applies to very smooth vertical surfaces, like window glass in low-rise buildings. Equation 4-1 shows the mathematic formula of the MoWiTT model.

$$h_c = \sqrt{h_n^{\,2} + h_f^{\,2}} \tag{4-1}$$

$$h_f = aV_f^b \tag{4-2}$$

$$h_n = C_t(\Delta T)^{1/3} \tag{4-3}$$

Where

h_c surface exterior convective heat transfer coefficient, W/(m^2-K);

h_f forced convective heat transfer coefficient, W/(m^2-K);

h_n natural convective heat transfer coefficient, W/(m^2-K);

ΔT the absolute value of temperature difference between surface temperature and ambient air temperature;

C_t turbulent natural convection constant;

V_f local free stream wind speed measured at 10 m height, m/s;

a, b model constant.

Table 4.3 MoWiTT coefficients [66]

Wind direction	C_t	a	b
(Units)	$W/m^2K^{4/3}$	$W/m^2K(m/s)^b$	-
Windward	0.84 ± 0.015	2.38 ± 0.036	0.89 ± 0.009
Leeward	0.84	2.86 ± 0.098	0.617 ± 0.017

□ DOE-2 model

The DOE-2 convection model is developed from the MoWiTT model. The convective heat transfer coefficient for very smooth surfaces (like window glass) is calculated using Equation 4-1.

For less smooth surfaces the convective heat transfer coefficient can be modified using the roughness multiplier R_f . Equation 4-4 shows the correction formula.

$$h_c = h_n + R_f (h_{c,glass} - h_n) \tag{4-4}$$

Where

R_f surface roughness multiplier, estimated based on the surface conductance and shown in Table 4.4.

Table 4.4 Surface roughness multipliers

Roughness index	R_f	Example materials
1 (very rough)	2.17	Stucco
2 (rough)	1.67	Brick
3 (medium rough)	1.52	Concrete
4 (medium smooth)	1.13	Clear pine
5 (smooth)	1.11	Smooth plaster
6 (very smooth)	1.00	Glass

□ Palyvos's linear model

The forced convective heat transfer in both MoWiTT model and DOE-2 model are expressed by the traditional power law equation as shown in Equation 4-2. Palyvos has conducted a recent extensive review on available modeling methods for external convective heat transfer coefficients caused by wind [67]. Paolyvos concludes that in

many cases the linear regression equations are equally in agreement with experimental data even though fundamental heat transfer theory predicts a power law relationship between external convective heat transfer coefficient and wind speed. When wind speed is within the range 0~4.5 m/s the maximum deviations of the external convective heat transfer coefficient predicted by Equation 4-5 for windward cases average to 18% and the maximum deviations by Equation 4-6 for leeward cases average to 22%.

$$h_f = 7.4 + 4.0V_{fs} \text{ (windward)} \quad (4\text{-}5)$$

$$h_f = 4.2 + 3.5V_{fs} \text{ (leeward)} \quad (4\text{-}6)$$

Where

V_{fs} free stream wind speed (~10 m above roof), m/s.

4.4.3 Infiltration

Air infiltration, i.e. uncontrolled ventilation, is always unavoidable. Moreover most residential houses rely on infiltration to provide ventilation to occupants. There are mainly two ways of measuring building infiltration: effective leakage area (ELA) and air exchange rate per hour (ACH). This study uses ELA as the major parameter in infiltration modeling. The exact ELA value of a residence is typically measured through a blow-door test. When onsite blow-door test data are not available typical values could be used for a reasonable estimate.

One classical infiltration model is the "Sherman-Grimsrud" model developed by Max Sherman and David Grimsrud [68]. Equation 4-7 and Equation 4-8 show the mathematical formulas. Table 4.5 and Table 4.6 show values of two model parameters respectively: stack coefficient and wind coefficient [68].

$$Q = \frac{A_L}{1000}\sqrt{C_s \Delta t + C_w U^2} \tag{4-7}$$

Where

Q airflow rate, m^3/s;

AL effective air leakage area, cm^2;

Cs stack coefficient, $(L/s)^2/(cm^4 \cdot K)$;

Δt average indoor-outdoor temperature difference for time interval of calculation, K;

Cw wind coefficient, $(L/s)^2/[cm^4 \cdot (m/s)^2]$;

U average wind speed measured at local weather station for time interval of calculation, m/s.

$$NL = 0.1\left(\frac{A_L}{A_f}\right)\left(\frac{H}{H_0}\right)^{0.3} \tag{4-8}$$

Where

NL normalized leakage area, dimensionless;

AL effective leakage area at 4 Pa (CD=1.0), cm^2;

Af gross floor area (within exterior walls), m^2;

H building height, m;

H0 reference height of one-story building, 2.5m.

Table 4.5 Stack coefficient C_s

	House height (Stories)		
	One	Two	Three
Stack coefficient	0.000145	0.00029	0.000435

Table 4.6 Wind coefficient C_W

	House height (Stories)			Description
	One	Three	Two	
1	0.000319	0.000494	0.000420	No obstructions or local shielding
2	0.000246	0.000382	0.000325	Typical shelter for an isolated rural house
3	0.000174	0.000271	0.000231	Typical shelter caused by other buildings across the street from the building under study
4	0.000104	0.000161	0.000137	Typical shelter for urban buildings on larger lots where sheltering obstacles are more than one building height away
5	0.000032	0.000049	0.000042	Typical shelter produced by buildings or other structures that are immediately adjacent (closer than one house height): e.g., neighboring houses on the same side of the street, trees, bushes, etc.

Sherman and Dickerhoff conducted tens of thousands leakage measurements of U.S. dwellings over the past decade and developed an air leakage database in 1998 [69]. Figure 4.8 shows the distribution of normalized leakage area they collected. Their data analysis shows that a single-story house in the U.S. has an average normalized leakage area of 1.6 with an error of the mean near 1%, which is 13% less leaky than multi-story dwellings. The houses built after 1980s have a mean NL value of 0.47 and this does not vary with house age. During the past decade advanced technology has enabled tighter construction in residential houses. The pursuit of energy efficient homes has pushed the

tightness of residential construction further. A recent report from Lawrence Berkeley National Laboratory (LBNL) by Chan et al. has verified this trend [70]. Chan et al. have conduct a data analysis using U.S. residential air leakage database and summarized the statistics of the NL area of different type of houses as a function of floor area, including low-income houses, conventional houses, and energy-efficient houses. Figure 4.9 shows the statistics of the normalized leakage area of energy-efficient houses according their floor areas.

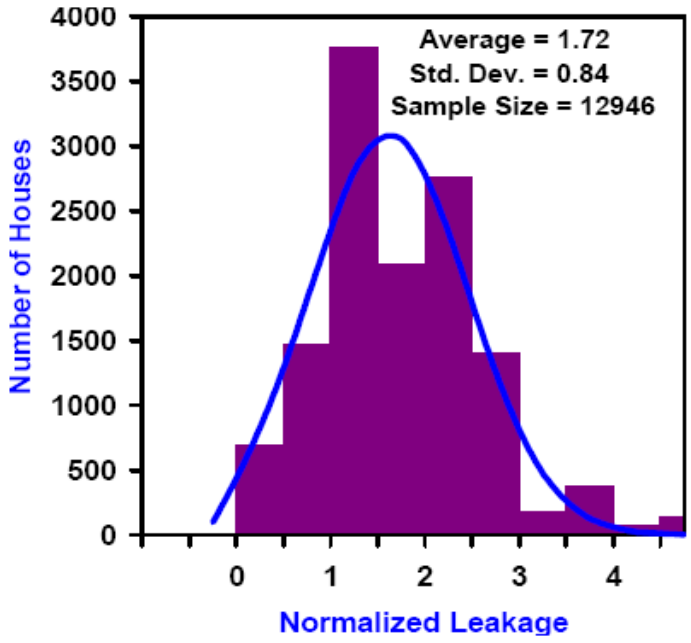

Figure 4.8 Distribution of leakage measurements by value

Floor Area	Year Built	# Data	GM	GSD	p05	p25	p50	p75	p95
<93 m^2	before 1950	10	0.85	1.69	0.00	0.50	0.67	1.47	1.81
	1950-1979	53	0.36	1.83	0.22	0.25	0.31	0.52	0.90
	1980-1995	52	0.32	1.52	0.17	0.24	0.30	0.39	0.65
	after 1995	366	0.25	1.80	0.08	0.19	0.30	0.36	0.52
93-139 m^2	before 1950	9	0.86	1.63					
	1950-1979	112	0.45	1.61	0.22	0.32	0.43	0.57	0.99
	1980-1995	127	0.36	1.69	0.14	0.26	0.37	0.50	0.82
	after 1995	1661	0.23	1.76	0.08	0.17	0.26	0.34	0.47
140-185 m^2	before 1950	9	0.86	1.96					
	1950-1979	75	0.44	1.76	0.19	0.30	0.40	0.64	1.09
	1980-1995	106	0.37	1.67	0.14	0.28	0.35	0.51	0.83
	after 1995	2205	0.24	1.61	0.09	0.20	0.27	0.33	0.42
186-232 m^2	before 1950	2							
	1950-1979	42	0.43	1.68	0.19	0.27	0.42	0.67	0.87
	1980-1995	57	0.37	1.72	0.16	0.26	0.40	0.51	1.05
	after 1995	1409	0.24	1.62	0.09	0.20	0.26	0.32	0.43
>232 m^2	before 1950	2							
	1950-1979	50	0.33	1.69	0.12	0.22	0.34	0.48	0.76
	1980-1995	88	0.34	1.64	0.12	0.25	0.39	0.49	0.56
	after 1995	1762	0.22	1.66	0.09	0.16	0.24	0.32	0.46

Figure 4.9 Statistics of the normalized leakage area of energy-efficient program houses according to [70]

4.4.4 Wind reduction factor

The wind reduction factor is the ratio of onsite local wind speed and the potential wind speed measured at an (typically undisturbed) meteorological station at 10m above ground level. In most cases an onsite weather station is not available. The Typical Meteorological Year (TMY) weather based on 30-year statistical data measured from city/regional weather stations is often used in building simulation. The wind reduction factor is used to estimate local wind speed based on wind speed in TMY data. Equation 4-9 is the classic wind reduction factor model [68]:

$$\gamma = \frac{V_{local}}{V_{pot}} = \left(\frac{\delta_{pot}}{H_{pot}}\right)^{\alpha_{pot}} \left(\frac{H}{\delta}\right)^{\alpha} \tag{4-9}$$

Where

V_{local} the hourly average wind speed at height H in the site of interest;

V_{pot} the wind speed measured at the reference height in meteorological station;

δ_{pot} wind boundary layer thickness for the meteorological station;

α_{pot} wind exponent for the meteorological station;

H_{pot} the height of measurements at the metrological station, usually 10m;

δ wind boundary layer thickness for the local building terrain;

α wind exponent for the local building terrain;

H the height of location of interest.

Identifying wind boundary layer thickness and wind exponent is part of meteorological research. ASHRAE has listed typical values of wind boundary layer thickness and wind exponent for four different types of terrain condition as shown in Table 4.7. The meteorological station often fits the atmospheric boundary layer characteristic of terrain category 3. A study from the Air Infiltration and Ventilation Center (AIVC) reformulated Equation 4-9 to a simpler version as shown in Equation 4-10 [71]. Comparing Equation 4-9 and Equation 4-10 we can estimate the constant K in Equation 4-10 as shown in Equation 4-11. This study will use Equation 4-10 to estimate wind reduction factor. Other studies or literature reviews on the estimate of wind reduction factor can be found in [55] and [54]. Table 4.9 summarizes the results and shows the uncertainty ranges of both constant K and wind exponent α.

$$\gamma = \frac{V_{local}}{V_{pot}} = KH^{\alpha} \tag{4-10}$$

$$K = \left(\frac{\delta_{pot}}{H_{pot}} \right)^{\alpha_{pot}} \left(\frac{1}{\delta} \right)^{\alpha} \tag{4-11}$$

Table 4.7 Atmospheric boundary layer parameters [68]

Terrain Category	Description	Exponent α	Layer thickness δ, m
1	Large city centers, in which at least 50% of buildings are higher than 21m, over a distance of at least 0.8 km or 10 times the height of the structure upwind, whichever is greater	0.33	460
2	Urban and suburban areas, wooded areas, or other terrain with numerous closely spaced obstructions having the size of single-family dwellings or larger, over a distance of at least 460 m or 10 times the height of the structure upwind, whichever is greater	0.22	370
3	Open terrain with scattered obstructions having heights generally less than 9.1 m, including flat open country typical of meteorological station surroundings	0.14	270
4	Flat, unobstructed areas exposed to wind flowing over water for at least 1.6 km, over a distance of 460 m or 10 times the height of the structure inland, whichever is greater	0.10	210

Table 4.8 Atmospheric boundary layer parameters [71]

Terrain Category	Description	Constant K	Exponent α
1	Large city centers, in which at least 50% of buildings are higher than 21m, over a distance of at least 0.8 km or 10 times the height of the structure upwind, whichever is greater	0.21	0.33
2	Urban and suburban areas, wooded areas, or other terrain with numerous closely spaced obstructions having the size of single-family dwellings or larger, over a distance of at least 460 m or 10 times the height of the structure upwind, whichever is greater	0.35	0.25
3	Open terrain with scattered obstructions having heights generally less than 9.1 m, including flat open country typical of meteorological station surroundings	0.52	0.20
4	Flat, unobstructed areas exposed to wind flowing over water for at least 1.6 km, over a distance of 460 m or 10 times the height of the structure inland, whichever is greater	0.68	0.17

Table 4.9 A summary of uncertain ranges for the constant K and wind exponent α

Terrain Category	Description	Constant K	Exponent α
1	Large city centers, in which at least 50% of buildings are higher than 21m, over a distance of at least 0.8 km or 10 times the height of the structure upwind, whichever is greater	0.14 ~ 0.21	0.33 ~ 0.4

Table 4.9 (continued)

2	Urban and suburban areas, wooded areas, or other terrain with numerous closely spaced obstructions having the size of single-family dwellings or larger, over a distance of at least 460 m or 10 times the height of the structure upwind, whichever is greater	0.35 ~ 0.43	0.22 ~ 0.28
3	Open terrain with scattered obstructions having heights generally less than 9.1 m, including flat open country typical of meteorological station surroundings	0.52 ~ 0.72	0.14 ~ 0.2
4	Flat, unobstructed areas exposed to wind flowing over water for at least 1.6 km, over a distance of 460 m or 10 times the height of the structure inland, whichever is greater	0.68 ~ 0.93	0.10 ~ 0.17

4.4.5 PV module efficiency

Modelling the PV module efficiency is difficult as it is a function of many factors, including ambient temperature, wind condition, installation method, module type, etc. Equation 4-12 represents the traditional simple linear expression for the PV electrical efficiency.

$$\eta_c = \eta_{T_{ref}} \times [1 - \beta_{ref}(T_c - T_{ref})] \quad (4\text{-}12)$$

Where

$\eta_{T_{ref}}$ the PV module efficiency at temperature T_{ref} and at solar radiation flux of 1000 W/m^2;

β_{ref} the efficiency correction coefficient for temperature that is included in the manufacturer data sheet;

T_c the PV operating temperature.

The increase of PV operating temperature T_c is well known to have an adverse impact on PV module efficiency which is also shown in Equation 4-12. As discussed earlier in this section the estimate of PV operating temperature T_c could be as complicated as conducting a full thermal analysis of the PV module and could be as simple as using an empirical equation from existing researches. This study will use the empirical equation developed by Skoplaki and Boudouvis [72], as shown in Equation 4-13.

$$T_c = T_a + \omega\left(\frac{0.32}{8.91 + 2.0V_f}\right)G_T \tag{4-13}$$

Where

T_a ambient air temperature;

ω the mounting coefficient and is estimated to be 1.2 for flat roof situation and 2.4 for a façade integrated condition;

G_T the incident solar radiation;

V_f the free stream wind speed in the windward side of the PV array and can be estimated through Equation 4-10.

The uncertainty related to PV module cell temperature estimate can be traced back to several parameters shown in Equation 4-13: 1) the uncertainty of wind speed estimate which is represented by the uncertainty in wind reduction factor estimate; 2) the uncertainty of incident solar radiation estimate which could be related to varying weather and the uncertainty in ground reflection factor.

Regarding other factors that might influence the PV module efficiency Detrick et al. investigated the difference between the actual power generated by a PV module and what it says on its nameplate (manufacturer data) and found out that the accuracy of manufacturer DC rating could range from -12% to +4% [45]. This estimate is in agreement with the conclusion reached from field measurements and individual tests. Figure 4.10 shows the suggested system loss factors determined from component specifications, analysis of measured data from fielded systems, and independent testing of individual losses [44, 45].

Item	Typical	Range
PV module nameplate d.c. rating	1.00	0.85 - 1.05
Initial light-induced degradation	0.98	0.90 - 0.99
d.c. cabling	0.98	0.97 - 0.99
Diodes and connections	0.995	0.99 - 0.997
Mismatch	0.98	0.97 - 0.995
Power-conditioning unit (inverter)	0.96	0.93 - 0.97
Transformers	0.97	0.96 - 0.99
a.c. wiring	0.99	0.98 - 0.993
Soiling	0.95	0.75 - 0.995
Shading**	1.00	0.0 - 1.0
Sun-tracking	1.00	0.98 - 1.00
Availability of system	0.98	0.0 - 0.995
Overall at STC	0.804	0.62* - 0.964

*Does not include soiling, shading, tracking, or availability losses
**Typically 0.975 for fixed-tilt rack-mounted systems

Figure 4.10 Suggested system loss factors [44, 45]

4.4.6 PV inverters and Balance of System (BOS) components

Off-grid applications of PV systems have to integrate a power storage component, typically batteries. The efficiency and service life varies depending on the specific technology a battery is manufactured with and at which depth of discharge the battery is

operated. Rydh and Sanden summarize the efficiency ranges for batteries employing 8 different technologies, including lithium-ion (Li-ion), sodium-sulphur (NaS), nickel-cadmium (NiCd), nickel-metal hydride (NiMH), lead-acid (PbA), vanadium-redox (VRB), zinc-bromine (ZnBr) and polysulfide-bromide (PSB) as shown in Table 4.10 [73]. Meanwhile Rydh and Sanden also summarize the efficiency ranges of inverters and charge regulators based on the literature review as shown in Table 4.11.

Table 4.10 The efficiency ranges of different types of batteries

Battery type	Efficiency range
Li-ion	0.85-0.95
NaS	0.75-0.83
PbA	0.70-0.84
NiCd	0.65-0.85
NiMH	0.65-0.85
VRB	0.65-0.80
ZnBr	0.60-0.73
PSB	0.60-0.65

Table 4.11 Efficiency ranges of inverters and battery charger regulators

Components	Efficiency range
Charge regulator	0.90-0.95
Inverter	0.92-0.94

4.4.7 HVAC system efficiency

The modeling of a HVAC system regarding both its performance of providing thermally comfortable environments and meeting its energy demand should be conducted at

multiple levels based on the available knowledge about the system and the purpose of the simulation studies (i.e. accuracy requirement).

At early design stages where the detailed system has not yet been established the simplest way and also the only available method of modeling a HVAC system is to use simple seasonal efficiency and/or coefficient of performance (COP). Table 4.12 lists the typical annual heating system seasonal efficiency for several typical heating systems [74]. Values shown in Table 4.12 include the effects of cycling and part load performance.

Table 4.13 shows typical values of COP for typical cooling systems [74]. The seasonal COP is a property of the air-conditioning device and represents the average expected performance over the cooling season and is expressed as the ratio of the cooling energy output of the device divided by the energy input to the device. All the efficiency values shown in Table 4.12 and Table 4.13 should be reduced by 10% if system ducts run outside of the insulated envelope.

Table 4.12 Typical heating system seasonal efficiencies

Heating system type	Typical annual heating system seasonal efficiency (%)
Standard boilers/furnaces (with pilot light)	55 ~ 65
Mid-efficiency boilers/furnaces (spark ignition)	65 ~ 75
High-efficiency or condensing boilers/furnaces	75 ~ 85
Electric resistance	100
Air-source heat pump	130 ~ 200
Ground-source heat pump	250 ~ 350

Table 4.13 Typical annual COP for air-conditioning systems

Cooling system type	Typical annual COP
Window air-conditioner	2.4
Standard DX (direct expansion)	3.0
Air-conditioner and air-source heat pumps	3.0
High-efficiency air-conditioner	3.5
High-efficiency commercial chiller	5.0
Ground-source heat pump	4.4

At later stages where either a detailed system configuration has been determined or even the specific mechanical equipments have been confirmed a more comprehensive computer model of the HVAC system can be built. Every type of HVAC system will need a specific model to capture their unique characteristics in terms of responding to building thermal loads and their primary energy consumption. Therefore a corresponding literature review will have to be conducted to pick up the appropriate uncertainty variables related to a HVAC model and to quantify the uncertainty ranges of selected variables. This following section is a review of HVAC systems with heat pump which is used in the case study presented in next chapter. For cases with other systems a similar study must be conducted.

Heat pumps have been widely used for both heating and cooling, especially in residential buildings. According to an EIA survey data in 2005 there are 9.2 million residential housing units in the USA using heat pump for space heating and 7.4 million of them are detached single-family houses; there are 12.3 million residential housing units using heat pump for space cooling and 9.7 million of them are detached single-family houses [75].

A heat pump is a device that extracts thermal energy from a low-temperature source and transfers it to a high-temperature sink [76]. Heat transfer always occurs from a higher-temperature object to a lower temperature one according to the second law of thermodynamics. Thus mechanical work (i.e. active energy) is required when heat pump transfers thermal energy from a lower-temperature object to a higher-temperature one. Figure 4.11 shows the diagram of the compression cycle in a heat pump. The COP of a heat pump is calculated using Equation 4-14.

$$COP_{heating} = \frac{Q_h}{W}$$
$$COP_{cooling} = \frac{Q_c}{W} \quad (4\text{-}14)$$

Where

Q_h the thermal energy delivered by the heat pump system to buildings;

Q_c the thermal energy taken away by the heat pump system from buildings;

W the mechanical work supplied to the heat pump system.

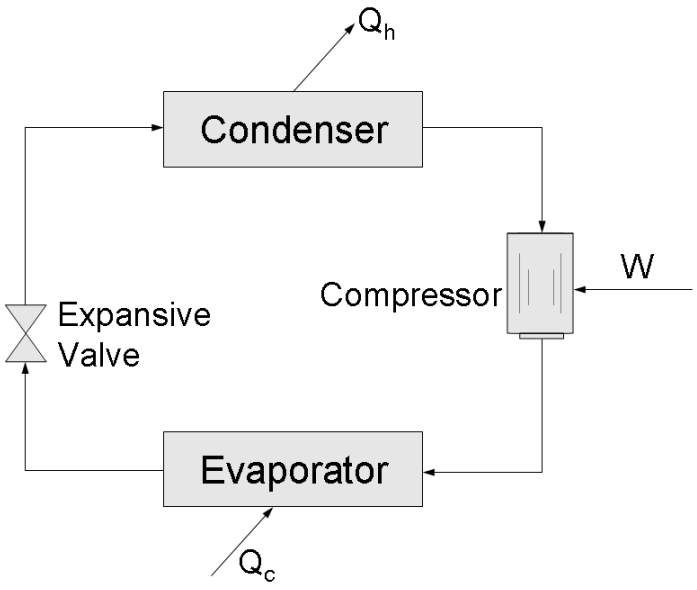

Figure 4.11 The diagram of compression cycle in heat pump

The steady state COP of all heat pumps will have been evaluated under testing conditions and stated in its product handbook. However the field COP is often different from that in the product handbook due to multiple factors including operating conditions, thermostat settings, cycling of the equipment on and off, and the system frosting and defrosting. The operating conditions often are different from the testing conditions and the COP of a heat pump has almost a linear relationship with outdoor temperature. Heat pump product handbooks often provide different COP curves at different operating conditions. Necessary corrections to the COP as a function of operating condition must therefore be considered. When heat pump systems are used in heating mode in a location with relatively low ambient temperatures the effects of frosting and defrosting might be significant. Goldschmidt has reviewed field measurements on heat pump system performance and his work reveals that the efficiency degradation due to frosting and defrosting could range from 2% to 16% [76]. Another significant efficiency degradation could be caused by cyclic effects. The steady state COP is measured at full capacity and under actual operating conditions it is common that the installed heat pump system may work at part load condition instead of full capacity. When operated under part load condition the compressor of a heat pump system will have to switch between on and off more often in order to respond to the dynamics especially when there is a narrow thermostat dead band. The extra cost of energy is called cyclic effect. Goldschmidt's field data review shows that the combination of cyclic effects and frosting effects could cause an efficiency degradation ranging from 17% to 40% [76]. The cyclic effects can be taken into account by a degradation coefficient in building simulation. Equation 4-15 shows the classic relationship between actual COP after considering cyclic effects and the steady

state COP through a factor called part load factor (PLF). The Air-Conditioning and Refrigeration Institute (ARI) suggests a generalized equation to estimate PLF [77], as shown in Equation 4-16.

$$COP_{cyclic} = COP_{ss} \times PLF \tag{4-15}$$

$$PLF = 1 - C_d \times (1 - PLR) \tag{4-16}$$

Where

COP_{cyclic} the heat pump COP after considering cyclic effects;

COP_{ss} the steady state heat pump COP;

PLF part load factor;

C_d degradation coefficient;

PLR partial load ratio, calculated as the ratio of the building requirement supplied by the machine in the time step to the maximum energy that could be supplied in the same time interval if continuing to work at full capacity.

The degradation coefficient C_d has a default value of 0.25. Kondepudi and Bhalerao proposed a range of C_d between 0.10 and 0.25 in their parametric analysis of system performance of air-source heat pumps [78]. One field measurement of effects of cycling, frosting, and defrosting losses on an air-source heat pump show the value of C_d as 0.11 at cooling mode and 0.26 at heating mode [79]. Another field measurement on transient performance of an air-source heat pump shows the value of C_d as 0.102 in heating mode and 0.066 in cooling mode [80]. Goldschmidt's another review on the cyclic effects of heat pump from field measurements concludes that the value of C_d could vary in the

range of between 0.07 to 0.26 in cooling mode and between 0.10 and 0.13 in heating mode [81]. Table 4.14 shows a summary of varying ranges of C_d for air-source heat pump systems.

Table 4.14 A summary of the degradation coefficient C_d for air-source heat pump systems

Mode	Minimum	Maximum
Heating	0.10	0.26
Cooling	0.066	0.26

4.4.8 Internal active thermal mass

Estimate of internal active thermal mass contributed by interior partitions and furniture can be crucial especially when passive designs are implemented. The building thermal mass has a positive effect on building indoor conditions. In winter solar radiation can be stored in thermal mass during the daytime and then released to the space at late afternoon or even in the evening when heating is most needed. In summer thermal mass absorbs part of the penetrating solar radiation and slowly releases it to inside space at later time where cooling demand is not as high as it is when solar radiation is stronger. The time shift reduces building peak load and provides opportunities of reducing HVAC system size. Therefore modeling of thermal mass effects is necessary in order to capture the dynamics of building thermal performance. Parameters that affect the performance of thermal mass include material thermal properties, thermal mass location and distribution, and etc. Detailed discussion can be found in a study by Balaras [82].

Thermal mass is mostly introduced deliberately into the building design and its thermal effects result from three sources: (1) the building exterior envelop like walls, roofs, and floors; (2) interior structural petitions; and (3) furniture. The thermal mass effects from different resources can be estimated separately or as a combined factor depending on the specific simulation technique. Antonopoulos has summarized the methods that may lead to a reliable estimate of thermal mass, such as direct measurement procedures, thermal network models, or solving a rigorous set of differential equations that describe the transient thermal behavior of buildings [83]. Multiple resources have been used to provide a rough estimate of thermal mass for typical constructions in residential buildings. Barakat and Sander estimate thermal capacities of typical residential constructions using thermal response factor program as shown in Table 4.15 [84]. Table 4.16 shows the ranges of effective thermal capacities for one-story detached houses with a floor area from 50 m^2 to 300 m^2 in Greece reported by Antonopoulos [83].

Table 4.15 Thermal capacities of typical residential constructions

Type	Thermal capacity MJ/ K-m^2 floor area	Description
Light	0.060	Standard frame construction, 12.7 mm gyproc walls and ceilings, carpet over wooden floor
Medium	0.153	As above, but 50.8 mm gyproc walls and 25.4 mm gyproc ceiling
Heavy	0.415	Interior wall finish of 101.6 mm brick, 12.7 mm gyproc ceiling, carpet over wooden floor
Very heavy	0.810	Very heavy commercial office building, 304.8 mm concrete floor

Table 4.16 The effective thermal capacities of one-story detached house with floor areas between 50 m^2 and 300 m^2

Insulation	Ranges MJ/°C
Fully-insulated	37 ~ 161
Un-insulated	18 ~ 59

However there is no explicit description that the thermal capacity estimate listed in Table 4.15 and Table 4.16 includes the thermal mass from interior furniture. In fact an estimate of thermal mass contributed from interior furniture would have to rely on field measurements after occupants move in. Meanwhile different occupants with different life styles may also lead to different levels of thermal mass (sparely furnished well organized interiors will have less active mass than the overly furnished interiors). Without detailed information collected from houses in use it is hard to offer a reliable estimate of thermal mass added by interior furniture. This study will treat it as a scenario uncertainty. The house energy consumption and power reliability at different thermal mass (added by interior furniture and partitions) levels will be studied.

4.4.9 Thermal bridges

Thermal bridges are parts of the building envelope where the otherwise uniform thermal resistance are significantly changed (e.g. structural joints with roofs, floors, ceilings, and other walls, or other building envelope details such as corners, window or door openings), resulting in a multi-dimensional heat flow. There are two main types of thermal bridges: 1) linear thermal bridge which is a thermal bridge with a uniform cross section in one direction; and 2) point thermal bridge which is the thermal bridge with no uniform cross section in any direction.

Equation 4-17 shows the corrected thermal performance of a building envelope after considering the effect of thermal bridges [85].

$$H = \sum U_i A_i + \sum \Psi_k l_k + \sum x_j \tag{4-17}$$

Where:

H thermal transfer coefficient;

U_i the thermal transmittance of part i of the building envelope;

A_i the area over which the value of U_i applies;

Ψ_k the linear thermal transmittance of the linear thermal bridge k;

l_k the length over which the value of Ψ_k applies;

x_j the point thermal transmittance of the point thermal bridge j.

Generally the heat loss caused by point thermal bridges can be neglected. The linear thermal transmittance of the linear thermal bridge, Ψ_k, can be calculated from Equation 4-18.

$$\Psi = L^{2D} - \sum U_i l_i \tag{4-18}$$

Where:

L^{2D} the linear thermal transfer coefficient obtained from a two-dimensional calculation of the building component;

U_i the thermal transmittance of the one-dimensional building component i;

l_i the length within the two-dimensional geometrical model over which the value of U_i applies.

Currently there are four types of methods available to estimate thermal loss due to the existence of thermal bridges. Depending on the particular method selected different

levels of accuracy will be achieved. Table 4.17 shows the available methods of estimating Ψ and their corresponding expected uncertainty. At early design stages building details may not be available. A rough estimate of Ψ can be made based on the size and main form of the building, using the default values of linear thermal transmittance provided in ISO 14683 [85]. At a later design development stage when global details are available more accurate estimates of Ψ can be obtained by comparing the particular details with the best fitting examples from a published thermal bridge catalogue which is based on numerical calculations. When full details about the building are available all methods can be used to calculate Ψ, including numerical methods which provide the most accurate results. There are a few computer tools available in the market to perform a detailed thermal analysis of building components with thermal bridges. A recent study by Larbi illustrates a numerical study of heat transfer through thermal bridges of buildings and the presented regression models based on simulation results show a global (combining uncertainty of the numerical method and regression analysis) uncertainty range of ±10% [86].

Table 4.17 Methods for calculating linear thermal transmittance

Methods	Expected uncertainty of Ψ
Numerical calculation	± 5%
Thermal bridge catalogue	± 20%
Manual calculation	± 20%
Default values	0% ~ 50%

4.4.10 Power consumption of domestic appliances

Domestic appliances are responsible for a significant part of the whole house electricity consumption and also produce significant internal gains. According to EIA, appliances use more than 60% of the electricity consumed in residential buildings. Table 4.18 lists the percentage of electricity consumed by appliances in residential buildings between 1987 and 2001. Meanwhile the advancement of technology has improved efficiencies of domestic appliances during the past decade. Energy Star lists a large number of energy efficient domestic appliances and their energy consumption data [87].

Table 4.18 Percentages of electricity consumption by end users [88]

End user	Survey year				
	1987	1990	1993	1997	2001
Air-Conditioning	15.8	15.9	13.9	11.8	16.0
Space heating	10.3	10.0	12.4	11.4	10.1
Water heating	11.4	11.2	10.3	11.0	9.1
Total appliances	62.5	63.0	63.4	65.9	64.7

Besides electricity consumed while in use, many electronic appliances draw power when switched off or not performing their principal functions actively. Standby power (sometimes also called “leaking electricity”) use for most appliances ranges from 1 to 20 watts and is responsible for 5~10% of residential electricity used in the USA [89]. Table 4.19 shows the standby power use of some major common residential appliances. Table 4.20 lists some minor standby power use by other home appliances. A more complete list of standby power consumption used for household and offices can be found in the book by Harvey [90].

Table 4.19 Standby power use of selected residential appliances [89]

	Minimum	Average	Maximum
Audio			
Portable stereo	0.7	2.2	3.2
Compact system	1.3	9.7	28.6
Component system	1.1	3	15.1
Radio	0.9	1.7	3.2
Video			
TV	0.3*	4.5	21.6
VCR	1.5	5.9	12.8
TV/VCR	1.1	7.6	19.5
Set-top			
Cable box	4.6	10.8	24.7
Satellite receiver	8.8	12.6	18.8
Video game	0.9	1.3	2
Telephony			
Answering machine	1.8	3	5.2
Cordless phone	1.1	2.6	5
Home office			
Personal computer	0.5*	1.7	3.5
Modem, analog	1	1.4	1.8

* Appliances with no standby losses are excluded.

Table 4.20 Standby power use in white goods [89]

Appliances	Average standby power use (Watts)
Clothes washer	0 ~ 3
Clothes dryer	0 ~ 3
Dishwasher	0 ~ 4
Microwave oven	0 ~ 3
Refrigerator/Freezer	0 ~ 3

4.4.11 Domestic hot water system

As shown in Table 4.18 hot water usage is responsible for about 10% of the electricity consumption in residential buildings in the USA. There are multiple ways of providing hot water for off-grid houses. The easiest way is to purchase an electric hot water heater. Another common way of generating hot water for residential usage is through solar thermal collectors. There are mainly three types of solar collectors available in the current market: unglazed collectors, glazed collectors, and evacuated collectors. The unglazed collectors are the cheapest among the three and not able to provide hot water at a high temperature. It is mainly used to supply hot water that doesn't require high supply temperature, for instance, to heat water in swimming pools. Compared to evacuated tubes the glazed collectors are relatively cheap and able to support higher temperature operations. The evacuated collectors are more expensive in terms of cost. However through its improved design an evacuated collector nearly has any convection heat loss and therefore can be used in cold climate and operated at higher system efficiency. Kalogirou has conducted a thorough survey study on all types of solar thermal collectors and their applications [91].

This section will focus on the domestic hot water (DHW) systems with evacuated tubes as they are used in the off-grid solar house design that will be introduced as a case study in the following chapters. There are two parameters that need to be defined to characterise the efficiency of an evacuated tube DHW system: collector efficiency and the incidence angle modifiers (IAMs). Equation 4-19 represents the typical efficiency model that has been used in the solar collector performance test methodology [92, 93]. Since the efficiency curve shown in Equation 4-19 is measured on the basis of normal

incidence angles, its use for arbitrary incident angles requires correction by the appropriate IAM. The instantaneous collector efficiency, at any incident angle, can be calculated using Equation 4-20.

$$\eta = \eta_0 - a_1 \times \frac{T_m - T_a}{G} - a_2 \times \frac{(T_m - T_a)^2}{G} \tag{4-19}$$

Where

η_0 the reference efficiency of evacuated tubes;

a_1 the global heat loss coefficient;

a_2 temperature dependence of global heat loss coefficient;

T_m the average manifold temperature;

T_a the ambient air temperature;

G the incident solar radiation on the tilted surface.

$$\eta_{corrected} = \eta \times K \tag{4-20}$$

K the IAM performance adjustment factor, calculated by multiplying two IAM factors.

In addition to the global heat loss and IAM correction presented in Equation 4-19 and 4-20 there is another environment related factor that also influences efficiency of evacuated collectors: duct accumulation. Dirt deposition could decrease hot water production as much as 40% in locations that suffer from sand storms [94]. El-Nashar's study found that dust deposition could cause a monthly drop in glass tube transmittance of 10% - 18% in the area near the city of Abu Dhabi, UAE [94]. During winter when less sand deposition takes place the monthly drop in glass tube transmittance only varies between 2% and 4%.

A monthly drop of 12.1% can be expected in a tropical climate condition over a period of 30 days [95].

4.4.12 User behavior

User behavior has a significant impact on power reliability in off-grid houses because it directly and indirectly determines the energy demand. For instance the electricity demand by hot water supply depends on the efficiency of the installed DHW system and obviously depends on the water usage as well as desired supply temperatures. The electricity demands on other home appliances are also highly dependent on the period of time in use. This usage information is subjective and varies for different individuals. This study will not consider usage profiles as uncertain variables but only investigate their impacts on power reliability through sensitivity analysis by treating assumed usage profiles as scenarios.

4.5 Identification of dominant parameters

As reviewed earlier there are a large number of sources of uncertainties that impact on the system reliability. Quantifying all uncertainties and finding the appropriate probability distribution function can be very time consuming. Since not all sources of uncertainty make equally significant contributions to the uncertainty of the outcome (i.e. power reliability in this case) it is more efficient to spend most efforts on significant factors only. A sensitivity analysis is an adequate instrument to rank all sources of uncertainty according to their importance of the uncertainty of outcomes.

Sensitivity analysis is defined as: “the study of how uncertainty in the output of a model (numerical or otherwise) can be apportioned to different sources of uncertainty in the

model input [96]". A sensitivity analysis may be performed for any of the following objectives [97]:

- Model corroboration: to check if the model is overly dependent on any fragile assumptions;
- Research prioritization: to identify which factor deserves further analysis or measurement;
- Model simplification: to check if any parameter can be fixed so that the overall model can be simplified;
- Parameter screening: to identify factors which interact and may thus generate extreme values.

Parameter screening fits the current need in this dissertation.

Multiple methods are available to perform parameter screening. The elementary effect method, originally contributed by Morris [98], is believed to be the most promising one in terms of computation time and resulting accuracy [97]. When the to-be-evaluated model is computationally expensive the elementary effect method is expected to be very effective in identifying the few important factors from a relatively large number of input factors by only using a relatively small number of samples. Two previous risk studies have demonstrated that the elementary effect method is adequate for parameter screening in building research areas [54, 55]. Below is a simple introduction of the elementary effect method developed by Morris.

The elementary effect method simply calculates an average of derivatives over the uncertain space of input factors. Consider a model with k independent (uncertain) input factors $X_i, (i = 1, k)$. The input space Ω is then discretized into a p-level grid and input

factors $X_i, (i = 1, k)$ will vary across p levels. For a given value of X, the elementary effect of the *ith* input factor is defined as Equation 4-21.

$$EE_i = \frac{Y(X_1, X_2, \cdots, X_{i-1}, X_i + \Delta, \cdots, X_k) - Y(X_1, X_2, \cdots, X_k)}{\Delta} \tag{4-21}$$

Where

p the number of levels;

Δ a value in $\left\{\frac{1}{p-1}, \cdots, 1 - \frac{1}{p-1}\right\}$;

$X = (X_1, X_2, \cdots, X_k)$ any selected value in Ω such that the transformed point $(X + e_i\Delta)$ is still in Ω for every single input;

e_i a vector of zeros but with a unit as its *ith* component.

The distribution of elementary effects caused by the *ith* input factor X_i can be obtained by randomly sampling different X in Ω. Denote it by F_i. The F_i distribution is finite if p is even and Δ is chosen to be $\frac{p}{2(p-1)}$. The number of elements of F_i can be calculated using Equation 4-22.

$$r = p^{k-1}[p - \Delta(p-1)] \tag{4-22}$$

The sensitivity measures, μ and σ, proposed by Morris, are the estimates of the mean and standard deviation of the sample F_i. The mean μ indicates the overall influence of the input X_i on the output and the standard deviation σ estimates the degree of how F_i is dependent on the values of other inputs $X_j\ (j \neq i)$. However the sensitivity measure μ may become vulnerable when the distribution F_i contains both positive and negative values in which case some effects may cancel each other out. Morris recommended to

look at both μ and σ simultaneously in order to avoid this problem. A graphic representation in the (μ,σ) plane is often used for a better interpretation. However Campolongo pointed out that it may still be problematic in the case of large models with multiple outputs and thus proposed to use another measure μ^* to replace the original μ [99]. The parameter μ^* is defined as the mean of the distribution of the absolute values of the elementary effects.

$$\mu = \frac{1}{r}\sum_{j=1}^{r} EE_i^j \tag{4-23}$$

$$\mu^* = \frac{1}{r}\sum_{j=1}^{r} |\, EE_i^j \,| \tag{4-24}$$

$$\sigma_i^{\,2} = \frac{1}{r-1}\sum_{j=1}^{r} (EE_i^j - \mu)^2 \tag{4-25}$$

Since there is no additional computation cost involved between the estimates of μ and μ^* all three sensitivity measures (μ, μ^*, σ) will be used in the following reliability analysis to get the maximum amount of sensitivity information.

The reliability analysis of an off-grid solar house design will calculate 3 basic performance indices (failure rate λ, outage hour r, power unavailability U) for every individual electricity consumer in the house, and two energy related performance indices (yearly wasted energy EW and yearly needed energy EN). Therefore the single measure μ^* will be used for parameter screening and results will then be verified through further simulation studies. Details about the verification process will be discussed in next chapter.

CHAPTER 5 A CASE STUDY

5.1 An off-grid solar house

The solar house used in this case study was designed by a Georgia Tech team for the Solar Decathlon 2007 competition, which is a bi-yearly international competition organized by the National Renewable Energy Laboratory (NREL) under the Department of Energy (DOE). Once every two years 20 universities/colleges compete against each other to design, build, and operate an 800 square foot house that is purely powered by sun. The following context will refer to this solar house as the "GTSD07 house".

5.1.1 Building design

The fundamental design theme of the GTSD07 house was "transparency" to be achieved through novel technologies that could be applied on single-family residential scale. This theme is reflected in the translucent envelope of the GTSD07 house.

Figure 5.1 shows the floor plan of GTSD07 house. As a small residential house it has a bedroom, a bathroom, a home office area, a kitchen, and a living room open to the kitchen. The GTSD07 house has overall dimension of 48.25 ft × 14 ft × 10.5 ft (14.7 m × 4.27m × 3.2m).

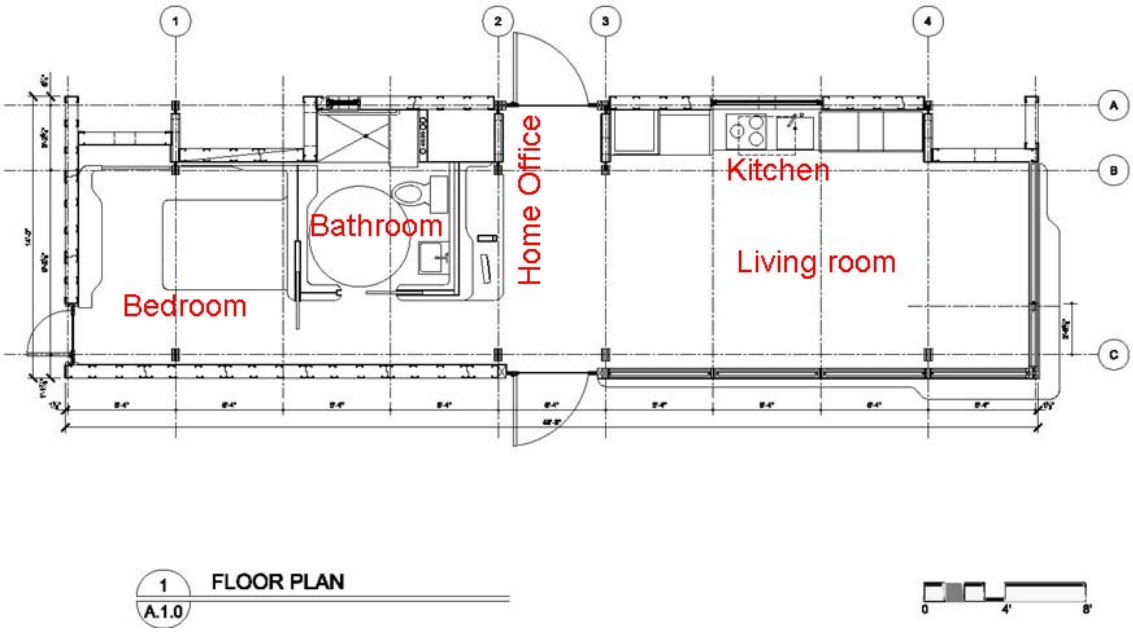

Figure 5.1 The floor plan of the GTSD07 house

Figure 5.2 shows a front view and rear view of the 3D image rendering of the GTSD07 house. The vertical house envelope has two types of materials: part of the southern wall and eastern wall (transparent area in Figure 5.2) are duo-guard which is made of polycarbonates filled with aerogel and has an R-value of R-20; the rest are structural insulated panels (SIP) walls (red area in Figure 5.2) which have an R-value of R-37. The roof is made of ETFE membranes filled with aerogel and has an R-value of R-20. Both the roof and duo-guard walls are translucent which allows sufficient natural light penetrating into interior spaces. Figure 5.3 shows the GTSD07 house during the competition in Washington DC.

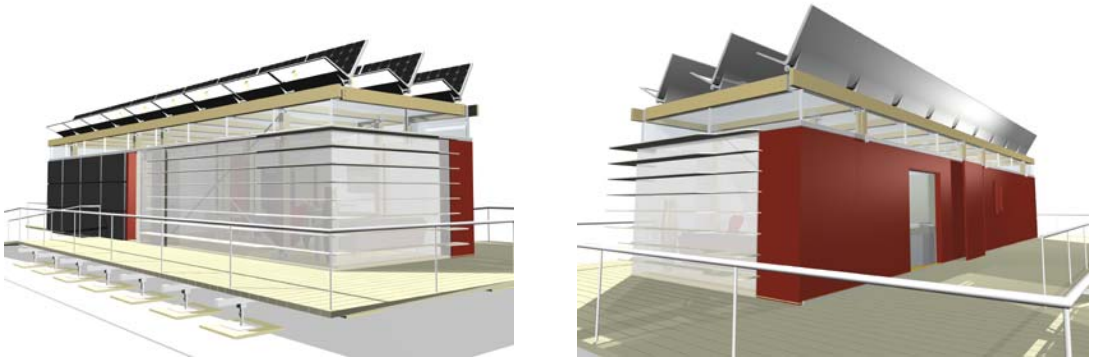

Figure 5.2 The front view (left) and the rear view (right) of the GTSD07 house

Figure 5.3 A picture of the GTSD07 house on the National Mall, DC

5.1.2 Solar power system

The electricity supplied to this house is produced by its PV system. It includes 27 PV modules on the roof providing a total power of 6.5 kW and 12 PV modules mounted to

the southern wall (black area in Figure 5.2) providing an additional 2 kW of electricity. All PV modules use monocrystalline cell technology. Table 5.1 and Table 5.2 list the major PV module parameters and their rated values given by manufacturers. There are two inverters installed to facilitate the roof PV modules and the southwall PV modules separately. The maximum alternating current (AC) output capacity is 6000 W for the inverter connecting to the roof PV modules and 3000 W for the one connecting to the southwall PV modules.

Table 5.1 The major roof PV module parameters and their rated values

Module parameters	Manufacture data
Peak power	215 W
Rated voltage	39.8 V
Rated current	5.40 A
Open circuit voltage	48.3 V
Short circuit current	5.80 A
Module efficiency	17.3%
Temperature coefficients	-0.38%/°C

Table 5.2 The major south wall PV module parameters and their rated values

Module parameters	Manufacture data
Peak power	220 W
Rated voltage	39.8 V
Rated current	5.53 A
Open circuit voltage	48.3 V
Short circuit current	5.95 A
Module efficiency	17.7%
Temperature coefficients	-0.38%/°C

The battery bank contains 8 battery modules providing a total voltage of 48 Volts. The total capacity of the installed battery bank is 98.4 kWh.

5.1.3 Domestic hot water system

The domestic hot water (DHW) is supplied by an evacuated tube solar collector system. And the hot water tank has a backup electric heating element that will meet the DHW need when solar radiation is not sufficient or not available. The DHW system is sized based on the DHW need of two residents. Figure 5.4 shows a view of the evacuated tube solar collector system located in the house backyard. The main DHW tank has a capacity of 80 Gallons and the solar water system contains 30 tubes.

Figure 5.4 A picture of the installed solar evacuated tube solar water system

5.1.4 The mechanical system

The mechanical system installed in the GTSD07 house includes a mini-split air source heat pump and a heat recovery ventilator. The mini-split air source heat pump has one outdoor unit and three indoor units which are located in the living room/kitchen, home

office area, and the bedroom respectively. The heat pump system provides a total cooling capacity of 28400 Btu/hr (8.32 kW) with the seasonal energy efficiency ratio (SEER) of 16.0 Btu/h/W (4.69 W/W). In terms of heating it has a rated heating capacity of 28600 Btu/hr (8.38 kW) with a SEER value of 13.1 Btu/h/W (3.84 W/W).

5.2 Building simulation models

5.2.1 The building simulation tool

The building simulation tool used for this study is called GTSim. It is a finite element based building simulation package developed in Matlab specifically for the Solar Decathlon project where it was used for building energy analysis [100]. In GTSim all house components are discretized into a finite element mesh and represented by the classic first-order heat balance equation, as shown in Equation 5-1. The mass matrix (M), stiffness matrix (S), and the load vector (f) can be functions of temperature, time, or both, depending on the formulation of the simulation model. For the details about the modelling of solar loads, shading, long and shortwave radiation, the reader is referred to Clarke's book [101]. Some of the main models used in GTSim and details on tool verification can be found in Appendix A. Figure 5.5 illustrates a schematic diagram of the GTSD07 house model finite element mesh (only the major nodes are shown).

$$M\dot{T} + ST = f \tag{5-1}$$

Where,

M the mass matrix;

S the stiffness matrix;

f the load vector;

T the temperature vector.

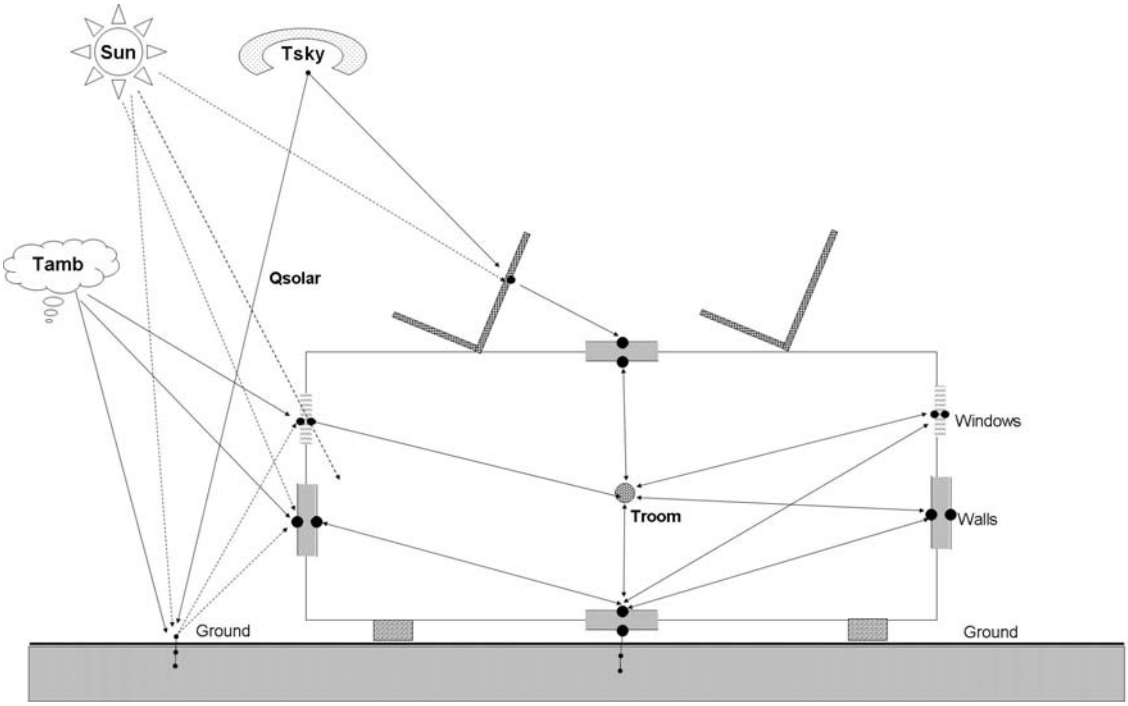

Figure 5.5 Schematic representation of the house's dynamic simulation

5.2.2 User profiles

Although the solar house was primarily designed for the Solar Decathlon competition it has been furnished and is technically fully functional as a residential house to accommodate one couple without kids. The house is ready to live in, i.e. it contains all normal appliances and is otherwise totally equipped. When the appliance information and other house equipment data is entered into the Building America analysis tool [102], a series of user profiles, intended to represent the behaviour of "standard" occupants (couple), are created. These "standard" user profiles will be used in all the following simulations and reliability analyses. Table 5.3 shows the normalized hourly profiles.

Table 5.3 The normalized Hourly Profiles

Hour	Occupant	Lights	Clothes Washer	Dishwasher	Fridge	Cooking	Misc Electric Loads
1	0.061	0.008	0.009	0.015	0.040	0.007	0.037
2	0.061	0.008	0.007	0.007	0.039	0.007	0.035
3	0.061	0.008	0.004	0.005	0.038	0.004	0.034
4	0.061	0.008	0.004	0.003	0.037	0.004	0.034
5	0.061	0.024	0.007	0.003	0.036	0.007	0.032
6	0.061	0.050	0.011	0.010	0.036	0.011	0.036
7	0.061	0.056	0.022	0.020	0.038	0.025	0.042
8	0.052	0.050	0.049	0.031	0.040	0.042	0.044
9	0.024	0.022	0.073	0.058	0.041	0.046	0.037
10	0.015	0.015	0.086	0.065	0.041	0.048	0.032
11	0.015	0.015	0.084	0.056	0.040	0.042	0.033
12	0.015	0.015	0.075	0.048	0.040	0.050	0.033
13	0.015	0.015	0.067	0.041	0.042	0.057	0.032
14	0.015	0.015	0.060	0.046	0.042	0.046	0.033
15	0.015	0.015	0.052	0.038	0.041	0.044	0.035
16	0.015	0.026	0.049	0.036	0.042	0.057	0.037
17	0.018	0.056	0.050	0.038	0.044	0.092	0.044
18	0.032	0.078	0.049	0.049	0.048	0.150	0.053
19	0.053	0.105	0.049	0.087	0.050	0.117	0.058
20	0.053	0.126	0.049	0.111	0.048	0.060	0.060
21	0.053	0.128	0.049	0.090	0.047	0.035	0.062
22	0.061	0.088	0.047	0.067	0.046	0.025	0.060
23	0.061	0.049	0.032	0.044	0.044	0.016	0.052
24	0.061	0.020	0.017	0.031	0.041	0.011	0.045

Table 5.4 shows the daily sensible internal gains and the corresponding electricity consumption from appliances. Figure 5.6 shows the daily DHW consumption for each

month whereas Figure 5.7 shows the typical usage profile for DHW. The hourly profile represents the percentage of daily total consumption that has been spent within each hour and is dimensionless. The hourly internal gains from each domestic appliance will be calculated as the product of the normalized hourly profile value and its daily load.

Table 5.4 Internal gains in the GTSD07 house

	Daily Sensible load (Wh)	Daily Machine Electricity (kWh)
Occupancy	1055.386	N/A
Lighting	5878	5.878
Clothes Washer	490	0.62
Dishwasher	126	0.211
Cooking Device	250	0.616
Misc. Electric loads	2670	2.97
Refrigerator	1270	1.27

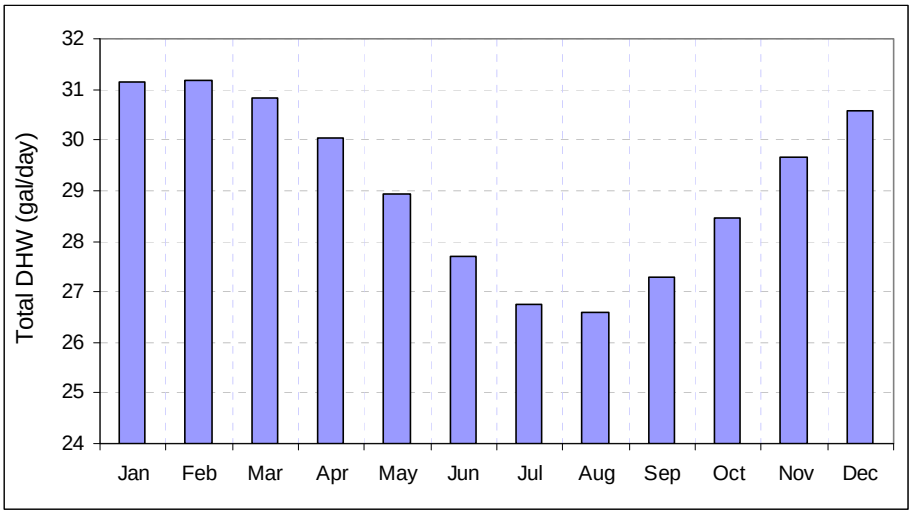

Figure 5.6 The daily total DHW usage in each month for the GTSD07 house

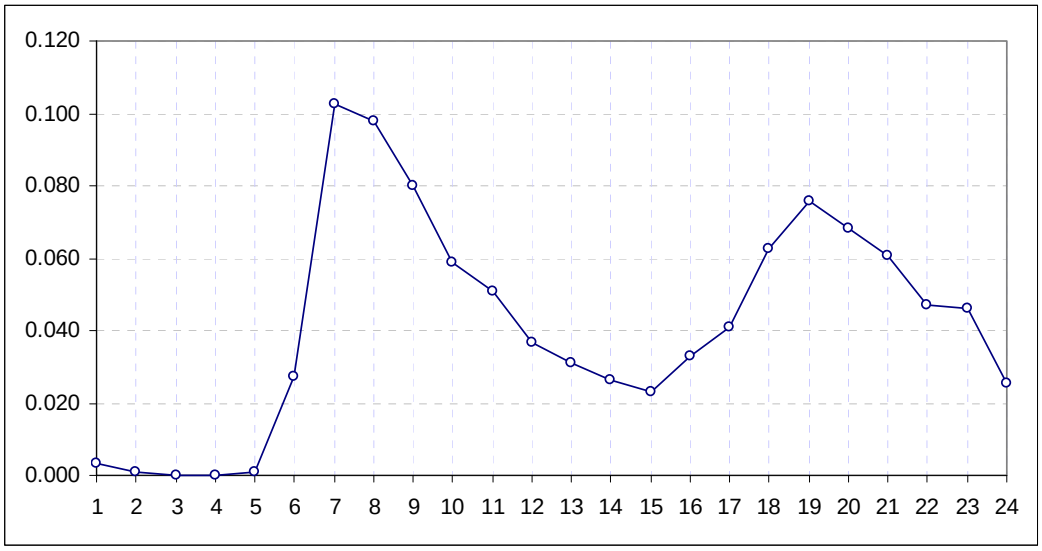

Figure 5.7 The normalized combined DHW hourly profile for the GTSD07 house

5.3 Quantifying uncertainties

The full set of uncertain parameters is identified for this specific case study, following the general methodology discussed in Chapter 4. The detailed calculations are presented as below.

5.3.1 Thermal bridge estimate

The thermal bridge effect is quantified based on ISO 16483 using Equation 4-17 and Equation 4-18. Table 5.5 lists the rough estimate of thermal bridge effect in this case study. The corresponding uncertainty range related to the calculation method is 0%~50%.

Table 5.5 Estimate of thermal bridge effect

Thermal bridge components	Thermal bridge type	Ψ_k	l_k	$\Psi_k \times l_k$ (W/K)
Wall/Roof	R8	0.40	37.95	15.18
Wall/Wall (SIP)	C2	-0.10	19.20	-1.92

Table 5.5 (continued)

Wall/Wall (Duo-guard)	C4	-0.15	3.20	-0.48
Wall/Floor (SIP)	R2	0.50	28.12	14.06
Wall/Floor (Duo-guard)	R4	0.30	9.82	2.95
Pillars	P2	1.20	0.23	0.27
Lintel, sill, reveal (clearstory-SIP)	W8	0.60	28.12	16.87
Lintel, sill, reveal (clearstory-Duo-guard)	W10	0.00	9.82	0.00
Door (South)	W8	0.60	7.04	4.23
Door (West)	W8	0.60	5.99	3.60
Door(North)	W8	0.60	7.04	4.23
Windows (North)	W8	0.60	12.37	7.42
Total				66.41

5.3.2 Uncertain parameters and their ranges

The uncertainty ranges of identified parameters are estimated based on specified (mostly manufacturer supplied) values of building component parameters and the modelling method chosen in GTSim. Table 5.6 shows the chosen 49 uncertain parameters, their uncertainty ranges, and main source of information used to assess the range. The "Ref" value represents the typical values that would be chosen in a deterministic building simulation where uncertainty is not considered. This is obviously only an estimate, but it should be noted that the choice of reference case is not relevant for the ultimate outcomes of the reliability outcomes. The reference is only chose as a convenient reference point for some of the analyses.

Table 5.6 Uncertain parameters and their uncertain ranges

Index	Variables	Min	Max	Ref	References
1	SIP wall - mCp per unit area	11586	14710	13018	[62]
2	SIP wall – U value	0.297	0.363	0.330	[62]
3	Duo-guard – mCp per unit area	11325	14379	12725	[62]
4	Duo-guard - U value	1.100	1.345	1.223	[62]
5	Floor – mCp per unit area	16565	21033	18613	[62]
6	Floor - U value	0.204	0.249	0.227	[62]
7	ETFE roof - mCp per unit area	2001	2541	2248	[62]
8	ETFE roof - U value	0.504	0.616	0.560	[62]
9	Envelope between roof and clearstory – mCp per unit area	82467	104705	92660	[62]
10	Envelope between roof and clearstory - U value	1.364	1.667	1.515	[62]
11	Single layer ETFE – mCp per unit area	79	100	88	[62]
12	Single layer ETFE - U value	1062	1299	1181	[62]
13	Polycarbonate - mCp per unit area	17095	21705	19208	[62]
14	Polycarbonate - U value	0.959	1.172	1.065	[62]
15	Window - mCp per unit area	20454	25970	22982	[62]
16	Window - U value	5.678	6.940	6.309	[62]
17	Door - mCp per unit area	20454	25970	22982	[62]
18	Door - U value	6.147	7.513	6.830	[62]
19	Absorption - SIPs	0.18	0.46	0.32	[62]
20	Roof - solar transmittance	0.14	0.22	0.18	Material specification

Table 5.6 (continued)

21	Duo-guard - solar transmittance	0.03	0.09	0.09	Material specification
22	MoWiTT model - Ct (windward)	0.825	0.855	0.84	[66]
23	MoWiTT model - a (windward)	2.344	2.416	2.38	[66]
24	MoWiTT model - b (windward)	0.792	0.988	0.89	[66]
25	MoWiTT model - a (leeward)	2.851	2.869	2.86	[66]
26	MoWiTT model - b (leeward)	0.6	0.634	0.617	[66]
27	Internal heat transfer coefficient - ceiling	0.3	0.8	0.5	[63]
28	Internal heat transfer coefficient - floor	3	5	3	[63]
29	Internal heat transfer coefficient - wall	1.59	4.1	2.5	[54, 63]
30	Normalized leakage area (NL)	0.08	0.52	0.25	[70]
31	Wind reduction factor - constant K	0.35	0.43	0.35	[71, 103]
32	Wind reduction factor - exponent δ	0.22	0.28	0.25	[71, 103]
33	Temperature setpoint control deviation	0	2	0	[54]
34	Heat pump - degradation coefficient: cooling	0.066	0.26	0.25	[78-81]
35	Heat pump - degradation coefficient: heating	0.1	0.26	0.25	[78-81]
36	PV - environmental factor	0.667	0.994	0.84	[44, 45]

Table 5.6 (continued)

37	Inverter	0.92	0.97	0.96	[73]
38	Charge regulator	0.9	0.95	0.95	[73]
39	Battery - efficiency	0.7	0.84	0.84	[73]
40	Evacuated tube - η0	0.96	0.98	1	[94]
41	Hot water tank - U	0.295	0.361	0.328	[62]
42	Distribution of incident solar gain - fraction to floor	0.22	1	1	[54]
43	Radiant temperature of surrounding environments	-5	5	0	[54]
44	Soils - ρ	1200	2200	1700	[62]
45	Soils - Cp	910	2500	1705	[62]
46	Soils - k	1.5	2	1.75	[62]
47	Ground - albedo	0.15	0.3	0.17	[54]
48	thermal bridge - U	0	99.6	66.4	[85]
49	Standby Power consumption - Appliances	13	86.9	41.8	[89]

5.4 Power reliability assessment

5.4.1 Occupants' preferences and reliability criteria

As described in previous chapters, different residents in off-grid houses may have different tolerances regarding power reliability for performing certain residential tasks. When power becomes insufficient to finish all residential tasks, distributing power to prioritized tasks will help reduce inconvenience. Table 5.7 shows an example of subjective occupants' preferences with respect to multiple residential tasks. In this case they reflect the preferences of the author of this thesis.

Table 5.7 shows the power reliability criteria in terms of power outage hour (r) and unavailability (U) to meet different residential functions. One shall notice that only the refrigerator has an outage hour requirement that is demanded by physical condition (i.e. to keep food fresh and good) whereas the rest is subjective to occupants' desires and reasonable expectations. The criteria for power unavailability (U) has been set based on the common settings in our current power industry practice [36, 37]. The needs from the first four most preferred consumers are considered as critical loads and the rest is considered as non-critical loads. The classification is rather subjective and may vary among individuals.

Table 5.7 An example of house function/service ranking and the occupants' corresponding tolerance for power outage r

Index (i)	Appliances	Rank	$r_{req,i}$	$U_{req,i}$
1	HVAC	5	4 days	5%
2	Lighting	3	3 days	1%
3	Clothes Washer	6	1 week	5%
4	Dishwasher	7	1 week	5%
5	Cooking Device	4	2 days	1%
6	Misc. Electric loads	8	1 week	5%
7	Refrigerator	1	4 hours [104]	1%
8	DHW	2	2 days	1%

5.4.2 Identifying dominant parameters

The improved elementary effects method (also referred to as the Morris method) is used in this study to identify dominant parameters. A total of 10 independent samples of the elementary effects are assessed and this leads to a total number of 500 simulation runs.

As shown in Table 3.1 there are five basic reliability performance indices at load-point and this study will use them to represent the off-grid power system's performance in providing reliable power service. Meanwhile the occupant oriented power reliability assessment has classified domestic electricity consumers into 8 subgroups, as shown in Table 5.7. Thus the first three basic reliability indices (failure rate λ, outage hour r, and power unavailability U) will be estimated for every consumer while the last two, energy based, indices will be estimated with respect to the whole house. Therefore a total of 26 reliability performance indices are used in the studies presented.

However, one should be aware that all five basic reliability indices mentioned above except outage hour r are indices on a yearly basis, which means that a power reliability analysis will only return one outcome per sample year. For outage hour r since there might be multiple times of power interruption and each of them will contribute to a record of outage hour. Thus a power reliability analysis will return a vector of outage hour per sample year. This nonmonotonic mapping between a sample year and system response (i.e. outage hour r) prevents the application of the Morris method which requires a monotonic mapping between a Morris experiment sample and a system response. Therefore the maximum consecutive outage hour $\max(r)$ within a year will be used instead of outage hour r for the following sensitivity analysis.

Table 5.8 shows the overall 10 dominant parameters for all chosen reliability PIs in this case study. The uncertain parameters related to the solar energy system show a significant impact on overall power reliability. The building envelope thermal resistance loss due to the existence of thermal bridge also plays a significant role in power reliability.

Table 5.8 The top 10 dominant uncertain parameters

Rank	Parameter index	Parameter name
1	36	PV efficiency loss
2	48	Thermal bridge
3	39	Battery efficiency
4	29	Internal heat transfer coefficient – walls
5	30	The Normalized leakage area
6	47	Ground albedo
7	37	Inverter efficiency
8	38	Charger regulator efficiency
9	43	The radiant temperature of surrounding environments
10	20	The total solar transmittance – ETFE roof

In order to verify whether the set of 10 uncertain parameters shown in Table 5.8 account for most of the variability of all power reliability PIs, a validation study is conducted using MC method with a sample number of 2000 (instead of 500). The selection of a larger sample size (i.e. 2000) is to avoid variations of power reliability PIs caused by the approximation of stochastic process itself (i.e. the MC method). Three sample matrices are built. The first sample (S1) contains all 49 uncertain parameters in Table 5.6. The second sample (S2) is identical to S1 for the 10 parameters shown in Table 5.8 but contains reference values for the remaining parameters. The third sample (S3) is a complementary matrix to S2: reference values for 10 parameters in Table 5.8 while identical to S1 for the rest of the uncertain parameters. Table 5.9 shows that variance obtained with S2 for all 26 PIs account for more than 94% of the total variance that results from S1 (with an exception to maximum outage hour $PI_9 \sim PI_{16}$ as their variances are dominated by weather). The variance obtained from S3 accounts for less

than 0.5% of the total variance. The results confirm the dominant position of the selected 10 parameters in Table 5.8.

Table 5.9 Verification of the screening results using elementary effects method

PI index	PI	$Var(S1)$	$Var(S2)$	$Var(S3)$	$\frac{Var(S2)}{Var(S1)}$ (%)	$\frac{Var(S3)}{Var(S1)}$ (%)
1	λ_1	9189.24	8658.49	45.65	94.22%	0.50%
2	λ_2	2998.37	2900.04	2.58	96.72%	0.09%
3	λ_3	8601.93	8092.00	46.15	94.07%	0.54%
4	λ_4	8374.95	7902.14	47.08	94.35%	0.56%
5	λ_5	3039.17	2931.38	1.76	96.45%	0.06%
6	λ_6	6049.29	5741.08	46.75	94.90%	0.77%
7	λ_7	1869.16	1812.10	3.32	96.95%	0.18%
8	λ_8	1813.41	1761.76	2.65	97.15%	0.15%
9	r_1	0.0976	0.1036	0.0647	106.10%	66.29%
10	r_2	0.0956	0.0921	0.0679	96.38%	71.05%
11	r_3	0.1075	0.1097	0.0638	102.02%	59.34%
12	r_4	0.1118	0.1135	0.0644	101.47%	57.59%
13	r_5	0.0864	0.0918	0.0480	106.21%	55.52%
14	r_6	0.6256	0.4464	0.0391	71.35%	6.25%
15	r_7	0.0948	0.0835	0.0511	88.08%	53.88%
16	r_8	0.1061	0.1051	0.0382	99.06%	36.02%
17	U_1	0.0013	0.0012	0.0000	94.18%	0.09%
18	U_2	0.0011	0.0011	0.0000	94.27%	0.08%
19	U_3	0.0013	0.0012	0.0000	94.21%	0.09%

Table 5.9 (continued)

20	U_4	0.0013	0.0012	0.0000	94.19%	0.09%
21	U_5	0.0012	0.0011	0.0000	94.25%	0.08%
22	U_6	0.0014	0.0013	0.0000	94.14%	0.09%
23	U_7	0.0010	0.0009	0.0000	94.70%	0.09%
24	U_8	0.0010	0.0009	0.0000	94.69%	0.09%
25	EW	445816.01	445621.83	1969.75	99.96%	0.44%
26	EN	23296.86	21956.50	34.68	94.25%	0.15%

5.4.3 Accuracy of Monte-Carlo simulation

In order to investigate the convergence of LHS technique and to find the most computationally economic sampling number the same building simulation model has been analyzed using different sample sizes ranging from 1 to 500. Three basic reliability indices (failure rate λ, outage duration r, and annual unavailability U) and two energy indices (energy not supplied ENS and energy wasted EW) are evaluated at each MC simulation when a different LHS sample size is chosen. As reviewed in Chapter 3 the parameter coefficient of variation (CoV) is chosen to evaluate the accuracy level of a MC simulation. The values of CoV are calculated according to equation (3-10) and compared to the selected CoV tolerance of 0.05. Figure 5.8, Figure 5.9, and Figure 5.10 show the plot of CoV value as a function of the LHS sample size for all 26 concerned PIs. It indicates that a sampling number of 200 will meet the accuracy requirement of MC simulations for all the concerned PIs.

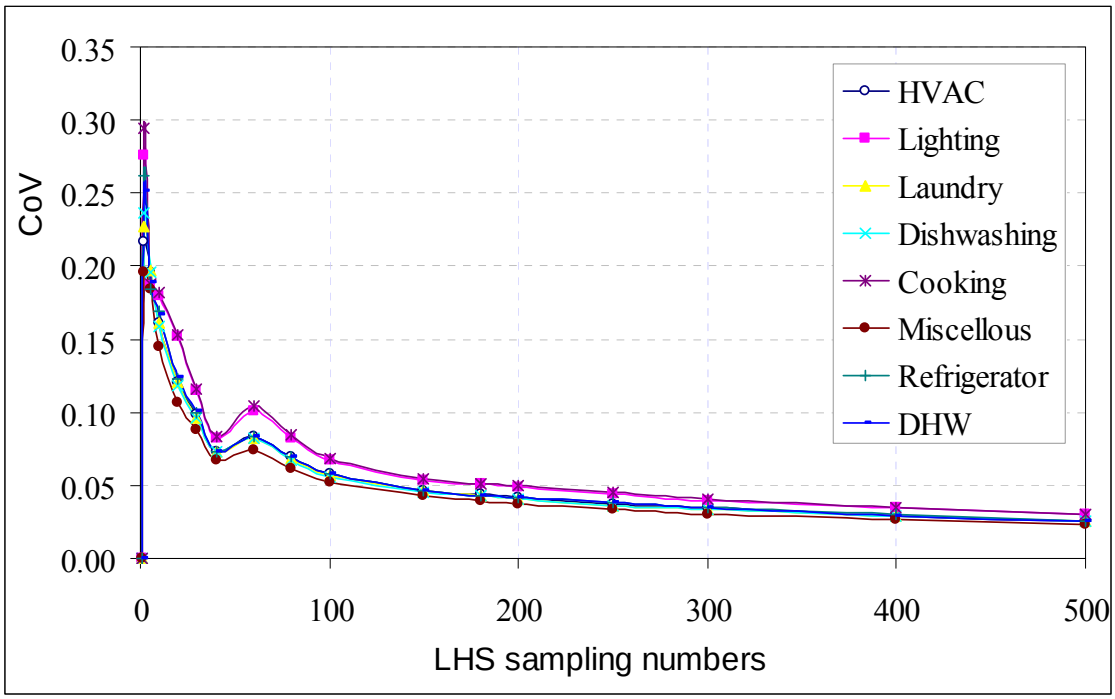

Figure 5.8 The CoV values of λ_i $(i = 1 \sim 8)$ corresponding to different LHS sampling numbers

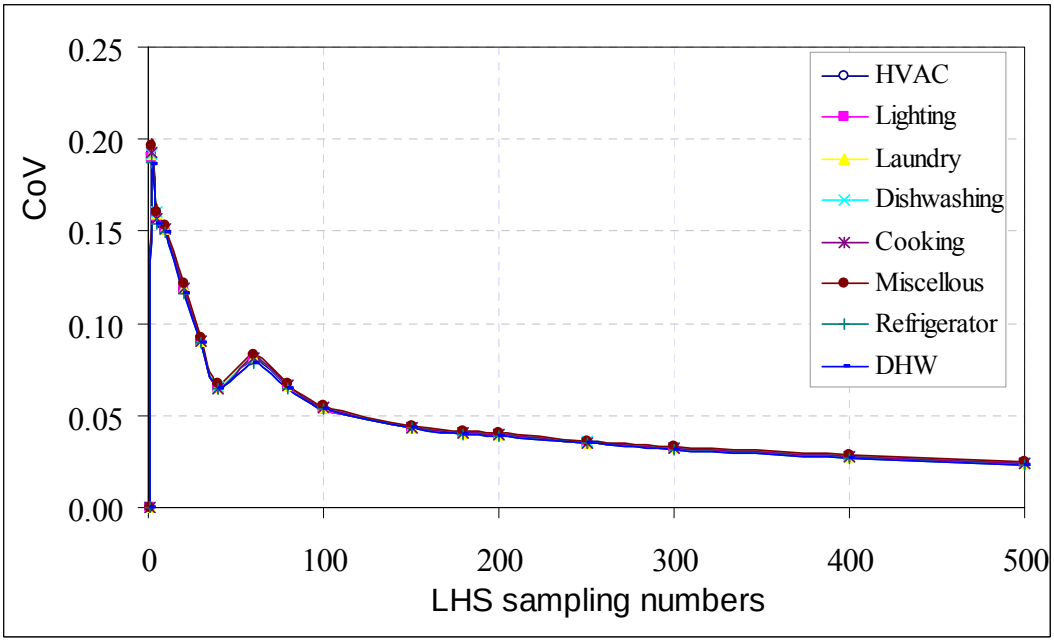

Figure 5.9 The CoV values of U_i $(i = 1 \sim 8)$ corresponding to different LHS sampling numbers

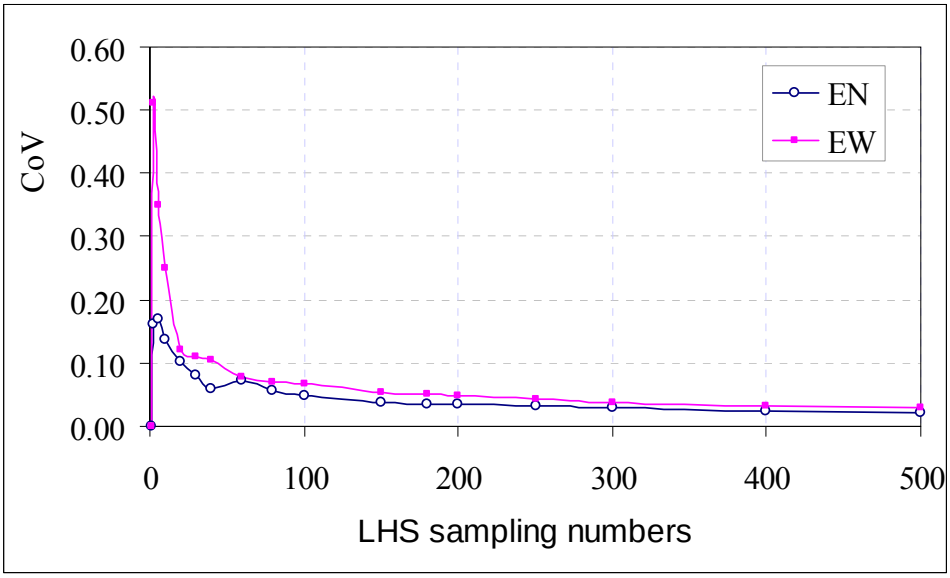

Figure 5.10 The CoV values of *EW* and *EN* corresponding to different LHS sampling numbers

5.4.4 Probability distribution of uncertain parameters

As discussed in Chapter 4 appropriate PDFs will be developed to quantity uncertainty in building energy systems. Macdonald has reviewed a few types of PDFs that are commonly used in uncertainty studies in building technology research and has given corresponding examples [62]. Below is a short summary of Macdonald's recommendations on typical PDF selection in building research area.

- Uniform distribution

The even distribution is a bounded continuous PDF where the probability of the variable taking a value between the bounds is equal. The distribution is the most suitable for modeling systematic errors that are not random and therefore the true value is equally spread over the given range.

- Normal distribution

As described in previous chapters the normal distribution is the most appropriate distribution for parameters quantified through measurements, including most of the material properties.

- Triangular distribution

Like uniform distribution the triangular distribution is also a bounded continuous distribution. In the building simulation context it is very useful as it can be easily described by minimum, maximum, and most likely values (often the typical values). Therefore it offers an easy transition from deterministic building simulation (where typical "reference" values are used) to uncertainty studies using building simulation (where uncertainty ranges are quantified).

- Log-normal distribution

The log-normal distribution is produced when multiple variables with normal distribution are combined as a product. For example the parameter mC_p of building envelope component in Table 5.6 is the result of the product of two measurements and thus will be log-normally distributed. However for small standard deviations the log-normal distribution can be approximated by the normal distribution. The log-normal distribution can not produce negative values and thus is unbounded towards positive infinity.

Table 5.10 shows the PDFs for all 10 dominant uncertain parameters selected and their corresponding PDF model parameters. For the normal distribution "Par1" and "Par2" refer to the mean and standard deviation. For uniform distribution "Par1" and "Par2" refer to the minimum and the maximum.

Table 5.10 the PDFs of the selected 10 uncertain parameters

Index	Variables	PDF	Par1	Par2
20	Roof - solar transmittance	Norm	0.18	0.02
29	internal heat transfer coefficient - wall	Uniform	1.59	4.10
30	Normalized leakage area	Norm	0.30	0.13
36	PV - environmental factor	Norm	0.84	0.08
37	Inverter efficiency	Uniform	0.92	0.97
38	Charge regulator efficiency	Uniform	0.90	0.95
39	battery efficiency	Uniform	0.70	0.84
43	Radiant temperature of surrounding environments	Norm	0.00	1.67
47	Ground - albedo	Uniform	0.15	0.30
48	thermal bridge - U	Uniform	66.40	99.60

5.4.5 Reliability assessment algorithm

Figure 5.11 shows the algorithm of the power reliability assessment. First the LHS generator generates the desired number of samples to approximate the stochastic process in power reliability studies. For each sample GTSim will simulate the corresponding electricity production and consumption information. The smartboard energy distribution module will compare the momentary production and consumption values to judge if there is a power interruption happening to any consumer. The power interruption, if taking place, will be recorded. And the same process will repeat until all the samples from the LHS generator are evaluated.

Figure 5.12 shows the flowchart of the smartboard operation. The smartboard is a sorting algorithm for house electricity distribution. It checks available electricity in the beginning of each time step and then compares the value against the individual end-user electricity demand. The comparison is executed in the sequence defined by the present rank based

on users' preference input, starting from the highest rank to the lowest one until either the available electricity runs out or all the end-users are served.

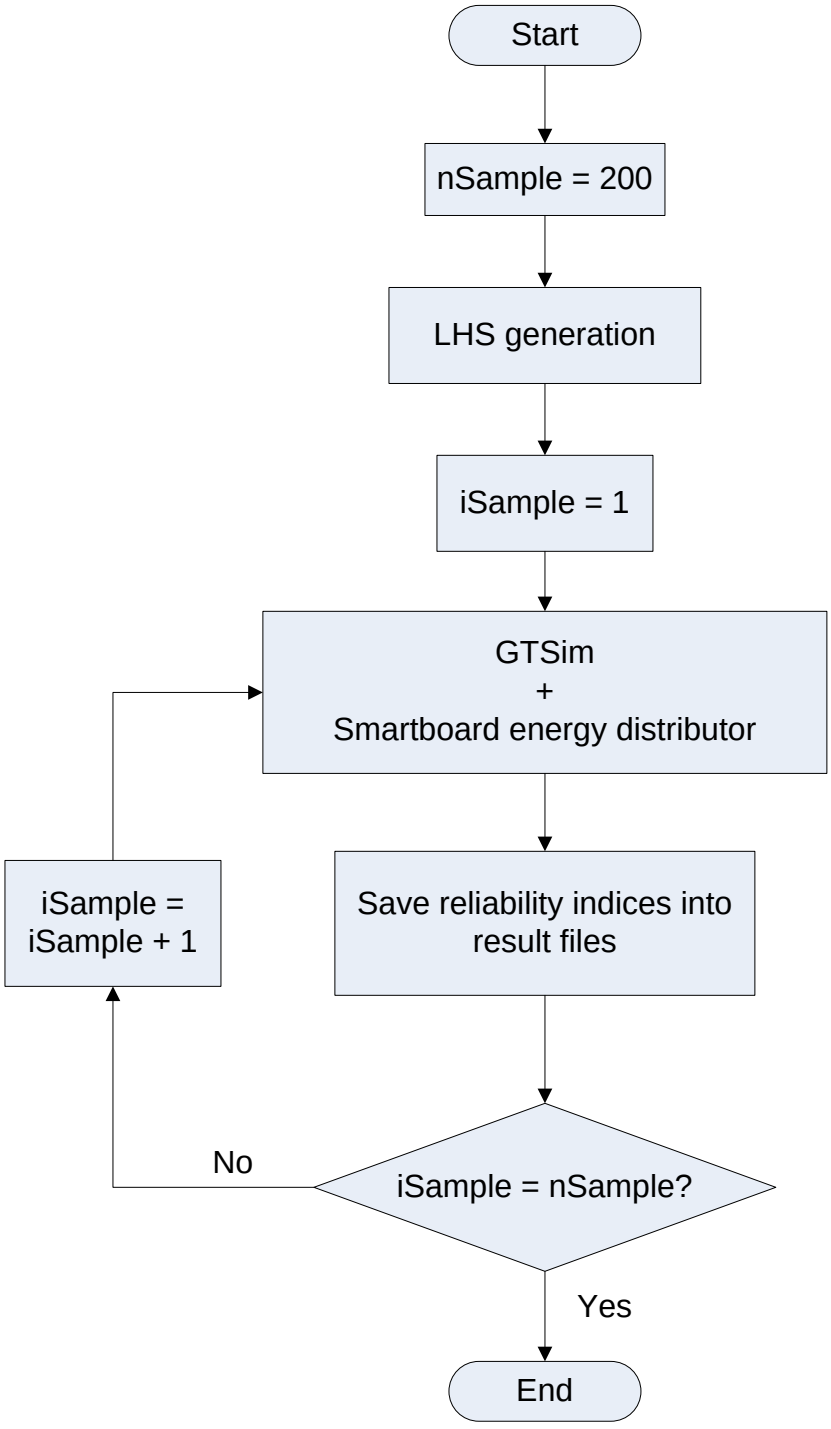

Figure 5.11 The diagram of computational power reliability assessment

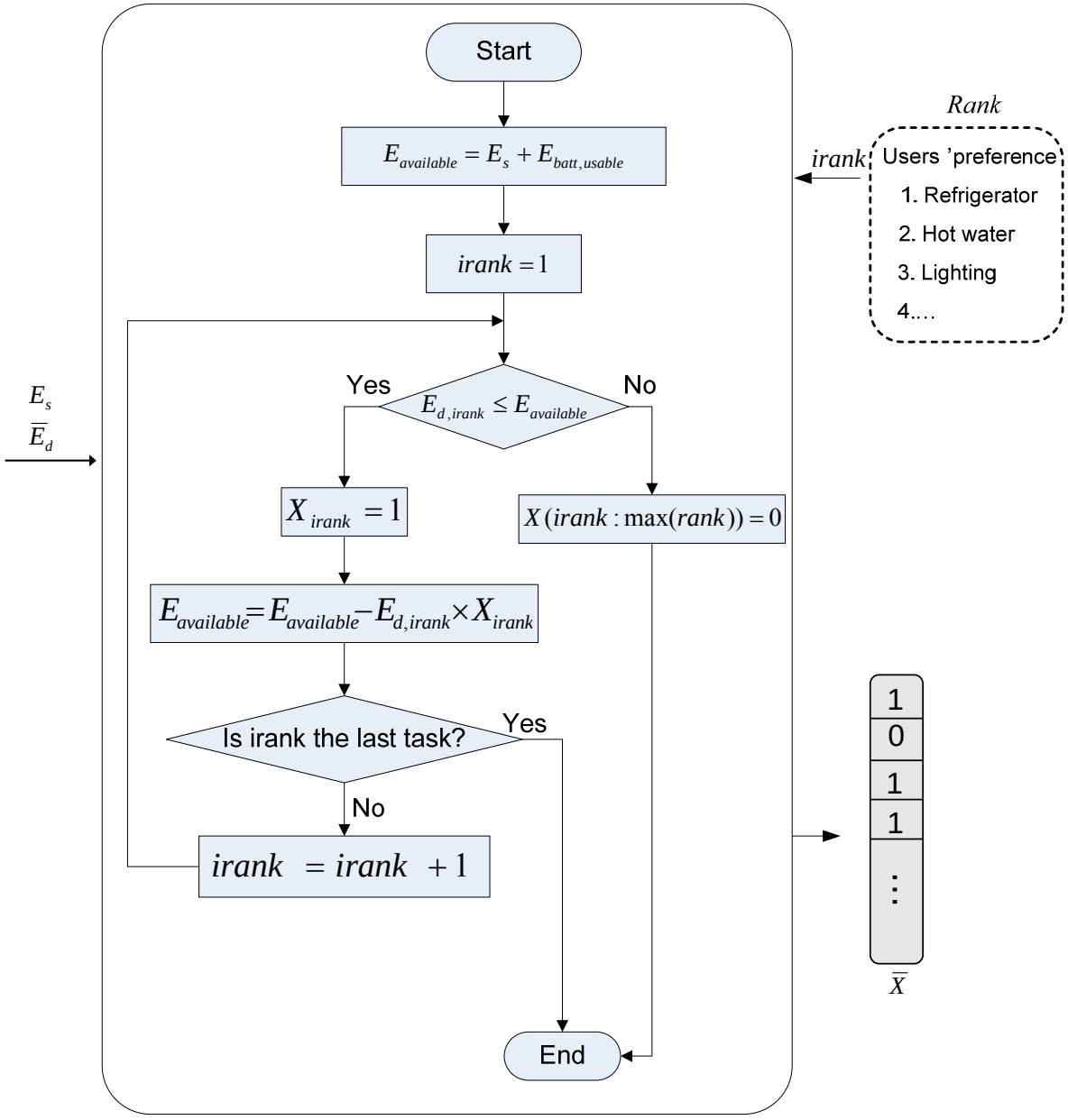

Figure 5.12 The flowchart of the smartboard operation

5.4.6 Reliability assessment results

An occupant-oriented power reliability study is conducted using the MC method. The available electricity is distributed to meet each residential power need according to the occupant's preference listed in Table 5.7. The selected 10 uncertain parameters are

quantified based on literature studies and entered into the MC simulation for uncertainty propagations. A sample size of 200 has been used in the LHS sampling to ensure the required accuracy level of the MC method. Two risk indices, regarding outage hour r and power unavailability U, are calculated based on Equation 5-2 and Equation 5-3.

$$risk(r_i) = 1 - \Pr(r_i \le r_{i,req}) \tag{5-2}$$

$$risk(U_i) = 1 - \Pr(U_i \le U_{i,req}) \tag{5-3}$$

Figure 5.13 to Figure 5.17 shows the histogram plots of five basic reliability indices (the refrigerator is chosen as an example of failure rate λ, outage hour r, unavailability U). Using the reliability criteria shown in Table 5.7 both power reliability and risk have been calculated in terms of outage hour r and unavailability U, as shown in Table 5.11 and Table 5.12 respectively. Results indicate that the refrigerator has a 61% chance that its outage hour will be larger than the threshold which is 4 hours as shown in Table 5.7. This may represent a relatively big risk to take for most of the occupants. All the other appliances are "safe" in terms of outage hour constraints, mostly because occupants have a larger tolerance with respect to their outage. An easy and practical way to resolve the refrigerator problem is to always reserve a certain level of electricity in the battery bank to ensure power supply to the refrigerator. As for the risk in terms of power unavailability (Table 5.12), all appliances have the risk of unacceptable power unavailability no less than 65% which most of occupants will perceive as a relatively great risk. Figure 5.16 suggests there is a significant energy waste due to the temporary mismatches of load and supply. The expected energy waste $E(EW)$ is more than two times larger than the expected energy need $E(EN)$ and it indicates that a certain adjustment in the system

components could lead to a better match, i.e. help increase system power reliability without increasing costs. This issue will be studied in the later chapters.

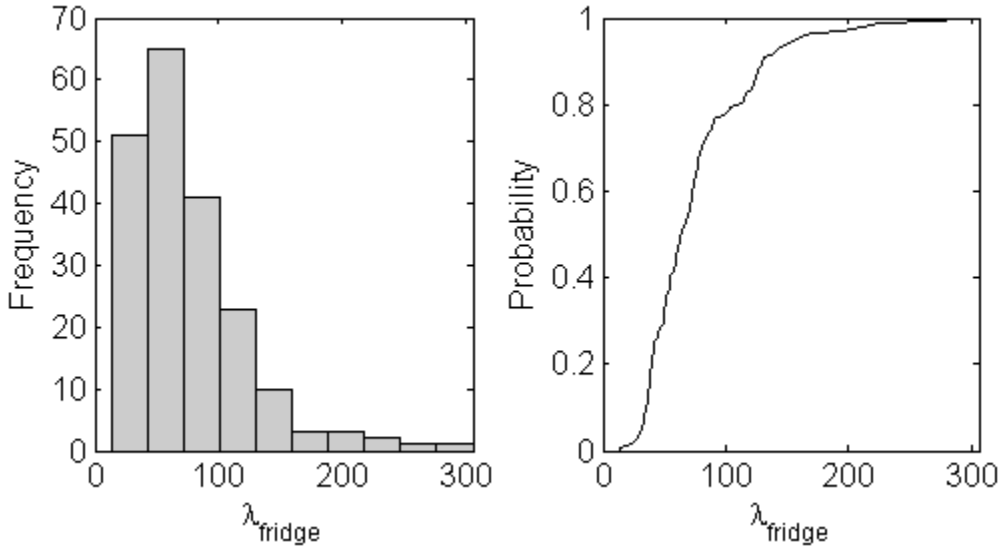

Figure 5.13 The histogram plot of λ_{fridge} (left) and its cumulative probability function plot (right)

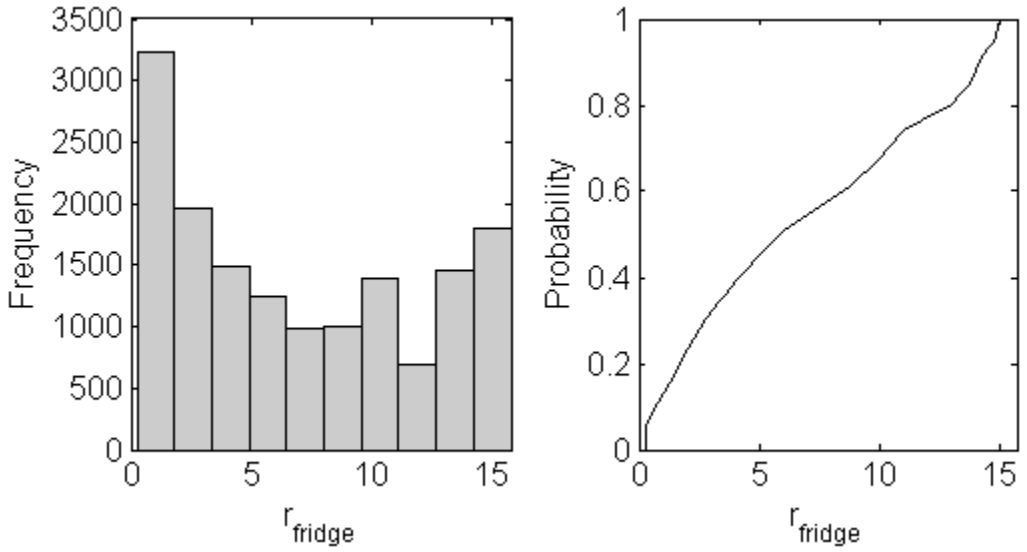

Figure 5.14 The histogram plot of r_{fridge} (left) and its cumulative probability function plot (right)

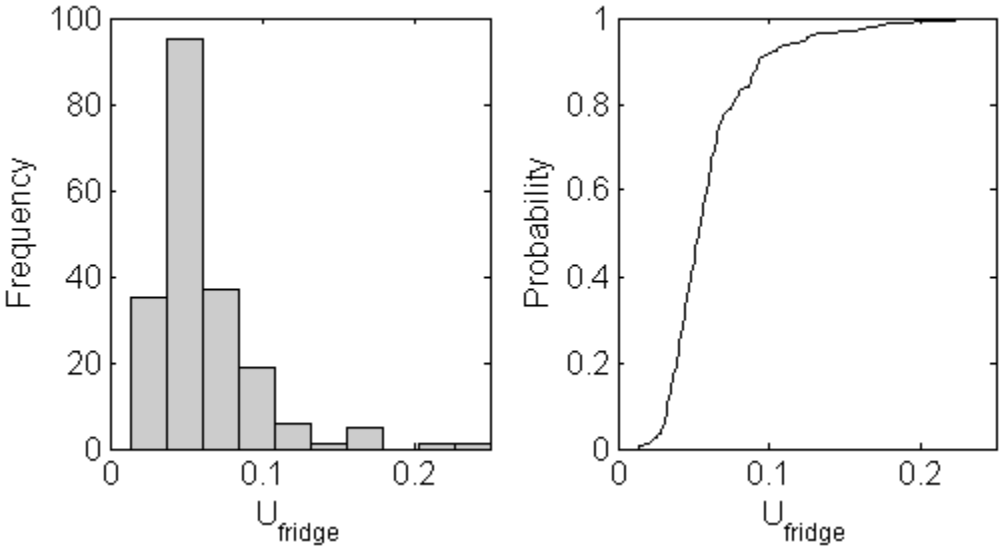

Figure 5.15 The histogram plot of U_{fridge} (left) and its cumulative probability function plot (right)

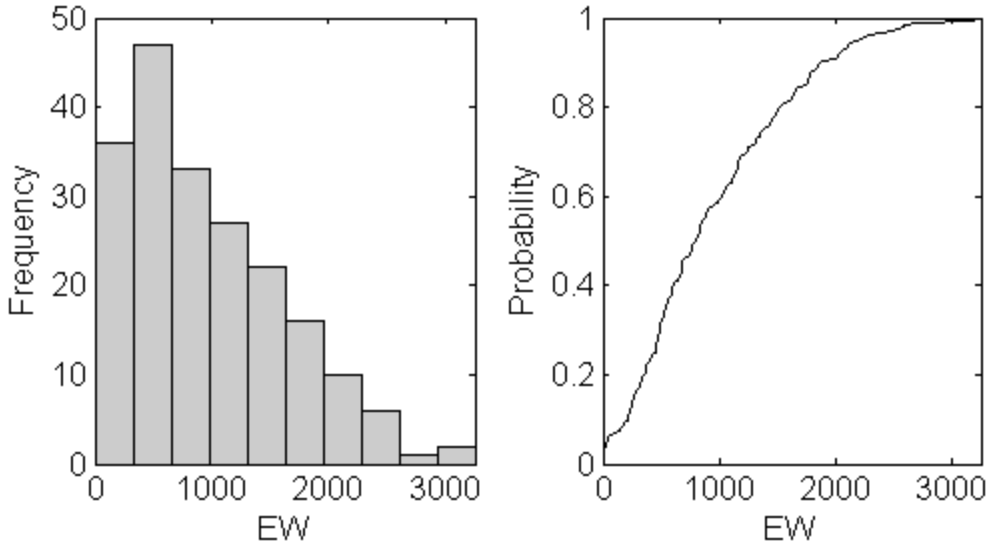

Figure 5.16 The histogram plot of EW (left) and its cumulative probability function plot (right)

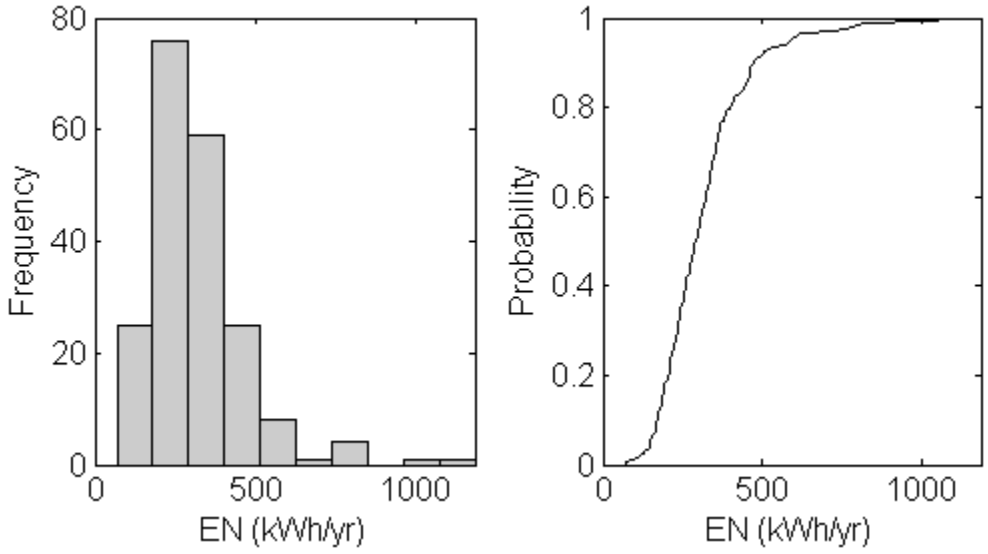

Figure 5.17 The histogram plot of EN (left) and its cumulative probability function plot (right)

Table 5.11 A summary of risk that violates occupants' tolerance in terms of r

Index (i)	Appliances	$\Pr(r_i \le r_{i,req})$	$risk(r_i)$
1	HVAC	100%	0%
2	Lighting	100%	0%
3	Clothes Washer	100%	0%
4	Dishwasher	100%	0%
5	Cooking Device	100%	0%
6	Misc. Electric loads	100%	0%
7	Refrigerator	39%	61%
8	DHW	100%	0%

Table 5.12 A summary of risk that violates occupants' tolerance in terms of U

Index (i)	Appliances	$\Pr(U_i \le U_{i,req})$	$risk(U_i)$
1	HVAC	33%	67%
2	Lighting	0%	100%
3	Clothes Washer	33%	67%

Table 5.12 (continued)

4	Dishwasher	33%	67%
5	Cooking Device	0%	100%
6	Misc. Electric loads	30%	70%
7	Refrigerator	0%	100%
8	DHW	0%	100%

5.5 Sensitivity analysis: modelling of external heat transfer coefficients

As discussed earlier in Chapter 4 it is extremely complicated to model external wind induced convective heat transfer coefficients accurately. This is relevant as outcomes could vary significantly if different external wind convective heat transfer coefficient models are used. Earlier in this chapter it was stated that GTSim uses the MoWiTT model. This section describes a power reliability analysis similar to the one in Section 5.4 but now use the Palyvos linear model to verify the effect that could be caused by a different external wind convective heat transfer coefficient model. Figure 5.18 shows a comparison between the MoWiTT model and the Palyvos linear model. It shows that the Palyvos model predicts larger external wind convective heat transfer coefficients at all wind speeds compared to MoWiTT model. It is hard to judge which model provides more accurate results due to the complexity of the heat transfer phenomena. This section intends to find how much effect the use a different convective heat transfer model will have on power reliability estimates.

The parameter screening using the elementary effects method (i.e. Morris method) show that none of the uncertain parameters related to Palyvos turns out to be the dominant

parameter and the following validation study also confirms the ranking shown in Table 5.8.

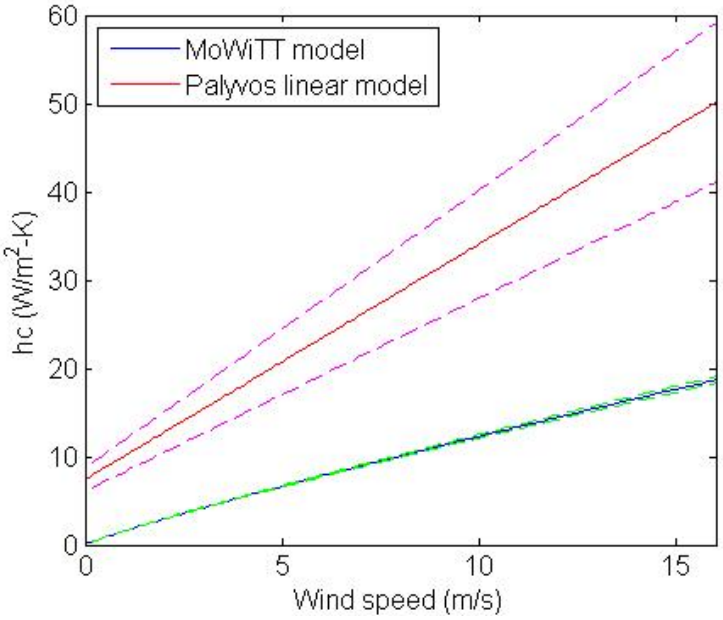

Figure 5.18 The comparison of external wind convective heat transfer coefficients from the MoWiTT model and the Palyvos linear model (windward) – the dotted lines represents the upper and lower bounds of the model outputs

Table 5.13 and Table 5.14 show the comparison of $risk(r)$ and $risk(U)$ respectively. Large convection heat loss/gain requires more active heating/cooling and further requires more power input to the house HVAC system. Therefore when the Palyvos model is used there is a larger power demand from the HVAC systems, which leads to higher risks in terms of both power outage and power unavailability. This risk increase is at the maximum of 5%. This study considers that the associated risk increase, caused by choosing a different external convective heat transfer coefficient, can be neglected. Thus this study will continue using the MoWiTT model for the estimate of external convective heat transfer coefficients and ignore the uncertainty brought on by the selection of a specific model. This again stipulates the necessity for model uncertainty inspection where

it has been proven that the risk assessment is highly dependent on better knowledge of the uncertainty. In this particular case there seems to be no immediate need for this.

Table 5.13 A comparison of $risk(r)$ using two different external convective heat transfer coefficient models

Index (i)	Appliances	MoWiTT model	Palyvos Model
1	HVAC	0%	0%
2	Lighting	0%	0%
3	Clothes Washer	0%	0%
4	Dishwasher	0%	0%
5	Cooking Device	0%	0%
6	Misc. Electric loads	0%	0%
7	Refrigerator	61%	62%
8	DHW	0%	0%

Table 5.14 A comparison of $risk(U)$ using two different external convective heat transfer coefficient models

Index (i)	Appliances	MoWiTT model	Palyvos Model
1	HVAC	67%	72%
2	Lighting	100%	100%
3	Clothes Washer	67%	72%
4	Dishwasher	67%	72%
5	Cooking Device	100%	100%
6	Misc. Electric loads	70%	74%
7	Refrigerator	100%	100%
8	DHW	100%	100%

5.6 Sensitivity analysis: interior thermal mass

As described in Chapter 4 the extra thermal mass contributed by furniture and interior partitions is difficult to estimate. An accurate estimate can be only obtained through careful model calibration against onsite measurements. Industry practice shows that the typical extra thermal mass from furniture and interior partitions is five times the thermal mass from indoor air for residential buildings and three times of indoor air mass for office buildings [105]. In Section 5.4 the typical value of 5 has been used. This section will investigate the influence of interior thermal mass on power reliability. Equation 5-4 shows the equation of calculating the total thermal capacity of building spaces in this case study.

$$Total\ Mass = (1 + f) \times AirMass \tag{5-4}$$

Where,

$AirMass$ the total thermal capacity of indoor air ($= \rho_{air} V_{room} C_{p,air}$);

f the ratio of the total thermal capacities from furniture and interior partitions and the thermal capacity of indoor air.

Table 5.15 and Table 5.16 show the comparisons of risk indices with different thermal mass levels (contributed from furniture and interior building partitions). It shows that the accuracy of internal mass level estimate does not impact the power risk significantly in terms of the outage hour but it does influence the risk estimate significantly in terms of power unavailability. A maximal risk difference of up to 11% in $Risk(U)$ can be observed in the sensitivity analysis, as shown in Table 5.16. Similar variations can be also observed in the expected values of all basic reliability indices, as shown in Table 5.17. Therefore internal mass level contributed by interior walls and furniture will be

considered as an uncertain variable and included in the power reliability analysis in the following studies. A normal distribution will be assumed for this uncertain variable with a mean of 5. Table 5.18 shows an updated list of uncertain parameters for the reliability studies in the rest of this thesis.

Table 5.15 A comparison of $risk(r)$ with different thermal mass levels

Index (i)	$f=1$	$f=2$	$f=3$	$f=4$	$f=5$	$f=6$	$f=7$	$f=8$	$f=9$
1	0%	0%	0%	0%	0%	0%	0%	0%	0%
2	0%	0%	0%	0%	0%	0%	0%	0%	0%
3	0%	0%	0%	0%	0%	0%	0%	0%	0%
4	0%	0%	0%	0%	0%	0%	0%	0%	0%
5	0%	0%	0%	0%	0%	0%	0%	0%	0%
6	0%	0%	0%	0%	0%	0%	0%	0%	0%
7	61%	62%	62%	61%	61%	62%	62%	62%	61%
8	0%	0%	0%	0%	0%	0%	0%	0%	0%

Table 5.16 A comparison of $risk(U)$ with different thermal mass levels

Index (i)	$f=1$	$f=2$	$f=3$	$f=4$	$f=5$	$f=6$	$f=7$	$f=8$	$f=9$
1	72%	70%	69%	68%	67%	67%	65%	61%	64%
2	100%	100%	100%	100%	100%	100%	100%	100%	100%
3	72%	70%	69%	69%	67%	67%	65%	61%	64%
4	72%	70%	69%	70%	67%	67%	65%	61%	64%
5	100%	100%	100%	100%	100%	100%	100%	100%	100%
6	73%	71%	71%	71%	70%	68%	67%	64%	65%
7	100%	100%	100%	100%	100%	100%	100%	100%	100%
8	100%	100%	100%	100%	100%	100%	100%	100%	100%

Table 5.17 A comparison of expected reliability PI values with different thermal mass levels

PI index	PI	$f=1$	$f=2$	$f=3$	$f=4$	$f=5$	$f=6$	$f=7$	$f=8$	$f=9$
1	λ_1	105.28	104.72	103.50	101.85	100.56	99.67	98.35	98.17	96.22
2	λ_2	75.40	75.68	75.11	74.01	73.48	73.02	72.59	72.23	71.23
3	λ_3	103.33	103.01	101.92	100.33	99.17	98.29	97.19	96.90	95.01
4	λ_4	103.00	102.67	101.57	100.09	98.91	97.96	96.87	96.63	94.82
5	λ_5	75.40	75.67	75.07	74.01	73.47	73.02	72.54	72.23	71.26
6	λ_6	96.68	96.54	95.65	94.19	93.22	92.51	91.57	91.09	89.52
7	λ_7	78.26	78.58	78.08	76.88	76.34	75.83	75.36	74.84	73.86
8	λ_8	77.06	77.53	77.00	75.68	75.15	74.77	74.37	73.86	72.83
9	r_1	5.86	5.95	5.98	5.93	5.95	6.05	6.07	6.04	6.02
10	r_2	7.55	7.61	7.62	7.55	7.54	7.66	7.64	7.63	7.55
11	r_3	6.01	6.09	6.11	6.06	6.07	6.17	6.19	6.16	6.14
12	r_4	6.04	6.11	6.14	6.08	6.10	6.20	6.22	6.19	6.16
13	r_5	7.59	7.64	7.65	7.58	7.57	7.69	7.68	7.66	7.58
14	r_6	6.54	6.62	6.64	6.58	6.59	6.69	6.70	6.70	6.65
15	r_7	6.97	7.02	7.02	6.96	6.95	7.05	7.04	7.05	6.98
16	r_8	7.15	7.18	7.18	7.14	7.13	7.22	7.20	7.21	7.15
17	U_1	0.07	0.07	0.07	0.07	0.07	0.07	0.07	0.07	0.07
18	U_2	0.07	0.07	0.07	0.06	0.06	0.06	0.06	0.06	0.06
19	U_3	0.07	0.07	0.07	0.07	0.07	0.07	0.07	0.07	0.07
20	U_4	0.07	0.07	0.07	0.07	0.07	0.07	0.07	0.07	0.07
21	U_5	0.07	0.07	0.07	0.06	0.06	0.06	0.06	0.06	0.06
22	U_6	0.07	0.07	0.07	0.07	0.07	0.07	0.07	0.07	0.07
23	U_7	0.06	0.06	0.06	0.06	0.06	0.06	0.06	0.06	0.06

Table 5.17 (continued)

24	U_8	0.06	0.06	0.06	0.06	0.06	0.06	0.06	0.06	0.06
25	*EW*	925	933	938	943	951	962	971	983	987
26	*EN*	329	330	327	321	318	318	316	312	307

Table 5.18 The PDFs of the selected 11 uncertain parameters

Variables	PDF	Par1	Par2
Roof - solar transmittance	Norm	0.18	0.02
Internal heat transfer coefficient - wall	Uniform	1.59	4.10
Normalized leakage area	Norm	0.30	0.13
PV - environmental factor	Norm	0.84	0.08
Inverter efficiency	Uniform	0.92	0.97
Charge regulator efficiency	Uniform	0.90	0.95
Battery efficiency	Uniform	0.70	0.84
Radiant temperature of surrounding environments	Norm	0.00	1.67
Ground - albedo	Uniform	0.15	0.30
Thermal bridge - U	Uniform	66.40	99.60
The extra internal mass - f	Norm	5.00	1.30

CHAPTER 6 MODEL-BASED PREDICTIVE CONTROL

6.1 Introduction

One major challenge in energy management when renewable energy systems are involved is to plan the operation against an unknown power generation amount. Wind and solar power generation is highly dependent on the condition of local natural resources (largely determined by the weather condition) and has only a limited level of predictability. This issue becomes even more difficult to resolve in off-grid solar house operation where both power generation and consumption vary with ambient weather condition (the energy demand for heating and cooling are the most directly correlated with the weather conditions). Conventional operation based on typical control logic cannot always guarantee a workable solution and in reality people often avoid this risk by purchasing either a backup generator or a large battery to prepare them for the worst situation. This chapter will take a closer look at how advanced control techniques may avoid the need for these extra investments.

6.2 Building automation system

Control engineering, by definition, is the engineering discipline that focuses on mathematical modeling of the systems of a diverse nature, analyzing their dynamic behavior, and using control theory to create a controller that will cause systems to behave in a desired manner [106].

Building control systems firstly appeared as pneumatic control where mechanical engineers could use their experience with air properties to control the flow of

heated/cooled air so that residents would stay in their comfort range. Pneumatic technologies dominated the industry until the late 1970s even in large commercial buildings [107]. As building science progressed and electronic technologies advanced computerized controllers became common. The current trend in building control is to use centralized monitoring and control systems, usually packaged with full blown building automation systems (BAS). The rapid advances in microelectronics and computer technology make BAS technologically feasible whereas increased labor costs make BAS not only economically feasible but economically necessary.

As building systems become more complicated, the BAS is required to process more and more complex information. They operate more building components to control multiple tasks, including maintaining thermal comfort and minimizing energy consumptions (or more precisely, minimizing utility costs, as load shedding and other paradigms reduce costs without necessarily saving energy). To stay competitive, buildings will need to operate optimally all the time and conventional controllers (proportional/integral/derivative, i.e. PID controllers) are challenged as means of optimal and flexible process control.

There are a few advanced control concepts that have been researched to solve the current multi-task building operation problem under dynamic operating conditions. Such approaches include model-based predictive control (MBPC), neural networks, fuzzy control, and adaptive control. More details about these advanced control concepts can be found in for instance the books by Camacho et al. [108] and Passino [109]. This research will focus on how MBPC can be used in off-grid houses to achieve better energy management. The MBPC is chosen because its capability in prediction a system's future

performance in advance. This ability in prediction also allows optimal control to be concluded within future time horizons which is the exact challenge that building operators are facing, especially when renewable systems onsite are part of the supply system.

6.3 The Model Based Predictive Control

The MBPC is broadly characterized as "proactive" in contrast to "reactive" that conventional control is considered to be. In MBPC a change in the state of a control device is decided based on the consideration of a number of candidate control options and the comparative evaluation of the simulated outcomes for these options [110]. The MBPC has been applied in various disciplines, including optimal control, stochastic control, and multi-variable control. In the area of building research, Kelly predicted that intelligent supervisory control system that use real-time building system models, expert systems, or a combination of both would probably be a "hot" research topic over the next few years in 1988 [107]. The MBPC has not attracted enough attention until enough computing power became available to support the novel controller.

Camacho et al. summarize the three main characteristics of MBPC based on its applications in the process industry, including 1) the explicit use of a model to predict the process output at future time instants, 2) calculation of a control sequence that minimizes a certain objective function, and 3) a receding strategy so that at each instant the horizon is shifted towards the future. The application of MBPC in the building industry is still in an experimental stage and is mainly investigated in research projects. Below is a short review of recent studies in this field. Special attention is devoted to inspect their model types and optimization algorithms.

Van Schijidel [111] has tried to apply a model-based optimal control to a complex hospital with a combined heating power and cooling plant. MBPC provides three modes of optimization of the system operations towards different objectives: a pure economic optimization, a pure energy optimization, and an energy optimization with economic constraints. The building model is based on vector equations for computational efficiency and shown to be time efficient for computation. This research demonstrates how MBPC can be used to optimize system operation towards multiple preset objectives. Wang and Jin [112] have designed another model-based optimal control on a VAV air-conditioning system using genetic algorithms (GA), driven by three objectives: 1) test the GA optimizer, i.e. test the tuning and stability of the strategy; 2) evaluate the performance of the optimal strategy; 3) investigate the effects of the weighting factors in the objective function on the performance of the strategy. In the end, the performance of MBPC is evaluated against a conventional control strategy through simulations. Their results show that the GA algorithm is a convenient tool in searching the optimal settings that minimize overall system cost. Meanwhile it also points out that a good selection of cost function and coefficient of cost function (weight factors) is important when multiple objectives are targeted (for instance thermal comfort and energy savings). The authors describe that this will require a certain number of tests. Sun and Reddy [113] have conducted a similar optimal control research on HVAC systems but using sequential quadratic programming. Their optimal control strategy covers two broad categories: 1) deciding on best operation mode; 2) deciding the optimal set points for local-controllers. The performance of MBPC is evaluated again through simulations but the authors also propose a method to apply

their complex controller in a real-time system which is to develop regression models for each control variable from the control map of that variable.

Zhang and Hanby [114] present recent research of applying a supervisory MBPC to renewable energy system control. The objective of their work is to evaluate the potential of an optimal supervisory control in a building/system that includes both active and passive thermal storage combined with an array of comparatively novel renewable energy systems. Their results indicate that a significant improvement in system operation is achievable through the proposed MBPC which however requires further significant improvements in execution time before it can be put in action to operate real buildings.

Although the MBPC has shown great potential to perform better than conventional control strategies in terms of handling dynamic and complicated operation issues, the benefits are only observed in virtual experiments. How these controllers will perform in actual buildings still remains to be tested on a larger scale. Henze et al. [115] demonstrate their model-based predictive optimal control of active and passive building storage inventory in a test facility in real time. Their supervisory MBPC successfully executes a three-step procedure: 1) short-term weather prediction, 2) optimization of control strategy over the next planning horizon using a calibrated building model, and 3) post-processing of the optimal strategy to yield a control command for the current time step that can be executed in the test facility. Results show that even when the optimal controller is given imperfect weather forecasts and when the building model does not match the actual building behavior perfectly, the measured utility cost savings relative to conventional control strategy can be substantial. This study might be the first onsite real-time

application of MBPC. Table 6.1 gives a summary of all the studies in terms of their simulation environments, optimization algorithms, and evaluation methods.

Table 6.1 A summary of previous studies on simulation-based control

	Simulation environments	Optimization algorithms	Evaluation in simulations	Testing in real-time
Van Schijindel [111]	Matlab	Sequential Quadratic Programming (SQP) optimization	Yes	No
Wang and Jin [112]	TRNSYS (only for building simulation)	Genetic algorithm	Yes	No
Sun and Reddy [113]	Sequential modular simulation	SQP	Yes	No
Zhang and Hanby [114]	Matlab/Simulink	Evolutionary algorithm	Yes	No
Henze et al. [115]	TRNSYS + Matlab	Quasi-Newton method	No	Yes

As the prediction capability of an MBPC is provided by the underlying system model it is critical for a successful MBPC to have a model that represents the system behavior appropriately. During the past few decades researchers have built large building models of different types, in different languages, and for different applications. Choosing appropriate and realistic building models for a certain application is highly dependent on the building modelers' experience and their engineering training. A recent study by Ahmad and Culp [116] shows that before model calibration the discrepancies between the simulated and the measured yearly building energy use varies over ± 30% and the

discrepancies ranges can be as high as ± 90% for individual consumption components such as chilled water, hot water and electricity consumption. Although non-calibrated models can still be very useful in a sensitivity analysis helping to determine trade-offs among multiple equipments it may have low accuracy in predicting energy use in buildings. The MBPC design will lose its advantage in predictability in such case. Moreover building model calibration is not easy as every building is composed of a massive number of components. Different methods for model calibrations have been discussed in previous studies [117-120]. Typically researchers calibrate the model parameters by solving the optimization problem to minimize the gap between simulation results and one or multiple measured dataset(s) under one/multiple experimental scenario(s). Sun and Reddy [121, 122] have conducted a research project with ASHRAE to establish a general analytic framework for calibrating building energy system simulation software/programs that has a firm mathematical and statistical basis. However regardless which calibration technique is used one of the necessary steps will be to compare simulated results and measured results. Since measurements are done under specific operating conditions one will not be able to guarantee the generality of a calibrated model. How to get an appropriate model for a MBPC design will continue to be challenging and more research is necessary.

Another challenge to a successful design of an MBPC is the need of a reliable optimizer when an optimization loop is included. It has to be recognized that in the domain of building simulation almost all building models are nonlinear. As pointed out by Camacho et al. there are two main difficulties when the embedded model in MBPC design is nonlinear [108]:

- The theoretical analysis of certain properties of a closed loop controller design, including stability and robustness, will become very complicated when nonlinear models appear in the formulation. Therefore a full evaluation of the controller design will not be possible and therefore the generality of controllers' performance can not be guaranteed;
- Due to the nonlinearity of the embedded model the objective function of the optimization problem is also nonlinear. It becomes difficult to guarantee the convergence of the algorithm especially within an adequate lapse of time when the MBPC is put online for a deployment. In fact the experimental work by Henze et al. [115] was actually compromised by the fact that the optimization converged on local minima.

6.4 A stochastic model-based predictive controller

The existing trial studies have shown how important it is to have a representative system model in achieving a successful MBPC design in reality. Model calibration has been proposed as a common solution in current practice. However, regardless how thoroughly a system is calibrated there is an intrinsic uncertainty one can not overcome: any future prediction is made based on past observation and is unavoidably associated with a degree of uncertainty [56]. Moreover not only is an appropriate model to represent system behaviors important it is equally important to have an accurate weather prediction model to represent the system's external condition, especially where a renewable energy system is involved. In off-grid cases the future weather condition basically determines the quantity of future energy production and therefore will dominate the operation

scheduling. These difficulties in both model calibration and weather prediction are the main challenges in the development of a MBPC design.

This research intends to face the uncertain nature of system behavior and integrate uncertainty as it is into the predictive controller design. A stochastic model based predictive controller (SMBPC) design is proposed as an alternative to the conventional MBPC design. Figure 6.1 shows the general diagram of the proposed SMBPC design. The SMBPC adopts the general concept of an MBPC and only replaces the conventional deterministic model by a stochastic model. Thus the SMBPC will not try to find a best fit (i.e. a deterministic model) through a series of model calibrations to represent the uncertain system behavior. Instead the SMBPC tries to quantify the range of uncertain behaviors (sometimes uncertain performance). The quantified uncertain future prediction will then be fed into the energy management system (EMS) module which is the decision-making module of a SMBPC. Then the EMS will calculate and export the control sequence as outputs.

Figure 6.2 shows the detailed algorithm of the EMS module. The EMS module accepts the distribution of energy production and energy demands by each individual task as the inputs, together with the preference rank of all tasks from occupants in terms of their subjective importance. According to the preference rank given by users the EMS module will calculate the probability that the energy demand of each individual task can be fulfilled by the installed PV system, from the highest preferred task to the lowest one. If the probability that any task can be done is larger than the probability threshold defined by users, the EMS module will export a positive control signal to the smartboard which will then distribute energy to the authorized task operator (i.e. domestic appliances).

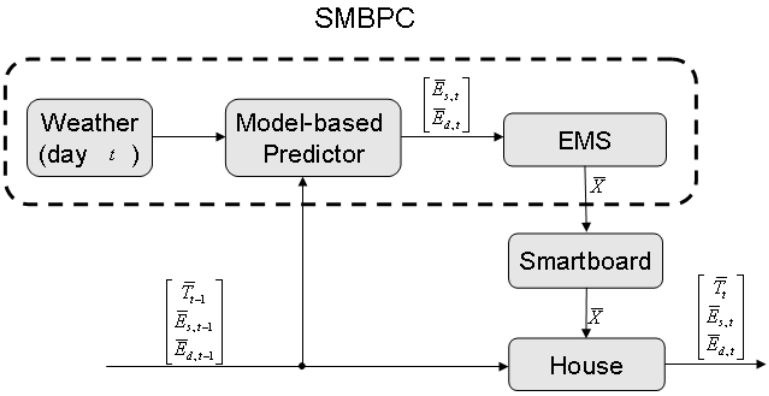

Figure 6.1 A module diagram of the designed SMBPC

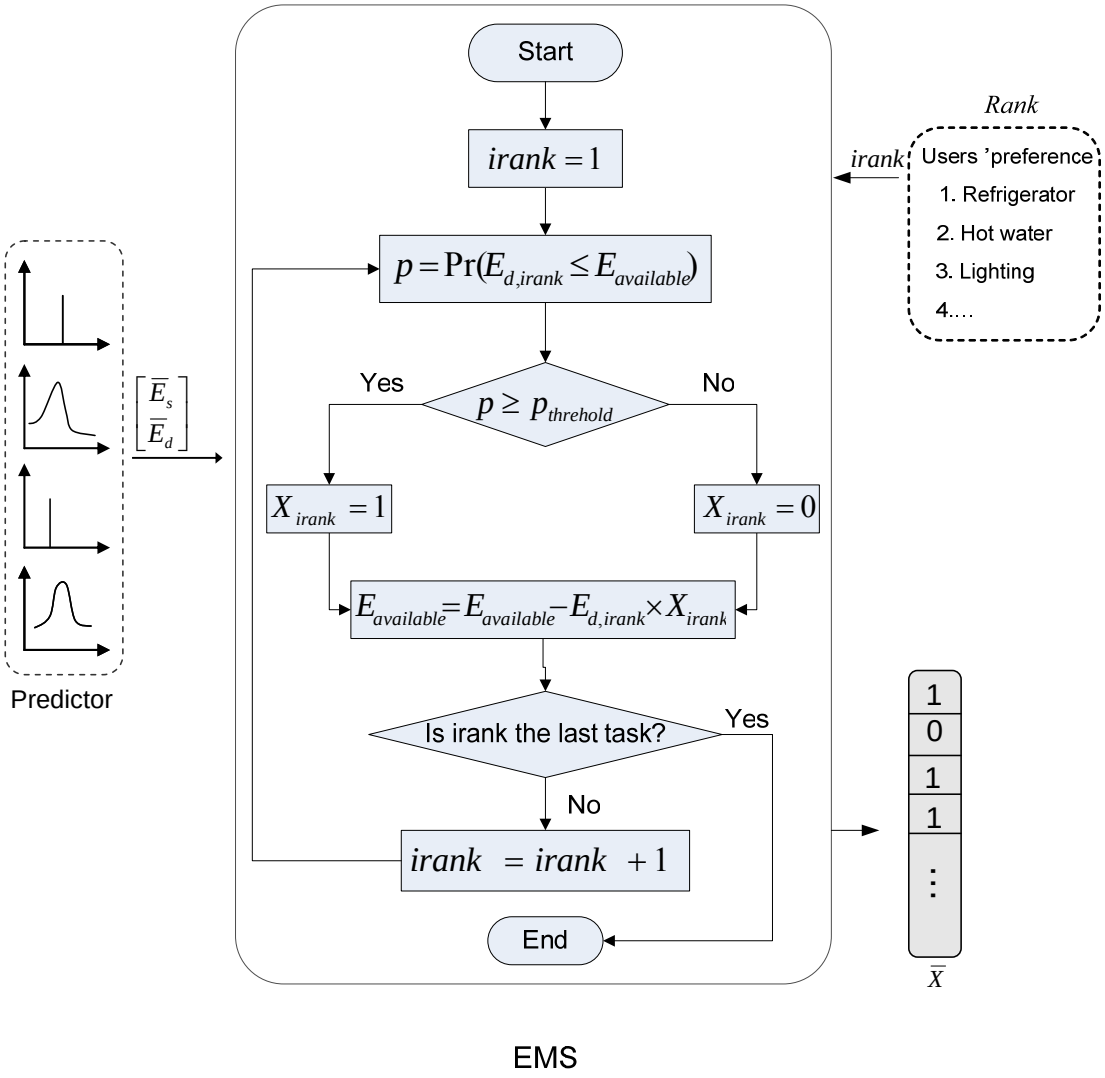

Figure 6.2 The flowchart of the EMS module

In the proposed SMBPC algorithm the model-based predictor uses one day as its time horizon and the EMS module generates daily control signals for the house operation. In other words, the SMBPC has been designed and implemented on a daily basis rather than an hourly basis. This decision is made because of two main reasons:

- Daily total electricity consumption and production have a stronger correlation with weather than hourly values. It reflects the fact that the hourly system performance prediction (i.e. house load and electricity generation in this case) from simulations will most likely have larger errors compared to actual values than is the case with daily estimates. Although the SMBPC design does not require an exact estimate of system performance a reasonable system model is still necessary for its success. The strong correlation between daily energy consumption and production will help future implementation of SMBPC and provide easy diagnosis for possible controller malfunction. In certain situations it may be possible to perform online model calibration which could be used to better quantify the uncertainty of system performance.
- The accuracy of weather forecast decreases when the prediction time horizon increases. The longer the prediction time horizon covers the less reliable the weather forecast is. People often underestimate the adverse effects that an unreliable weather forecast could causes in reality as it is hard to estimate through computer simulations. An effective and accurate 24-hour weather prediction is currently available based on the work by Zhang and Hanby [123]. They propose a short-term weather prediction method using a combination of local observation

data and meteorological forecast data which effectively improves the accuracy of the short-term (24 hours) prediction.

6.5 The performance evaluation of the proposed MBPC

The improvement that a SMBPC design could bring to an off-grid solar house in power reliability has been studied through simulations. Figure 6.3 shows the flow diagram of the evaluation process. In this study the power reliability assessment algorithm and the SMBPC algorithm use the same uncertainty information. But one shall be aware that during the operation stage there might be more information available about the system and therefore the system uncertainty shall be further quantified. The more information the SMBPC can access the more accurate decision a SMBPC could make regarding optimal house operation.

The GTSD07 house is used again to study the benefits that an SMBPC could achieve in terms of power reliability. The uncertainty information has remained the same as presented in Chapter 5. The number of LHS samples (*nsample*) is also the same (=200) as used previous chapters.

Figure 6.4, Figure 6.5, and Figure 6.6 show the comparison of failure rate, outage hour, and unavailability in histograms for the house refrigerator which has the highest rank in the users' preference list. As shown in the histograms after implementing the SMBPC the refrigerator failure rate, outage hour, and general unavailability all shift to the left hand side of the histogram which indicate higher occurrences of smaller failure rate, outage hour, and unavailability. The most obvious improvement can be observed in Figure 6.6. The cumulative plot of unavailability for the refrigerator indicates a significant decrease in power unavailability for the refrigerator after implementing the SMBPC.

Figure 6.7 shows the comparison of the power waste in the histogram. There is only very little improvement made in terms of reducing power waste by implementing a SMBPC design. Obviously the energy waste is mainly determined by the system design itself. Figure 6.8 shows the comparison of histograms of the needed energy. The cumulative plot of the needed energy is also shifted to the left and it suggests that the needed energy is reduced by implementing the SMBPC. In another word the SMBPC has helped manage energy flow more efficiently in the studied off-grid solar house.

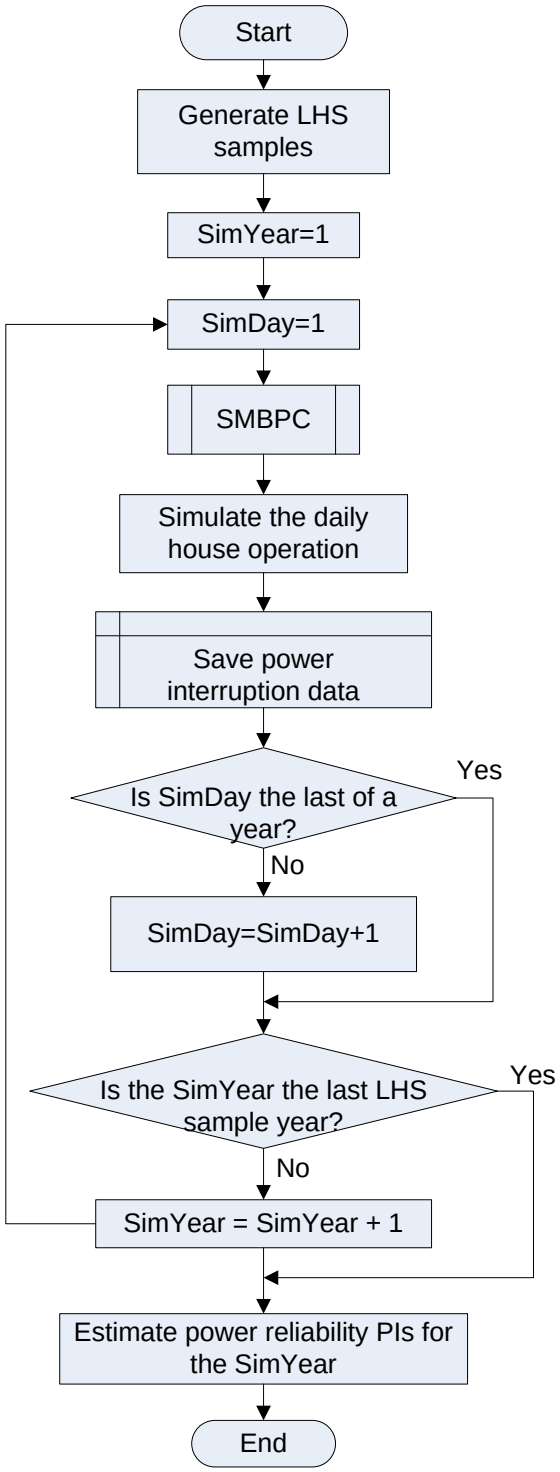

Figure 6.3 Flow diagram showing the power reliability evaluation process with a SMBPC design implemented

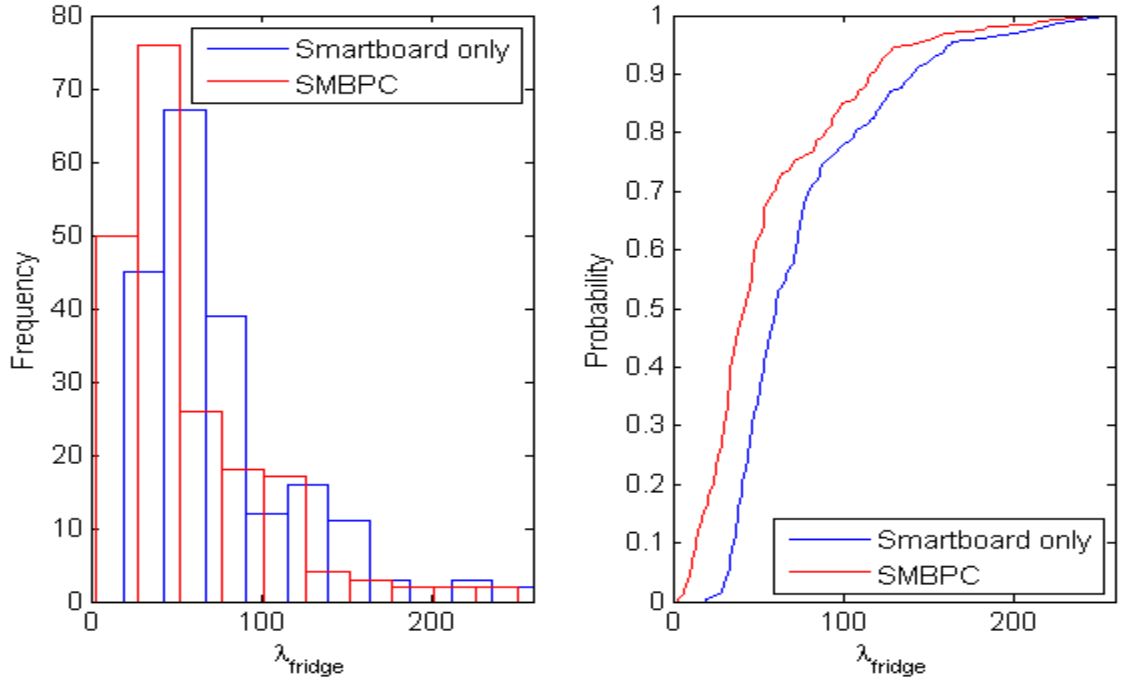

Figure 6.4 A comparison of the histogram plot of λ_{fridge} (left) and its cumulative probability function plot (right)

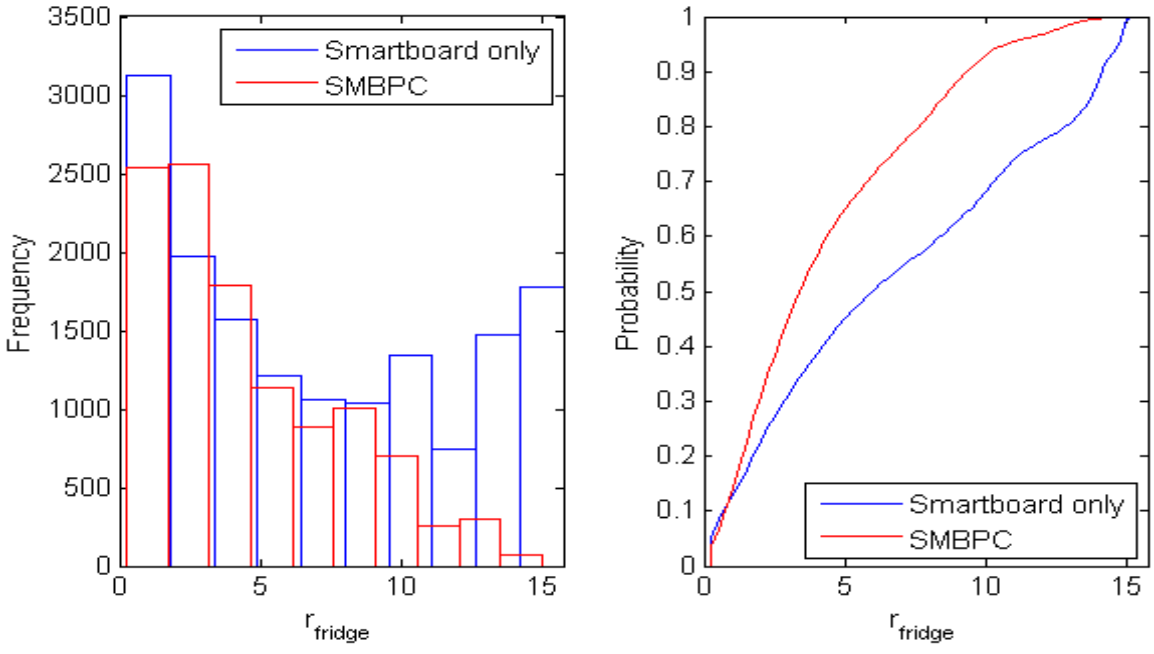

Figure 6.5 A comparison of the histogram plot of r_{fridge} (left) and its cumulative probability function plot (right)

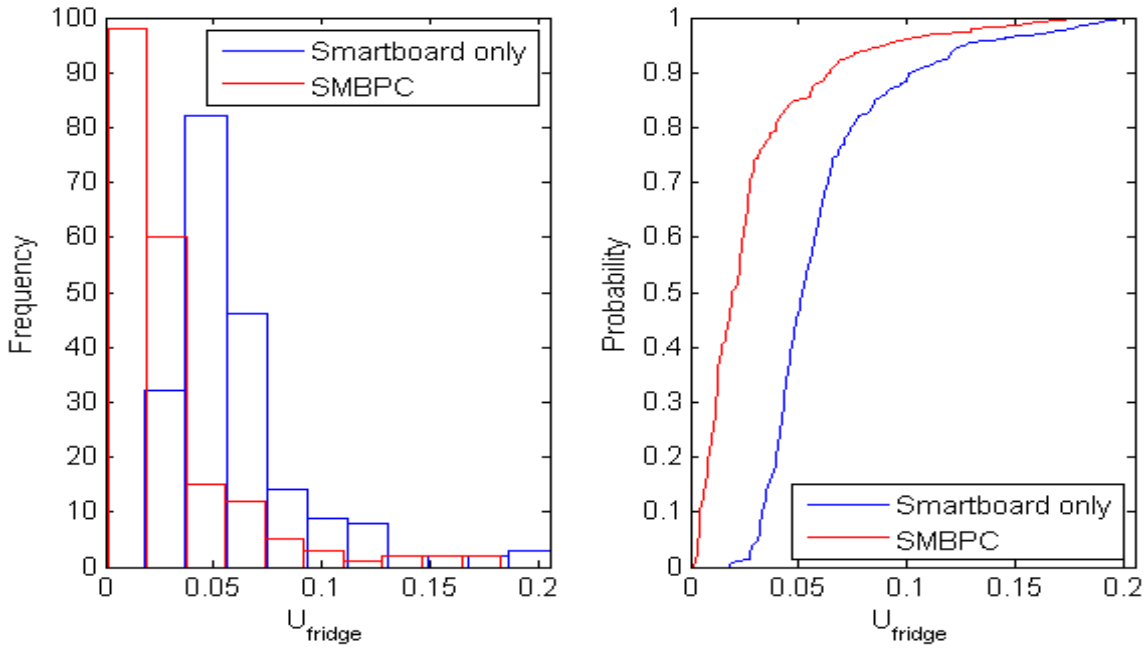

Figure 6.6 A comparison of the histogram plot of U_{fridge} (left) and its cumulative probability function plot (right)

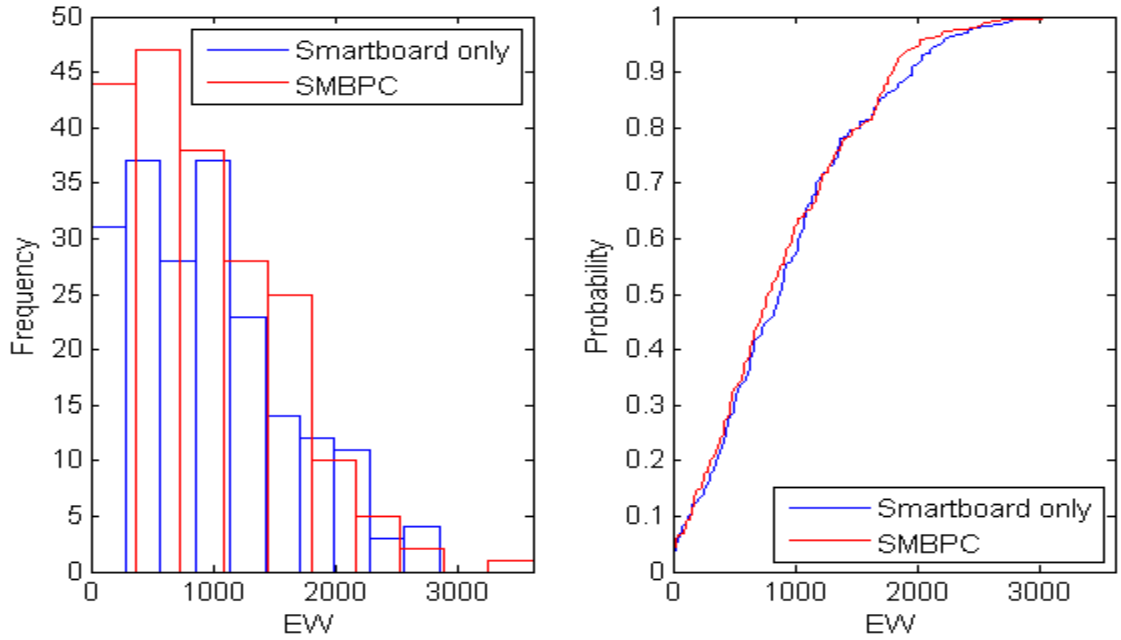

Figure 6.7 A comparison of the histogram plot of EW (left) and its cumulative probability function plot (right)

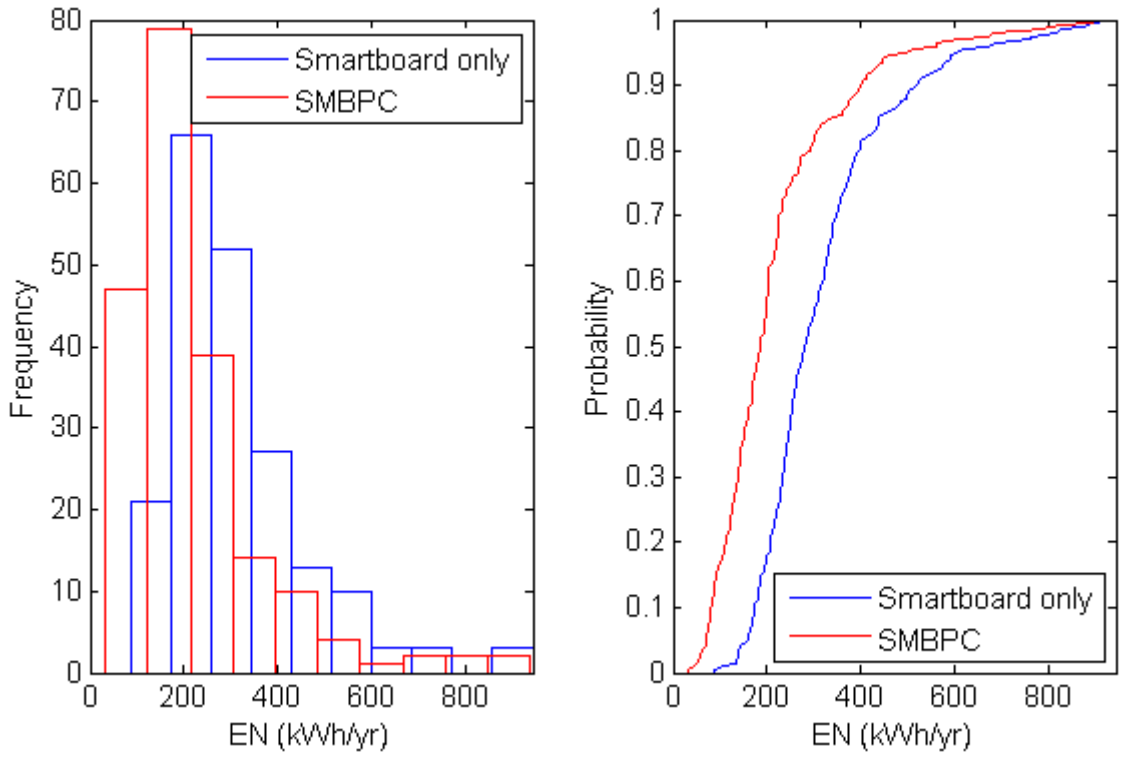

Figure 6.8 A comparison of the histogram plot of EN (left) and its cumulative probability function plot (right)

Table 6.2 shows a comparison of expected values of all reliability indices. The expected failure rates decrease after implementing the SMBPC. This suggests that the SMBPC will lead to fewer power interruptions in the off-grid house. However the expected outage hours do not follow the trend. Most of the expected outage hours decrease, except for those of the HVAC system and the miscellaneous electric loads. The expected outage hour for the HVAC system has almost tripled. This is due to the fact that the HVAC system is the biggest energy consumer in the house. Compared to the rest of the energy consumers, even those less preferred to the HVAC system by the users, the HVAC system will have a smaller probability to be fulfilled by the available energy in the house due to its relatively large demand. When this probability drops below the threshold

($p_{threshold}$ in Figure 6.2) set by the users the SMBPC will give a negative signal to the smartboard and decide not to distribute energy to run the HVAC system. As for the miscellaneous electric loads, since it is the least preferred consumer in the preference rank list its need of energy will always be scarified whenever energy is not sufficient for all consumers. The same increase is also observed in the expected unavailability for the HVAC system and the miscellaneous electric loads due to same reason.

Table 6.3 shows the comparison of $risk(r)$ values. After implementing the SMBPC the risk for the refrigerator to exceed maximum outage hour allowance decreases from 61.3% to 43.5%. In the meantime the risk of the HVAC system exceeding its maximum outage hour allowance increases from 0% to 4.0%. As for the $risk(U)$ most of the energy consumers, except the HVAC system and the miscellaneous electric loads, benefit from the SMBPC and show to have smaller probabilities of exceeding the maximum allowance of power unavailability compared to the original case with a smartboard only (Table 6.4). The risk of the HVAC system exceeding its maximum unavailability allowance increases from 65.3% to 98.2%. The risk increase for the miscellaneous electric loads is however relatively smaller (from 67.8% to 70.0%).

Table 6.2 A comparison of expected reliability PI values with and without SMBPC

PI index	PI	Smartboard only	SMBPC
1	λ_1	101.60	62.02
2	λ_2	73.94	58.22
3	λ_3	100.14	65.53
4	λ_4	99.82	65.45
5	λ_5	73.92	57.27

Table 6.2 (continued)

6	λ_6	93.95	58.07
7	λ_7	76.64	56.21
8	λ_8	75.60	56.23
9	r_1	5.94	13.69
10	r_2	7.56	5.94
11	r_3	6.06	5.06
12	r_4	6.09	4.83
13	r_5	7.59	4.77
14	r_6	6.60	10.75
15	r_7	6.98	4.48
16	r_8	7.14	4.48
17	U_1	0.07	0.11
18	U_2	0.06	0.04
19	U_3	0.07	0.04
20	U_4	0.07	0.04
21	U_5	0.06	0.03
22	U_6	0.07	0.08
23	U_7	0.06	0.03
24	U_8	0.06	0.03
25	EW	952	913
26	EN	319	218

Table 6.3 A comparison of $risk(r_i)$ between with and without the SMBPC

Index (i)	Appliances	Smartboard only	SMBPC
1	HVAC	0.0%	4.0%
2	Lighting	0.0%	0.0%
3	Clothes Washer	0.0%	0.0%
4	Dishwasher	0.0%	0.0%
5	Cooking Device	0.0%	0.0%
6	Misc. Electric loads	0.0%	0.0%
7	Refrigerator	61.3%	43.5%
8	DHW	0.0%	0.0%

Table 6.4 A comparison of $risk(U_i)$ between with and without the SMBPC

Index (i)	Appliances	Smartboard only	SMBPC
1	HVAC	65.3%	98.2%
2	Lighting	100.0%	85.9%
3	Clothes Washer	66.0%	20.4%
4	Dishwasher	66.1%	19.3%
5	Cooking Device	100.0%	80.2%
6	Misc. Electric loads	67.8%	70.0%
7	Refrigerator	100.0%	76.1%
8	DHW	100.0%	76.1%

6.6 Sensitivity analysis: the probabilistic decision-making threshold

As shown in Figure 6.2 the SMBPC requires a new user input, called probability threshold $p_{threshold}$, in addition to distribution of energy demands and supplies and preference rank list. The EMS module needs $p_{threshold}$ to judge whether it shall give a

positive signal to authorize energy distribution to the evaluated energy consumer. Basically the selection of $p_{threshold}$ reflects an individual attitude to acceptable risk. For instance on a day when weather forecast says that there is a 85% chance of rain, some people may choose to bring their umbrellas and some may choose not to. The action whether they bring umbrellas or not depends on individual's perception of "the chance" and the threshold on which one starts to translate "the chance" into a firm incident: from "chance to rain" to "will rain". The exact threshold value varies among individuals. Table 6.5 shows an example of three sets of threshold values representing individuals with different attitudes towards risk taken – normal, conservative, and aggressive. Different individuals may have their own understanding on normal, conservative, and aggressive attitudes towards risk taken.

Table 6.6 shows a comparison of $risk(r)$ values while taking different $p_{threshold}$ values. It suggests that an aggressive attitude will lead users to the lower risk for the HVAC system and to the higher risk for the miscellaneous electric loads in terms of violating the maximum allowance of the outage hour. The results in Table 6.7 indicate that an aggressive attitude will lead to a relatively lower risk in terms of power unavailability for the HVAC system but higher risks for the rest energy consumers. Table 6.8 shows the comparison of the expected power reliability PIs among three threshold settings. The results indicate that a conservative attitude will result in fewer expected power interruptions for all consumers. In terms of the expected outage hours the conservative attitude will result in shorter expected outage hours for most of the energy consumers except the HVAC system and the miscellaneous electric loads which matches the results shown in Table 6.6. For the expected power unavailability the conservative attitude leads

to lower power unavailability for all the consumers except the HVAC system which matches the results shown in Table 6.7.

Table 6.5 The $p_{threshold}$ values for individuals with different risk acceptance

Attitude towards risk perception	$p_{threhold}$
Normal	85%
Conservative	95%
Aggressive	75%

Table 6.6 A comparison of $risk(r_i)$ among different $p_{threshold}$ settings

Index (i)	Normal	Conservative	Aggressive
1	4.0%	4.2%	3.6%
2	0.0%	0.0%	0.0%
3	0.0%	0.0%	0.0%
4	0.0%	0.0%	0.0%
5	0.0%	0.0%	0.0%
6	0.0%	0.0%	0.0%
7	43.5%	37.8%	46.5%
8	0.0%	0.0%	0.0%

Table 6.7 A comparison of $risk(U_i)$ among different $p_{threshold}$ settings

Index (i)	Normal	Conservative	Aggressive
1	98.2%	98.4%	98.2%
2	85.9%	83.5%	89.9%
3	20.4%	18.1%	23.6%
4	19.3%	16.8%	23.5%

Table 6.7 (continued)

5	80.2%	67.6%	83.1%
6	70.0%	69.2%	76.5%
7	76.1%	64.7%	80.0%
8	76.1%	64.7%	80.0%

Table 6.8 A comparison of expected reliability PI values among different $p_{threshold}$ settings

PI index	PI	Normal	Conservative	Aggressive
1	λ_1	62.02	59.06	64.84
2	λ_2	58.22	52.89	61.58
3	λ_3	65.53	58.75	69.78
4	λ_4	65.45	58.91	69.74
5	λ_5	57.27	51.29	61.05
6	λ_6	58.07	52.63	61.78
7	λ_7	56.21	50.37	59.84
8	λ_8	56.23	50.37	59.87
9	r_1	13.69	14.82	12.83
10	r_2	5.94	5.63	6.17
11	r_3	5.06	4.88	5.09
12	r_4	4.83	4.59	4.93
13	r_5	4.77	4.52	5.01
14	r_6	10.75	11.40	10.61
15	r_7	4.48	4.10	4.75
16	r_8	4.48	4.10	4.76
17	U_1	0.11	0.11	0.11

Table 6.8 (continued)

18	U_2	0.04	0.03	0.04
19	U_3	0.04	0.03	0.04
20	U_4	0.04	0.03	0.04
21	U_5	0.03	0.03	0.04
22	U_6	0.08	0.08	0.08
23	U_7	0.03	0.02	0.03
24	U_8	0.03	0.02	0.03
25	EW	913	913	913
26	EN	218	201	232

One shall notice that the above section only presents one particular example. In general which risk attitude works the best in a certain situation depends on the characteristics of the system, how well the system uncertainty is quantified, and of course on users' preference. In practice a user may be able to diagnose the system based on daily operation data and set an appropriate $p_{threshold}$ value to achieve the best performance on the SMBPC.

6.7 Computation efforts

Figure 6.9 shows the data flow of a power reliability assessment when a SMBPC is implemented in an off-grid house design. Both the power reliability assessment and the execution of a SMBPC require uncertainty analysis. These two sets of uncertainty analysis are independent from each other. In practice the SMBPC and the power reliability assessment may or may not share: 1) the same set of uncertain variables; 2) the

same uncertainty in all uncertain variables; and 3) both 1 and 2. This study has assumed case 3 in the overall performance evaluation. As presented earlier in this chapter a SMBPC relies on uncertainty analysis to predict possible building performance for the next day. Thus it requires a total number of *nsample* building performance simulation (done by running *GTSim*) runs over the time horizon of a day. While a full power reliability analysis (with a SMBPC implemented) will require a total number of $nsample \times (nsample + 1)$ building performance simulations runs over the time horizon of a year.

In this study the *nsample* has been chosen to be 200 in order to meet the accuracy requirement on the LHS technique. It leads to a total run of 40200 which makes the design optimization of design alternatives with a SMBPC implemented computationally expensive. Due to the heavy computation required in design optimization a two-stage optimization approach has been proposed and will be demonstrated in the following chapters.

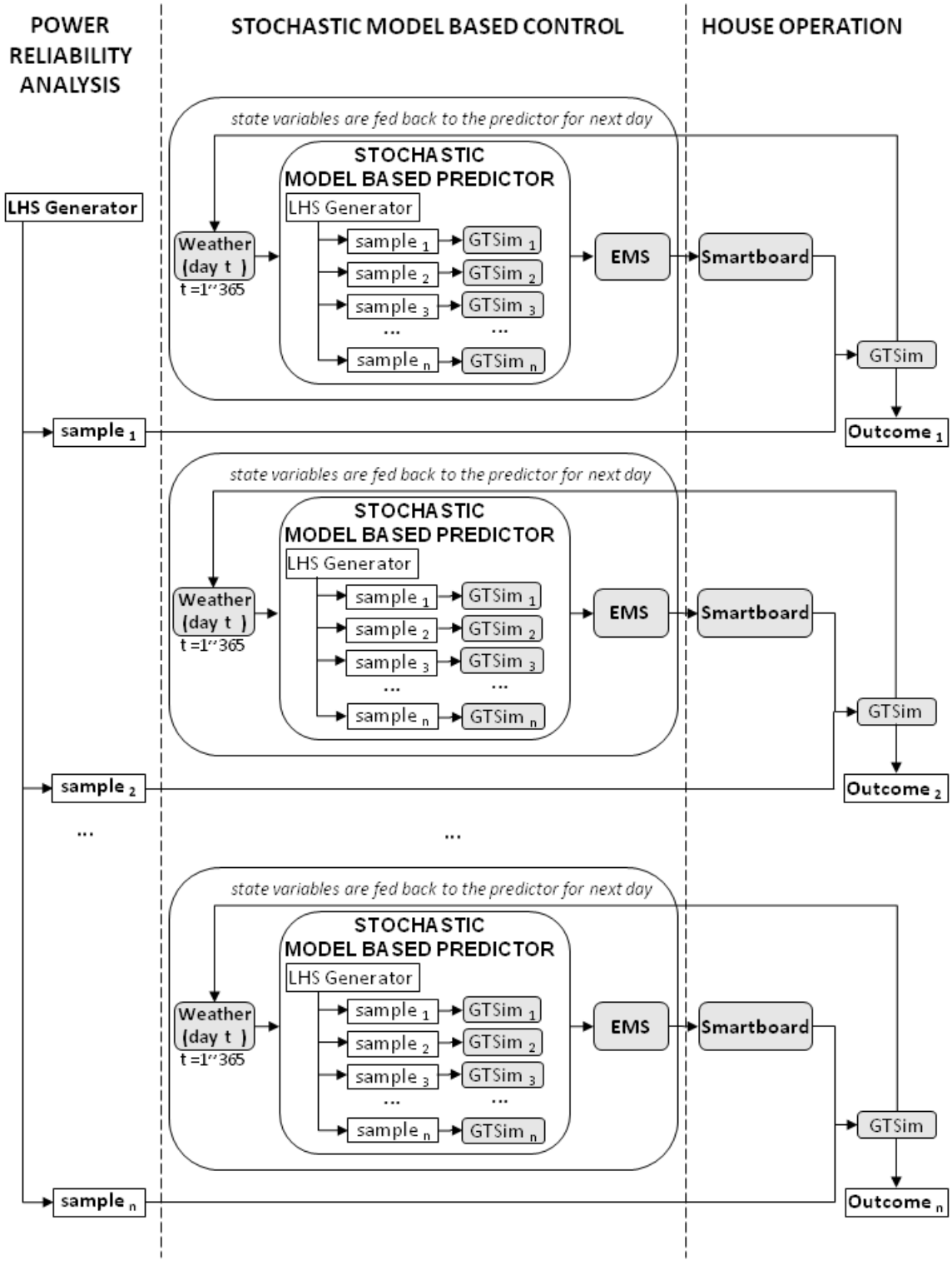

Figure 6.9 A data flow chart of power reliability analysis when a SMBPC is implemented

6.8 Conclusions

This chapter presents a SMBPC design to improve the energy management efficiency in off-grid solar houses. Compared to a conventional MBPC the SMBPC approach integrates the uncertain nature of system behavior into controller design and therefore provides an alternative solution to model calibration problems in the conventional MBPC design. Although this study assumes known information about the future weather (using TMY weather data) and does not investigate how the proposed SMBPC design will perform under an uncertain future weather it is expected to be easy and natural to integrate uncertainty in weather forecast into the SMBPC design and implementation in practice because of the way that a SMBPC handles uncertainty.

CHAPTER 7 A VALUE-BASED APPROACH

7.1 Background

Sizing an off-grid solar residential home design mainly includes PV array sizing, battery sizing, domestic hot water system sizing, and home heating, ventilation, and air conditioning (HVAC) system sizing. Typically, every system or sometimes even every single main component of a system has its own well-established sizing methodology. For instance a PV system is commonly sized either according to worst case scenarios (usually in the winter when there is limited solar irradiation) or according to the typical day of the local weather data [48, 124]. HVAC systems are usually sized according to a worst case scenario or extreme design day. The requirements of specialties in specific disciplines result in rather isolated sizing procedures at pre-defined stages of the building design. This reduction of interrelation among different components during the design stage is contrary to their intensive interactions that actually occur in the operation stage. From the operation perspective none of these system parts can be sized in isolation, as their performances are highly interrelated and need to be studied through holistic assessment based on dynamic simulations. In off-grid solar house design energy self-sufficiency is one of the key performance aspects. All involved design components and building loads, the HVAC system, ambient weather, battery or other type storage system, and solar power system are interacting with each other all the time. Many of these interactions are not well accounted for by the current disjointed and often individual system design tasks. This often leads to mismatches among different components and systems and eventually causes underperformance, in particular unnecessary energy waste. Celik investigated the

effects of different load profiles on the performance of stand-alone PV systems and his research results show that the reliability of a PV power system varies considerably when it works with different load profiles, especially for small battery capacities [125]. Anis and Nour studied energy losses in PV systems and their results show that the mismatch between the array and the load or battery capacity could cause big energy losses [126]. The main reason is that the PV array is usually sized to meet the load during the winter season when solar irradiation is low. As a result the system is oversized for the summer and energy loss from the PV system can be as high as 40%. These results reveal the importance to integrate building load, renewable power generation system, battery bank and their instantaneous interaction together in the design, system balancing and performance evaluation processes of off-grid solar houses.

Another common issue that confronts the off-grid solar house design is that designers in each field tend to oversize their components. This is due to the liability issue which demands full responsibilities from designers to ensure that their design meets the performance requirements under all conditions. In response to the increasing need to provide liability protection designers have to either oversize the system or add an extra parallel system to ensure system reliability, which in off-grid solar house design, often results in purchasing large backup electricity generators or oversizing the PV power generation systems. This justifies the question whether the decision to "buy" reliability guarantees is really cost effective.

This chapter develops a strategy to right size the complete system based on the prediction of outcomes under uncertainty. The uncertainty remains the same as in previous chapters. The complete list of ranges of uncertainty in parameters is given in Table 5.18.

7.2 A value-based sizing approach

As discussed in Chapter 2 a commonly used performance parameter to evaluate the reliability of off-grid solar power systems is loss of load probability (LOLP). The LOLP "connects" a PV power system with its electricity consumers. It should be noted that in current practice, most building (electricity) load simulations are conducted separately from the LOLP evaluation of a PV system. This disconnect can lead to the neglect of energy reliability impacts that result from system sizing mismatches.

The value-based approach was first proposed in the power planning industry to help utility companies make the most promising investments in their utilities service business [127]. This approach combines customer-value with the cost to design the power generation and distribution system at various levels of reliability and "power quality" and then uses it to identify the optimum balance between service reliability and utility company's investments [128]. The customer interruption cost is the economic loss (or "damage" customers incur as a result of power interruption or power quality problems [129]. Customer interruption cost has been used to represent the customer value since 1994 [130-132]. Figure 7.1 shows the concept of value-based planning in the power industry. The total cost of a power system configuration is the sum of utility investment cost, operating cost, and customer interruption cost. The point of minimum of total cost is the balancing point that power planners look for.

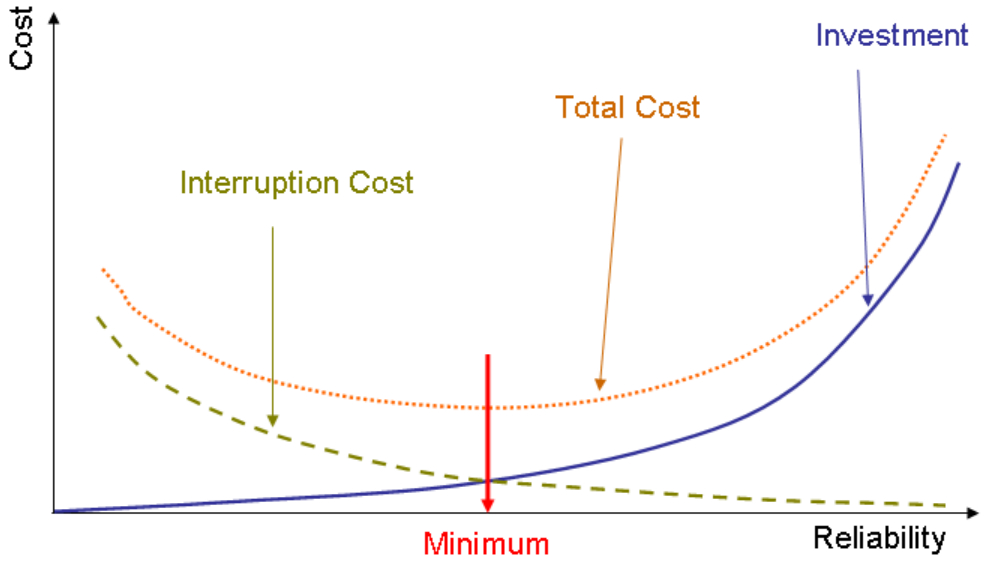

Figure 7.1 The concept of value-based planning [132]

The value-based sizing approach adopts the same concept of value-based planning described above. In fact an off-grid solar house could be considered as a small scale power plant with multiple (internal) electricity consumers. However the operating cost in an off-grid solar house is close to zero and the total cost becomes a sum of customer interruption cost and system investments. The design objective is to find the most economic system sizing match which corresponds to the minimum total cost.

7.3 Design space and performance evaluation

The objective of the case study is to investigate the relationship between the sophistication of system sizing, energy consumption, power reliability, and the house capital cost. The parameter screening based on the elementary effects method in previous chapters has revealed that the efficiency of the installed PV power system has a dominant effect on the overall system power reliability. Therefore this case study will be focusing

on the balance between the PV system sizing and the total system cost. However the same concept can be easily applied to HVAC system sizing and others.

7.3.1 Design problem statements

The studied off-grid house currently has 27 PV modules installed on the roof with a rated power of 203.2 W each and 12 more modules mounted to the southern wall with a rated power of 197.6 W each. It uses eight batteries with an individual capacity of 12.6 kWh. The installed solar power system is designed based on conventional PV sizing method in current practice. Table 7.1 lists all the investigated design values. All the design variables are integer variables. The design options are generated with different combinations of three design variables at different discrete values. Table 7.2 shows the design variable values of 12 selected design options. Obviously the Option 8 is the current design.

Table 7.1 Design variables – reference values, varying ranges

	Installed original design	Design options
$N_{battery}$	8	7, 8, 9
$N_{pv,roof}$	27	24, 27
$N_{pv,south}$	12	8, 12

Table 7.2 A list of investigated design options

	$N_{battery}$	$N_{pv,roof}$	$N_{pv,south}$
Option 1	7	24	8
Option 2	7	24	12
Option 3	7	27	8
Option 4	7	27	12

Table 7.2 (continued)

Option 5	8	24	8
Option 6	8	24	12
Option 7	8	27	8
Option 8	8	27	12
Option 9	9	24	8
Option 10	9	24	12
Option 11	9	27	8
Option 12	9	27	12

7.3.2 The estimate of total cost

The total cost of an off-grid solar house is the sum of capital cost, maintenance cost, and customer interruption cost. In the off-grid solar house case, power will not be available all the time and certain inconveniences or even damages will result. The damage that an electricity interruption causes is quantified to represent the value of power quality. The interruption cost is taken from the customers. The following section will discuss how to calculate the total cost.

- PV system cost

The annualized life cycle cost (ALCC) of the installed PV system is calculated as the yearly cost related to PV power system investments. The ALCC spreads the total life cycle cost of the installed PV power system to its life span and is the same for every year operation [133]. The cost of a PV power system includes costs of the PV modules, inverters, Battery costs, other Balance of System (BOS) costs (hardware costs), installation costs, indirect costs (includes design, engineering, site-related costs, permitting, and profits), and the operation and maintenance (O&M) costs. Table 7.3

shows the 2005 benchmarked parameters for life cycle cost estimate that are calculated from a sample set of more than 60 installed systems and laboratory-based measurements and modeling [134]. Table 7.4 lists all the necessary parameters for this case study. As the GTSD07 house is built by college students whose work is rewarded by school credits but not dollars some of the cost parameters in Table 7.4 are taken from benchmark data.

Table 7.3 2005 benchmarked parameters, 2011 and 2020 projections for modeling of off-grid reference systems

System element	Units	2005	2011	2020
Module price	$/$W_{dc}$*	4.00	2.20	1.25
Inverter price	$/$W_{ac}$	0.90	0.69	0.30
Other BOS	$/$W_{dc}$	0.61	0.50	0.40
Installation	$/$W_{dc}$	1.00	0.90	0.80
Storage	$/$W_{dc}$	1.47	1.49	1.49
Other/indirect	$/$W_{dc}$	4.71	4.20	3.71
Installed system price	$/$W_{dc}$	13.61	10.69	8.26
Lifetime	Years	30	35	35
degradation	%/yr	1	1	1
O&M cost (not including replacement cost)	% installed price	3.6	2.7	2.1

*W_{dc} represents power wattage in the form of direct current (dc) and W_{ac} represents power wattage in the form of alternating current (ac).

Table 7.4 The cost information for calculating ALCC

	Prices	sources
PV modules on the roof	$1056/module	Project data
Inverter for roof PV modules	$0.56/$W_{ac}$	Project data
PV modules on the SW	$1032/module	Project data

Table 7.4 (continued)

Inverter for SW PV modules	\$0.67/W_{ac}	Project data
Installation	\$1.00/W_p	[134]
Indirect cost	\$4.71/W_p	[134]
Other BOS costs	\$0.61/W_p	[134]
Battery cost	\$4200/module	Project data
O&M cost	0.5% of gross cost (not including inverter replacements)	[134]

Table 7.5 The cost estimate of the currently installed PV system

	Cost (\$)	NPV(\$)
Module cost -roof	28,512	28,512
Inverter cost -roof	3,094	3,094
Module cost -SW	12,384	12,384
Inverter cost -SW	1,608	1,608
Installation cost	8,520	8,520
Other BOS cost	5,197	5,197
Battery cost	33,600	33,600
Maintenance cost	465	9,106
Battery replace (11^{th} yr)	33,600	24,273
Battery replace (21^{st} yr)	33,600	18,062
Total LLC	-	144,355
ALCC	7365	-

The inverter is assumed to have a life time of 5 years and the PV power system is assumed to have a life time of 30 years in residential applications [134]. The batteries are assumed to be replaced once every 5 years [133]. The real discount rate used for life-cycle cost estimate in 2008 is taken as 3.0% according to the latest release from National

Institute of Standards and Technology (NIST) [135]. Table 7.5 shows a sample of ALCC estimate for the currently installed PV system in the GTSD07 house.

- The customer interruption cost

Power interruption reflects one aspect of power quality. The damage a power interruption causes is mostly physical but may have different consequences for different customers depending on how they are affected by every occurrence of power interruption. Thus customer interruption costs varies from one to another as a function of a number of factors, including customers' dependence on electricity, the nature and timing of the power disturbance, and the economic value of the activity being disrupted [129]. The establishment of value functions to estimate customer interruption costs requires a survey to a representative sample of customers. The details of surveying technique and the resulting questionnaires are described in [127]. Figure 4 shows typical interruption cost characteristics in residential applications based on industry practice [128]. This interruption cost value function includes a fixed cost caused when an interruption occurs, and a variable cost that increases as the interruption continues.

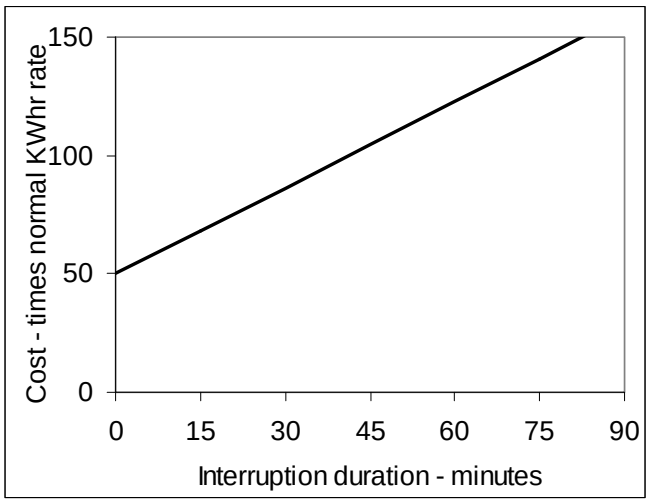

Figure 7.2 Typical interruption cost characteristics for residential customers [128]

7.3.3 Performance evaluation

As addressed above the design objective is to minimize the total cost which can be calculated using Equation 7-1.

$$C_{total} = ALCC + C_{\text{int } pt} \tag{7-1}$$

Where,

C_{total} the system total cost;

$C_{\text{int } pt}$ the interruption cost.

7.4 Simulation results

As indicated in Equation 7-1 the power reliability analysis will lead to a distribution of the total cost C_{total}. There is no true optimality when the objective is a stochastic variable. In practice the expected value of the stochastic objective variable is often chosen for design optimization, as calculated in Equation 7-2.

$$C_{EV} = E(C_{total}) \tag{7-2}$$

However the expected value of the stochastic objective variable only shows the average of the possible outcomes and may not capture the full picture. This research proposes a second type of PI as a supplementary measure to the expected value. It is the absolute probability of design option i better than design option j. This probabilistic PI can be calculated based on their distribution of C_{total}, using Equation 7-3.

$$C_{prob} = \Pr(C_{total,i} \le C_{total,j}) \tag{7-3}$$

7.4.1 Performance evaluation using PIs based on expected values

Figure 7.3 shows the comparison of C_{EV} values of all investigated design options. And the Option 4 turns out to have the lowest total cost. It refers to a PV system with 7 battery modules, 27 PV modules on the roof, and 12 PV modules mounted to the southern wall. Compared to the original design (i.e. Option 8) the optimal option, Option 4, has a lower system cost and higher interruption cost (i.e. worse power reliability). The difference of C_{EV} values between Option 4 and Option 8 is only \$440, which is small compared to the average total cost C_{total}. Therefore the rank among design options could be different if the interruption cost function is slightly different.

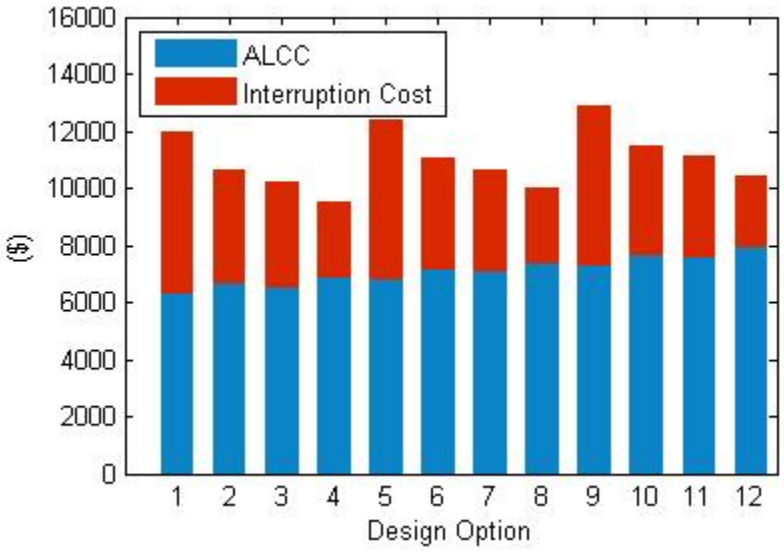

Figure 7.3 A comparison of the expected total costs C_{EV} of different design options

7.4.2 Performance evaluation using probabilistic PIs

Figure 7.3 shows the mean values of the total cost value of each design option. However it does not reflect the full spread of the cost value of each design option. Figure 7.4 shows the mean value C_{EV} along with its variation for every design option. The green square

represents the mean value C_{EV} of each design option. The upper and the lower bar represent the minimum and maximum values of C_{total} of each design option. As shown in Figure 7.4 most of the distribution function of C_{total} are not symmetrical and therefore the mean value alone may not be a good indicator for decision-making in this case study since it does not reflect the full range probability of the occurrence of C_{EV} to the same extent for all design options.

Figure 7.5 shows the comparison of the probabilistic PI, C_{prob}, of all design options. The original design (i.e. design option 8) is used as the reference option during the calculation. The probability of Option 4 having a lower cost than Option 8 is 65.8%, which is larger than 50% and is the highest among all the other design option. Therefore Option 4 remains the most competitive one when using the probabilistic PI for decision-making rather than expected value C_{EV}. However the rank of other design options has changed using C_{EV}. Table 7.6 shows the top 10 design options based on both sets of PIs.

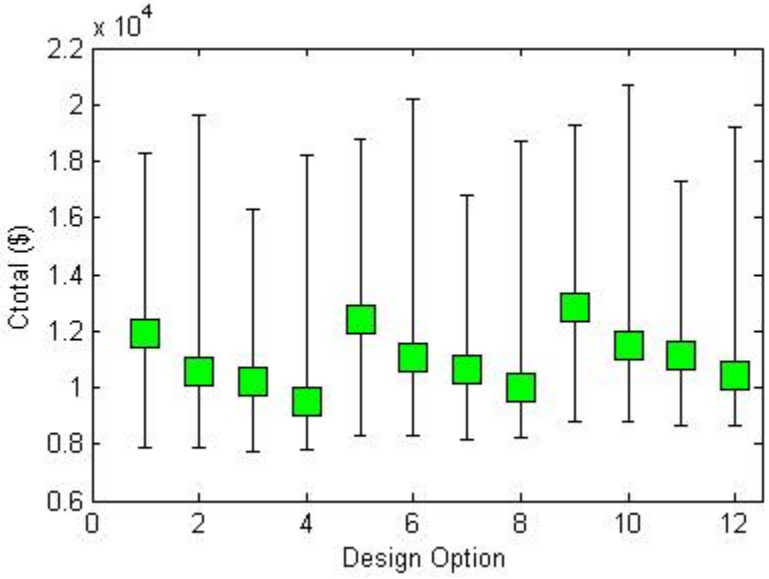

Figure 7.4 The variance of the total cost C_{total} of all design options

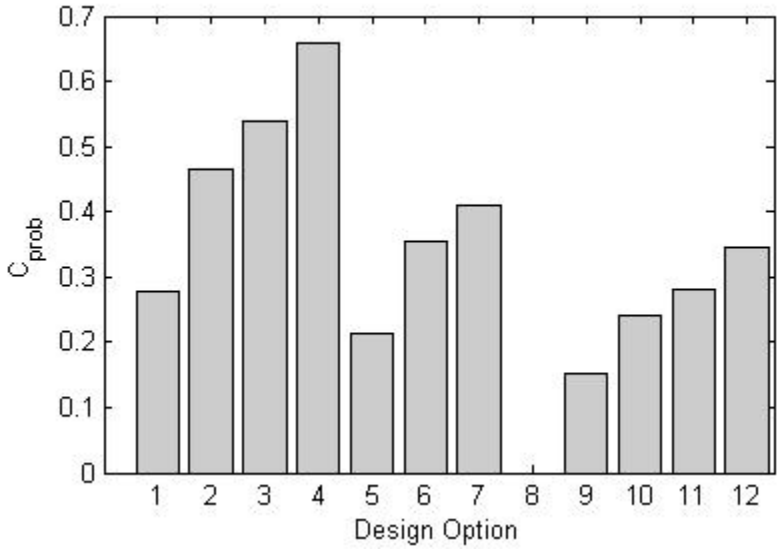

Figure 7.5 A comparison of C_{prob} values of all design options

Table 7.6 A comparison of rank of design options based on C_{EV} and C_{prob} PI values

Rank	Base on C_{EV}	Base on C_{prob}
1	4	4
2	8	3
3	3	8
4	12	2
5	2	7
6	7	6
7	6	12
8	11	11
9	10	1
10	1	10

7.5 Impacts of a SMBPC implementation on interruption cost estimate

Willis and Welch point out that if given sufficient time to prepare for a power interruption most of the momentary interruption cost (the fixed part) and a major part of the variable cost can be eliminated [128]. Figure 7.6 shows the interruption cost reduction that a 24-hour notice could yield.

A SMBPC design has been proposed to achieve a more efficient energy management in the GTSD07 house in Chapter 6. With the help from the SMBPC occupants will be aware of any possible power interruption to a specific energy consumer 24 hours ahead. This section will re-evaluate the 12 design options Table 7.2 assuming a SMBPC will be installed in the house.

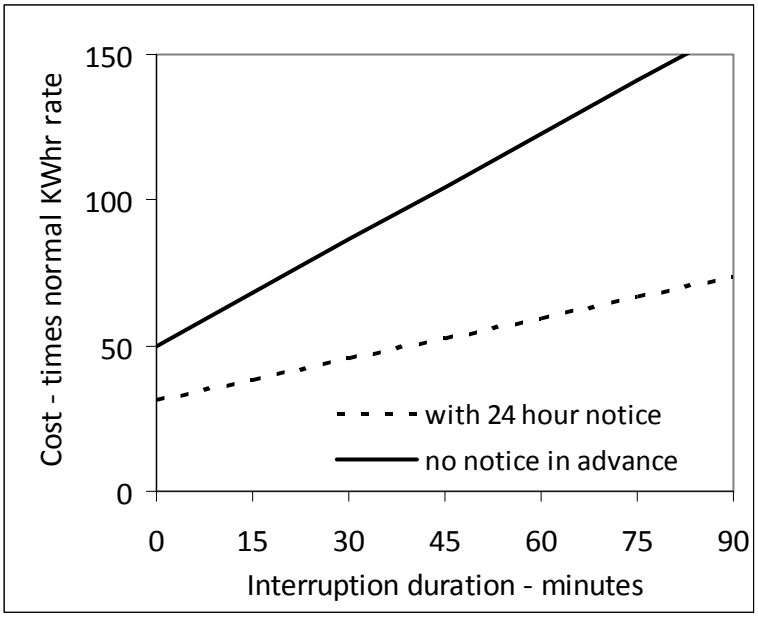

Figure 7.6 The reduced cost impact if power interruption is noticed to customers 24 hours ahead [128]

As presented in Chapter 6 a SMBPC requires an uncertainty analysis to quantify the distribution of energy demands and supplies in order to make a decision about future

control sequences. A full power reliability analysis (with a SMBPC implemented) will require a total run of $nsample \times (nsample + 1)$ yearly simulations. In this study a total of 40200 runs which makes the design optimization computationally expensive.

This study proposes a two-stage optimization process to solve this computationally expense problem. At the first stage a conventional MBPC model assuming known information about the future will be used to replace the original SMBPC module. Since it assumes that system behavior is fully known it will not need an uncertainty analysis to make a prediction on future energy demands and supplies. Therefore compared to a regular power reliability analysis the power reliability analysis of an off-grid house with a conventional MBPC will require a total run of $2 \times nsample$ years which becomes affordable in design optimization. A small group of competitive design options will be selected at the end of the first stage design optimization. In the second stage the optimal choice among the selected small group of design options will be evaluated using the original SMBPC design (The flow diagram of power reliability analysis when involving a SMBPC design can be found in Figure 6.3). The final optimal design option can be selected at the end of the second stage optimization.

Figure 7.7 shows the comparison of C_{EV} from the first stage optimization (i.e. a MBPC with full certainty about the future system behavior). The design Option 3 (7 batteries, 27 PV modules on the roof, and 8 PV modules mounted to the southern wall) becomes the optimal option with the lowest expected total cost. The results also show that the interruption cost has been significantly reduced because the MPC and the system investment become dominant in the design optimization. When using the probabilistic PI option 4 becomes the most economic design option, as shown in Figure 7.8. Based on the

findings there are now four design options that should be chosen for the second stage optimization using the SMBPC algorithm. They are: Option1, 2, 3, and 4.

Figure 7.9 shows the comparison of C_{EV} values for the four selected design options and Option 8 (the current design). Option 4 turns out to be the most economic design option; the comparison using C_{prob} leads to the same optimal design option, as shown in Figure 7.10. But as shown in Figure 7.9 and Figure 7.10 the Option 3 and 4 are competitive: Option 3 costs only $22 more than Option 4, which is less than 0.3% of the total expected cost of Option 4. In terms of the probabilistic PI C_{prob} the Option 4 has 80.6% probability to be better than the original design and Option 3 has 73.7% of probability. The difference is only about 7%. The SMBPC largely reduces the interruption costs. In turn it diminishes the difference between Option 3 and Option 4 and makes the optimal design option (Option 4) less competitive compared to the rest.

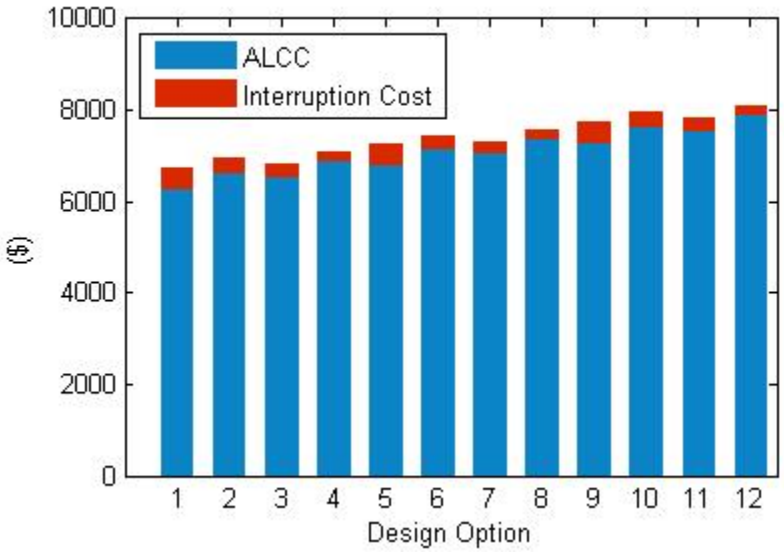

Figure 7.7 A comparison of the expected total costs C_{EV} with 24 hour notice (Stage 1)

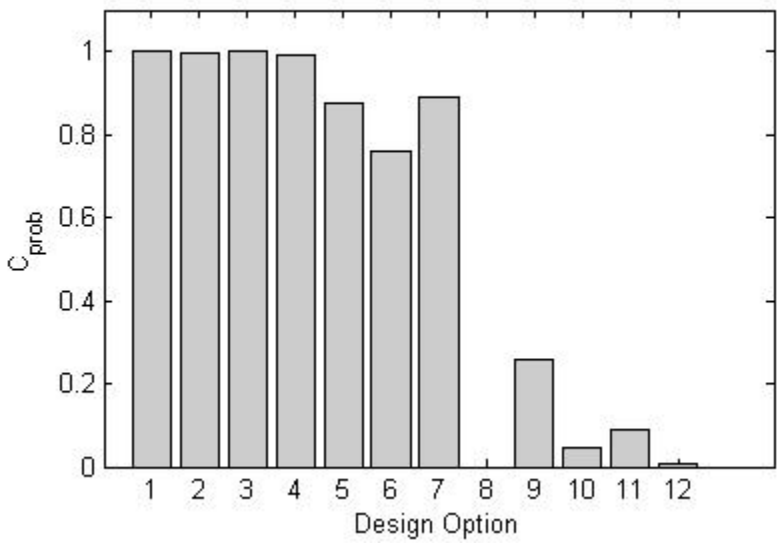

Figure 7.8 A comparison of C_{prob} values with 24 hour notice (Stage 1)

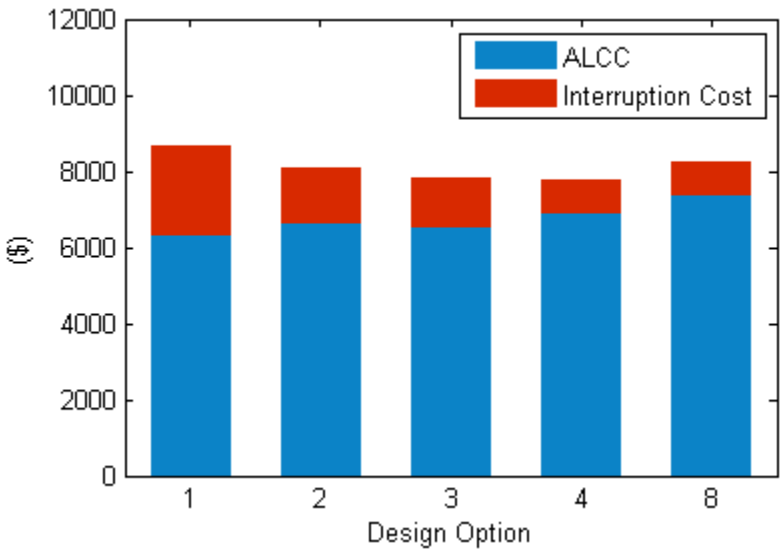

Figure 7.9 A comparison of the expected total costs C_{EV} with 24 hour notice (Stage 2)

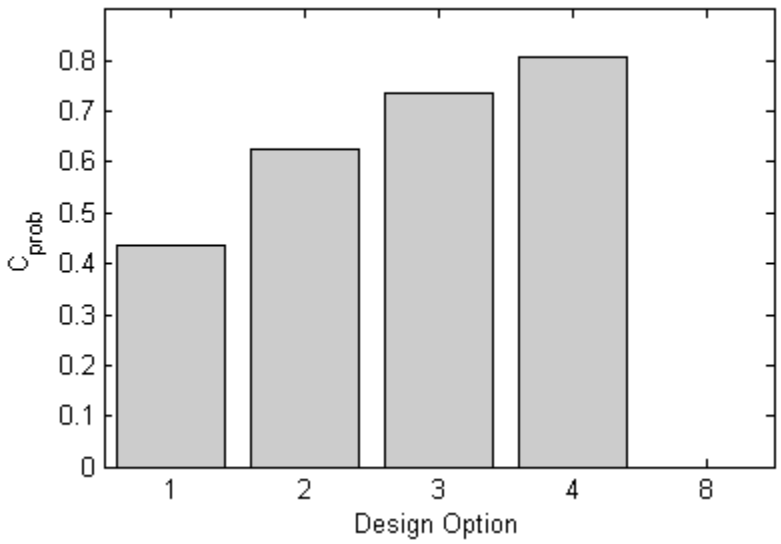

Figure 7.10 A comparison of C_{prob} values with 24 hour notice (Stage 2)

7.6 Discussion

7.6.1 The task dependent interruption cost functions

In the previous section, all electricity consumers in the off-grid solar house are assumed to require the same level of electricity quality, which is not true in reality. For instance the hot water temperature will not be influenced much even if the DHW system suffers from a (small) electricity shortage. But occupants may suffer critical data loss if their home computers encounter a power shortage. Moreover, subjectively occupants have different preferences to individual house functions. Between having a cold sandwich and having a cold shower different individuals may have completely different choices. Therefore the consequence of a power outage for any individual electricity consumer may vary for different occupants. Figure 7.11 shows a sample of the varying quality requirement by different house electricity consumers.

An energy smart board could be implemented to distribute electricity (in cases of shortage) to different house electricity consumers according to their preset priority rank as discussed in Chapter 3 and Chapter 5. The prioritized energy distribution network will help maximize occupants' satisfaction level with a fixed amount of available electricity.

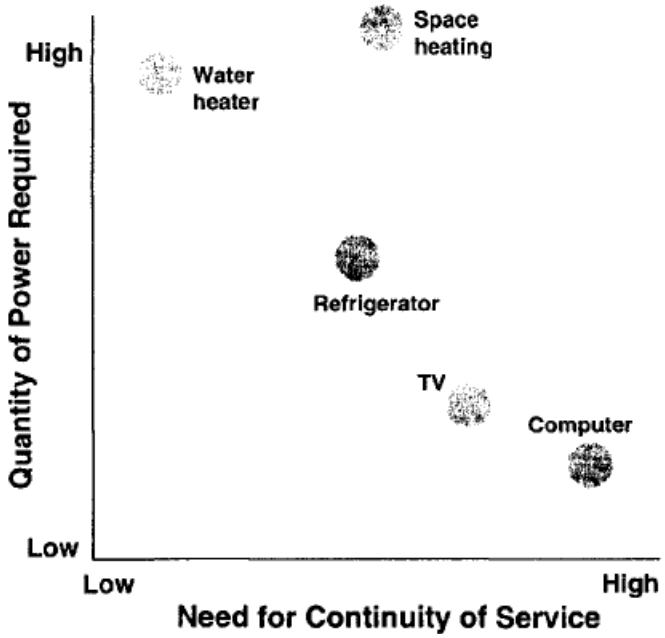

Figure 7.11 Electrical appliances vary in the amount of electricity they demand, and the level of continuity of service they require to perform their function adequately [128]

Recall the form of the value function for interruption cost estimate as shown in Equation 7-4:

$$C_{\text{int } pt} = a + b \times r \tag{7-4}$$

Where,

$C_{\text{int } pt}$ the interruption cost, dollars;

a the fixed cost related to every occurrence of power outage;

b the varying cost proportional to the duration of every power outage;

r the duration of each power outage, minutes.

The values of parameter a and b for overall residential applications can be found in Figure 7.2. Theoretically the value function of customer interruption cost for each individual electricity consumer in an off-grid house shall be developed based on results concluded form a survey to all household members. This study uses the value function of overall residential consumer as the base function and applies correction factors to both parameter a and b to every electricity consumer respectively. Equation 7-5 shows the corrected formula for an interruption cost estimate of each individual electricity consumer. The correction factors are based on the author's personal perception concerning future power interruption to every individual residential activity. Figure 7.12 shows a sample of correction factors assuming the author is a potential off-grid resident. The total customer interruption cost will be a normalized cost of all household electricity consumers, as shown in Equation 7-6. Different selections of weight functions could lead to different final design decisions. Further work needs be conducted to estimate weight factors based on perceptions of all household members. This study will conduct the design optimization under two sets of weight factors: 1) the weight factors of all electricity consumers are equal; 2) the weight factors are linearly proportional to the rank of every electricity consumer and the top ranked appliance has the highest weight in the overall interruption cost calculation. Table 7.7 shows the numeric values of both sets of weight factors.

$$C_{\text{int}\,pt,i} = (f_{a,i} \times a) + (f_{b,i} \times b) \times r \tag{7-5}$$

Where,

$f_{a,i}$ the correction factor for parameter a with respect to appliance i;

$f_{a,i}$ the correction factor for parameter b with respect to appliance i.

$$C_{\text{int } pt} = \sum_{i=1}^{8} w_i C_{\text{int } pt,i} \tag{7-6}$$

Where,

w_i the weight factor for appliance i and $\sum_{i=1}^{8} w_i = 1$.

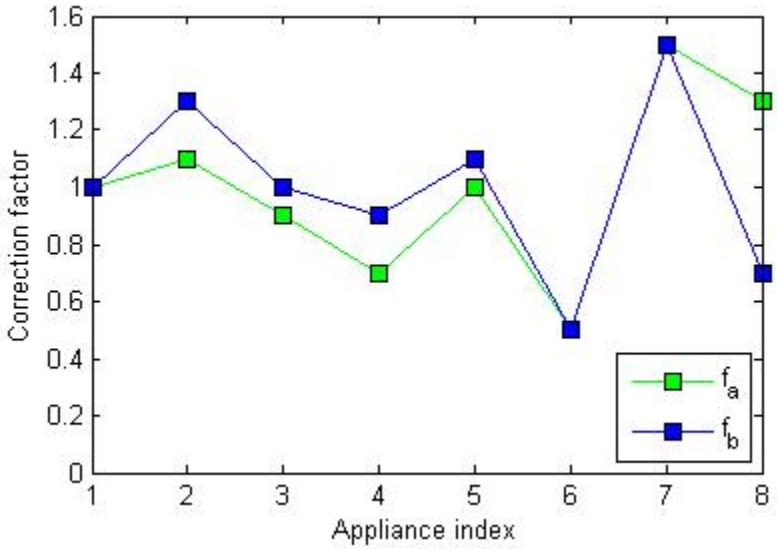

Figure 7.12 The correction factors for interruption cost estimate

Table 7.7 Two sets of weight factors w_i

Index (i)	Appliances	Equal weight	Proportional weight
1	HVAC	0.125	0.111
2	Lighting	0.125	0.167
3	Clothes Washer	0.125	0.083
4	Dishwasher	0.125	0.056
5	Cooking Device	0.125	0.139
6	Misc. Electric loads	0.125	0.028
7	Refrigerator	0.125	0.222
8	DHW	0.125	0.194

□ Equal weight factors

Figure 7.13 shows the comparison of all design options using C_{EV} values with equal cost weight factors in Equation 6-6. It turns out that Option 4 is still the optimal option with the lowest expected total cost. The optimal design option remains when using the probabilistic PI C_{prob} for decision making (Figure 7.14).

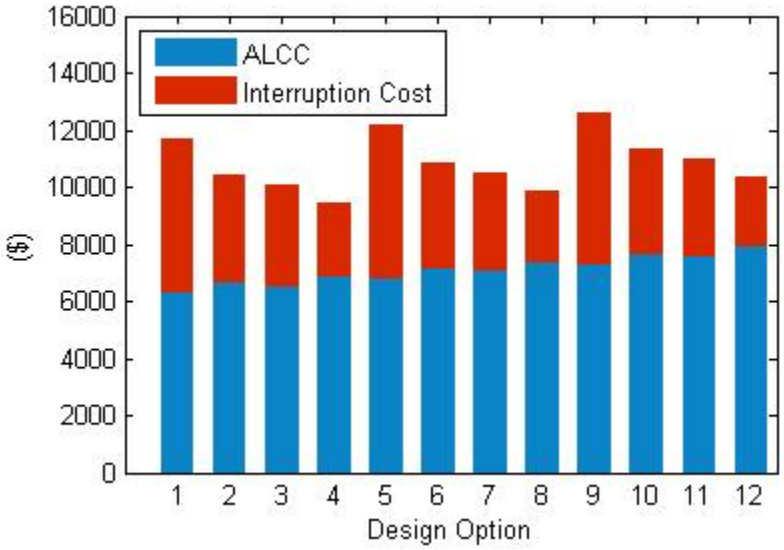

Figure 7.13 A comparison of C_{EV} using equal cost weight factors

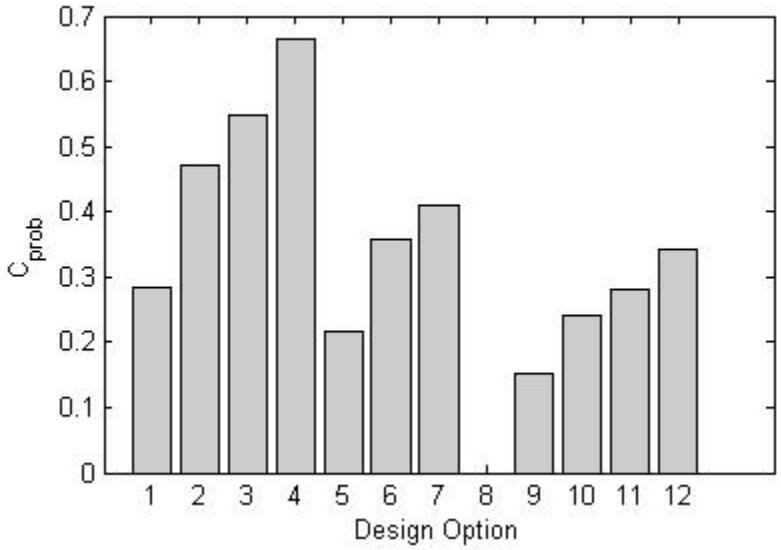

Figure 7.14 A comparison of C_{prob} using equal cost weight factors

□ Proportional weight factors

When using the proportional weight factors for customer interruption cost estimates, the optimal design option continues to be Option 4 regardless which PI is used for performance comparisons (Figure 7.15 and Figure 7.16).

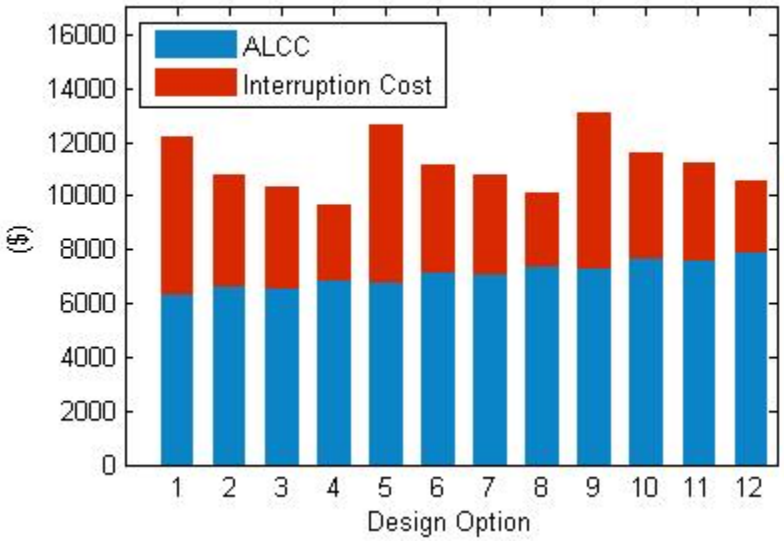

Figure 7.15 A comparison of C_{EV} using proportional cost weight factors

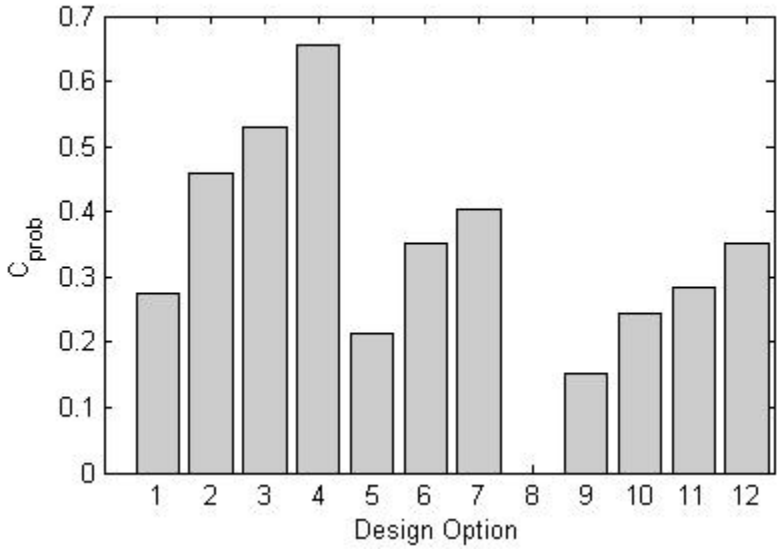

Figure 7.16 A comparison of C_{prob} using proportional cost weight factors

7.6.2 Degradation of a PV power system

The efficiency of a PV module degrades with time. The yearly degradation rate depends on the type of PV modules, PV operating environment, the effectiveness of the system maintenance, etc. A case study of an existing 1 kW roof PV system shows that its amorphous silicon PV system has a degradation rate of 0.985% per year (DC) and 1.09% per year (AC) [52]. This degradation is in agreement with benchmarked data shown in Table 7.3. The degradation rate of 1% per year is used in this case study.

Figure 7.17 shows the system total cost change along service life time of Design option 4 (i.e. the optimal design option). The green square represents the expected value. The error bars show the maximum and minimum values of the total cost. Obviously power reliability drops along the time due to PV efficiency degradations. The system reliability indices, shown in Figure 7.18, confirm this trend. Over the 30 year service life time the mean overall system failure rate increase from 105 times per year to 392 times per year

and the mean unmet electricity amount increases from 602 kWh/year to 1674 kWh/year. The mean overall power unavailability increases from 8.4% to 27.5%. It suggests that certain system upgrade will be necessary during its lifetime in order to provide a reasonable quality level of electric service to off-grid residents consistently.

Figure 7.19 shows the total cost over service lifetime for the original design (i.e. Design option 8). It indicates that Option 4 will continue to have the lowest total cost over the whole lifetime even when degradation effects are taken into accounts.

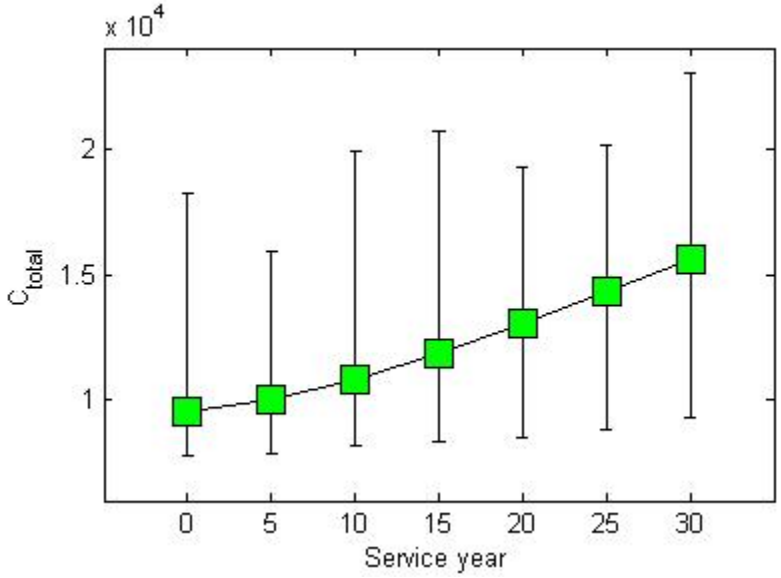

Figure 7.17 Design option 4 - A plot of C_{EV} over service life

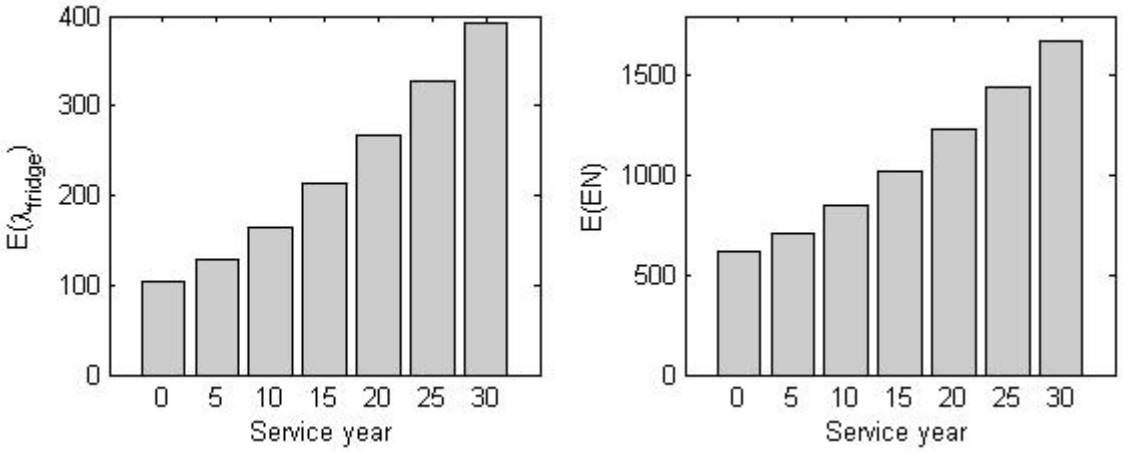

Figure 7.18 Design option 4 – Plots of $E(\lambda_{fridge})$ and $E(EN)$ over service life

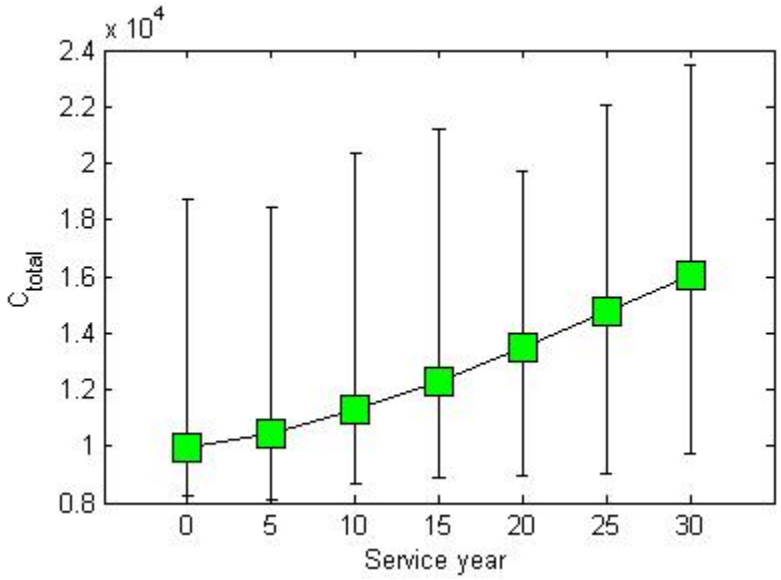

Figure 7.19 Design option 8 - A plot of C_{EV} over service life

7.7 Conclusions

This chapter applies a value-based approach to designing a cost effective PV power system for an existing off-grid solar house – the GTSD07 house. The design objective is to find the balancing point between the acceptable power reliability level and affordable capital cost.

Two sets of PIs used in this case study for decision making: the expected value based PI and the probability based PI. In this case study both sets of PIs lead to the same optimal design option. The installation of a SMBPC largely reduces the difference between the top two design options and it makes the optimal design option less competitive. Meanwhile the reliability study over system service life time reveals that the designed PV system requires an upgrade during its lifetime in order to provide satisfactory electric service consistently.

CHAPTER 8 A RISK-BASED APPROACH

8.1 The overall comfort measure in an off-grid solar house

The earlier chapters of this dissertation have focused on power reliability analysis of an off-grid solar house. Onsite generated energy is distributed to different house consumers to fulfill occupants' basic needs, such as providing food (which requires energy inputs to the refrigerator and cooking devices), individual entertainments (which may include energy inputs to TV, computers, DVD players and etc.), emergency responses (which may include energy inputs to different alarms) and other. The HVAC system, which accounts for 20 to 50% of the energy use in residential buildings, is one of the biggest energy consumers in an off-grid house. The energy consumed by the HVAC system is used to maintain thermal comfort in indoor spaces whenever they are occupied. The more closely thermal comfort is maintained to the optimum, the more energy a HVAC system will need. The sophistication of balancing thermal comfort and energy consumption has been raised in building control research [136]. In the light of this, it would not be appropriate to use only power reliability with respect to the HVAC system, if it is not linked to the realized performance of thermal comfort. It can be expected that a lower acceptable thermal comfort performance will lead to increased HVAC power reliability. Finding this relationship (under uncertainty) is one of the objectives of this chapter.

8.2 The trade-off between of users' thermal comfort and power reliability

8.2.1 Design criteria for thermal comfort requirement in buildings

This research uses the customary heating/cooling setpoints to express indoor thermal comfort targets. They are 76°F (~24.4°C) with a setback temperature of 80°F (~26.7°C) for cooling and 68°F (20°C) with a setback of 60°F (~15.6°C) for heating. ASHRAE defines design conditions of a HVAC system such that their values represent the value that is exceeded on average 99.0% (hot season) and 99.6% (cold-season) of the total number of hours in a year (8760 hours). This definition of design conditions can be understood as a thermal comfort compliance criterion to some degree but in reality it is a sizing criterion. There are no relevant official compliance codes available in the U.S. to define how strictly the thermal comfort criteria have to be met over the course of a year (i.e. the maximum hours of thermally uncomfortable environment allowed over a year). The thermal comfort compliance studies in Europe commonly use two sets of criteria:

1) 25°C may be exceeded during max 10% of the working hours in a year (100 hour per year); and 28°C may be exceeded during max 1%-2% of working hours in a year (10-20 hour per year). It is an example setting of exceeding hour limits of desired temperatures released by the Dutch Governmental Occupational health Service and has been described in a thermal comfort study by van der Linden et al. [137].
2) 25°C may be exceeded during max 5% of occupied hours in a year; and 28°C may be exceeded during max 1% of occupied hours. This criterion is given by a UK guideline [138] and discussed in several studies [139, 140].

This research will use the first criterion mentioned above, but with the proviso that residential occupants are more flexible in terms of reacting to a varying thermal environment. As in the U.S. there is no established definition of extreme thermal environments (i.e. 28°C in the above contexts) we will use an arbitrary but plausible range for that purpose. This range is chosen to be identical with the setback temperature setpoints. This leads to the following thermal comfort criteria: the temperature range of [68°F, 76°F] ([20°C, 24.4°C]) can be exceeded at the most during 10% of occupied hours per year and the temperature range of [60°F, 80°F] (15.6°C, 26.7°C) can be "deceeds" at the most of 1.5% of occupied hours in a year (deceed is used as the opposite of exceed). This setting of thermal comfort compliance criteria results in the formulation of two PIs related to thermal comfort as shown in Equation 8-1 and 8-2. They are percentage of exceeding and deceeding hours of the comfort range (68°F, 76°F) and the extreme temperature range (60°F, 80°F). Two corresponding risk measures can be calculated using Equation 8-3 and 8-4 respectively.

$$PercentageT_c = \frac{hr(T \notin [68°F, 76°F])}{TotalOccupiedHours} \times 100\% \quad (8\text{-}1)$$

$$PercentageT_e = \frac{hr(T \notin [60°F, 80°F])}{TotalOccupiedHours} \times 100\% \quad (8\text{-}2)$$

$$Risk(T_c) = \Pr(PercentageT_c > 10\%) \quad (8\text{-}3)$$

$$Risk(T_e) = \Pr(PercentageT_e > 1.5\%) \quad (8\text{-}4)$$

8.2.2 A temperature tuning module

In order to adjust the energy allocation between general power consumers and the HVAC system a temperature (setpoint) tuning module has been implemented into the SMBPC.

Figure 8.1 shows the relationship and data exchange between the temperature tuning module and components of the SMBPC.

Figure 8.2 shows the detailed flowchart of the temperature tuning module. Compared to the original system with a SMBPC, the temperature tuning module is added to allow users to move the HVAC system up in priority when indoor temperature reaches a certain temperature range due to lack of power. Thus the HVAC system will have two modes: a regular mode and a new mode called "relax mode" in this study. As shown in Figure 8.2 the temperature tuning module will check indoor temperature when the HVAC runs in regular mode. If the indoor temperature goes beyond a set range the tuning module will set the HVAC system to relax mode. This mode change is accomplished by two actions: 1) to set the heating/cooling setpoints to setback values and meanwhile shift setback values correspondingly; and 2) to promote the rank of HVAC system in the SMBPC from $Rank_{HVAC,original}$ to $Rank_{HVAC,pro}$ if the HVAC system is not on the top of the preference list given by users in the first place. The reverse mode change (i.e. switch from relax mode to regular mode) happens when the ratio of battery storage to battery capacity is larger than a preset value $f_{s,HVAC}$. When the mode changes from relax mode to regular mode the rank of HVAC system in SMBPC and its setpoints will be changed accordingly.

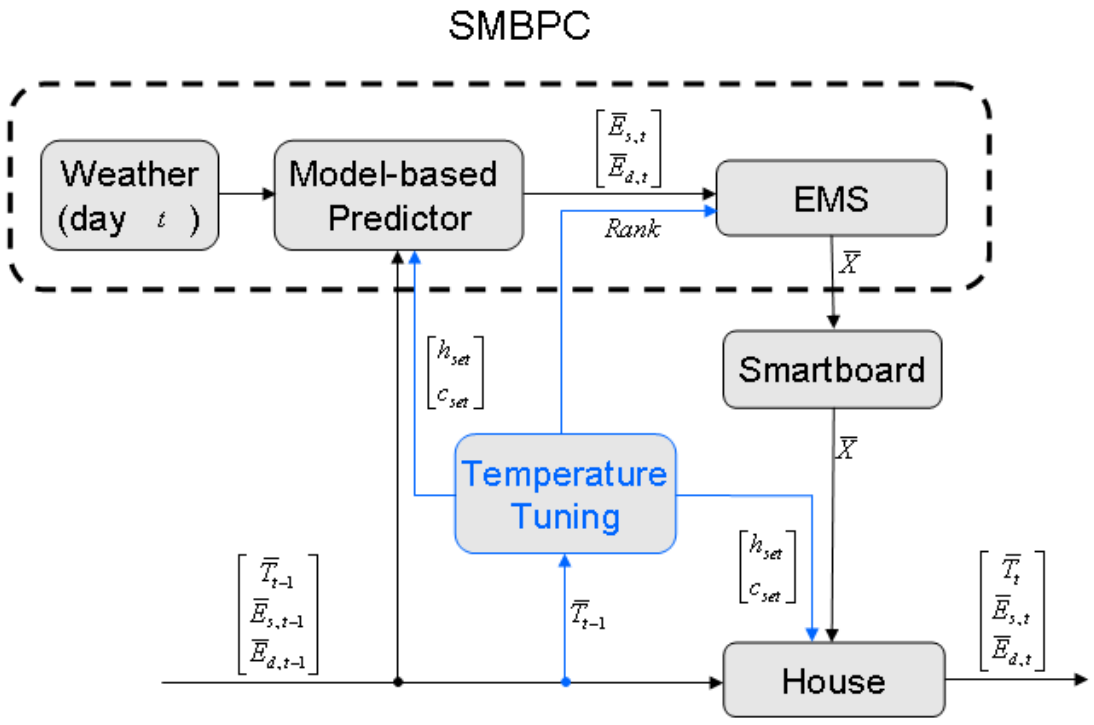

Figure 8.1 The concept diagram of a SMBPC equipped with a temperature tuning module

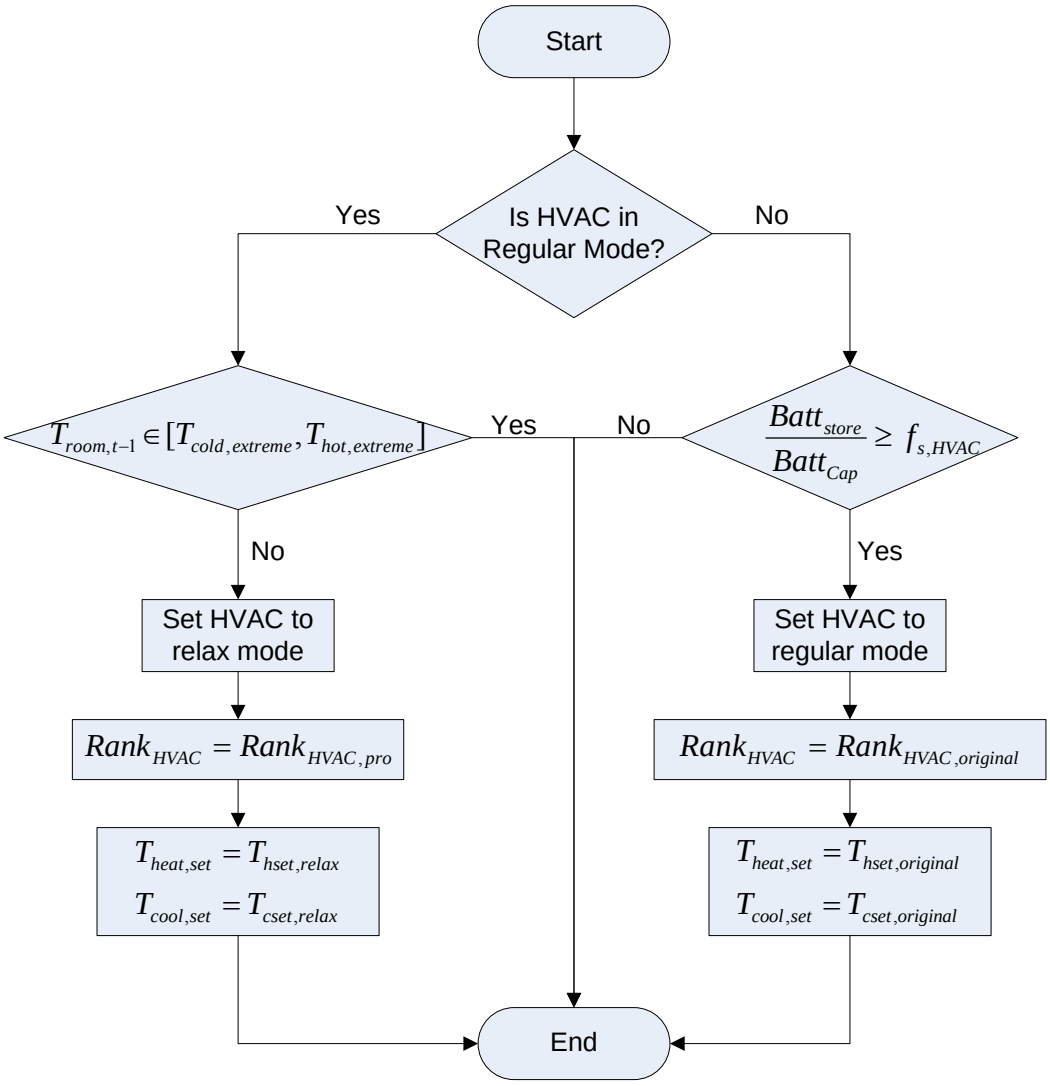

Figure 8.2 Flow diagram of the proposed temperature tuning module

8.2.3 The trade-off

The subtle trade-off between meeting thermal comfort requirement and meeting general power reliability requirement can be achieved through proper tuning of the controller parameters $f_{s,HVAC}$ and $Rank_{HVAC,pro}$ of the proposed temperature tuning module. The GTSD07 house is used again here as the case to evaluate the adequateness and performance of the proposed tuning module.

The value of $f_{s,HVAC}$ is set to vary between 0.3 and 0.9. The minimum value for $f_{s,HVAC}$ is set to be 0.3 because the maximum allowable depth of discharge of the batteries is 0.8. It becomes pointless if $f_{s,HVAC}$ is assigned a very small value. The original rank of the HVAC system given by users is 5 which leaves four possible values for $Rank_{HVAC,pro}$. They are 2, 3, 4, and 5. When $Rank_{HVAC,pro}$ is set to be 2 the temperature tuning module aims to promote thermal comfort needs. In turn the rest of the energy consumers will be allocated less energy and as a result, the general power reliability for these consumers will decrease.

As discussed in Chapter 7 the evaluation of the SMBPC's impact on power reliability in an off-grid house is very computing intensive if done in one pass. A conventional MPC with known information has been proposed in Chapter 7 to replace the SMBPC for a preliminary (first pass) performance investigation. The same approach is adopted in this chapter and for simplicity the chosen conventional MPC with known information will be referred to as a deterministic model based predictive controller (DMBPC) in the rest of this chapter.

Table 8.1 shows the impact that the temperature tuning module has on the risks in terms of outage hour $Risk(r)$. Although minor changes are observed the results indicate that $Risk(r)$ values are neither sensitive to the existence of a temperature tuning module nor to the change of $f_{s,HVAC}$ values. Another risk factor, $Risk(U)$, turns out to be more sensitive to the temperature tuning module and its parameter variations, as shown in Table 8.2 . The results show that power unavailability decreases for the HVAC system while it increases for the rest of house electricity consumers. Table 8.3 lists the mean

values of two thermal comfort PIs and their corresponding risk measure values. The results are in agreement with results shown in Table 8.2. Although there is nearly no reduction observed in exceeding hours of comfort range there is a maximum 1.7% reduction in the mean exceeding hours of the extreme temperature range. Figure 8.3 shows the variation of $Risk(T_c)$ as a function of the temperature tuning module parameter $Rank_{HVAC,\,pro}$ and $f_{s,\,HVAC}$. Despite the swing in the middle the $Risk(T_c)$ value increases when $f_{s,\,HVAC}$ increases. For GTSD07 house the minimum $Risk(T_c)$ is achieved at the following point $f_{s,\,HVAC}$ = 0.3, and $Rank_{HVAC,\,pro}$=3.

Table 8.1 The comparison of $Risk(r_i)$ between with and without a temperature tuning module ($Rank_{HVAC,\,pro}$ = 2)

i	No MPC	DMBPC Only	DMBPC + Temperature tuning module ($f_{s,\,HVAC}$)						
			0.3	0.4	0.5	0.6	0.7	0.8	0.9
1	0.0%	3.0%	1.1%	1.0%	1.1%	1.1%	1.1%	1.1%	1.1%
2	0.0%	0.0%	0.1%	0.1%	0.1%	0.1%	0.1%	0.1%	0.1%
3	0.0%	0.0%	0.0%	0.0%	0.0%	0.0%	0.0%	0.0%	0.0%
4	0.0%	0.0%	0.0%	0.0%	0.0%	0.0%	0.0%	0.0%	0.0%
5	0.0%	0.0%	0.0%	0.0%	0.1%	0.1%	0.0%	0.0%	0.1%
6	0.0%	0.0%	0.0%	0.0%	0.0%	0.0%	0.0%	0.0%	0.0%
7	61.3%	45.4%	44.8%	45.4%	45.7%	45.8%	45.6%	45.4%	46.2%
8	0.0%	0.0%	0.0%	0.0%	0.0%	0.0%	0.0%	0.0%	0.0%

Table 8.2 The comparison of $Risk(U_i)$ between with and without a temperature tuning module ($Rank_{HVAC,\,pro} = 2$)

i	No MPC	DMBPC Only	DMBPC + Temperature tuning module ($f_{s,HVAC}$)						
			0.3	0.4	0.5	0.6	0.7	0.8	0.9
1	65.3%	95.1%	95.1%	89.1%	84.3%	84.8%	82.9%	83.5%	83.1%
2	100.0%	98.1%	100.0%	100.0%	100.0%	100.0%	99.3%	100.0%	100.0%
3	66.0%	21.1%	32.0%	28.5%	31.3%	31.1%	29.6%	30.8%	29.5%
4	66.1%	20.1%	27.8%	25.7%	24.8%	26.5%	25.1%	28.2%	23.4%
5	100.0%	96.7%	100.0%	99.0%	100.0%	100.0%	99.2%	100.0%	100.0%
6	67.8%	77.6%	81.8%	81.5%	85.1%	84.5%	83.8%	85.9%	83.2%
7	100.0%	93.9%	100.0%	98.3%	100.0%	100.0%	98.3%	98.8%	100.0%
8	100.0%	94.0%	100.0%	98.4%	100.0%	100.0%	98.4%	99.0%	100.0%

Table 8.3 The comparison of $Risk(T_c)$ and $Risk(T_e)$ between with and without a temperature tuning module ($Rank_{HVAC,\,pro} = 2$)

	No MPC	DMBPC Only	DMBPC + Temperature tuning module ($f_{s,HVAC}$)						
			0.3	0.4	0.5	0.6	0.7	0.8	0.9
$Risk(T_c)$	54.8%	72.7%	72.0%	78.5%	79.5%	81.6%	84.9%	89.4%	86.8%
$Risk(T_e)$	100.0%	100.0%	100.0%	100.0%	100.0%	100.0%	100.0%	100.0%	100.0%
$E(\text{PercentageT}_c)$	11.4%	12.5%	12.5%	13.2%	13.7%	14.2%	14.6%	14.9%	15.2%
$E(\text{PercentageT}_e)$	6.9%	8.3%	7.4%	6.9%	6.8%	6.7%	6.6%	6.6%	6.6%

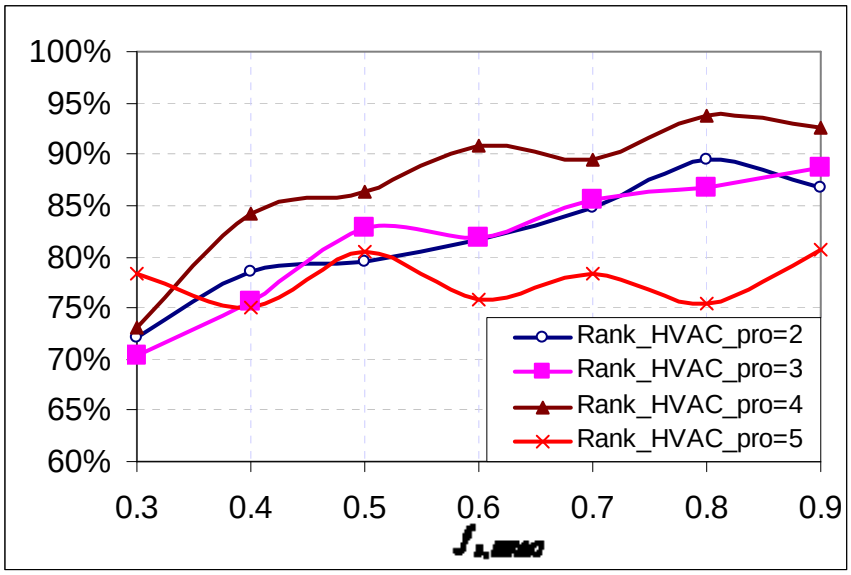

Figure 8.3 A comparison of $Risk(T_c)$ when $Rank_{HVAC,\,pro}$ and $f_{s,HVAC}$ vary

8.3 A risk-based approach

As addressed earlier, each kWh of onsite generated energy is eventually allocated to the individual systems that fulfill a variety of occupant's needs. Current design practice will have to provide guarantees to the developers, buyers and occupants, most likely in the form of some level of power reliability compliances. It turns out that strict power reliability compliance is often hard to meet without incurring significant extra costs and substantial energy waste (i.e. the supply system is oversized during most of the year). In order to reach a reliable and affordable solution for all stakeholders, it is the designer's responsibility to conduct design optimization that balances system investments and resulting power reliability.

Chapter 7 has presented an approach commonly used in the current power industry practices. But the effectiveness of the value-based approach highly depends on how well the interruption cost function represents the damage that a power interruption causes to

off-grid residents. Due to of the way that researchers have developed interruption cost functions, the results have mostly been rather subjective. It should also be recognized that the interruption cost function varies across individual residents. In addition, the value-based approach translates power reliability into dollar values in the objective function; this tends to blur the designers' perspective on power reliability compliances. A slight variation is therefore proposed, i.e. a risk-based approach to design optimization which applies power reliability compliances as optimization constrains while minimizing system costs as the objective function. As a result it provides a direct and more intuitive solution to the above design problem. The GTSD07 house is used as a case study to demonstrate this approach.

8.3.1 The mathematical expression of design problems

Mathematically the design optimization problem in this study is a stochastic programming problem. The proposed risk-based approach solves it as an optimization problem with probabilistic constraints (sometimes also called chance constraints). The mathematical form of the optimization problem is shown below:

$$\min cX \tag{8-5}$$

s.t.

$$\begin{cases} \Pr(r_i > r_{i,req}) \le \varepsilon_{r_i,tolerance} \ (i = 1 \sim 8) \\ \Pr(U_i > U_{i,req}) \le \varepsilon_{U_i,tolerance} \ (i = 1 \sim 8) \\ \Pr(PercentageT_c > 10\%) \le \varepsilon_{Tc,tolerance} \\ \Pr(PercentageT_e > 1.5\%) \le \varepsilon_{Te,tolerance} \end{cases}$$

Where,

X Design variables;

c The cost function;

$r, U, PercentageT_c, PercentageT_e$ Performance measures that are functions of design variables X and uncertain parameters ω embedded in the system model (the same set of uncertain parameters as introduced in Chapter 2);

$\varepsilon_{r,tolerance}, \varepsilon_{U,tolerance}, \varepsilon_{Tc,tolerance}, \varepsilon_{Te,tolerance}$ Risk parameters chosen by decision makers, i.e. developers, buyers or (prospecting) occupants in our case. It represents people's attitude towards unwanted events and is often a small value like 0.01, 0.05 depending on quality control of specific situations. This is in fact subject to research that needs to be carried out in the future. For simplicity, this study uses the plausible value of 0.1 for all risk thresholds.

8.3.2 A practical solution towards the optimal design

Stochastic programming is generally difficult to solve, especially when probabilistic constraints exist. Moreover the stochastic programming problem in the building research domain relies on (in most cases non-linear) building simulations to evaluate constraint satisfaction at each value of the design variables. The problem is harder as there is also no explicit mathematical relationship between design variables and constraints. The fact that the constraints are implicit disqualifies most advanced techniques developed to solve stochastic programming problems.

Therefore this research will rely on a traditional sizing method to find a starting design option which is typically close enough to the optimal solution and then explore its neighboring area for a more economic design by exhaustive search. There are two strategies taken in the exhaustive search to reduce computing time. They are:

1) Replace the SMBPC by the DMBPC module in the search. A reliability analysis using the DMBPC model only uses about 1% of the computational efforts that the

same analysis but using the SMBPC model needs. According to statistic theory the profit estimated by a stochastic optimization with know information about demand parameters will always be larger than that estimated when demand parameters are unknown. People always make the best decision if future need is known. Thus the reliability analysis using the DMBPC model will overestimate power reliability and the resulting optimal solution is indeed not feasible as it will not satisfy constraints. But the optimization using the DMBPC model will generate a smaller design space for the ensuing search of a real and feasible optimal solution using the SMBPC model.

2) Replace a full scanning of the temperature tuning module parameters by a strategic search algorithm. The temperature tuning module has two module parameters - $Rank_{HVAC,pro}$ and $f_{s,HVAC}$. A complete scanning of all possible combinations will require 21 full power reliability analyses. Earlier analysis in the previous section shows that the general power unavailability decreases when $f_{s,HVAC}$ increases and meanwhile thermal comfort worsens. As power unavailability decreases when $Rank_{HVAC,pro}$ decreases, instead of conducting a full scan on all possible combinations, the search algorithm will always start from the biggest $Rank_{HVAC,pro}$ value (i.e. $Rank_{HVAC,pro}$=5) and the biggest $f_{s,HVAC}$ value ($f_{s,HVAC}$=0.9) which represents the controller's best effort to increase power reliability. If the risk constraints for power reliability are not satisfied the search algorithm will move to the next design option otherwise it will continue the search within the current design option by decreasing $f_{s,HVAC}$ and $Rank_{HVAC,pro}$.

Figure 8.4 shows the flow diagram of a practical solution to the risk-based design optimization problem. Table 8.4 shows all the risk values (i.e. constraints in Equation 8-5) for all investigated design options. As is shown, none of the investigated design options satisfies all risk constraints and there is no feasible solution reached in the selected design space.

Experiments are designed and conducted to search a feasible region before the finer search is conducted within this region. In order to simply the design problem, the PV modules mounted to the southern wall is repositioned to be the same as the PV modules on the roof. Thus the design variables reduce to two: the number of PV modules and the number of batteries. Table 8.5 shows all risk indices and two energy related power reliability indices from an experiment with fixed number of PV modules. It shows that when the number of PV modules is large enough the improvement of the risk indices caused by increasing number of batteries is limited and seems to be bounded. The same trend is observed for the number of PV modules when the battery capacity is large enough, as shown in Table 8.6. Figure 8.5 shows the expected values of two energy related power reliability indices EW and EN when different numbers of PV modules are installed ($N_{battery} = 32$, about 400 kWh total capacity). It shows that when the number of N_{PV} is larger than 34 the gradient with which $E(EW)$ increases becomes steeper than the gradient that $E(EN)$ decreases. This indicates that additional investment makes nearly no sense from this point. An extremely large system would have to be installed to meet the risk thresholds.

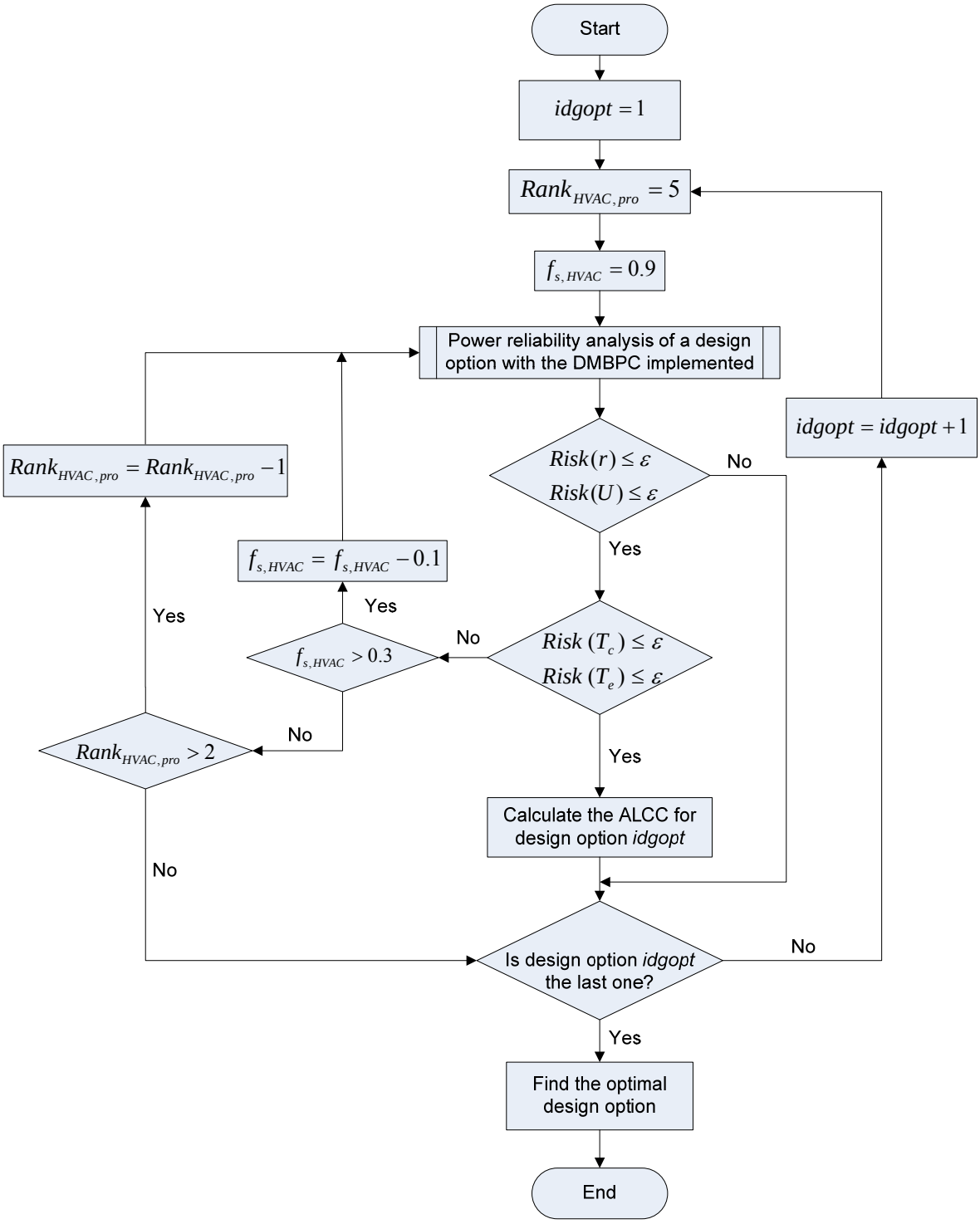

Figure 8.4 Flow diagram of the risk-based design optimization

Table 8.4 The risk PI values of all design options

	Option 1	Option 2	Option 3	Option 4	Option 5	Option 6	Option 7	Option 8	Option 9	Option 10	Option 11	Option 12
Risk(r)	1.9%	2.0%	2.4%	2.4%	1.9%	2.1%	2.4%	2.5%	1.9%	2.1%	2.5%	2.5%
	0.1%	0.0%	0.0%	0.0%	0.1%	0.0%	0.0%	0.0%	0.1%	0.0%	0.0%	0.0%
	0.0%	0.0%	0.0%	0.0%	0.0%	0.0%	0.0%	0.0%	0.0%	0.0%	0.0%	0.0%
	0.0%	0.0%	0.0%	0.0%	0.0%	0.0%	0.0%	0.0%	0.0%	0.0%	0.0%	0.0%
	0.0%	0.0%	0.0%	0.0%	0.0%	0.0%	0.0%	0.0%	0.0%	0.0%	0.0%	0.0%
	0.1%	0.0%	0.0%	0.0%	0.1%	0.0%	0.0%	0.0%	0.1%	0.0%	0.0%	0.0%
	53.7%	50.3%	47.5%	45.4%	53.9%	50.3%	47.5%	45.4%	54.0%	50.4%	47.7%	45.2%
	0.0%	0.0%	0.0%	0.0%	0.0%	0.0%	0.0%	0.0%	0.0%	0.0%	0.0%	0.0%
Risk(U)	100.0%	100.0%	100.0%	97.7%	100.0%	100.0%	100.0%	96.5%	100.0%	100.0%	100.0%	94.4%
	100.0%	100.0%	100.0%	99.1%	100.0%	100.0%	100.0%	98.8%	100.0%	100.0%	100.0%	98.6%
	80.6%	58.4%	45.9%	23.5%	79.1%	54.4%	42.0%	22.4%	76.1%	51.9%	39.1%	21.4%
	76.2%	55.9%	41.6%	23.0%	73.5%	53.1%	38.8%	21.8%	73.3%	50.1%	36.8%	20.6%
	100.0%	100.0%	100.0%	98.9%	100.0%	100.0%	100.0%	97.9%	100.0%	100.0%	100.0%	96.0%
	100.0%	95.2%	95.1%	80.1%	100.0%	93.8%	94.6%	76.2%	99.4%	92.6%	93.6%	72.2%
	100.0%	100.0%	100.0%	98.3%	100.0%	100.0%	99.5%	96.5%	100.0%	100.0%	100.0%	95.1%
	100.0%	100.0%	100.0%	98.3%	100.0%	100.0%	99.5%	96.5%	100.0%	100.0%	100.0%	95.2%
Risk(Tc)	100.0%	95.7%	95.5%	82.1%	100.0%	92.5%	92.7%	78.3%	100.0%	91.5%	91.8%	73.8%
Risk(Te)	100.0%	100.0%	100.0%	100.0%	100.0%	100.0%	100.0%	100.0%	100.0%	100.0%	100.0%	100.0%

Table 8.5 Risk results from a design of experiment with fixed PV module numbers

N_{PV}	36	36	36	36	36	39	39	39	39	39
$N_{battery}$	16	20	24	28	32	16	20	24	28	32
Risk(r)	3.4%	3.2%	3.2%	3.2%	3.4%	2.4%	2.4%	2.3%	2.3%	2.3%
	0.0%	0.0%	0.0%	0.0%	0.0%	0.0%	0.0%	0.0%	0.0%	0.0%
	0.0%	0.0%	0.0%	0.0%	0.0%	0.0%	0.0%	0.0%	0.0%	0.0%
	0.0%	0.0%	0.0%	0.0%	0.0%	0.0%	0.0%	0.0%	0.0%	0.0%
	0.0%	0.0%	0.0%	0.0%	0.0%	0.0%	0.0%	0.0%	0.0%	0.0%
	0.0%	0.0%	0.0%	0.0%	0.0%	0.0%	0.0%	0.0%	0.0%	0.0%
	42.2%	43.5%	42.1%	42.2%	42.4%	39.9%	39.9%	40.5%	39.5%	40.1%
	0.0%	0.0%	0.0%	0.0%	0.0%	0.0%	0.0%	0.0%	0.0%	0.0%
Risk(U)	91.1%	91.1%	89.7%	93.1%	90.8%	77.0%	71.5%	72.1%	69.9%	75.3%
	95.5%	97.6%	98.1%	97.1%	97.0%	89.6%	87.6%	89.8%	91.1%	89.8%
	6.5%	7.7%	6.4%	6.7%	6.1%	0.5%	2.0%	2.0%	1.7%	1.3%
	4.3%	5.9%	4.9%	4.7%	5.0%	0.5%	1.9%	1.5%	1.3%	0.6%
	91.8%	93.6%	92.9%	93.3%	92.5%	79.8%	80.8%	78.8%	78.8%	84.6%
	73.1%	68.0%	68.9%	65.8%	70.8%	44.6%	41.0%	44.3%	43.1%	44.1%
	91.1%	90.9%	92.1%	92.2%	91.6%	77.4%	78.5%	75.1%	76.0%	79.4%
	91.1%	90.9%	92.1%	92.3%	91.6%	78.0%	78.8%	76.3%	76.0%	79.9%

Table 8.5 (continued)

Risk(Tc)	71.4%	67.8%	66.8%	66.0%	71.1%	42.6%	42.8%	42.1%	41.0%	41.8%
Risk(Te)	100.0%	100.0%	100.0%	99.5%	100.0%	98.8%	97.8%	98.9%	98.4%	97.8%
Mean(EW)	1239	1253	1246	1246	1246	1853	1863	1856	1862	1856
Mean(EN)	193	195	193	191	194	145	142	143	142	142

Table 8.6 Risk results from a design of experiment with fixed battery numbers

N_{PV}	28	30	32	34	28	30	32	34	36	39
$N_{battery}$	24	24	24	24	32	32	32	32	32	32
Risk(r)	2.3%	2.9%	3.8%	3.7%	2.0%	2.4%	2.8%	2.6%	3.4%	2.3%
	0.2%	0.1%	0.0%	0.0%	0.2%	0.1%	0.0%	0.0%	0.0%	0.0%
	0.0%	0.0%	0.0%	0.0%	0.0%	0.0%	0.0%	0.0%	0.0%	0.0%
	0.0%	0.0%	0.0%	0.0%	0.0%	0.0%	0.0%	0.0%	0.0%	0.0%
	0.0%	0.0%	0.0%	0.0%	0.0%	0.0%	0.0%	0.0%	0.0%	0.0%
	0.1%	0.1%	0.0%	0.0%	0.1%	0.1%	0.0%	0.0%	0.0%	0.0%
	53.7%	50.0%	47.1%	44.2%	54.0%	50.3%	47.5%	44.7%	42.4%	40.1%
	0.0%	0.0%	0.0%	0.0%	0.0%	0.0%	0.0%	0.0%	0.0%	0.0%

Table 8.6 (continued)

Risk(U)	100.0%	99.1%	94.6%	87.3%	98.9%	96.4%	91.0%	73.7%	90.8%	75.3%
	100.0%	100.0%	100.0%	97.3%	100.0%	100.0%	100.0%	96.6%	97.0%	89.8%
	69.1%	45.7%	22.2%	9.4%	69.5%	46.3%	23.5%	9.7%	6.1%	1.3%
	67.2%	42.5%	21.4%	8.0%	68.5%	43.8%	21.2%	8.3%	5.0%	0.6%
	100.0%	99.3%	98.8%	94.8%	99.4%	99.1%	97.6%	92.9%	92.5%	84.6%
	98.4%	94.9%	87.3%	69.9%	97.5%	90.7%	80.9%	60.1%	70.8%	44.1%
	100.0%	99.3%	98.1%	94.5%	99.2%	98.9%	94.7%	89.5%	91.6%	79.4%
	100.0%	99.3%	98.2%	94.6%	99.2%	99.0%	94.9%	90.8%	91.6%	79.9%
Risk(Tc)	98.7%	94.8%	87.3%	67.6%	95.3%	90.6%	74.3%	56.3%	71.1%	41.8%
Risk(Te)	100.0%	100.0%	100.0%	100.0%	100.0%	100.0%	100.0%	100.0%	100.0%	97.8%
Mean(EW)	73	226	455	779	58	193	399	710	1246	1856
Mean(EN)	539	377	269	204	538	372	259	190	194	142

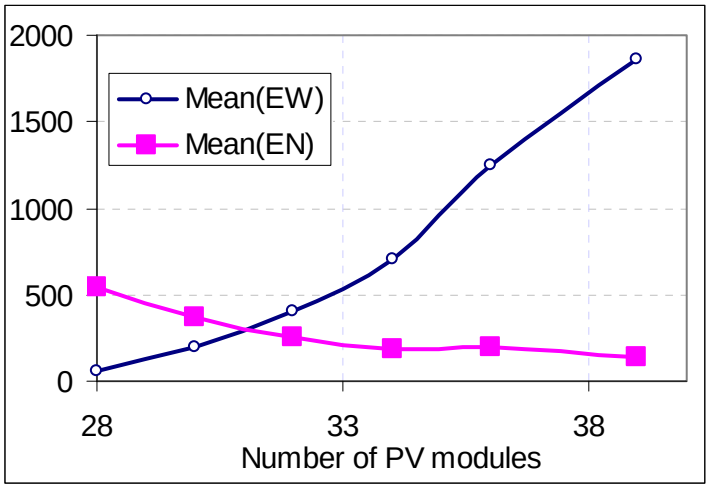

Figure 8.5 A comparison of expected *EW* and *EN* at different number of PV modules with a fixed 32 batteries

8.4 Discussions

Results in this chapter indicate that close to a certain "near optimum" level of performance, the risk factors become insensitive to further change of the design variables. It proves that further investment leads to more energy waste due to oversizing and yields only marginal improvement in the risk indices. This suggests that the risk indices of the GTSD07 house are primarily affected by factors other than the capacity of onsite energy generation and storage systems. The most plausible cause for this "system design independent" risk is obviously the weather, as both energy generation and consumption in off-grid solar house are highly dependent on the dynamics of the ambient weather conditions. It suggests that the frequency with which cloudy days occur pose the irreducible risk in a near optimal design space. It also shows that the system may have to go to extreme oversizing to reduce the risk indices to the desired level. This insight has two important ramifications: (1) risk thresholds may have to be chosen in a location

dependent manner as different locations may have feasible design space that respond to certain risk thresholds; (2) it may require a use of more adequate time series of weather in risk based design. The latter deserves further exploration.

As addressed in the beginning of this thesis the TMY3 weather file for Atlanta, GA (365 day time series which is widely used in current building performance simulation and PV system design) is used in all uncertainty analysis and reliability/risk studies. A deterministic simulation of the GTSD07 house using reference values for all uncertain variables and the TMY3 weather reveals that the longest consecutive period during which its onsite generation amount is less than the daily energy need is seven days. It is between Dec 28th and Jan 3rd. The total unmet electricity during this period is about 100 kWh. Between Dec 28th and Jan 10th the total unmet electricity accumulates to 189 kWh. The last period that the house has a sufficient positive storage is back on Dec 7th. The above only addresses power unavailability on a daily basis and power unavailability in real time will be more severe because of energy waste due to possible instantaneous mismatches between power demand and supply.

A small experiment has been designed and conducted to investigate the impact of weather uncertainty on power reliability assessment of an off-grid solar house. Power reliability assessment is conducted on the GTSD07 house (without any advanced control and the house is considered as one single consumer) under two different scenarios as shown below:

- Scenario 1: the TMY3 weather data set is used;
- Scenario 2: all 15 weather data sets between 1991 and 2005 are used [141]. The 1991-2005 weather dataset is based mainly on measurements but also contains

modeled data. They are the original data source used for the TMY3 data set development.

In both scenarios system uncertainty (uncertainties shown in Table 5.18) remains the same and the sample number of MC simulations is 200.

Table 8.7 shows the comparison of total variances of the basic reliability indices between Scenario 1 and Scenario 2. The variance of outage hour r is not listed because unlike other basic reliability indices there is no monotonic mapping between the LHS sample and outage hour r (i.e. there are more than 1 outage event during a sample year). The results show that the system uncertainty is responsible for most of the variances in failure rate λ (98%). And it is also responsible for about 74% of the variances in general power unavailability U. Table 8.7 also indicates that the system uncertainty contributes almost of the same to variances of power unavailability U and the needed energy EN. It is because that the yearly needed energy EN is a product of yearly house load and general unavailability U. And as proved through cases studies the yearly house load evaluated using TMY data is very close to the average using its corresponding actual weather data sets [40]. The total variance in yearly wasted energy EW using TMY3 data set is larger than that using 15 actual weather data sets. It is due to the fact that the yearly total radiation in TMY3 is larger than the average of 15 actual weather data sets and thus more energy gets wasted.

Table 8.8 shows the expected values of all power reliability indices. The results indicate that the inclusion of a larger data set of weather files does not influence the expected total number of power interruptions in a year. However it does influence the rest of power

reliability indices. The percentage difference of expected power reliability indices is shown in the last column of Table 8.8.

Table 8.9 shows the value of $Risk(U)$ when 5% is used as the design criterion for power unavailability U. The inclusion of larger weather data sets instead of TMY3 weather only will lead to an increase of 12.57% in risk in terms of power unavailability U. This increased value is larger than the general setting of risk tolerance $\varepsilon_{tolerance}$ (10% is chosen in this study).

Table 8.7 A comparison of $Var(PI)$ between Scenario 1 and Scenario2

PI	Units	Var(Scenario1)	Var(Scenario2)	$\frac{Var(Scenario1)}{Var(Scenario2)}$
λ	# per year	40747.61	41577.27	98.0%
U	% of a year	0.027	0.036	73.7%
EW	kWh/year	6917311.62	5319906.66	130.0%
EN	kWh/year	379021.15	531774.52	71.3%

Table 8.8 A comparison of $E(PI)$ values between Scenario 1 and Scenario2

PI	Units	Scenario1	Scenario2	$\frac{E(PI)_1 - E(PI)_2}{E(PI)_2}$
λ	# per year	94.07	92.00	2.3%
r	hr	6.66	7.41	-10.1%
U	% of a year	0.072	0.093	-22.7%
EW	kWh/year	958.09	777.51	23.2%
EN	kWh/year	321.07	412.54	-22.2%

Table 8.9 A comparison of $Risk(U)$ value between Scenario 1 and Scenario2

	Scenario1	Scenario2
Risk(U)	68.3%	80.8%

This analysis obviously raises the following question: "Is the TMY3 weather file adequate for risk-based design of zero energy systems"? The TMY data set is developed to provide designers an adequate meteorological data set that sufficiently characterizes ambient conditions at a specific location over a long period of time. It was not designed to represent meteorological extremes in such a way that risk based design is adequately supported. Developing an appropriate weather data set for power reliability analysis of off-grid house design is challenging because of the non-linear and complicated relationship among ambient temperature, local solar radiation intensity, onsite energy generation, and house loads. A TMY data set with associated occurrence frequencies at each time point may be a feasible solution to this need. A comprehensive statistical weather analysis over a long period of historical data will be necessary. Meanwhile one should also be aware that no matter how sophisticated the statistical weather analysis is conducted it will not change the fact that we are designing based on past climate and there will always be the intrinsic uncertainty not investigated as discussed in previous chapters.

8.5 Conclusions

This chapter presents a risk-based approach which formulates the design problem of an off-grid house as a stochastic programming problem where power reliability and thermal comfort requirements serve as probabilistic constraints. It reflects the point of view that for a given design option one will not reject the statistical hypothesis that the probabilistic

performance constraints are satisfied but a small amount of system failure occurrences due to extreme conditions may be allowed. It prevents the system from being oversized in order to ensure system performance under all circumstances, and provides more design space for certain energy efficient technologies especially those whose performances depend on dynamic ambient conditions. Compared to expected value based constraints it better represents occupants' attitude to undesirable shortfalls of power service.

An application of this approach to sizing the onsite solar power system for an existing off-grid house design indicates that the probabilistic constraint compliance will result in an oversized system design if the current TMY3 weather data set is used. A more appropriate weather data set needs to be developed before the risk-based approach demonstrates its merit in industrial design practices.

CHAPTER 9 SUMMARY AND DISCUSSIONS

9.1 Summary and conclusions

Zero energy houses and (near) zero energy buildings are expanding their market penetration from experimental individual cases to industrial applications. This ambitious target is driven by current worldwide energy and environmental crisis. This study has developed a risk based design method to integrate occupants' needs with respect to the key performance aspect – power self-sufficiency – into off-grid system design evolution and has provided detailed information about aspects of future power service in an off-grid residence. It is hoped that the comprehensive approach can be used to provide better evidence to stakeholders, showing when a design works and what risks are inherent. This may remove some suspicion from the public regarding the living quality in (near) zero energy houses and speed up its market penetration towards a new generation of sustainable living. The main contributions of this study are the following:

- Occupant driven power reliability assessment: This research classifies off-grid power demands into different levels according to occupants' need, develops risk performance indicators and integrates occupant's need into design evolution. This occupant driven power reliability analysis provides occupants options to choose what they want and ensures users' satisfaction by responding to what they desire.
- Risk based power reliability assessment: The implementation of risk based power reliability indicators enables the occupant's attitude towards undesired performance to be integrated as decision criteria into design evolution. In a design process where large uncertainties exist and reliability is the essential issue,

imposing constraints on probability of undesired events is more appropriate. The traditional manner of imposing constraints on the expected values (i.e. adding safe factors) is not sufficient to reflect occupants' attitude to inadequate power service. A risk conscious method may also prevent unnecessary energy waste due to oversized systems which are designed to meet all performance requirements under all circumstances including infrequent extreme conditions.

- Stochastic model based controller design: The stochastic model based controller uses uncertainty analysis to project the likelihood of future system performance and then manages energy allocation to different domestic energy consumers accordingly. It bypasses the extreme difficulty in calibrating a deterministic system model that serves in the conventional model based control and provides more flexibility in the future to integrate weather forecast with uncertainty into model based controller design. In addition the developed stochastic model-based control design contains a temperature tuning module which determines the power priority between certain appliances and the HVAC system. The priority settings are adjustable and therefore it allows users to adjust between two kinds of user needs: power reliability and thermal comfort. It should be noted that such a temperature tuning module is very similar to demand control modules, potentially used in grid-connected buildings to reap utility cost savings through relaxing thermal comfort criteria during peak load periods (i.e. during high utility price periods).

- All studies are carried out on design idealizations that cover expected and irreducible uncertainties. A systematic survey of uncertainties and their quantification has been accomplished.

In conclusion, the proposed risk based approach formulates the off-grid design problem as stochastic programming with probabilistic constraints, which successfully reflects occupants' true attitude to undesired power services. It provides an instrument to evaluate power reliability analysis for an off-grid solar house. The stochastic model based controller exploits the advantage of stochastic modeling in representing uncertain system performance under dynamic operating conditions and integrates it with an occupant driven smartboard to provide a more desired energy management service according to occupants' needs. The developed risk based reliability compliance framework opens a new door to sustainable design process where performance assurance is always mandatory and yet challenging due to their dependence on ambient weather. Meanwhile it provides more intuitive information regarding the occurrences of undesired system performance of potential new technology to users and mitigates their fears to the emerging innovative design/systems.

9.2 Limitations and future work

This dissertation has provided the methodology and experimental demonstrations of a risk based approach for off-grid solar house design. The risk based approach is expected to guide designers to a more reliable design compared to the conventional deterministic approach. Its capability to examine risk and execute "risk control" can be extremely helpful and to a certain extent indispensable when experimental technologies or design features are implemented in a design. Future work is required before it can be applied in

field design practice. The following are the most critical aspects that need to be addressed:

1) A weather data set for risk based design practices

Results from design optimization using the risk based approach have revealed the importance of developing a more appropriate weather set. The TMY3 weather data set used in current design practice may contain certain scenarios that alone causes power unavailability larger than design criterion unless extra capacities of sustainable energy system are added. Design practice such as advocated in this thesis will require a more appropriate weather data sets that not only provide typical weather condition in a particular location but also provide probability of certain risk related weather conditions.

2) A simplified building model for robust stochastic optimization

As shown in Chapter 8 the risk based approach formulates the off-grid design problem as stochastic programming with probabilistic constraints. The probabilistic constraints of each design option are examined through a sample approximation using Monte-Carlo technique. It makes each design option evaluation computationally expensive, especially where novel control strategies are implemented such as the stochastic model based control demonstrated in Chapter 8. Meanwhile the power reliability is evaluated through a building simulation package which is a black box simulator and provides no clear mathematical relationship between design variables and power reliability indices. This implicit expression prevents application of any advanced numerical methods that have been developed to solve stochastic programming efficiently. A simplified and explicit building simulator needs to be developed for future robust stochastic optimization.

3) A systematic database for building uncertainty quantifications

The quality of a power reliability assessment depends on how well the relevant uncertainties are quantified. Every power reliability analysis requires an extensive amount of time and efforts on quantifying case relevant uncertainties. A comprehensive database for uncertainties in building simulation ought to be developed so that information can be shared among analysts and fewer efforts are wasted on the same task. Meanwhile a standard uncertainty quantification database would help ensure the quality of uncertainty analysis in building research, including power reliability analysis.

4) Further verification on different climates and different load patterns

This research demonstrates the risk based approach on only one exiting off-grid solar house design for the climate of Atlanta, GA in the USA. Although the general methodology can be consistently applied on other designs and in other climates, further insights will be gathered by large scale applications to other off-grid house designs in different climates.

5) Online calibration module for the stochastic model based predictive controller

The proposed stochastic model based predictive control no longer requires extensive model calibration like a conventional model based predictive control does. But further calibration of the stochastic model is expected to improve its performance greatly. The field application of the proposed stochastic model based controller requires an extra calibration module which will refine uncertainties in the stochastic model using observed occupancy and detailed operation data and provide increasingly more plausible estimate of building energy consumption over time.

6) Application of the principles developed in this thesis on commercial buildings

In commercial buildings the zero energy off-grid target is usually replaced by the net zero energy target. Considering the fact that more and more buildings with experimental renewable technologies report to fall short of their expectations there is good potential to support design decisions of those buildings with risk based strategies.

APPENDIX A THE GTSIM

A.1 Background

GTSim is a building energy simulation program developed in MATLAB environment by the author as part of the work for the Solar Decathlon project. It imports an external TMY3 weather file and provides hourly energy simulation results.

A.2 Framework

GTSim is a finite element based building simulation package with a simple self developed predictor-corrector (p-c) solver. The p-c method was chosen to reduce computation time in the computing intensive reliability analyses. Generally there are three main heat transfer means: conduction, convection, and radiation. All of them are modeled in the finite element method by using different element types. More specifically they are:

- Conduction: conductive heat transfer through house envelope;
- Convection: convective heat transfer at interior and exterior surfaces;
- Radiation: a) longwave radiation between exterior surfaces and ambient environment, sky, and ground; b) longwave radiation between every two interior surfaces; c) shortwave solar radiation through transparent and translucent house envelope;
- Ventilation: heat transfer caused by ventilation and infiltration/exfiltration through the house envelope.

Figure A.2 shows an example of a discretized house. All the involved heat transfer means between two nodes are formulated numerically into the following general form, as shown in Equation A-1.

$$M\dot{T} + ST - f = 0 \tag{A-1}$$

Where,

M the thermal capacity, J/K;

S the stiffness matrix, W/K;

f the gain vector, W.

Each matrix (M, S, f) can be a function of time.

Figure A.2 shows the infrastructure of GTSim and how information flows. In fact the GTSim follows the same structure like most programs do:

First, the GTSim loads in all necessary building information as well as simulation parameters, including internal gains and daily usage profile.

Second, the GTSim will form the three basic matrices (M, S, f) in Equation A-1.

Third, the GTSim will run an initialization to estimate the initial temperatures.

Fourth, GTSim will run the simulation time-step by time-step for the given simulation period. This is the major part of the simulation package. At each time step GTSim will call weather info from the TMY3 weather file and update all three matrices (M, S, f) if necessary. Then the updated equation A-1 will be solved using the p-c method. Temperature at each node is the output. Space heating/cooling loads will then be estimated based on user-supplied heating/cooling setpoints.

The last is postprocessing. All the customized postprocessing can be added in the end.

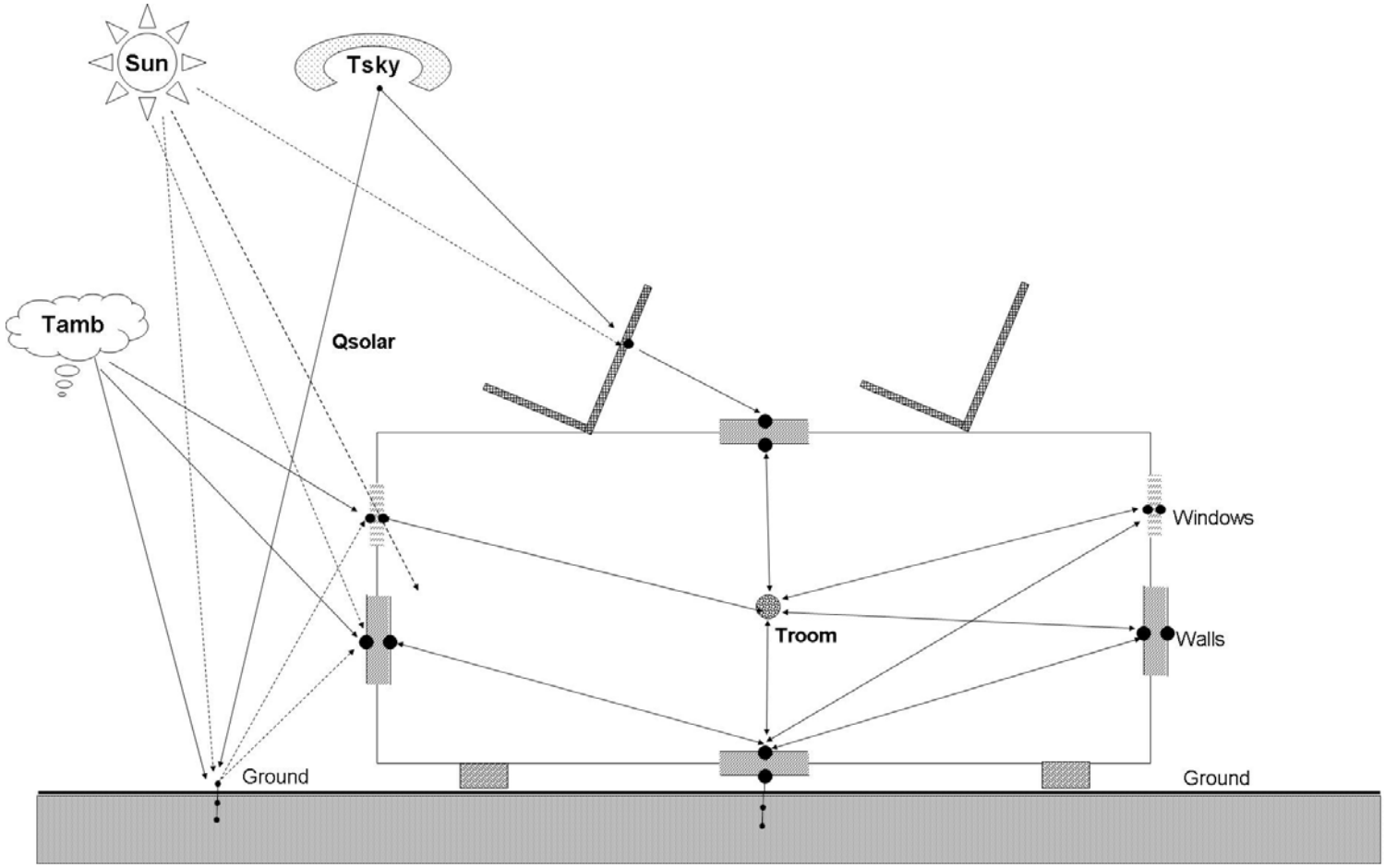

Figure A.1 An example of discretizing a physical house into a node network

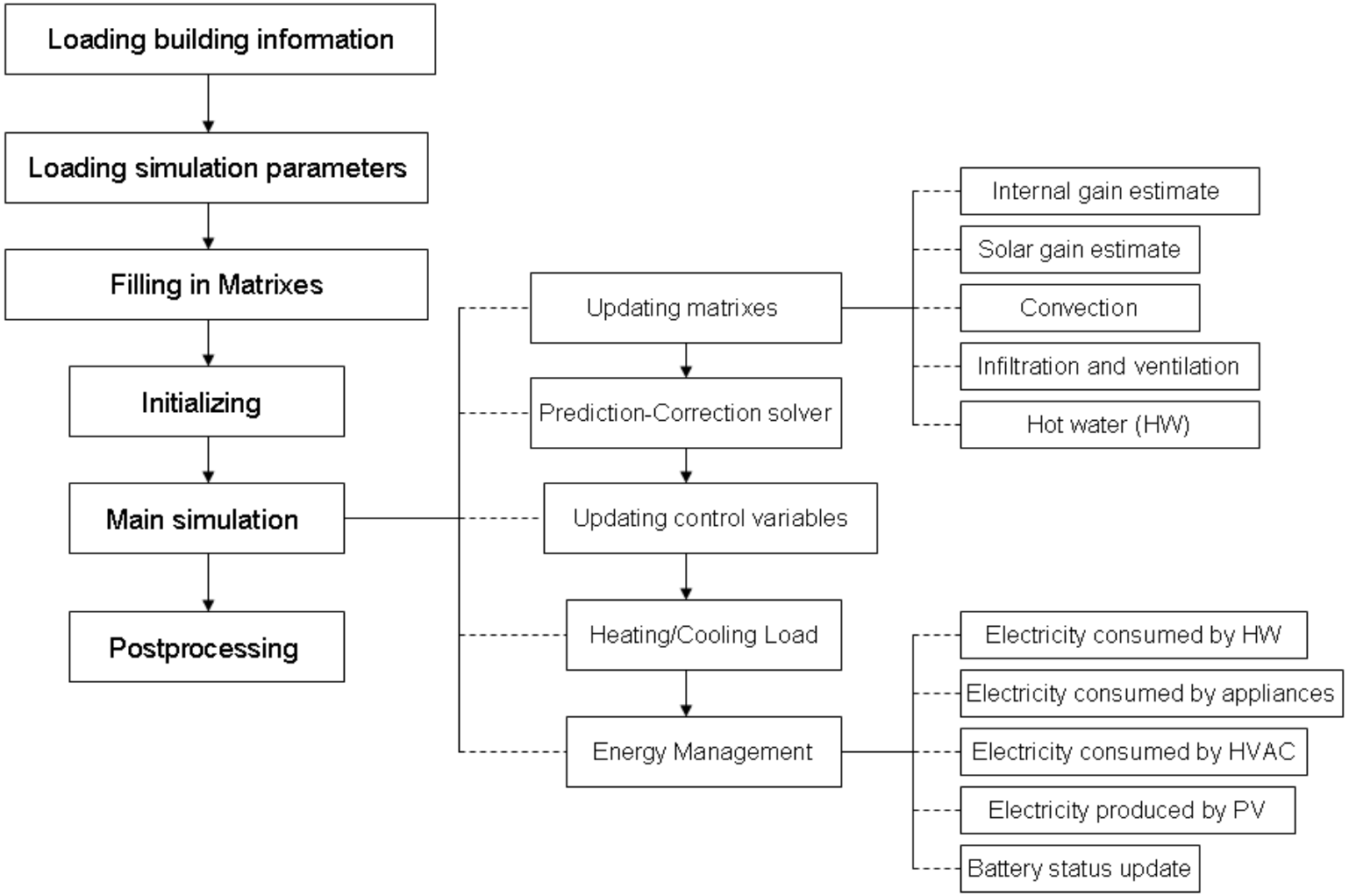

Figure A.2 The Framework of GTSim

A.3 Physical Models used in GTSim

This section introduces all the important physical models used in GTSim.

A.3.1 Solar Model

The total short-wave irradiance incident on an exposed opaque or transparent surface of arbitrary inclination β_f and azimuth α_f has three components: beam, diffuse and ground reflected. They will be estimated based on the following equations.

- Beam radiation:

$$I_{d\beta} = I_{dn} \times \cos i_{\beta} \tag{A-2}$$

$$\beta_s = \sin^{-1}(\cos L \cos d \cos \theta_h + \sin L \sin d) \tag{A-3}$$

$$d = 23.45 \sin(280.1 + 0.9863Y) \tag{A-4}$$

$$\theta_h = 15 \times (12 - t_s) \tag{A-5}$$

$$\alpha_s = \sin^{-1}(\cos d \sin \theta_h / \cos \beta_s) \tag{A-6}$$

$$i_{\beta} = \cos^{-1}(\sin \beta_s \cos \beta_f + \cos \beta_s \cos w \sin \beta_f) \tag{A-7}$$

Where:

$I_{d\beta}$ The direct intensity on the inclined surface (W/m^2);

I_{dn} The direct normal radiation (W/m^2), read from imported TMY2 weather file;

β_s The solar altitude;

L The site latitude;

d The solar declination (deg);

Y The year day number (January 1 = 1, Febrary 1 = 32 etc.);

θ_h The hour angle;

t_s The solar time (or local apparent time);

i_β The angle between the incident beam and the surface's normal vector;

w The surface solar azimuth ($=|\alpha_s - \alpha_f|$);

α_f The surface azimuth;

β_f The tilt angle.

□ Diffuse radiation:

The diffuse solar radiation is estimated using the Perez model [142]. In this model the sky diffuse irradiance is considered to be fully anisotropic. The main equations are listed below:

$$I_{s\beta} = I_{fh} \times [(1 - F_1)\cos^2 0.5\beta_f + F_1(a_0 / a_1) + F_2 \sin\beta_f] \quad \text{(A-8)}$$

$$a_0 = \max[0, \cos i_\beta] \quad \text{(A-9)}$$

$$a_1 = \max(\cos 85^\circ, \cos Z) \quad \text{(A-10)}$$

$$F_1 = \max[0, (f_{11} + f_{12}\Delta + Zf_{13})] \quad \text{(A-11)}$$

$$F_2 = f_{21} + f_{22}\Delta + Zf_{23} \quad \text{(A-12)}$$

$$\Delta = mI_{fh} / I_{sc} \quad \text{(A-13)}$$

$$\varepsilon_i = \frac{[(I_{fh} + I_{dn}) / I_{fh}] + 1.041Z^3}{1 + 1.041Z^3} \quad \text{(A-14)}$$

Where,

$I_{s\beta}$ The sky diffuse radiation incident on a surface of inclination, W/m^2;

I_{fh} The horizontal diffuse radiation for clear sky condition, W/m^2;

I_{sc} The solar constant evaluated at the equinox, normally assigned to be 1353, W/m^2;

F_1 The circumsolar brightness coefficient;

F_2 The horizon brightness coefficient;

a_0, a_1 Correct for the angle of incidence of the circumsolar radiation on the inclined and horizontal surface respectively;

Z The zenith angle, in radians;

Δ The sky's brightness;

m The air mass corresponding to the prevailing solar altitude and atmospheric pressure;

ε_i The sky clearness.

The factors f_i used to calculate brightness coefficients are listed in Table A.1.

TableA.1 "f_i" factors used in Perez model

ε_i	1	2	3	4	5	6	7	8
from	1.000	1.065	1.230	1.500	1.950	2.800	4.500	6.200
to	1.065	1.230	1.500	1.950	2.800	4.500	6.200	-
f_{11}	-0.0083	0.1299	0.3297	0.5682	0.8730	1.1326	1.0602	0.6777
f_{12}	0.5877	0.6826	0.4869	0.1875	-0.3920	-1.2367	-1.5999	-0.3273
f_{13}	-0.0621	-0.1514	-0.2211	-0.2951	-0.3616	-0.4118	-0.3589	-0.2504
f_{21}	-0.0596	-0.0189	0.0554	0.1089	0.2256	0.2878	0.2642	0.1561
f_{22}	0.0721	0.0660	-0.0640	-0.1519	-0.4620	-0.8230	-1.1272	-1.3765
f_{23}	-0.0220	-0.0289	-0.0261	-0.0140	0.0012	0.0559	0.1311	0.2506

The air mass varies with various solar elevation angles and can be evaluated based on Equation 15 if under a standard pressure (P_0 = 101.325 Pa) at sea level [143]. Otherwise air mass has to be corrected according to Equation 16. The local pressure p can be read from the imported TMY3 weather file.

$$m = \frac{1}{\sin\beta_s + 0.00176759[\beta_s \times (94.37515 - \beta_s)^{-1.21563}]} \quad \text{(A-15)}$$

$$m' = m \times \frac{p}{p_0} \quad \text{(A-16)}$$

□ Ground reflected radiation:

The total ground reflected solar radiation incident on any inclined surface can be estimated as below:

$$I_{rv} = 0.5 \times (1 - \cos\beta_f) \times I_{gh} \times r_g \quad \text{(A-17)}$$

Where,

I_{rv} The ground reflected total radiation incident on a surface of inclination β_f, W/m^2;

I_{gh} The global horizontal radiation, W/m^2;

r_g The ground reflectivity.

A.3.2 Ground model

GTSim has an individual ground temperature simulation package. Figure A.3 shows the node network of the ground model. This ground model assumes that the soil temperature at 1.2m below ground surface is constant for a certain location. Then instant heat balance equations can be built between soil nodes, ambient air node, sky node, and incident solar radiation as shown in Figure A.3. The resulting equation will share the same form as that

in Equation A-1. The ground surface temperature T_{gnd} will then be solved as the output. The constant soil temperature at 1.2m below ground surface is listed in the TMY statistics file.

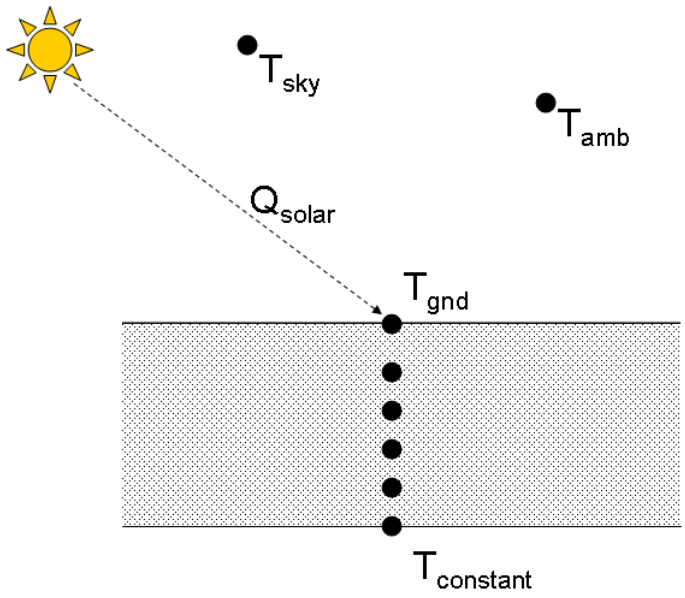

Figure A.3 The node network for ground model

A.3.3 The Domestic Hot Water System

GTSim includes a DHW model using evacuated tubes which is part of the DHW design in GTSD07 project. This DHW contains three components: evacuated tubes, DHW tank, and backup electric heat pump. Figure A.4 shows the diagram of DHW system in GTSD07 house.

The efficiency of evacuated tubes is estimated based on technical literature provided by the manufacturer[144].

The DHW module solves the following governing equation (Equation A-18) to estimate instant hot water temperature, assuming no heat loss through heat transfer process from evacuated tubes to main tank:

$$m_{\tan k} C_{pw} \frac{dT_w}{dt} = Q_{solar} - h(T_w - T_{air}) \quad \text{(A-18)}$$

Where,

$m_{\tan k}$ mass capacity of the main tank, kg;

C_{pw} the specific heat capacity of water, J/(kg-K);

T_w hot water temperature, K;

T_{air} the ambient air temperature, K;

Q_{solar} the collected solar heat (estimated from evacuated tube model), W;

h the total heat transfer coefficient between water in tank and ambient environment (air), W/m^2.

The backup electric heat pump model (Equation A-19) estimates how much extra electricity residents need to consume to heat water up to the desired temperature for every specific household function when instantaneous solar heat is not enough, assuming there is no temperature stratification in the water tank and the embedded electric heater has an efficiency of 1.

$$E_{backup} = m_{\tan k} \times C_{pw} \times (T_{w,req} - T_w) \quad \text{(A-19)}$$

Where,

E_{backup} the electricity consumption used by backup heating element, J;

$T_{w,req}$ the required hot water temperature, K.

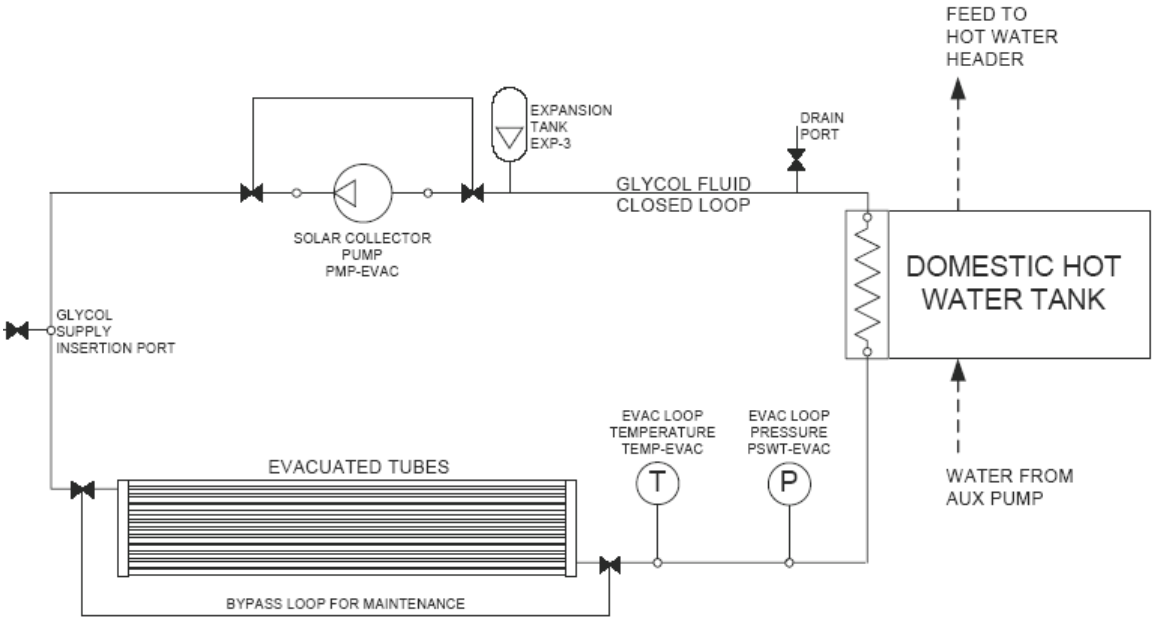

Figure A.4 The diagram of DHW using evacuated tubes

A.3.4 Room Element

GTSim has a special element named Room-element. It aggregates all convective and radiative heat transfers together in one macro element. Right now the Room-element is limited to rectangular space geometry.

A.4 Verification

A series of verifications have been conducted along with GTSim's development. Two cases have been built to verify GTSim's capacities as well as credibility on different prospects. They are:

- Case 1: A simple box-type room with ventilation only. This space has two windows: one in the northern wall right below the ceiling and the other one in the

southern wall near the floor. Both windows are in the same size of 10 m × 1m. Figure A.5 shows the space geometry information.

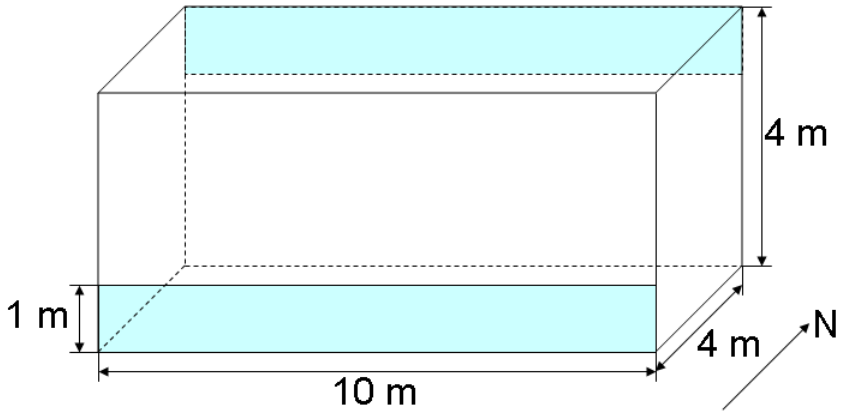

Figure A.5 The testing space in case 1 and case 2

□ Case 2: The same space in case 1 but with abstract mechanical system (purchased heating/cooling).

A.4.1 Case1: ventilation only

A ventilation rate of 0.35ACH was set in this case. The intention of conducting this test was to check whether GTSim models the phenomena with acceptable accuracy. The simulation period is chosen to be May 25~June 5 because this is a period when a house can survive without mechanical systems. Internal gains and corresponding schedules are set to be the same in GTSim and EnergyPlus.

Figure A.6 shows the hourly room air temperature comparison between GTSim and EnergyPlus. The average room air temperature from GTSim simulation is 22.43 °C and that from EnergyPlus is 22.31°C. The average room air temperature difference is 0.12°C. The hourly room air temperature curves from GTSim and EnergyPlus match and

conclusively GTSim demonstrates its capability and reliability in simple ventilation mode.

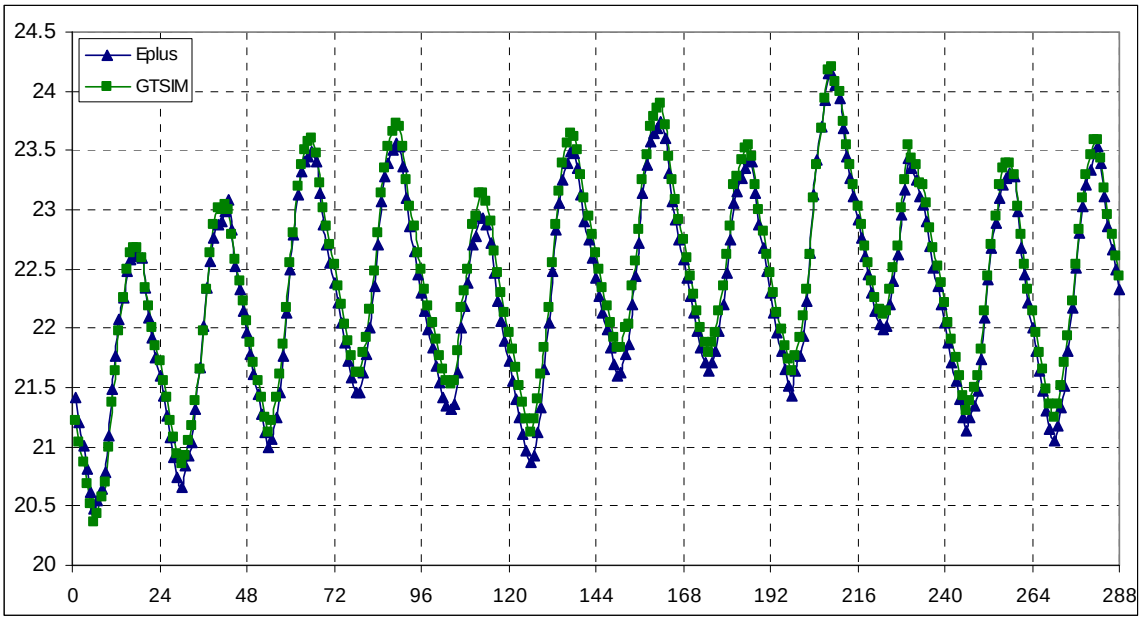

Figure A.6 Mean air temperature comparison for case 1

A.4.2 Case2: mechanical ventilation (purchased heating/cooling)

Figure A.7 shows the comparison of hourly room air temperature between GTSim and EnergyPlus. The trends are very much similar but in the simulation by GTSim room air temperature increases more rapidly. The higher room air temperatures also result in higher cooling loads in GTSim as shown in Figure A.8. Since EnergyPlus is not completely transparent especially in terms of the HVAC control implementation the cause of the differences can not be identified.

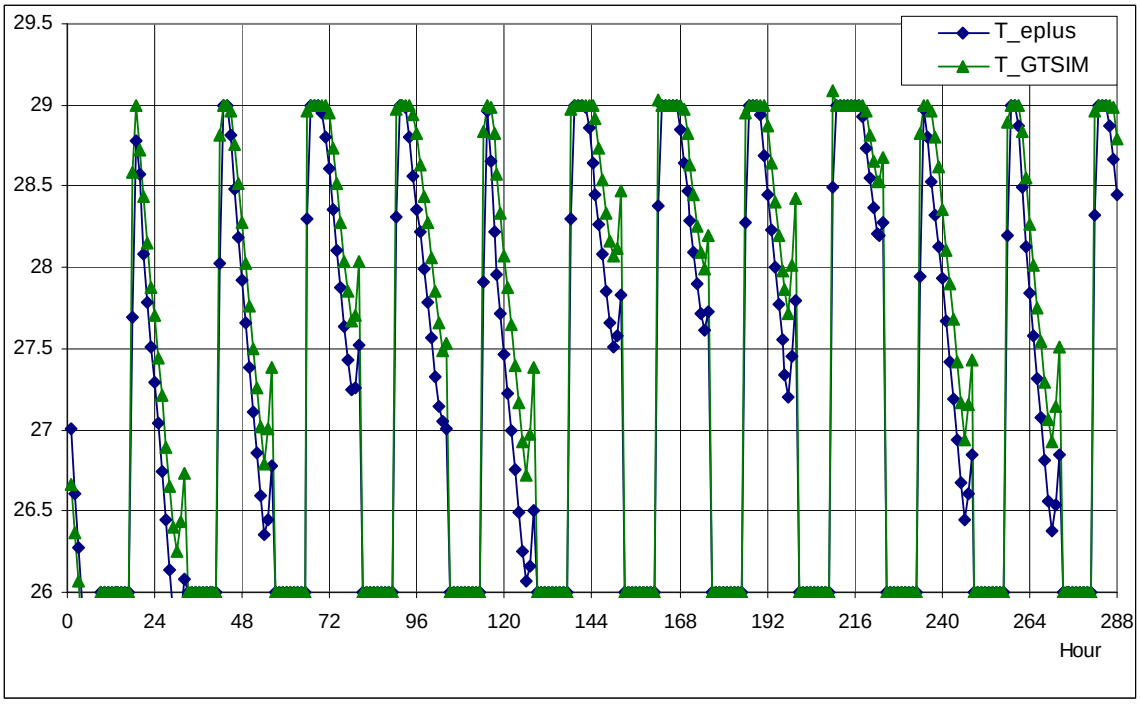

Figure A.7 Mean air temperature comparison for mechanical ventilation case

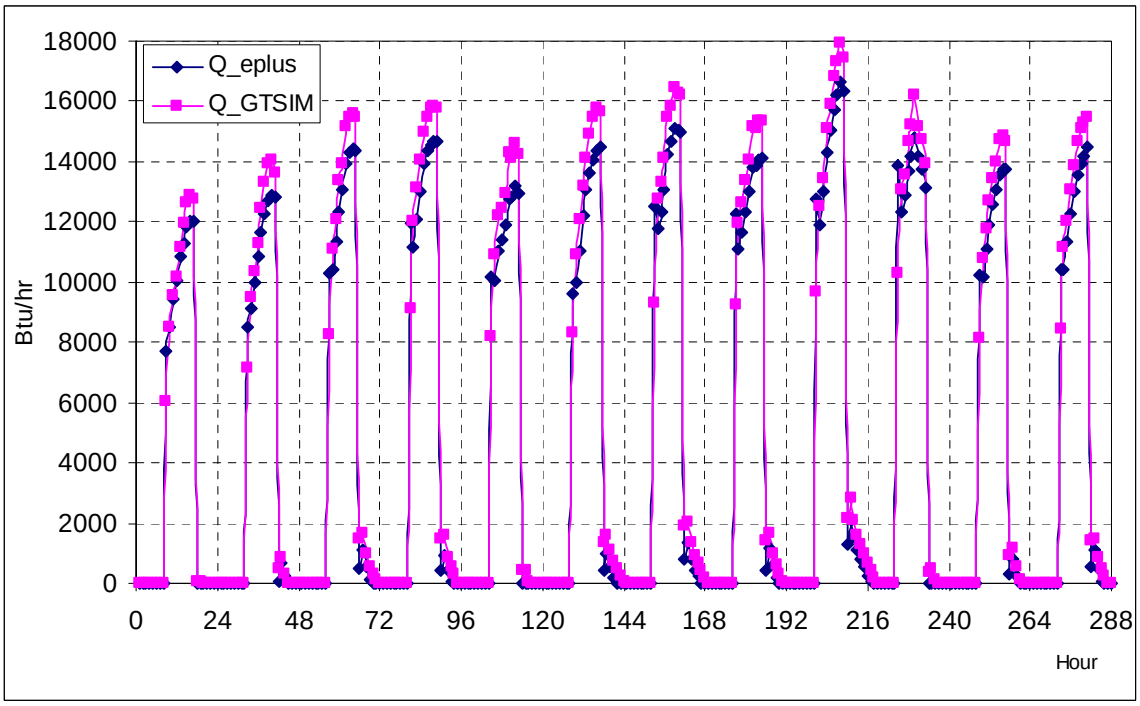

Figure A.8 Hourly cooling load comparison for mechanical ventilation case

APPENDIX B RISK CALCULATION FORMULAS

Below shows mathematical formulas to calculate risk indices at two different scenarios: 1) the criterion is a discrete value; 2) the criterion is a distribution of series of values.

- The criterion is a discrete value x_{req}

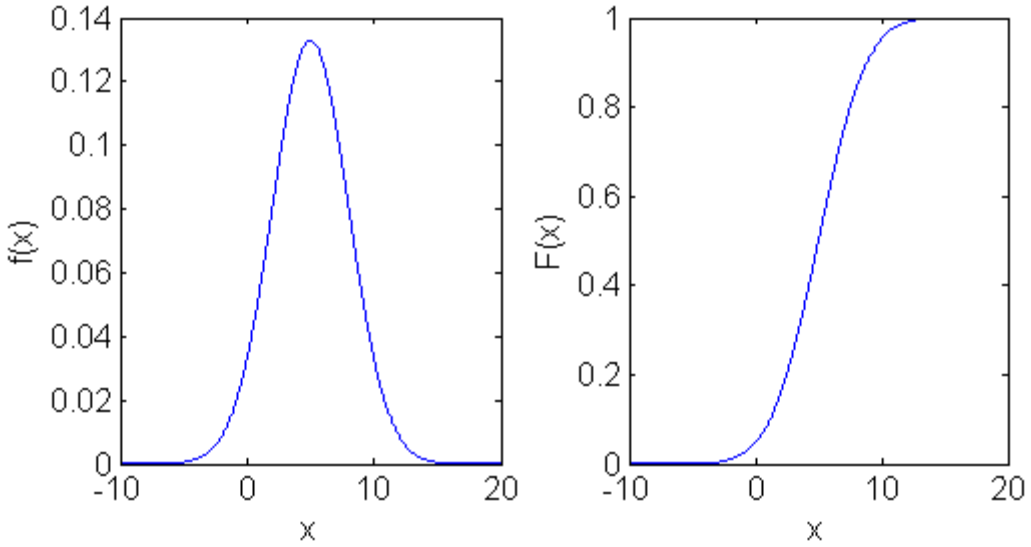

Figure B.1 A plot of probability density function (PDF) and cumulative distribution function (CDF)

Figure B.1 shows the probability density function of the simulation outcome X (usually denoted by $f(x)$) and its corresponding cumulative distribution function (usually denoted by $F(x)$). The relationship between $f(x)$ and $F(x)$ is written in Equation B-1. The risk index p can be calculated using Equation B-2.

$$F(x) = \Pr(X \le x) = \int_{-\infty}^{x} f(t)dt \tag{B-1}$$

$$p = \Pr(X \le x_{req}) = F(x_{req}) \tag{B-2}$$

□ The criterion is a distribution of series of values (Y)

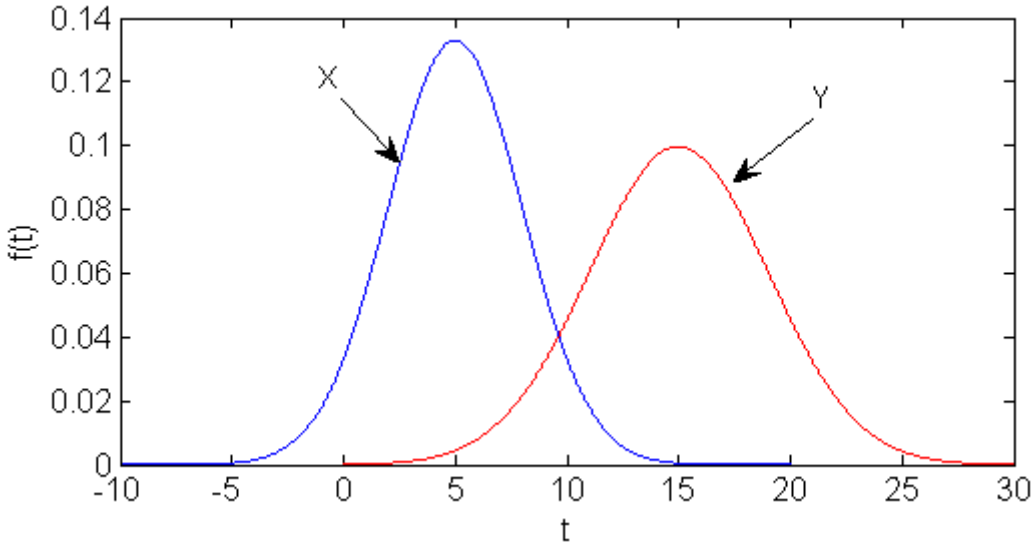

Figure B.2 The PDFs of two variables X and Y

Figure B.2 shows the PDFs of two variables X and Y. The probability of variable X no larger than Y can be calculated using Equation B-3 analytically.

$$p = \Pr(\overline{X} \le \overline{Y}) = \int \Pr(\overline{X} \le y) g(y) dy = \int_{-\infty}^{\infty} \left(\int_{-\infty}^{y} f(x) dx \right) g(y) dy \qquad \text{(B-3)}$$

In this study sample approximation method has been used to represent the stochastic process. Samples of X and Y (donated by $\overline{X}$ and $\overline{Y}$) are achieved instead of the PDFs of X and Y. Therefore Equation B-4 has been used to estimate the above probability instead.

$$p = \sum_{i=1}^{N} F(y_i) g(y_i) \Delta y_i \qquad \text{(B-4)}$$

Where,

$$\Delta y_i = \frac{\max(y) - \min(y)}{N}$$

REFERENCES

1. Energy Information Administration, *Annual Energy Review 2006*. 2007: Washington DC.
2. Scheer, H., *Energy Autonomy*. 2007, London, UK: Earthscan.
3. Energy Information Administration, *Annual Energy Outlook 2008 (Early Release)*. 2008.
4. Sandia National Laboratories, *The Photovoltaic Industry Roadmap*. 2000.
5. Solar Energy Industries Association. *Our Solar Power Future*. 2004; Available from: http://www.seia.org/roadmap.pdf.
6. Energy Information Administration, *Table 8.10 Average retail prices of electricity, 1960-2008*, Annual energy review 2008, Editor. 2009: Washington DC.
7. RenewableEnergyAccess.com, *PV Costs to Decrease 40% by 2010* in *RenewableEnergyWorld.com*. 2007.
8. Davis, F.D., R.P. Bagozzi, and P.R. Warshaw, *User acceptance of computer technology: a comparison of two theoretical models.* Management Science, 1989. **35**(8): p. 982-1003.
9. Rogers, E.M., *Diffusion of innovations*. 3rd ed. 1983, New York: Free Press. 453.
10. Fanger, P.O., *Thermal comfort: analysis and applications in environmental engineering*. 1970: Danish Technical Press.
11. Brager, G.S. and R. de Dear, *A standard for natural ventilation.* ASHRAE journal, 2000. **42**(10): p. 21-29.
12. de Dear, R.J. and G.S. Brager, *Thermal comfort in naturally ventilated buildings: revisions to ASHRAE Standard 55.* Energy and Buildings, 2002. **34**(6): p. 549-561.
13. Nicol, J.F. and M.A. Humphreys, *Adaptive thermal comfort and sustainable thermal standards for buildings.* Energy & Buildings, 2002. **34**(6): p. 563-572.
14. Shove, E., *Users, technologies and expectations of comfort, cleanliness and convenience.* Innovation: The European Journal of Social Sciences, 2003. **16**(2): p. 193-206.
15. Wener, R. and H. Carmalt, *Environmental psychology and sustainability in high-rise structures.* Technology in Society, 2006. **28**(1-2): p. 157-167.
16. Meguro, W., *Beyond blue and red arrows : optimizing natural ventilation in large buildings*, in *Department of Architecture*. 2005, Massachusetts Institute of Technology. p. 140.
17. McConahey, E., *Finding the Right Mix.* ASHRAE Journal, 2008. **50**(9): p. 36-48.
18. Bourgeois, D.J., *Detailed occupancy prediction, occupancy-sensing control and advanced behavioural modelling within whole-building energy simulation*. 2005, Université Laval: Quebec, Canada.
19. Kueck, J.D., et al., *Measurement practices for reliability and power quality*. 2004, Oak Ridge National Laboratory: Oak Ridge, Tennessee. p. 54.
20. Kueck, J.D. and B.J. Kirby, *The Distribution System of the Future.* The Electricity Journal, 2003. **16**(5): p. 78-87.

21. Georgia Power. *Power credit*. 2008; Available from: http://www.georgiapower.com/powercredit/powercredit.asp.
22. Nevada Power. *Cool Share*. 2008; Available from: http://www.coolshareprogram.com/.
23. Idaho Power. *A/C cool credit*. 2008; Available from: http://www.idahopower.com/accoolcredit/coolCredit_faqs.htm.
24. Rausand, M. and A. Høyland, *System Reliability Theory: Models, Statistical Methods, and Applications*. 2004: Wiley-IEEE. 636.
25. Billinton, R. and W. Li, *Reliability assessment of electric power systems using Monte Carlo methods*. 1994, New York: Plenum Press. 351.
26. Yang, F., *A comprehensive approach for bulk power system reliability assessment*, in *School of Electrical and Computer Engineering*. 2007, Georgia Institute of Technology Atlanta, GA. p. 150.
27. Bagen, *Reliability and Cost/Worth Evaluation of Generating Systems Utilizing Wind and Solar Energy*, in *Department of Electrical Engineering*. 2005, University of Saskatchewan: Saskatoon. p. 253.
28. Karki, R., *Reliability and cost evaluation of small isolated power systems containing photovoltaic and wind energy*, in *Department of electrical engineering*. 2000, University of Saskatchewan: Saskatoon. p. 245.
29. Patel, J., *Reliability/Cost Evaluation of a Wind Power Delivery System*, in *Department of Electrical Engineering*. 2006, University of Saskatchewan: Saskatoon. p. 94.
30. Gao, Y., *Adequacy assessment of electric power systems incorporating wind and solar energy*, in *Department of electrical engineering*. 2006, University of Saskatchewan. p. 180.
31. El-Maghraby, M.H., Y.A. Abed, and M.A. El-Sayes, *Proposed generalized models for estimating the reliability of a stand-alone solar photovoltaic power system.* Electric Power Systems Research, 1985. **8**(2): p. 111-118.
32. Tsalides, P. and A. Thanailakis, *Loss-of-load probability and related parameters in optimum computer-aided design of stand-alone photovoltaic systems.* Solar Cells, 1986. **18**(2): p. 115-127.
33. Garvey, P., *Analytical methods for risk management : a systems engineering perspective*. 2009, Boca Raton: CRC Press. 264.
34. ISO, *Buildings and constructed assets - Service life planning - Part 1: General principles*, in *ISO 15686-1*. 2000.
35. Aven, T., *Reliability analysis as a tool for expressing and communicating uncertainty*, in *Recent advances in reliability theory: methodology, practice, and inference*, N. Limnios and M. Nikulin, Editors. 2000, Birkhauser: Boston, MA.
36. Messenger, R.A. and J. Ventre, *Photovoltaic systems engineering*. 2004, Boca Raton: CRC Press. 455.
37. Kaplanis, S. and E. Kaplani. *The effect of statistical fluctuations of solar radiation on PV-system sizing*. in *Proceedings of the 5th IASTED International Conference on Power and Energy Systems*. 2005. Benalmadena, Spain: Acta Press, Anaheim, CA, United States.

38. Wilcox, S. and W. Marion, *Users Manual for TMY3 Data Sets*. 2008, Technical Report NREL/TP 581 43156, National Renewable Energy Laboratory, Golden CO.
39. Marion, W. and K. Urban, *User's Manual for TMY2s*. 1995, National Renewable Energy Laboratory Golden, CO.
40. Huang, Y.J. and D.B. Crawley. *Does it matter which weather data you use in energy simulations?* in *American Council for an Energy-Efficieny Economy (ACEEE) summer study on energy efficiency in buildings*. 1996. Pacific Grove, CA
41. Hopfe, C., et al. *The impact of future climate scenarios on decision making in building performance simulation: a case study*. in *The 12th EuropIA international conference*. 2009. Paris, France.
42. Wyss, G. and K. Jorgensen, *A user's guide to LHS: Sandia's Latin Hypercube Sampling Software*. 1998, Sandia National Laboratories: Albuquerque, NM. p. 148.
43. Dows, R.N. and E.J. Gough, *PVUSA procurement, acceptance, and rating practices for photovoltaic power plants*, in *Other Information: PBD: Sep 1995*. 1995. p. Size: 200 p.
44. Marion, B., et al. *Performance parameters for grid-connected PV systems*. in *The 31st IEEE Photovoltaic Specialists Conference*. 2005. Lake Buena Vista, FL, United States: Institute of Electrical and Electronics Engineers Inc., Piscataway, NJ 08855-1331, United States.
45. Detrick, A., A. Kimber, and L. Mitchell. *Performance evaluation standards for photovoltaic modules and systems*. in *Conference Record of the IEEE Photovoltaic Specialists Conference*. 2005. Lake Buena Vista, FL, United States: Institute of Electrical and Electronics Engineers Inc., Piscataway, NJ 08855-1331, United States.
46. Emery, K., et al. *Trust but verify: Procedures to achieve accurate efficiency measurements for all photovoltaic technologies*. in *Conference Record of the IEEE Photovoltaic Specialists Conference*. 2005. Lake Buena Vista, FL, United States: Institute of Electrical and Electronics Engineers Inc., Piscataway, NJ 08855-1331, United States.
47. de Wit, S. and G. Augenbroe, *Analysis of uncertainty in building design evaluations and its implications.* Energy and Buildings, 2002. **34**(9): p. 951-958.
48. Bhuiyan, M.M.H. and M. Ali Asgar, *Sizing of a stand-alone photovoltaic power system at Dhaka.* Renewable Energy, 2003. **28**(6): p. 929-938.
49. Deshmukh, M.K. and S.S. Deshmukh, *Modeling of hybrid renewable energy systems.* Renewable and Sustainable Energy Reviews, 2008. **12**(1): p. 235-249.
50. Sidrach-de-Cardona, M. and L. Mora Lopez, *A general multivariate qualitative model for sizing stand-alone photovoltaic systems.* Solar Energy Materials and Solar Cells, 1999. **59**(3): p. 185-197.
51. Labed, S. and E. Lorenzo, *The impact of solar radiation variability and data discrepancies on the design of PV systems.* Renewable Energy, 2004. **29**(7): p. 1007-1022.
52. Adelstein, J. and B. Sekulic. *Performance and reliability of a 1-kW amorphous silicon photovoltaic roofing system*. in *The 31st IEEE Photovoltaic Specialists*

Conference. 2005. Lake Buena Vista, FL, United States: Institute of Electrical and Electronics Engineers Inc., Piscataway, NJ 08855-1331, United States.
53. King, D.L., J.A. Kratochvil, and W.E. Boyson. *Stabilization and performance characteristics of commercial amorphous-silicon PV modules*. 2000. Anchorage, AK, USA: IEEE.
54. de Wit, S., *Uncertainty in predictions of thermal comfort in buildings*. 2001, Technical University of Delft (The Netherlands) Delft. p. 228.
55. Moon, H.J., *Assessing mold risks in buildings under uncertainty*, in *College of Architecture*. 2005, Georgia Institute of Technology: Atlanta, GA. p. 245.
56. Lorenzo, E. and L. Narvarte, *On the usefulness of stand-alone PV sizing methods.* Progress in Photovoltaics: Research and Applications, 2000. **8**(4): p. 391-409.
57. Birta, L.G. and G. Arbez, *Modelling and Simulation: Exploring Dynamic System Behaviour*. 2007: Springer. 454.
58. Judkoff, R. and J. Neymark, *International Energy Agency Building Energy Simulation Test (BESTEST) and Diagnostic Method* 1995, National Renewable Energy Laboratory: Golden, CO.
59. EIA. *Winter Energy Savings from Lower Thermostat Settings*. 2000; Available from: http://www.eia.doe.gov/emeu/consumptionbriefs/recs/thermostat_settings/thermostat.html.
60. Skoplaki, E. and J.A. Palyvos, *Operating temperature of photovoltaic modules: A survey of pertinent correlations.* Renewable Energy, 2009. **34**(1): p. 23-29.
61. Spiegel, M.R., *Schaum's outline of theory and problems of probability and statistics*. 1975, New York: McGraw-Hill.
62. Macdonald, I.A., *Quantifying the effects of uncertainty in building simulation*, in *Department of Mechanical Engineering*. 2002, University of Strathclyde. p. 267.
63. Beausoleil-Morrison, I. *Modelling mixed convection heat transfer at internal building surfaces*. 1999.
64. Awbi, H.B., *Calculation of convective heat transfer coefficients of room surfaces for natural convection.* Energy & Buildings, 1998. **28**(2): p. 219-227.
65. U.S. Department of Energy, *EnergyPlus*. 2009, http://apps1.eere.energy.gov/buildings/energyplus/.
66. Yazdanian, M. and J.H. Klems, *Measurement of the exterior convective film coefficient for windows in low-rise buildings.* ASHRAE transactions, 1994. **100**(1): p. 1087-1096.
67. Palyvos, J.A., *A survey of wind convection coefficient correlations for building envelope energy systems' modeling.* Applied Thermal Engineering, 2008. **28**(8-9): p. 801-808.
68. ASHRAE, *ASHRAE Handbook of fundamentals*. 2001.
69. Sherman, M.H. and D.J. Dickerhoff. *Airtightness of U.S. dwellings*. 1998. Toronto, Can: ASHRAE.
70. Chan, W.R., et al., *Analysis of U.S. residential air leakage database*. 2003, Lawrence Berkeley National Laboratory: Berkeley, CA. p. 52.
71. Orme, M., M.W. Liddament, and A. Wilson, *Numerical data for air infiltration & natural ventilation calculations*. 1994, Air Infiltration and Ventilation Center: Great Britain.

72. Skoplaki, E., A.G. Boudouvis, and J.A. Palyvos, *A simple correlation for the operating temperature of photovoltaic modules of arbitrary mounting.* Solar Energy Materials and Solar Cells, 2008. **92**(11): p. 1393-1402.
73. Rydh, C.J. and B.A. Sandén, *Energy analysis of batteries in photovoltaic systems. Part I: Performance and energy requirements.* Energy Conversion and Management, 2005. **46**(11-12): p. 1957-1979.
74. International, R., *RETScreen software online user manual - ground-source heat pump project model*. 2005, Canada: Natural Resources Canada.
75. EIA, *2005 Residential Energy Consumption Survey*. 2008: Washington DC.
76. Goldschmidt, V.W., *Heat Pumps: Basics, Types, and Performance Characteristics.* Annual Review of Energy, 1984. **9**(1): p. 447-472.
77. ARI, *Unitary air-conditioning and air-source heat pump equipment*. 1989, Air Conditioning & Refrigeration Institute.
78. Kondepudi, S.N. and A.A. Bhalerao, *Parametric analysis on the seasonal heating coefficient of performance (SHCOP) of air to air heat pumps.* Recent Research in Heat Pump Design, Analysis, and Application, 1992. **28**: p. 79-87.
79. Baxter, V.D. and J.C. Moyers, *Field-measured cycling, frosting, and defrosting losses for a high-efficiency air-source heat pump.* ASHRAE transactions, 1985. **91**(2B): p. 537-554.
80. Goldschmidt, V.W., G.H. Hart, and R.C. Reiner, *A note on the transient performance and degradation coefficient of a field tested heat pump--cooling and heating mode.* ASHRAE Trans, 1980. **86**(2): p. 368-375.
81. Goldschmidt, V.W., *Effects of cyclic response of residential air conditioners on seasonal performance.* ASHRAE Transaction, 1981. **87**(2): p. 757-770.
82. Balaras, C.A., *The role of thermal mass on the cooling load of buildings. An overview of computational methods.* Energy and Buildings, 1996. **24**(1): p. 1-10.
83. Antonopoulos, K.A. and E. Koronaki, *Apparent and effective thermal capacitance of buildings.* Energy, 1998. **23**(3): p. 183-192.
84. Barakat, S.A. and D.M. Sander, *Utilization of solar gain through windows for heating houses*. 1982, Division of building research, National Research Council of Canada: Ottawa, Canada.
85. ISO 14683, *Thermal bridges in building construction - Linear thermal transmittance - Simplified methods and default values*, ISO, Editor. 1999.
86. Larbi, A.B., *Statistical modelling of heat transfer for thermal bridges of buildings.* Energy and Buildings, 2005. **37**(9): p. 945-951.
87. Energy Star. *Appliances*. 2009; Available from: http://www.energystar.gov/index.cfm?c=appliances.pr_appliances.
88. EIA, *End-Use Consumption of Electricity 2001*. 2009: Washington DC.
89. Meier, A. and K. Rosen, *Leaking electricity in domestic appliances*. 2002, Lawrence Berkeley National Laboratory, University of California: Berkeley, CA.
90. Harvey, L.D.D., *A handbook on low-energy buildings and district-energy systems: fundamentals, techniques and examples*. 2006, London, UK: Earthscan.
91. Kalogirou, S.A., *Solar thermal collectors and applications.* Progress in Energy and Combustion Science, 2004. **30**(3): p. 231-295.
92. EN 12975-2, *Thermal solar systems and components - Solar collectors*, European Standard, Editor. 2006.

93. ISO 9806-1, *Test methods for solar collectors* ISO, Editor. 1994.
94. El-Nashar, A.M., *Seasonal effect of dust deposition on a field of evacuated tube collectors on the performance of a solar desalination plant.* Desalination, 2009. **239**(1-3): p. 66-81.
95. Mastekbayeva, G.A. and S. Kumar, *Effect of dust on the transmittance of low density polyethylene glazing in a tropical climate.* Solar Energy, 2000. **68**(2): p. 135-141.
96. Saltelli, A., et al., *Sensitivity Analysis in Practice: A Guide to Assessing Scientific Models*. 2004, West Sussex, England: John Wiley & Sons Ltd. 232.
97. Saltelli, A., et al., *Global Sensitivity Analysis: The Primer*. 2008, West Sussex, England: John Wiley & Sons Ltd. 304.
98. Morris, M.D., *Factorial sampling plans for preliminary computational experiments.* Technometrics, 1991. **33**(2): p. 14.
99. Campolongo, F., J. Cariboni, and A. Saltelli, *An effective screening design for sensitivity analysis of large models.* Environmental Modelling and Software, 2007. **22**(10): p. 1509-1518.
100. Choudhary, R., et al. *Simulation enhanced prototying of an exprimental solar house*. in *Building Simulation 2007*. 2007. Beijing, China.
101. Clarke, J.A., *Energy simulation in building design*. 2001: Butterworth-Heinemann.
102. Hendron, R., *Building America Research Benchmark Definition*. 2007, National Renewable Energy Laboratory: Golden, Colorado.
103. ASHRAE, *Airflow around buildings*, in *2001 ASHRAE Handbook of Fundamentals*. 2001, ASHRAE: Atlanta, GA.
104. Altafullah, A., *Keep Food Safe When Power Goes Off*, in *Daily Press*. 2006: Newport News, Va.
105. Augenbroe, G., *Private communication*. May, 2009.
106. Wikipedia. *Control engineering*. 2007; Available from: http://en.wikipedia.org/wiki/Control_engineering.
107. Kelly, G.E., *Control system simulation in North America.* Energy and Buildings, 1988. **10**(3): p. 193-202.
108. Camacho, E.F., M. Berenguel, and F.R. Rubio, *Advanced control of solar plants*. 1997: New York : Springer. 267.
109. Passino, K.M., *Biomimicry for optimization, control, and automation*. 2004: Springer.
110. *Advanced building simulation*, ed. A.M. Malkawi and G. Augenbroe. 2004: Spon Press.
111. van Schijndel, A.W.M., *Optimal operation of a hospital power plant.* Energy and Buildings, 2002. **34**(10): p. 1055-1065.
112. Wang, S. and X. Jin, *Model-based optimal control of VAV air-conditioning system using genetic algorithm.* Building and Environment, 2000. **35**(6): p. 471-487.
113. Sun, J. and A. Reddy, *Optimal control of building HVAC&R systems using complete simulation-based sequential quadratic programming (CSB-SQP).* Building and Environment, 2005. **40**(5): p. 657-669.

114. Zhang, Y. and V.I. Hanby, *Model-based control of renewable energy systems in buildings.* HVAC and R Research, 2006. **12**(3 A): p. 577-598.
115. Henze, G.P., et al., *Experimental Analysis of Model-Based Predictive Optimal Control for Active and Passive Building Thermal Storage Inventory.* HVAC&R Research Journal, 2005. **11**(2): p. 189-213.
116. Ahmad, M. and C.H. Culp, *Uncalibrated Building Energy Simulation Modeling Results.* HVAC&R Research, 2006. **12**(4): p. 1141-1155.
117. Clarke, J.A., P.A. Strachan, and C. Pernot. *Approach to the calibration of building energy simulation models*. in *ASHRAE Transactions*. 1993. Denver, CO, USA: Publ by ASHRAE, Atlanta, GA, USA.
118. Manke, J.M., D.C. Hittle, and C.E. Hancock. *Calibrating building energy analysis models using short term test data*. in *International Solar Energy Conference*. 1996. San Antonio, TX, USA: ASME, New York, NY, USA.
119. Pan, Y., Z. Huang, and G. Wu, *Calibrated building energy simulation and its application in a high-rise commercial building in Shanghai.* Energy and Buildings, 2007. **39**(6): p. 651-657.
120. Pedrini, A., F.S. Westphal, and R. Lamberts, *A methodology for building energy modelling and calibration in warm climates.* Building and Environment, 2002. **37**(8-9): p. 903-912.
121. Sun, J. and T.A. Reddy, *Calibration of building energy simulation programs using the analytic optimization approach (RP-1051).* HVAC and R Research, 2006. **12**(1): p. 177-196.
122. Reddy, T.A., *Literature Review on Calibration of Building Energy Simulation Programs: Uses, Problems, Procedures, Uncertainty, and Tools.* ASHRAE Transactions, 2006. **112**(1): p. 226-240.
123. Zhang, Y. and V. Hanby. *Short-term prediction of weather parameters using online weather forecasts*. in *Building Simulation*. 2007. Beijing, China.
124. Celik, A.N., *Techno-economic analysis of autonomous PV-wind hybrid energy systems using different sizing methods.* Energy Conversion and Management, 2003. **44**(12): p. 1951-1968.
125. Celik, A.N., *Effect of different load profiles on the loss-of-load probability of stand-alone photovoltaic systems.* Renewable Energy, 2007. **32**(12): p. 2096-2115.
126. Anis, W.R. and M.A.-S. Nour, *Energy losses in photovoltaic systems.* Energy Conversion and Management, 1995. **36**(11): p. 1107-1113.
127. Wacker, G. and R. Billinton, *Customer cost of electric service interruptions.* Proceedings of the IEEE, 1989. **77**(6): p. 919-930.
128. Willis, H.L., G.V. Welch, and R.R. Schrieber, *Aging power delivery infrastructures*. 2001, New York: M. Dekker. 551.
129. Sullivan, M. and V. President, *Interruption costs, customer satisfaction and expectations for service reliability.* IEEE Transactions on Power Systems, 1996. **11**(2): p. 989.
130. Rau, N.S., *The use of probability techniques in value-based planning.* Power Systems, IEEE Transactions on, 1994. **9**(4): p. 2001-2013.

131. Chowdhury, A.A. and D.O. Koval, *Application of customer interruption costs in transmission network reliability planning.* Industry Applications, IEEE Transactions on, 2001. **37**(6): p. 1590-1596.
132. Kaur, N., et al. *Evaluation of customer interruption cost for reliability planning of power systems in developing economies*. in *Probabilistic Methods Applied to Power Systems, 2004 International Conference on*. 2004.
133. Dakkak, M., et al., *Operation strategy of residential centralized photovoltaic system in remote areas.* Renewable Energy, 2003. **28**(7): p. 997-1012.
134. US DOE, *Solar Energy Technologies Program: Multi-Year Technical Plan 2007-2011 and Beyond*. 2007, Golden CO: National Renewable Energy Laboratory.
135. Rushing, A.S. and B.C. Lippiatt, *Energy price indices and discount factors for lifecycle cost analysis - April 2008*. 2008, National Institute of Standards and Technology. p. 75.
136. Pargfrieder, J. and H.P. Jorgl. *An integrated control system for optimizing the energy consumption and user comfort in buildings*. in *Computer Aided Control System Design, 2002. Proceedings. 2002 IEEE International Symposium on*. 2002.
137. van der Linden, K., et al., *Thermal indoor climate building performance characterized by human comfort response.* Energy & Buildings, 2002. **34**(7): p. 737-744.
138. *Performance specification for the energy efficient office of the future*. General Information Report 30. 1995: Building Research Energy Conservation Support Unit.
139. Robinson, D. and F. Haldi, *Model to predict overheating risk based on an electrical capacitor analogy.* Energy & Buildings, 2008. **40**(7): p. 1240-1245.
140. Holmes, M.J. and J.N. Hacker, *Climate change, thermal comfort and energy: Meeting the design challenges of the 21st century.* Energy & Buildings, 2007. **39**(7): p. 802-814.
141. National Renewable Energy Laboratory, *National Solar Radiation Database 1991–2005 Update: User's Manual*. 2007, Office of Energy Efficiency and Renewable Energy: Golden, CO.
142. Perez, R., et al., *Modeling daylight availability and irradiance components from direct and global irradiance.* Solar Energy, 1990. **44**(5): p. 271-289.
143. Gueymard, C., *Critical analysis and performance assessment of clear sky solar irradiance models using theoretical and measured data.* Solar Energy, 1993. **51**: p. 121.
144. Apricus. *Collector Efficiency*. 2006; Available from: http://www.apricus.com/html/solar_collector_efficiency.htm.